ILLUMINATING THE NEURAL CIRCUITRY UNDERLYING LARVAL ZEBRAFISH BEHAVIOR

Dissertation der Fakultät für Biologie
der Ludwig-Maximilians-Universität München
zur Erlangung des Grades eines Doktors
der Naturwissenschaften

vorgelegt von
Eva Aimable Naumann

Cambridge, Massachusetts, USA 2010

Erstgutachter: Prof. Dr. Alexander Borst
Zweitgutachter: Prof. Dr. Hans Straka

Tag der Annahme zur Beurteilung: 8. Oktober 2010
Tag der mündlichen Prüfung: 21. Dezember 2010

ILLUMINATING THE NEURAL CIRCUITRY UNDERLYING LARVAL ZEBRAFISH BEHAVIOR

A dissertation presented
by
Eva Aimable Naumann
to Ludwig-Maximilians-Universität München
in partial fulfillment of the requirements
for the degree of
Doctor rerum naturalium
in the subject of
Biology

Cambridge, Massachusetts, USA 2010

Dissertation Advisors: Dr. Florian Engert, Dr. Oliver Griesbeck & Dr. Alexander Borst

© 2010 – Eva Aimable Naumann

All rights reserved. iii

TABLE OF CONTENTS:

Acknowledgments 5

Summary 7

1 Introduction 10

1.1 The investigation of neural circuits 10

- 1.1.1 Motivation 10
- 1.1.2 Neural circuits 11
- 1.1.3 Neuroethological approach to the investigation of neural circuits 13
- 1.1.4 Criteria for choosing a preparation for neural circuit investigations 14

1.2 The larval zebrafish: A translucent vertebrate brain 15

- 1.2.1 The zebrafish in biological research 15
- 1.2.2 Benefits for larval zebrafish for neural circuit mapping 16
- 1.2.3 Behavioral paradigms in larval zebrafish: What behavior to study? 18
- 1.2.4 Functional imaging of neural activity for neuronal circuit identification 20
- 1.2.5 Establishing causality between behavior and neurons 23
- 1.2.6 Strategy to investigate neural circuits in larval zebrafish 25
- 1.2.7 Specific aims of the dissertation 27

1.3 Background and introduction to aim 1: Whole-field motion discrimination in larval zebrafish 28

- 1.3.1 Optomotor behaviors: Visually guided behavioral choices 28
- 1.3.2 Optomotor response of zebrafish as visual discrimination task 30
- 1.3.3 Neural substrates of the optomotor response in the zebrafish 32
- 1.3.4 Aim1: Investigating the neural circuitry of visual whole-field motion discrimination 37

1.4 Background and introduction to aim 2: Monitoring neural activity with bioluminescence during natural behavior 38

- 1.4.1 Non imaging strategies 39
- 1.4.2 Aequorin as calcium indicator in neurons 40
- 1.4.3 Aim 2: Using bioluminescence to record from genetically specified neurons while monitoring behavior simultaneously 41

2 Materials and methods 43

2.1 Material and methods of aim 1 43

2.1.1 Zebrafish 43

2.1.2 Behavioral testing 43

2.1.3 Two photon Calcium imaging 44

2.1.4 Two photon laser ablation 45

2.1.5 Generation of transgenic zebrafish lines 46

2.2 Material and Methods of aim 2: 47

2.2.1 Zebrafish 47

2.2.2 Vector construction and transgenic lines 47

2.2.3 Aequorin reconstitution 48

2.2.4 Bioluminescence detection and behavior monitoring 48

2.2.5 *In vivo* two photon imaging 49

2.2.6 Single photon imaging 50

2.2.7 Bioluminescence detection during natural lighting 50

3 Results 52

3.1 Results of aim 1: Neural circuitry underlying whole-field motion discrimination in larval zebrafish 52

3.1.1 Behavioral responses to monocular whole-field motion in freely swimming zebrafish 52

3.1.2 Behavioral responses to monocular motion in head restrained zebrafish 60

3.1.3 Neural responses to monocular motion stimulation 62

3.1.4 Neural responses of hindbrain spinal projection neurons reflect the behavior 63

3.1.5 Generation and evaluation of pan neuronal transgenic lines 65

3.1.6 Neural responses of retinal ganglion arborization fields reflect sensory information 67

3.1.7 Neural responses of pretectal neurons resemble the behavior 71

3.1.8 Laser ablations of functionally identified neural structures 77

3.1.9 Comparison of behavioral responses and neural correlates 82

3.2 Results of aim 2: Monitoring neural activity with bioluminescence during natural behavior 84

3.2.1 Neuroluminescence reports neural activity in freely behaving zebrafish 84

3.2.2 Monitoring neuroluminescence in genetically targeted neurons 97

3.2.3 Aequorin responses in serotonergic neurons 108

3.2.4 Monitoring neuroluminescence during visual behavior 111

4 Discussion 113
4.1 General discussion 113
4.1.1 General significance 113
4.1.2 Methodological considerations for using larval zebrafish in the investigation of neural circuits 115
4.1.3 Progress in understanding the neural circuitry of larval zebrafish 117
4.2 Specific discussion of aim 1: Neural circuitry of visual whole-field motion discrimination 119
4.2.1 Psychophysics and neural circuit identification 119
4.2.2 Components of the zebrafish motion discrimination circuit 121
4.2.3 Comparison to other motion discrimination neural circuitry 124
4.2.4 Conclusion and future directions for aim 1 126
4.3 Specific discussion of Aim 2: Monitoring neural activity with bioluminescence during natural behavior 128
4.3.1 The relation between neuroluminescence and neural activity 128
4.3.2 Correlation of bioluminescence signals with locomotion 130
4.3.3 Investigation of neural circuits with neuroluminescence 132
4.3.4 Optogenetics and neuroluminescence 133
4.3.5 Conclusion and future directions of aim 2 133
4.4 Conclusion 135
5 Contributions and acknowledgements 136
5.1 Aim 1 136
5.2 Aim 2 136
6 References 137
Curriculum Vitae 144
Ehrenwörtliche Versicherung und Erklärung 148

ACKNOWLEDGMENTS

First and foremost, I would like to thank Dr. Oliver Griesbeck, Dr. Florian Engert and Dr. Alexander Borst for the opportunity to do the research that led to this thesis. I am immensely grateful for their continuous support of my graduate studies at the Max Planck Institute for Neurobiology, Munich and the Molecular Cellullar Biology Department at Harvard University. Besides my advisors, I would like to thank my 'Prüfungskommission' for their willingness to read the following (now) 150 odd pages of my dissertation.

In particular, I would like to thank Dr. Oliver Griesbeck and Dr. Alexander Borst for their patience, motivation, advice and sharing of their immense knowledge, especially during my first year which I spent at the MPI. It was my honor to be part of their vibrant scientific laboratories and to participate in their insightful lab meetings. Although my project could not be finished in time, this training period was invaluable for the following years of my graduate career. Specifically, I also would like to thank many of the excellent researchers at the MPI for their scientific help and support and their cheerful presence: Dr. Marco Mank and Dr. Michael Friedrich for their help and advice about genetically encoded optical probes and molecular biology. Dr. Yong Choe and Dr. Corette Wierenga for their priceless advice about patch clamp recordings. Furthermore, I would like to thank the whole group of Dr. Frank Bradke, in particular Liane Breyn and Dr. Susana Gomis-Ruet for sharing their knowledge and spectacular hippocampal cell cultures with me. In general, I wish to thank the MPI researchers of the Borst and Bonhoeffer laboratories for both insightful scientific conversation and their pleasant company. Specifically, it was my pleasure to get to know and become friends with Dr. Virginia Flanigin, Dr. T. Gaborsian, Dr. Sonja Hofer, Dr. Mark Huebener, Dr. Miriam Mann and many others.

For my time in Cambridge, I owe my deepest gratitude to Dr. Florian Engert, whose enthusiasm for scientific endeavors and everything else, encouragement, guidance and support on so many levels leaves me speechless. Even if I would find the right words, it would fill more pages than anybody would be willing to read. For the last four years of my graduate life, I could not have imagined a better advisor, mentor and friend. Thanks!

I would like to thank my collaborators in the Engert and Schier laboratories for all their scientific and non scientific support. In particular, it was my absolute pleasure to work very closely with Dr. Adam Kampff. I would like to thank him for his collaboration on a seemingly

impossible project[1] and sleepless nights we were working together to make the brain of zebrafish glow, for the endless stream of information about computer science and optics and the design and construction of the two-photon laser scanning microscope that was used for many of the experiments presented in this thesis. I am grateful for many insightful discussions, help and their gracious sharing of resources to my collaborators on different transgenic zebrafish lines, Dr. Alex Schier, Dr. David Prober, Dr. Michael Orger, Jen Li, Drew Robson and Dr. Adam Douglass. Next to their scientific support and advice I would like to thank many of the brilliant minds of the Engert, Schier, Murthy, Meister, Maniatis and Ölveczky and other laboratories that made my life fun and the slow days of the scientific drudgery bearable. In particular, I also would like to thank my female scientist friends Dr. Polina Kehayova, Dr. Nadine Vastenhouw, Dr. Wen-ye Choi, Dr. Rebecca Vislay, Dr. Jamila Newton, Kristin Severi and Annie Wang for being so inspiring. I thank Dr. Dinu Florin Albeanu for chats about thesis titles.

Moreover, I would like to thank the professors that gave me the opportunity to work for them as a teaching fellow: Dr. Florian Engert, Dr. John Dowling, Dr. Mark Hauser, Dr. Alan Viel, Dr. Naoshige Uchida, Dr. Bence Ölveczky and Dr. Naomi Pierce. It was an immensely enriching experience and I am particularly grateful to my advisor Dr. Florian Engert that let me have it.

Furthermore, unless mentioned above, I would like to thank all my friends (those that were smart enough not to embark on this lengthy quest for an academic title -perhaps wisely so- and those that did or will). Thanks for just being and also forgiving me whenever I was only ‘just’ on time; to name just a very few: Anna Huber, Dr. Veronika Huber, Dr. Roland Puettmann-Holgado, Dr. Fabia Mueller-Groh, Myriam Darmstaedter and Anja Lueckenkemper .

Last, but not the least I would like to thank my family: my mother Regine Naumann for her endless efforts, support and patience. I am grateful to my siblings, Olaf, Lena, Sven, Agnes and Christian and my father Nils Naumann for enormous enrichment throughout childhood and their friendship and help over all those years. In particular, I would like to thank my brother Olaf who always encouraged and supported me in so many ways. Danke! Likewise, I hope to be able to express my gratitude to my uncle Dr. Hermann Schwarz, his wife Maren and my grandmother Dr. Marlene Schwarz (although I never met her) for their inspiration throughout my life.

Thanks, zebrafish! Thanks, reader!

SUMMARY

Neurons collaborate to give rise to the brain's diverse functions. Their interactions generate the astonishing repertoire of behaviors that distinguish animals from inanimate objects. These behaviors result from information processing carried out within the brain's neural circuits. The first goal of this dissertation is to describe a strategy for identifying the neurons that participate in neural circuits underlying specific behaviors. Implementing this strategy, I next report the results of an investigation of a neural circuit involved in simple sensory motor transformation. To complement a noted limitation of the circuit identification strategy, I also developed a new technique that was used to study the elements of a neural circuit important for the regulation of resting and spontaneous behaviors. For all of these studies, I have utilized the larval zebrafish as a model system. The zebrafish offers a fortunate combination of useful properties: translucence, genetic accessibility and easily quantifiable behaviors. When combined with behavior analysis, the zebrafish represents a powerful model for the study of systems neuroscience.

In the introduction, I will first discuss generally investigations of neural circuits as well as the larval zebrafish as a neuroscience model system. I then review some of the relevant tools that can be combined in an experimental strategy for studying the neural basis of natural behaviors and the underlying neural circuits of the zebrafish brain. Using these available tools, I next outline a strategy to identify and investigate the neural circuitry underlying specific behaviors of the larval zebrafish. The two aims of this thesis are: 1. The implementation of an experimental strategy that uses behavioral analysis and functional whole brain imaging in transgenic zebrafish expressing genetically encoded Ca^{2+}-indicators to study the motion discrimination neural circuitry guiding the optomotor response. 2. The development of a novel technique employing bioluminescence to monitor neural activity from genetically identified candidate neurons in freely swimming zebrafish, which allows assessing the role of distinct neural circuits in the execution of specific behaviors. Although both these aims share the goal of investigating neural circuits, their specific questions, implementation, and background are quite different and will be introduced in separate sub sections of the introduction.

In the results section, I report on experiments performed for aim 1 that successfully revealed putative components of a neural circuit that discriminates whole field motion and translates this information into appropriate behaviors. I developed a visual behavioral assay for larval zebrafish that uses the optomotor response (OMR) as a discrimination task, and tested

whether unambiguous and ambiguous stimuli differentially affect directed turns. Unambiguous whole field motion stimuli evoked consistent behavioral responses, directed turns in the stimulus direction, and drove neural activity in a subset of spinal cord projection neurons of the hindbrain. However, when presented with monocular or ambiguous (conflicting) motion stimuli, both the behavior and neural activity provided new insight into how the visual input is translated into behavior. Interestingly, monocular inward motion (lateral to medial) was able to evoke a rate of directed turning similar to the rate elicited by unambiguous whole field motion, whereas monocular outward (medial to lateral) stimuli caused very few directed turns. Furthermore, while any stimulus containing monocular inward motion drove increased locomotion, monocular outward motion only directionally biased spontaneous locomotion and even suppressed the spontaneous rate of locomotion altogether. Notably, the conflicting binocular inward stimuli did not evoke bistable behavioral responses, demonstrated by the reduced number of large angle turns to either side. I next identified neuronal populations that exhibited activity related to each stimulus condition, with single cell resolution, throughout the brain of transgenic zebrafish expressing a Ca^{2+}-reporter, GCaMP2, using *in vivo* two photon microscopy. With this method, I could identify a retino-recipient arbourization field (AF6) that is the likely site of entry for the relevant whole field visual motion information, which I could confirm by laser ablations. Furthermore, neurons in the pretectum were found to combine inward and outward information from either eye, suggesting its role as the combining processing stage of the sensory information. Such response properties could arise by specifically connecting to different direction selective retinal ganglion cells, which is supported by the finding that AF6 is segregated into inward and outward responsive regions. Furthermore, the neural activity in these pretectal neurons strongly resembles the behavior and therefore may directly activate hindbrain neurons known to send the motor command to the spinal cord that controls directed turns. From these results, I present a “working model” for the complete visual whole field motion discrimination circuit of the zebrafish brain.

In the result section for aim two, I describe a novel technique that I developed to monitor neuronal activity in freely swimming zebrafish. Existing techniques for monitoring neural activity in awake, freely behaving vertebrates are invasive and difficult to target to genetically identified neurons. I utilized bioluminescence to non-invasively monitor the activity of genetically specified neurons in freely behaving zebrafish. The photoprotein GFP-apoAequorin (Ga) was expressed in neurons of larval zebrafish and constituted *in vivo* with its substrate coelenterazine (CLZN) to form the Ca^{2+}-sensitive bioluminescent sensor GFP-Aequorin (GA).

After 24hour exposure to CLZN, flashes of luminescence were detected that reported spontaneous and evoked Ca^{2+} signals from targeted neurons. These 'neuroluminescence' responses were recorded with a large-area photon-counting detector while simultaneously monitoring behavior with an infrared-sensitive camera. Transgenic fish, in which the neuro-β-tubulin promoter (Nβt) drives expression of GA in most neurons, produced large and fast neuroluminescent signals that could be recorded continuously for many days. To test the limits of this technique, GA was specifically targeted to the hypocretin-positive neurons of the hypothalamus. I found that neuroluminescence generated by this group of ~20 neurons was associated with periods of increased locomotor activity and identified two classes of neural activity corresponding to distinct swim latencies. To overcome a major limitation of existing bioluminescence monitoring strategies, which require a completely dark environment, I developed and tested a method for fast temporal gating of the detector that is able to count single photons during normal lighting conditions. Furthermore, I have begun to use this technology to study a small population of serotonergic neurons during prey capture. Thus, this neuroluminescence assay can report, with high temporal resolution and stability, the activity of small subsets of neurons during unrestrained, visual behavior. This technique holds great potential in its application to other neuroscience models, such as *Drosophila* larvae or *C.elegans*, as an alternative strategy to study neuronal circuits and behavior.

Finally, I examine how the presented results can be generalized to extend current strategies for investigating the neural circuitry underlying zebrafish behaviors. A combination of the different techniques used, developed and reviewed in this thesis presents a powerful method for unraveling the neural circuitry that zebrafish use to perform simple behaviors. However, many insights and conclusions can already be gained from this level of neural circuit investigation within larval zebrafish; some limitations of the system and future directions will also be discussed. Following this general discussion is a more specific discussion of the results from aim 1 and aim 2, which provides more focused interpretations and evaluations of the associated experimental results. In conclusion, I demonstrate that the strategy described in the introduction of this dissertation promises an unprecedented understanding of vertebrate brain function at the cellular level of neural circuits, exemplified by the knowledge gained about the whole-field motion discrimination circuitry and the development of the neuroluminescence assay.

1 INTRODUCTION

1.1 THE INVESTIGATION OF NEURAL CIRCUITS

1.1.1 MOTIVATION

Modern neuroscience is divided into many sub-fields and many different motivations drive investigations of the nervous system. A full understanding of the development, function and failure of (human) brains will require a multi-level approach. Studies of the molecular components, physiological properties, anatomy and psychological and behavioral phenomena will all contribute to our comprehension. My personal interest is to understand how information is processed in vertebrate brains, at the level of single neurons that are arranged into specific neural circuits. As there are few examples of well characterized neural circuits, I started by developing a strategy to identify and investigate the neural circuitry underlying “simple” behaviors. The first important step in this strategy was the choice of an appropriate model system. The zebrafish has a rich behavioral repertoire, is optically accessible, small in size, and has numerous available molecular and genetic tools; these impressive benefits can be combined to develop a complete approach to the investigation of neural circuits. In the following, I describe how investigations of neural circuits can contribute to understanding information processing within the brain and then review why the larval zebrafish is suited for this level of circuit investigation. Given these methodological considerations, I will then present a strategy to identify and study the components of neural circuits in the larval zebrafish.

Readers familiar with this model system and the technical methods may prefer to skip directly to the introduction sections 1.3 (which introduces the optomotor response and underlying neural circuitry together with the results in section 3.1 as an implementation of the outlined experiment strategy) and 1.4 (introducing the considerations and problems of recording from freely behaving animals and introduces the background and technical details of a solution to one of the strategy’s major limitations presented in 3.2)[1].

1.1.2 NEURAL CIRCUITS

Animal behavior is generated by the animal’s nervous system, a collection of discrete cellular units called neurons. These neurons function together to sense the animal’s environment, extract relevant determinants, store information and generate appropriate immediate and future behaviors. In many cases, neurons are specifically connected with other neurons to form circuits that accomplish specific tasks. Knowing what these neural circuits are, and how they work, is essential to understanding how the brain processes sensory information and generates the motor commands that allow the animal to survive and reproduce. If we can identify and understand multiple neural circuits, we will be in a position to extract general principles of brain function, and ultimately, to model the neural computations underlying behavior[i].

The foundational idea that the brain is the seat of cognitive processes is very young[ii]. Still younger is the realization that different mental processes may be localized in different brain structures (Figure 1.1a). However, especially in the last century, evidence has accumulated in favor of this ‘localized’ brain theory: the intriguing case of *Phineas Gage*, who’s specific loss of prefrontal cortex led to distinct personality changes[4], famous lesions in the left brain hemisphere incapacitating language faculties [5], damage to a portion of temporal medial cortex eliminating the ability to form new memories[6], and many other examples support, at least, a coarse functional partitioning of the brain. However, in the last century, neuroscience was revolutionized by the finding that the brain is composed of cellular units that process and exchange information: neurons (Figure1.1b). With the development of techniques to record the activity from single neurons, specific brain structures have been associated with many different aspects of sensory motor processing, and have even been shown to be responsive for more “abstract” phenomena, such as subjective perception[7,8], valuation[9], and intention[10]. However, it can be dangerous to mistake the mapping of active brain locations with an understanding of neural processing. To understand the brain’s function, it is necessary to investigate the brain at the level of single neurons and identify neural circuits, the interconnected cellular pathways that integrate sensory information and execute behaviors. To achieve such an understanding, single neurons must first be identified that participate in these dedicated neural circuits. Subsequent experiments could then focus on gaining insight into their function and attempt to predict (model) the neural processes implemented by the circuit.

---

[i] Whether this is possible, and even whether a human brain can ever understand a human brain, is an interesting discussion.

[ii] The first modern investigation of the brain, which begins the transition into the modern ‘neurocentric age’, was performed by Thomas Willis in Beam Hall in Oxford, England [2]. With the dissection of brains belonging to convicts, he and his colleagues introduced the fundamental idea that our mind is nothing other than biochemical processes in neural tissue. Then 300 years later, the German physician Franz Joseph Gall developed ‘phrenology’ (Greek: *phrēn*, "mind"; and *logos* "knowledge"), a theory stating that certain brain regions have localized specific functions or even modules. This popular discipline was based on the concept that the brain, as the organ of the mind, was believed to be partitioned into different brain areas dedicated to various mental faculties. Today, much of phrenology is recognized as pseudoscience, but it certainly influenced the development of modern neuroscience [3].

Attempts to investigate *simple* neural circuits have been very successful in identifying the neural components and their function, i.e. the stomatogastric ganglion[11-13] or the spinal monosynaptic reflex circuitry (knee jerk reflex)[14]. So far, the progress towards understanding more complex neural circuits (e.g. a ‘simple’ cortical column) has been very slow. Notable exceptions have all benefited from the fact that a quantifiable, robust behavior is known to be controlled by the circuit in question, i.e. the vestibulo ocular reflex (VOR)[15,16], parts of the cerebellar neural circuitry[17] and the jamming avoidance reflex (JAR) in weakly electric fish (Figure 1.1c, d)[18]. Therefore, I propose that investigations of neural circuits should be carried out with an emphasis on a specific behavior and, preferably, in organisms that possess a readily accessible nervous system to allow the investigation on the level of single neurons.

Figure 1.1

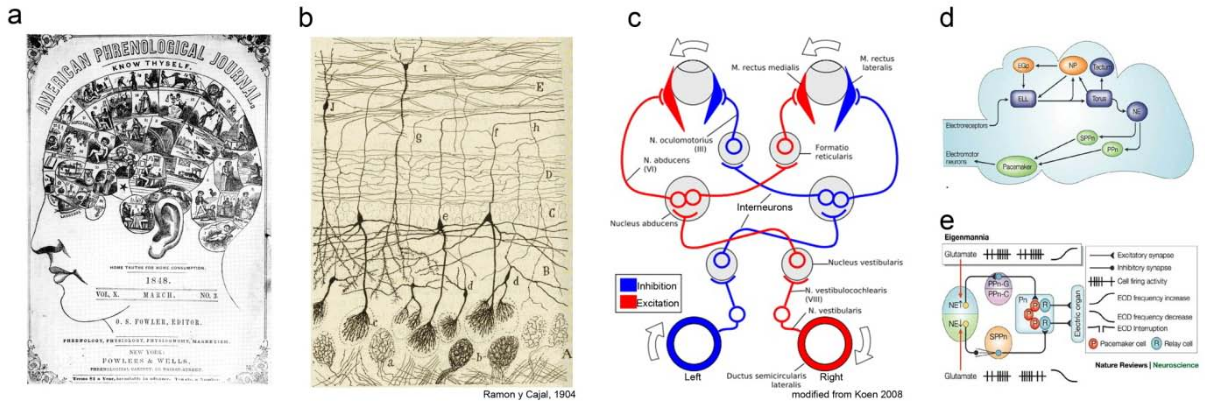
a
b
c
d
e
AMERICAN PHRENOLOGICAL JOURNAL
KNOW THYSELF.
1848.
O. S. FOWLER, EDITOR.
M. rectus medialis
M. rectus lateralis
N. oculomotorius (III)
N. abducens (VI)
Formatio reticularis
Interneurons
Nucleus abducens
Nucleus vestibularis
N. vestibulocochlearis (VIII)
N. vestibularis
Inhibition
Excitation
Left
Ductus semicircularis lateralis
Right
Electroreceptors
Electromotor neurons
ELL
Torus
Tectum
NP
NE
SPPn
PPn
Pacemaker
Eigenmannia
Glutamate
PPn-G
PPn-C
Electric organ
Excitatory synapse
Inhibitory synapse
Cell firing activity
EOD frequency increase
EOD frequency decrease
EOD interruption
Pacemaker cell
Relay cell
Nature Reviews | Neuroscience

Ramon y Cajal, 1904

modified from Koen 2008

Figure 1.1 - Neural circuits: **a** Cover of the American Phrenology Journal, VolumeX, March 1848, conveying the then popular idea that brain function was spatially localized. **b** Drawing by Ramon y Cajal of a portion of the cat brain that illustrates that the nervous system is made of single cellular units (neuron doctrine) **c** Schematic depiction of the neural circuit underlying the vestibular ocular reflex: If rotation is detected in the *ductus semicircularis*, a compensating eye movement is evoked by excitation of extraocular muscles on the contralateral side and inhibition of those on the ipsilateral side. **d** Organization of the weakly electric fish brain highlighting the brain nuclei that are involved in the detection and modulation of electric organ discharge. **e** A more detailed schematic of the neural circuitry that controls the modulation of the frequency of the electric organ discharge during the jamming avoidance response (JAR)[18].

1.1.3 NEUROETHOLOGICAL APPROACH TO THE INVESTIGATION OF NEURAL CIRCUITS

How can we identify neurons that participate in distinct neural circuits governing animal behaviors? One possibility is to focus on the neurons whose activity is associated with a particular, well-understood behavior; a strategy that could be called the "neuroethological approach" to neural circuit identification. Ethologists, such as Max von Frisch, Konrad Lorenz and Nicholas Tinbergen, argued that the behavior of different animals is intrinsically different due to different natural ecology and unique evolutionary history[19]. One of their main contributions to the understanding of animal behavior is that certain stimuli are able to reliably evoke specific behaviors. These specific stimuli are often called 'trigger' or 'releasing' stimuli, since they trigger a behavioral sequence of actions (or 'fixed action pattern')[20]. If such a stimulus can trigger a behavior, it is a required that the brain must not only have the necessary sensory equipment to detect the behaviorally relevant stimulus, but also the processing power to evaluate and then translate the information into a motor command that initiates the muscle contractions that constitute the behavior. This knowledge can direct investigations of the brain, as a 'trigger' stimulus will be a powerful tool for identifying dedicated neuronal circuitry, which begins with the sensory input and ends with the motor output. In the ideal experimental situation, it would be possible to present such a stimulus and monitor the activity of every single neuron, or even every individual synapses, throughout the entire nervous system while the brain is processing the information and, eventually, performing the behavior[iii]. This specific stimulus dependent activity would isolate the putative circuit components, those that could be responsible for controlling the triggered behavior. However, even with an identified neural substrate, often the details of circuit function are not accessible. Ethologists, by varying the trigger stimulus, could determine not only the most salient stimulus components but also design stimuli that were even stronger than a naturally occurring stimulus (a supernormal stimulus). They also found that small changes to a stimulus would sometimes eliminate or specifically alter the behavioral response[21,20]. Probing the nervous system with variations of the 'trigger' stimuli provides a powerful framework for studying the specific neural activation that leads to the behavioral output. Combining a stimulus that can trigger a specific behavior with different methods of anatomical mapping, neuronal recordings and manipulations of single or groups of functionally similar neurons *in vivo* provides a holistic approach to the investigation of neural circuits; a neuroethological approach. However, this approach's success will require an appropriate model organism, one that allows the necessary recordings and manipulations.

[iii] If such a dream preparation existed, one could simply "read out" information about whether, how and when, during the time course of the processing and execution phase, a neuron was activated or inhibited.

1.1.4 CRITERIA FOR CHOOSING A PREPARATION FOR NEURAL CIRCUIT INVESTIGATIONS

The decision to use a particular animal preparation to study neural circuits should depend on the currently available technologies to investigate the brain. Another criteria, however, is finding a model system that displays behaviors that are of interest. For humans, and funding agencies, behaviors related to their own behaviors, or that of their close evolutionary relatives, are often the most interesting. For this reason, it is useful to study animals that exhibit such behaviors. Furthermore, focusing on specific behaviors that are important for many species would be preferred, as the underlying neural circuitry dedicated to such a behavior might reveal a specific neural solution to a general problem, one that must be solved by most, if not all, brains. In this regard, rodents have been useful for understanding diverse mammalian brain processes, determining which brain regions are involved in different behavioral processes, i.e. fear, stress, learning and memory [22]. However, neuroscience also has benefited tremendously from less complex model organisms, like the invertebrates *Drosophila melanogaster,* the nematode *Caenorhabditis elegans* or marine mollusk, *Aplysia californica*. They have served admirably as model organism to understand the genetic and molecular basis of different behaviors and in particular memory formation at the synaptic level[22]. However, shedding light on the function of vertebrate brains, which includes the colossal human brain, will require the investigation of a potentially more complex, vertebrate preparation. From mice[23,24], barn owls[25], via electric fish[26], to gerbils[27] and zebrafinches[28], a variety of different vertebrate models have emerged and provided insight into different neural computations that produce very specific behaviors. However, each model organism comes with its own advantages and disadvantages. As the ideal investigation of vertebrate neural circuits requires the study of single or groups of functionally similar neurons involved in specific behaviors, the ability to easily record from the entire, intact brain, is a very daunting task[iv]. In the following, I will explain the virtues of a particularly well suited model organism in systems neuroscience, the larval zebrafish[29-32].

[iv] This complexity is particularly overwhelming when one considers the estimated 100 billion neurons of the human brain.

1.2 THE LARVAL ZEBRAFISH: A TRANSLUCENT VERTEBRATE BRAIN

1.2.1 THE ZEBRAFISH IN BIOLOGICAL RESEARCH

The zebrafish (*Danio rerio*) is a small freshwater teleost native to the rice patties and rivers of India (Figure 1.2). George Streisinger[33] at the University of Oregon established its utility as a model organism, and it has since developed into a popular and successful preparation for studies of vertebrate development and gene function [34]. Few other vertebrate organisms can offer a similar wealth of information and technologies for scientific inquiry. Although, zebrafish still largely supplement, rather than preclude, research on other vertebrate models, e.g. mice and rats. Its attractive characteristics have allowed a new community of researchers to expand rapidly. The zebrafish's advantages include the following: a fully sequenced genome and annotated gene data base, rapid embryonic development *ex utero*, easy breeding of large numbers, robust health in captivity, body translucence, availability of mutants, well described, easily observable behaviors early in development, and numerous other features that make it a good laboratory model organism. As small vertebrates, they serve as the model of choice for research on gene networks, regeneration and development and even many developmental and neurodegenerative disorders. Given the small size and permissible skin of the zebrafish embryo, compounds can be simply added to the water, and their affect on hundreds of embryos analyzed[35]. High throughput drug screens can identify molecules with therapeutic potential. For pharmacological research, this is not only a fast and cost effective alternative to widely used rodent models, but is also more ethically acceptable to the public interest.

What really brought the zebrafish its fame, were the large scale forward genetic screens that were particularly successful for identifying genes involved in developmental processes; the generation of germ layers, organ systems, neural[36] and vascular architecture[37]. These impressive experiments involve the characterization of a particular phenotype in fish that were previously treated with a mutagen, and then identifying the gene mutation(s) that caused this change. Fortunately, the Zebrafish Information Network (ZFIN) is organizing resulting data concerning the genetic, genomic and developmental information gleaned from these screens. Together with the development of many complementary techniques, such as imaging[38-40] and novel behavioral assays[41,42], our knowledge of the relationship between genes and phenotypes has increased remarkably. Due to the similarity between human and zebrafish genetics, many of the insights gained from these studies can be expected to apply to humans. Also, given the ongoing development of technologies for transgenesis[43], gene expression analysis, and proteomics, the zebrafish will surely continue to contribute to our understanding of gene regulation networks. New molecular tools coupled to advances in modern microscopy, also promise new the qualitative and quantitative insights into the molecular and cellular processes underlying vertebrate development. Zebrafish have already contributed greatly to our understanding of many different aspects of vertebrate biology. More recently, they have also attracted the interest of neuroscientists.

Figure 1.2

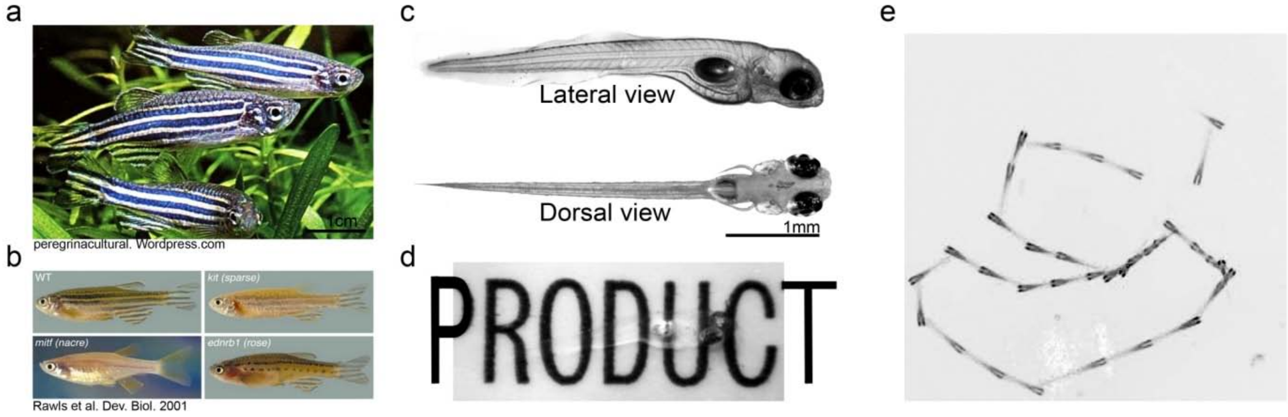

peregrinacultural. Wordpress.com

Rawls et al. Dev. Biol. 2001

Figure 1.2 - Zebrafish: **a** Wild type adult female and male zebrafish (*Dario rerio*). **b** Adult zebrafish strains with pigmentation mutations. **c** Lateral and dorsal view of a nacre zebrafish larva at 6 days post fertilization (dpf). Although the eyes retain normal pigmentation, the body is completely clear. **d** 6 dpf nacre larva embedded in low melting agarose and placed *above* a background with printed text. The larva is so translucent that it is possible to read through the animal. **e** A projection through time of a 10 second movie of a freely swimming zebrafish. Zebrafish larvae swim in discrete bursts, demonstrated by the fact that instead of forming a continuous trace of their body outline, distinct images of their body are visible in the projection.

1.2.2 BENEFITS FOR LARVAL ZEBRAFISH FOR NEURAL CIRCUIT MAPPING

Zebrafish are an emerging model organism in systems neuroscience and have become increasingly popular for many different investigations of vertebrate neural function, ranging from motor control[44] to perceptual memory[45]. In contrast to other small neuroscience model organisms, such as *Drosophila* or *C.elegans,* zebrafish neurotransmitter and receptor systems are very similar to their mammalian counterparts[34]. This similarity promises that findings will better translate, and perhaps facilitate general insights about the vertebrate nervous system.

Admittedly, some neuroscientific questions, such as the role of cortical structures in cognition and learning, cannot be studied in zebrafish, since some structures are not readily evident or even clearly existent. However, the zebrafish offers a unique opportunity to study the evolutionary old vertebrate brain, from which many structures have clear homologues in today's human brain, and to use techniques that are otherwise only available for invertebrates.

Importantly, larval zebrafish show many behaviors at the earliest larval stages when they are mostly translucent, and thus the same technologies developed for investigations of development and gene regulation networks will directly benefit the analysis of the developing nervous system. Arguably, the most useful tool for the dissection of neural circuits is the use of transgenic animals that express a reporter gene in specific neurons[46,23]. In the translucent zebrafish brain, many transgenes can be used to visualize, investigate and manipulate the elements of distinct neural circuits[46]. However, until recently, the generation of DNA constructs with the desired promoter and reporter elements required a lot of time and effort, but now many tricks are available that have made this process easier and faster. In addition, transposon-mediated methods for transgenesis have greatly simplified the generation of transgenic zebrafish[47], which was previously the slowest step in the generation of stable transgenic lines. The diagram in Figure 1.3 shows how stable transgenic lines can be generated by microinjection of DNA into the one cell stage. Although the specificity of tissue or celltype-specific promoters to target reporter genes is still a challenge, many useful zebrafish promoter elements have been isolated and ongoing research in mechanisms of expression promises further improvement[48-50]. With the current and future promoters, an explosion of various colored fluorescent proteins allows visualizing neuronal morphology. In addition, many types of genetically encoded optical tools can be inserted into the desired neuronal population. These technologies make possible the mapping, monitoring and controlling of neural activity, within an intact zebrafish, using light.

Since light can penetrate the translucent brain of the zebrafish easily, this model organism benefits directly from developments in modern microscopy. For many applications and simple fish screening, excitation light can be easily delivered to the zebrafish with wide field illumination. To achieve optical sectioning however, confocal or two-photon microscopy is necessary. The optical sectioning effect of a confocal configuration is achieved by spatial filtering of all emission light that is not generated at the focal plane, however, neural tissue above and below are still excited by the laser illumination. With two photon microscopy, the optical sectioning is intrinsic to the excitation process: ultra fast pulses of infrared light will only excite fluorophores contained in a very small volume at the beam focus. In addition to improving depth penetration (by using infrared excitation), minimizing out-of-focal-plane photo bleaching and photo toxicity, the infrared light is conveniently invisible to the zebrafish, which allows simultaneous visual stimulation while avoiding the unwanted behavioral effects arising from the intense excitation light. These advantages have been routinely exploited for imaging of visually evoked neural activity in the zebrafish[51-53]

Even for these impressive optical techniques, pigmentation still poses a problem as it prevents light penetration and causes phototoxic heating. Complete transparency is necessary for a detailed visualization of the development and function of the entire nervous system in the living animal. Fortunately for neuroscientists, a zebrafish pigment mutant, which lacks the expression of the nacre gene (nacre-/-)[54], does not produce any melanophores throughout its body, but retains eye pigmentation and normal visual behaviors[55], thus making them particularly well suited for imaging studies and (for more subtle reasons discussed below) behavioral analysis.

Figure 1.3

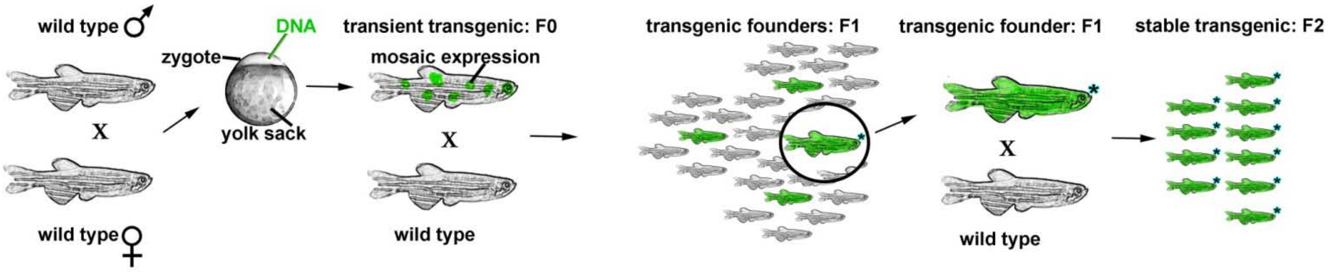

Figure 1.3 - Generation of stable transgenic zebrafish: Wild type female and male zebrafish are mated and eggs collected 5-10 minutes post fertilization. DNA constructs that contain fish specific promoter elements upstream of the reporter gene of interest (green), which drive expression within specific cell types, are injected into the single cell (zygote). This cell will divide and grow into an embryo that expresses the gene of interest ectopically, in a mosaic fashion, in some cells that contain the DNA and posses the necessary transcription profile to activate the promoter. Fish with expression are selected and raised to adulthood. These potential founders (F0) are then out crossed to wild typed fish. Offspring (F1) that have integrated the promoter and reporter gene into their genome, at a position such that the desired expression is achieved (*), are again raised to adulthood. These fish are the transgenic founders of the stable line; all share the same positional integration of the transgene.

1.2.3 BEHAVIORAL PARADIGMS IN LARVAL ZEBRAFISH: WHAT BEHAVIOR TO STUDY?

General principles of neural circuits are more likely to be gleaned from studying a behavior common to many species. Such behaviors will likely address problems that many animals must solve and, therefore, the neural implementation is potentially of broad relevance. Some visual behaviors are displayed across taxa, from insects to humans, such as the optokinetic (OKR) and optomotor responses (OMR) to global motion of the visual scene [56]. Both behaviors can be easily studied in the larval zebrafish[57,58,34,59]. The OKR is a visually evoked sweeping of the eyes following a horizontally moving visual stimulus, with occasionally saccades back to a starting position, thus beginning another stimulus tracking. Whereas the OKR is only concerned with the visually induced motion of the eyes, the OMR describes a visually evoked locomotion behavior in which the fish reorients his body axis and swims in the direction of visual motion. Such a behavioral response would keep the fish, in its natural environment, stationary with respect to the external world. Importantly, the OMR can be elicited in immobilized zebrafish larvae, which are presented with whole field motion from below. The wild-type zebrafish OMR and OKR, and even mutations with anatomical phenotypes and deficits in these behaviors[60-62], have been described. However, the details of the underlying neural circuitry are still largely unknown.

Another particularly interesting behavior paradigm for the investigation of visual attraction and avoidance, is prey capture and predator escape. Zebrafish use vision to track and reorient towards moving prey prior to a capture attempt[63]. When presented with prey-like stimuli (small moving spots), zebrafish reliably reorient towards the stimulus, but will turn away from spots that are just a few angular degrees larger, possibly reflecting a visually-driven escape behavior. This behavior, despite its simplicity, represents a model for sensory motor transformation in appetitive and aversive behaviors[64]. Here, sensory information about a moving object must be detected, classified and neural signals transformed into appropriate motor commands. The necessity of high acuity vision and behavioral output has been characterized in detail[65,66]. Ablations of the tectum, and some other retino-recipient areas, as well as the fact that zebrafish cannot hunt in the dark, have suggested a prominent role for the optic tectum in prey capture [63,67].

In addition, many other behaviors have been described in larva and a number of more complex behaviors have been successfully studied in adult fish[68,69]. However, since adult zebrafish lose most of their translucence, develop a hard skull and require the gills to be perfused when immobilized, they are less amenable to imaging experiments. However, with improved protocols, many techniques could probably extend the period in which imaging experiments are feasible and thus allow exploiting the advantages the larval zebrafish is offering in older, juvenile animals. Extending the time window in which zebrafish can be used for imaging experiments is very promising for the investigation of neural circuits underlying more complex behaviors.

Unfortunately, there are also other limitations for imaging approaches to systems neuroscience questions with zebrafish. For example, the visual prey capture behavior is difficult to evoke, and thus study, in immobilized zebrafish larvae, which has held back the elucidation of the underlying neural circuitry. Similarly, many other behaviors cannot be studied in the immobilized or paralyzed preparation. Therefore it would be ideal if recordings could be done in freely behaving animals. In this case, again the zebrafish' translucence offers an optical solution. In the section 3.2 of this thesis, I report a new technique[1] for monitoring neural activity in free, unrestrained animals by measuring the light emission from a calcium dependent photoprotein (Aequorin)[70-72]. This technique provides an opportunity to study even more delicate behaviors, such as sleep and arousal. In particular, this technique allows investigating the neural activity of genetically identified neurons associated with particular behaviors. However, for the behaviors that do occur in immobilized zebrafish, mapping of the neural circuitry is possible with well established methods for functional imaging.

1.2.4 FUNCTIONAL IMAGING OF NEURAL ACTIVITY FOR NEURONAL CIRCUIT IDENTIFICATION

Circuit identification requires the ability to monitor the activity of individual neurons, ideally of all neurons, simultaneously during the presentation of stimuli and execution of behavior. Although electrophysiology represents a useful method to record from individual neurons in behaving animals, this is only useful if the putative components of a neural circuit are known and can be accurately targeted. For the task of identifying unknown circuit components, imaging techniques, which monitor the activity of populations of neurons, have proven very useful [73]. Since the translucent larval zebrafish brain allows complete, non-invasive optical access to every neuron in the live animal, it presents an ideal preparation for circuit identification with optical methods. Although any method that can optically monitor the activation state of neurons could be employed for circuit identification, monitoring calcium concentration in neurons has emerged as a well established and oft used method.

1.2.4.1 MEASURING NEURAL ACTIVITY WITH OPTICAL CALCIUM INDICATORS

The divalent calcium ion (Ca^{2+}) is a ubiquitous second messenger that is involved in the regulation of many cellular functions [74]. In particular, its strict regulation in neurons makes the measurement of physiological changes in Ca^{2+} informative: the arrival of an action potential (AP) triggers a large influx of Ca^{2+} ions through voltage-gated Ca^{2+} channels and neurotransmitter receptors located in dendritic processes. Since this modulation of intracellular Ca^{2+} is correlated with neural electrical activity, it is possible to predict the timing of spikes and patterns of synaptic events by observing neuronal Ca^{2+}[75].Thirty years ago, Roger Tsien[76] synthesized one of the most powerful tools to visualize Ca^{2+}, a fluorescent probe linked to the Ca^{2+} chelator BAPTA[v]. This class of reporters exhibited large, Ca^{2+}- dependent changes in fluorescence, fast kinetics, and high affinity and specificity for Ca^{2+} over other divalent cations. These synthetic dyes have been able to reliably report changes of intracellular Ca^{2+} associated with neural activity in many preparations, including zebrafish[77].

Loading a synthetic Ca^{2+} indicator into zebrafish neurons, however, has required the development of novel, often invasive strategies. For studies of neurons in the zebrafish hindbrain and spinal cord, neurons were “backfilled” with dextran-conjugated calcium green BAPTA by injecting the dye directly into the axons of the spinal cord[53,78,79]. Another successful loading strategy employed bolus loading with acetoxymethyl (AM) conjugated dyes, which readily permeate neuronal membranes, injected directly into the targeted brain region, such as the optic tectum[52,51,77,45].

1.2.4.2 GENETICALLY ENCODED CALCIUM INDICATORS

However, even when a tolerably invasive loading technique for synthetic dyes is available, chronically recording from the same cells is difficult and dyes cannot be targeted to specific cell types or sub cellular compartments. In contrast to synthetic indicators, genetically encoded calcium indicators (GECIs) can be stably expressed in neurons and targeted to specific cell types/sub cellular structures. Importantly, *any* temporal or spatial expression pattern can be mimicked by GECIs, if the reporter gene is driven by an appropriate promoter.

---

[v] Interestingly, the first optical measurements of intracellular [Ca2+] have been made by microinjection of bioluminescent proteins by Shimomura & Johnson in 1972.

With a GECI, it is possible to investigate a specified neuronal population, i.e. inhibitory or excitatory neurons, and measure neuronal Ca^{2+} repeatedly, over long periods of time.

GECIs are artificially designed proteins, consisting of natural amino acids encoded by recombinant DNA. Their relatively short, easily modifiable DNA sequences can be delivered, with various techniques, to the cell type in question. Once the GECI gene is expressed *in situ*, the protein sensor allows measuring intracellular Ca^{2+} with florescence imaging techniques. The general design of a GECI is as follows: a calcium-binding domain (Ca^{2+} sensor) is allosterically coupled to a fluorescent protein (reporter) element. In most GECIs, the calcium binding domain is a naturally evolved calcium binding protein with large Ca^{2+} -dependent conformational changes, such as calmodulin (CaM)[80] or troponin-C (TnC)[81]. There are two main classes of GECIs. They are either constructed of single fluorescent proteins or utilize Fluorescence/Förster Resonance Energy Transfer (FRET) protein donor–acceptor pairs. Single fluorescent protein sensors, typically a circularly permuted fluorescent protein, are altered by the conformational change initiated by the Ca^{2+} binding domain and thus local changes in Ca^{2+} can be visualized by measuring the emission of the GECI at a single wavelength. The most prominent single fluorophore sensor is GCaMP and its variants[82]. In contrast, FRET indicators consist of a Ca^{2+} binding domain sandwiched between a donor and an acceptor fluorescent protein, each with different excitation and emission wavelengths. For FRET sensors, the conformational change of the Ca^{2+} binding domain alters the FRET transfer efficiency between the donor–acceptor pair and thereby changes the ratio of emission between the two wavelengths; changes in Ca^{2+} are detected, ratiometrically, as reduced donor and increased acceptor emission. The ratiometric indicator TN-XXL has been used successfully used for demanding applications like *in vivo* two photon imaging of specific neurons in the fly visual system [83] and cortical neurons in the mouse[82].

GECIs are very promising, but thus far, they have been most successful for *in vivo* detection of strong neural activity and the detection of sparse spike train remains the field's greatest challenge[82,84]. Although reliable *in vivo* single spike detection is still difficult with available indicators, using GECIs to identify neurons that consistently show strong activation associated with a specific stimulus or behavior offers an excellent opportunity to identify the components of underlying neural circuits. The genetically tractable larval zebrafish, offering optical access to the entire brain, represents a near ideal model system for the use of GECIs in the identification and investigation of neural circuitry.

1.2.4.3 USING GENETICALLY ENCODED CA^{2+} INDICATORS IN ZEBRAFISH FOR CIRCUIT IDENTIFICATION

Recently, a transgenic zebrafish was generated that expressed an early form of Chameleon, a FRET-based GECI, in all (or almost all) neurons [85]. This quasi panneuronal expression was achieved with the HuC promoter, which drives the endogenous expression of the HuC gene, a specific marker for differentiated cells [48]. Given that every neuron in the larval zebrafish brain is optically accessible, monitoring the neural activity throughout the entire brain now appeared feasible, a possibility that will be further advanced with the development of transgenic, panneuronal zebrafish expressing improved GECIs. Functional imaging of the entire nervous is an excellent starting point for the identification of neural circuits, as, ideally, it can reveal the neurons whose activity is correlated with the stimulus or response characterizing a specific behavior. However, the role of these identified neural correlates must then be confirmed and evaluated using other methods that establish the necessity and/or sufficiency of these neurons for the circuit's function.

1.2.5 ESTABLISHING CAUSALITY BETWEEN BEHAVIOR AND NEURONS

Particularly for the translucent zebrafish, the development of genetically encoded optical tools for the control of membrane potential is quite promising, especially for studies of the sufficiency and necessity of neural populations for behavior[86]. Since the perturbations are reversible and can be controlled with high temporal resolution, they offer an opportunity to compare their behavioral effects on a trial by trial basis.

Recently, a receptor tethered glutamate mimic, photo activation method (LiGluR) was able to manipulate neural activity in zebrafish[31]. LiGluR is an ionotropic glutamate receptor of the AMPA type. With a modified cysteine close to the ligand binding site, this cysteine reacts with a synthetic tethered agonist, maleimide azobenzene glutamate (MAG), yielding a light-gated ion channel, LiGluR[87]. Excitation with UV light brings this tethered agonist into contact with ligand site and thus opens the channel. Influx of Na^+ ions through this channel lead to the depolarization of the neuron. Conveniently, this channel can be closed by illumination with blue light and can therefore be used as bistable switch. LiGluR has already been used in zebrafish to elucidate the function of specific spinal cord neurons identified in a Gal4 enhancer trap screen [31].

The activity in zebrafish neurons can also be manipulated with the light activated cation channel Channelrhodopsin-2(ChR2)[88]. Unlike invertebrate models, zebrafish do not require external addition of the all-trans retinal required for ChR2 activity. Fine temporal and spatial control over neural activity was demonstrated in zebrafish when ChR2 mediated activation of a single action potential, in a specific group of somatosensory neurons, reliably triggered escape behaviors in 24 hr old zebrafish.

To test the necessity of neurons, Halorhodopsin (NpHR), a light-activated chloride pump from the bacterium *Natronomas pharaonis*, can be used to hyperpolarize neurons exposed to yellow light. In zebrafish, NpHR has been used to link localized areas of the brain to some behavioral functions[89].

Permanently removing neurons has the advantage that there are no concerns about residual activity, which is possible with other temporal inactivation techniques, and thus provides a method for establishing whether the ablated neural component is necessary to execute a behavior. In zebrafish, there exist multiple molecular and physical techniques for permanently ablating neurons. Laser ablations, in combination with the labeling of specific neurons or their processes, can be accurately targeted to small regions of interest[53]. Increasing the incident laser light intensity results in the formation of localized plasma that is energetic enough to destroy single cells and disrupt neuropil regions[53,60]. The *Escherichia coli* enzyme nitroreductase (NTR) can molecularly ablate genetically specified neurons[90]. NTR converts a harmless substance into a potent cytotoxin, effectively killing cells expressing the substrate. This method has the advantage that many animals can be treated simultaneously. However, the targeting of ablation with NTR relies on the expression pattern, which often lacks the necessary specificity. A technique that circumvents this dilemma utilizes KillerRed, a fluorophore that releases cytotoxic reactive oxygen species when specifically illuminated with green light, otherwise harmless to non expressing cells[91]. Alternatively, Tetanus toxin light chain (TeTxLC) has also been successfully used in zebrafish to block synaptic exocytosis[92]. Applying any of the above techniques in the right context has the power to assess the causal role of neural components within a neural circuit.

1.2.6 STRATEGY TO INVESTIGATE NEURAL CIRCUITS IN LARVAL ZEBRAFISH

Incorporating available methods, I will now describe my strategy for investigating neural circuits. The work presented in this thesis represents the progress that was made, thus far, using such strategy. As emphasized previously, it was important that the behavior controlled by the investigated neural circuit be well described and the key variables quantifiable; this includes both a characterization of the stimulus space that can trigger the behavior as well as the motor response itself. Therefore, the first step to unravel the complex function of a neural circuit is to develop a detailed description of the behavior under study. Secondly, once such a behavior is characterized, neurons involved in this circuit must be identified. Such circuit component identification is possible by either measuring neural activity correlates in response to behaviorally relevant stimuli, or alternatively, measuring neural activity of specific candidate neurons during behavioral execution and/or in response to the same behaviorally relevant stimuli. During this step, the response properties of these circuit components must be determined which allows the prediction of their role within the circuitry. Third, the necessity and sufficiency of these neurons for the behavior must be established. Fourth, and finally, a full understanding of the neural circuit is completed when the acquired data from behavior, neural recordings, and knowledge of interconnections and cellular mechanisms of the neural components is integrated into a testable computational model of the circuit. In the following, I will briefly outline the general strategy that I used to investigate neural circuits in zebrafish.

Step 1: Identify, characterize, and quantify a specific behavior and trigger stimuli:

To identify and characterize different behaviorally relevant stimuli and their associated behaviors in zebrafish, one can draw from a wide repertoire of experimental paradigms. Once a behavior, and the stimulus (e.g. visual motion stimuli) that triggers the behavior, is identified, an assay must be developed to probe and quantify the behavioral events that is sufficiently detailed to assess the effects of stimulus variation as well as neural perturbations, such as ablation or stimulation.

Step 2: Identify circuit components by monitoring neural responses:

Monitoring neural responses to trigger stimuli: In order to identify neurons involved in a behavior with physiological methods, neural activity must be measured *in vivo,* ideally during the execution of the behavior in question. If this is not possible, neural activity should be monitored during the presentation of stimuli that trigger the behavior. Physiological measurements, such as single-cell recordings or functional imaging, can reveal which neural activity patterns are associated with the presentation of behaviorally relevant stimuli. Neurons that show activity changes in response to these relevant stimuli can be assumed as candidate circuit components. The advantages of the zebrafish suggest the use of functional imaging of GECIs, throughout the whole brain, to map regions activated by these specific stimuli. This part of the strategy is used in part one of the results section to elucidate visual motion discrimination circuitry that guides optomotor responses in the larval zebrafish.

Monitoring neural activity of candidate neurons during behavioral execution: To identify specific behaviors that are associated with neural activity of genetically identified candidate neurons, both should be measured simultaneously. Such correlations of neural activity and specific behaviors would similarly implicate these specific neurons in the responsible neural circuitry. Such approach is not only desirable, but absolutely necessary for behaviors that cannot be studied in restrained preparations (i.e. prey capture or sleep). Since no technique existed that would allow such recordings, I developed a technique that allows such recordings within freely swimming fish; this technique is presented as part two of the results section.

Step 3: Establishing a causal link between the correlated neurons and the behavior:

Historically, neural perturbation has been a powerful method to test whether a structure is necessary (inactivation) and or sufficient (activation) for a particular brain function. When paired with detailed behavioral analysis, temporal or permanent activation/inactivation of neuronal structures is able to identify components of the neural circuit underlying the behavior. If the ablation of neural activity in a neuron or population of neurons abolishes a specific behavior, these neurons are presumed necessary elements of this behavior's circuit. Sufficiency is claimed, if the stimulation of particular neurons can reliably evoke the behavior. Perhaps better than permanent ablations, reversible control over membrane potential with genetically encoded methods allow establishing neurons' necessity (NpHR) and sufficiency (LiGluR and CHR2) on a trial by trial basis.

Step 4: Integration of available information to develop circuit models:

By collecting, organizing and evaluating the behavioral, anatomical and physiological data available for a putative neural circuit, a model can be developed. Even simple computational models, with testable predictions about neural activity and behavioral outcomes, can provide a useful descriptor of the neuronal processing within the circuit and an important tool to evaluate our current level of understanding. Successful models should not only be able to explain the circuit itself, but contribute to a general understanding about how information is processed by nervous system. We can then compare it with other systems and address the evolutionary history that allowed brains to gain such a diversity of function. Understanding several different implementations, for comparison, may ultimately reveal which features of these brain circuits are essential and which are specific to each particular implementation.

1.2.7 SPECIFIC AIMS OF THE DISSERTATION

To understand the brain's function, the study of functional cellular components of neural circuits is a fundamentally important level of investigation. Zebrafish offer great biological and technical advantages for studies seeking to anatomically and functionally describe the circuitry involved in vertebrate behaviors. A range of established behaviors in the larval zebrafish await the elucidation of their neural implementation. Numerous available tools for mapping neural circuits and to gain experimental control over neurons can be used to address the neural circuitry underlying behaviors that are compatible with the need to restrain the fish. However, for the behaviors that only occur when the fish is freely swimming, a new technology is required. In order to study the neural circuits underlying freely swimming behaviors in the larval zebrafish, I developed and worked on the two major aims presented in this thesis:

1. The identification and functional description of the neural whole-field motion discrimination circuitry underlying the zebrafish optomotor response, using the above described experimental strategy, relying on available methods (employing whole brain functional imaging to identify neural circuit components).
2. The development of a new technique that uses bioluminescence for recording of neural activity from genetically specified neurons in freely behaving zebrafish.

The relevant background and specific questions concerning these two aims will be introduced in the following sections.

1.3 BACKGROUND AND INTRODUCTION TO AIM 1:

WHOLE-FIELD MOTION DISCRIMINATION IN LARVAL ZEBRAFISH

How do neural networks process sensory information from the environment and choose the appropriate behavior? Recent research on the neural basis of decision making[93] has demonstrated that when simple sensory discrimination tasks are performed by primates[93,94] or rodents[95,96], the underlying neural activity can be correlated with the integration of relevant sensory information and even expected reward value[9]. In most of these tasks, the animal is required to learn an association between particular perceptual stimuli and associated reward values, and then use this information to make the behavioral decision that is most likely to "pay off"[9,97,95]. However, even after such an accurate association is learned and correct choices are made, the stimulus information must still be integrated, compared and sufficiently processed to execute the favorable decision[93]. Similarly, innate behaviors, which don't require the prior learning of value for a particular behavioral choice, must rely on sensory information that has to be integrated and analyzed to select appropriate behaviors. However, how even these "simple" sensory-motor transformations are accomplished within the neural circuitry of the brain is poorly understood. Understanding the principles of neural circuits that implement simple sensory motor transformations promises to of inform how more complex behaviors, such as value based decision making, are achieved by networks of neurons within the brain. In vertebrates, the evolutionary old brain circuitry performs many such sensory motor transformations. The zebrafish model organism offers numerous practical advantages for the mapping and analysis of neural circuits that integrate and process sensory stimuli, such as visual motion, and use this information to guide behavioral choices[53,98,32].

1.3.1 OPTOMOTOR BEHAVIORS: VISUALLY GUIDED BEHAVIORAL CHOICES

There are few sensory processes as universal and essential as the detection of whole field visual motion[56]. Perceptual judgment of global motion allows the estimation one's own velocity with respect to a stationary world[99,100]. Therefore, many species exhibit compensatory behaviors that work to stabilize the visual world and thereby cancel the animal's self-motion: smooth pursuit (saccadic tracking of the visual scene)[15], optomotor responses (OMR)[53,60,98,99,101,102], optokinetic reflexes (OKR)[57,41,60,34,103,104]. Since global motion must be integrated over time and space, this visual information cannot be represented at the level of photoreceptors. Rather, the perception of global motion must be computed from locally detected changes in light intensities by the downstream nervous system. Some invertebrates, such as flies and bees, possess remarkable visual motion detection[102,105,106]. Motion vision in flies and the consequential compensatory behavior, the OMR, has been extensively studied on the neural circuit level[102,106]. From the non-directional responses of the fly photoreceptors, local Reichhardt-type motion detectors provide spatially organized input to the global motion selective tangential cells of the *lobula* plate. Functioning as a filter for directional optic flow, tangential cells pass their information on to descending neurons, which control motor centers of the thoracic ganglion that guide flight and locomotion. Although not all details are known, the rapid progress in neurobiological tool development in *drosophila melongaster* promises to uncover and understand this and other neural circuits within insects in the near future[102,107].

In comparison, the neural circuits of vertebrates that underlie similar visual stabilizing behaviors are not well understood. In mammals, our knowledge is particularly patchy. We know of direction selective retinal ganglion cells[105,108-110], simple and complex cells in the primary visual cortex, and the global motion selective neurons in the medial temporal lobe (MT), which receive input from neurons in the primary visual cortex[105]. MT provides input to the medial superior temporal lobe (MST), where neurons are also responsive to self motion and involved in the generation of 'smooth pursuit'[15], a tracking motion of the eyes which keeps a moving object within the fovea of the retina. However, a more basic stabilization of the entire retinal image in response to self-motion induced visual whole-field motion is termed the optokinetic reflex (OKR)[103,111,112] in which the eyes move in the same direction, and with the same speed, as the visual scene moving across the retina.

With their excellent vision, fish present an enticing model for the investigation of the vertebrate OKR[57,62]. The OKR is a robust response, already present in four day old larval zebrafish[113], which has allowed the development of high-throughput assays to rapidly screen genetic mutants for defects of the visual system[114,34,41]. Similar to the OKR, the optomotor response (OMR) is also evoked by motion of the whole visual scene, but it describes an attempt to stabilize the visual environment by inducing counter-acting locomotion of the body. This compensatory movement might provide benefits beyond simple image stabilization, since it also allows the animal to 'stay in one place'. For example, young zebrafish would be easily swept along with slow water currents of a river, and all the fish would experience is the resulting whole field motion of the underlying river bottom. To compensate for this perceived self motion, fish will reorient to and swim in the direction of visual motion. This behavior, the

OMR, may serve an ethologically valuable role as it allows the fish to ultimately stay in the same location, and thus avoid being swept downstream. That such behavior could be crucial for survival might explain why the OMR is such a remarkably robust behavior in larval zebrafish.

For these innate behaviors, the OKR and OMR, the associated value of the stimuli and actions do not have to be learned, but nonetheless, one could characterize the behavior as a “choice” based on incoming visual information that has an intrinsic value to the animal. To investigate the circuit underlying this sensory guided decision, I will focus on the robust and relatively well-understood zebrafish OMR.

1.3.2 OPTOMOTOR RESPONSE OF ZEBRAFISH AS VISUAL DISCRIMINATION TASK

The optomotor response of larval zebrafish is a behavior that combines a number of characteristics useful for the identification and investigation of a neural circuit underlying visual guided behavioral choices. Importantly, the zebrafish OMR can be easily elicited by computer generated visual stimuli and the behavior is composed of distinct locomotion events that can be easily recorded and quantified. Furthermore, larval zebrafish are willing to perform the OMR continually for hours, and even days. These features make the OMR an ideal candidate for computer controlled behavioral assays. Automatic monitoring of the visually-evoked responses at the level of single swim events and the automated analysis of the high-speed kinematics, has revealed that three typical locomotion events are evoked by whole field patterns moving in different directions beneath the fish (Figure 1.4a, b)[53,66]. Sinusoidal grating patterns, moving across the fish body-axis, evoke reorientation turns, tail flicks to one side resulting from the unilateral contraction of axial tail muscles. Thus, these motion stimuli can be used to isolate distinct elements of zebrafish behavioral responses, i.e. left versus right tail bends.

The easy classification of distinct behavioral responses allows using the OMR as a visual discrimination task, for which the fish reports the “perceived” direction of visual motion with a directed tail flick. With complete control over the stimulus, it is then possible to test how changes to the stimulus lead to changes in the discrimination/behavior. For example, it is possible to investigate how the different eyes contribute to the behavioral output by stimulating each eye independently, and similarly, the stability and dynamics of the neural circuit can be studied by presenting ambiguous stimuli (conflicting information to each eye). Furthermore, eye independent (monocular) stimulation represents a powerful psychophysics approach for identifying the circuitry responsible transmitting and ultimately combining the information gathered from each eye.

Figure 1.4

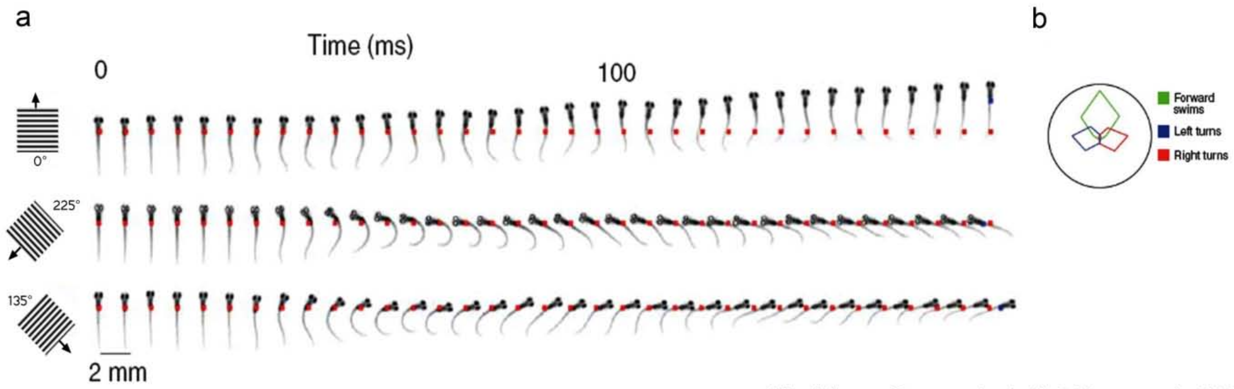

modified from Orger et al. Nat.Neurosci. 2008

Figure 1.4 - Optomotor behavior in larval zebrafish: a High speed kinematics of body movements to moving gratings in three different directions (top row: tail to head motion: forward, middle row: back left motion, bottom row: back right motion). Single images of fish taken in 5 ms intervals during 3 modes of swimming are presented from left to right. Colored arrows show the stimulus direction. Red dots indicate the starting position of the fish. **b** Polar plot of swim-type frequency (forward swim, 0-5mm forward, less than 10º turned and turns, angle change over 30º) versus stimulus direction

1.3.3 NEURAL SUBSTRATES OF THE OPTOMOTOR RESPONSE IN THE ZEBRAFISH

Much is already known about the early-stage sensory processing and late-stage motor control of the neural circuit underlying the OMR. This research will provide a start and end point for my investigations of the intervening circuitry. I review this previous work in this section.

1.3.3.1 INPUT TO THE OMR CIRCUITRY: SENSORY PROCESSING OF WHOLE-FIELD MOTION BY THE RETINA

Visual perception begins in the retina. The circuitry, anatomy, histology, and neurotransmitter biochemistry of the retina is conserved among most extant vertebrates[34]. As a vertebrate, the zebrafish "developed" into a model system for retinal development and function. The zebrafish possesses all major vertebrate retina cell types, photo receptors, horizontal, bipolar, amacrine and retinal ganglion cells[105,34]. Like humans, zebrafish are diurnal and its retina contains cone photoreceptors (red, green, blue and ultraviolet UV) in additions to rods[34]. Interestingly, the cone types most important for the larval optomotor response are the red and green cones, but none of the short-wavelength cones; they do, however, contribute to phototactic behaviors. Intriguingly, moving color gratings, which stimulate the different cone types out of phase with one another, do not evoke the OMR, whereas the OMR is enhanced when the cones are stimulated together, suggests that red and green cone signals are pooled at a stage before motion detection[115,116]. So, the obvious question arises of where does motion and/or direction detection occur? While the photoreceptors are non-directional, other retinal cells like amacrine[117] and some subtypes of retinal ganglion cells[108-110,118] are known to be direction selective along specific axes of the visual field[109]. Such direction selective retinal ganglion cells have also been found in the goldfish retina[115]. In addition, general evidence is accumulating that the retina already solves specific computations within the local circuitry and provide the results to various brain regions[119]. As recently found for particular types of retinal ganglion cells in the mouse, such direction selective cells could specifically connect to their downstream partners to allow for efficient processing of information already computed by the retina[120,110,121,122,118].

1.3.3.2 DOWNSTREAM TARGETS OF THE RETINA

Presumably because fish do not have eyes with overlapping visual fields, all retinal ganglion cells project to the contralateral side of the brain[123,124] (Figure 1.5a). Most of the retinal ganglion cell afferents (~95%) project to the optic tectum where they fan out in an arbourization field (AF) and form topographic and layer specific synapses with downstream neurons guided by chemical cues[105]. The tectum is the final, and largest, AF for retinal ganglion cells leaving the retina (AF10), however, other sites along the path from the retina also receive ganglion cell synapses (AF1-9) (Figure1.5b, c)[125].

Figure 1.5

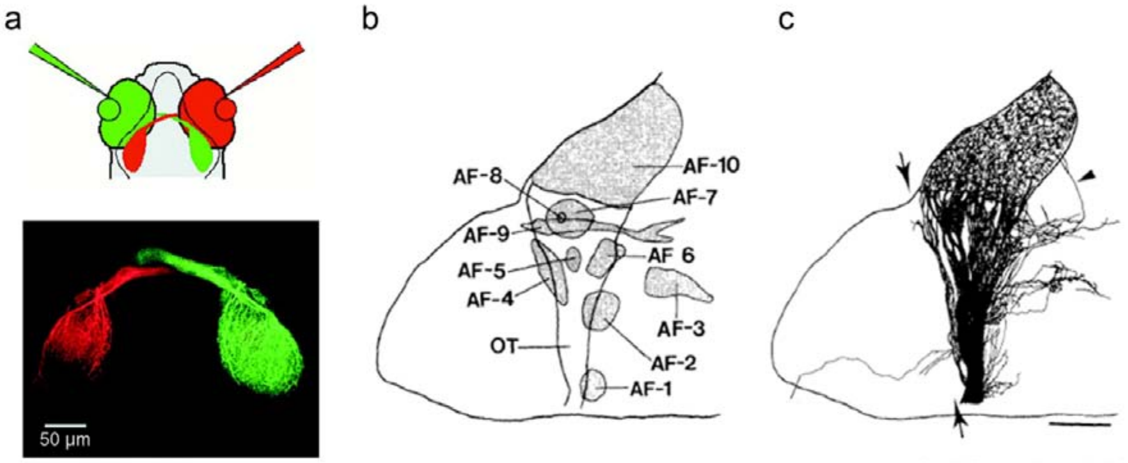

Fricke et al. Science 2001

Burril & Easter J. Neurosci. 1995

Figure 1.5 - Retinal projections in the zebrafish: **a** Schematic view of the technique for double labeling retinal ganglion cells with diI (red) and diO (green) fluorescent dyes injected directly into the eye of a larval zebrafish. Lower: confocal micrograph of retinotectal projection at 5 dpf. Retinal ganglion cells exclusively innervate the contralateral tectal and pretectal neuropils. **b** Schematic, lateral view (rostral, left; dorsal, up) of the 10 retinorecipient areas found in a 6 dpf larval zebrafish. These areas were identified by intraocular injections of DiI. **c** Camera lucida drawing of DiI labeled optic axons and their arborizations in a whole mount preparation. The cell bodies of the retinopetal projection were removed during the dissection of the larvae. The approximate locations of AF-5 and AF-8 are also shown, but they are not visible in this drawing. Scale bar = 50 µm.

Unfortunately, which of these arbourisation fields receive input from the retinal ganglion cells that provides the visual information necessary for the OMR is not known [126,60]. The little that is known is controversial: Although Springer et al.[126] reports that the OMR in goldfish depends on an intact optic tectum, normal OMR behavioral results after bilateral laser ablation of the ganglion cell axons entering the optic tectum in zebrafish larvae suggests that other regions than the tectum might be involved in the OMR (Figure 1.6)[60]. This apparent contradiction could be explained by the difference of the extent of ablations in the different studies. Whereas the mechanical ablation in the goldfish might have eliminated more than just the tectum, the laser ablation in zebrafish targeted only the retino-recipient layers of the tectum and presumably left deeper layers intact. These deeper layers are in close proximity to other retinal arbourisation fields. Laser ablation of another easily discernable AF, AF7, also had no detectable effect on the OMR. As motion information must enter the brain via the retinal ganglion cell afferents, any of the remaining AFs are potential carriers of the whole field motion information. Whole field motion processing beyond the retina has been investigated in a variety of vertebrates[127,112,128,105], direct input from the retina to direction selective neurons in the pretectal areas, accessory optic system (AOS) or the pretectal nucleus lentiformis mesencephali (nLM) is necessary for the OKR[31]. In teleost fish, the homolog retinorecipient structures, the pretectal area ventral to the optic tectum have been shown to be direction selective[127] and thus appear to be involved in gaze stabilization. Whether the pretectal area functionally overlaps with the OMR and utilizes whole-field visual information to guide compensatory behaviors is poorly understood. However, it presents itself as possible candidate of the neural substrate that allows the transformation of sensory inputs into motor commands.

Figure 1.6

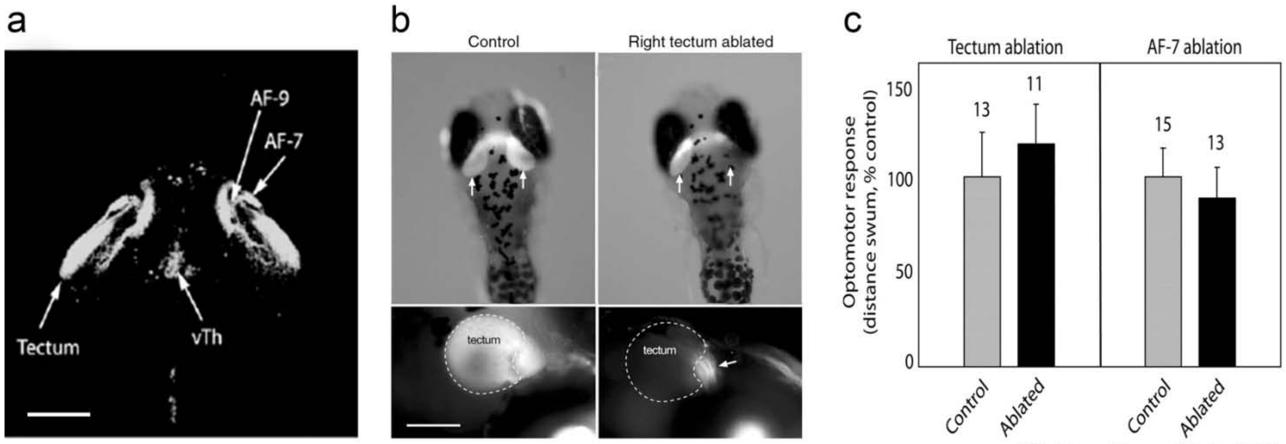

modified from Roeser&Baier 2003

Figure 1.6 - Effects of ablating the tectal neuropil and of AF7 on the OMR: a Dorsal view of a projection through confocal z-sections showing the lower tectal neuropils (tectum) and retinorecipient arbourisation fields(AF7 and AF9) in *Shh:GFP* transgenic fish(6 dpf). The ventral thalamic cells (vTh) are also labeled by GFP in this line. The optic chiasm and other retinorecipient arborization fields are located more ventrally and thus are not visible in this projection. b After the behavioral tests, the extent of laser ablation was assessed by an injection of DiI into both eyes of paraformaldehyde-fixed fish (upper panels). DiI labels the retinofugal projection, including the tectum. In control fish, both tectal lobes are clearly visible, whereas in the tectum-ablated fish, labeled fibers are absent from the ablated tectum. Lower panels: Higher-magnification, dorsolateral views of a control and ablated tectum (dotted line). Arrow in lower images indicates the pretectal arborization field AF7. Scale bar in a and b: 100µm. c Behavioral effects of laser ablations are measured as magnitudes of the OMR swimming and expressed as percentage ± SEM of control (sham-ablated). Neither tectum ablation nor AF7 ablation noticeably affected the OMR.

1.3.3.3 OUTPUT OF THE OMR CIRCUITRY:
DESCENDING MOTOR CONTROL OF TURNING BEHAVIORS

Neuronal motor commands are sent by descending projection neurons to the local networks of the spinal cord, where the actual behavior, patterns of muscle contractions, is coordinated and executed[53]. A recent study demonstrated that the OMR in fish is controlled by an identifiable subset of reticulospinal cord neurons [53]. These roughly 300 neurons can be easily labled retrogradely by injection of fluorescent indicators into the spinal cord. Unique for a vertebrate, these neurons are identifiable. Although arranged in a stereotyped pattern, their distinct response properties, morphological diversity and the different axonal and dendritic projection patterns suggest that they serve different behavioral functions. One particular well studied neuron of this group is the Mauthner neuron, known to be sufficient to initiate the escape response[129]. Whereas almost all descending motor control neurons seem to respond to tactile stimuli in widespread activation[130], specific neurons are necessary to activate specific visually evoked tail behaviors, swims and turns, in the larval zebrafish[53]. Calcium imaging of the descending spinal cord neurons during presentation of the moving gratings in different directions revealed a specific functional organization[53]. Most cells either did not respond or preferred forward motion and only a few prefer gratings moving in directions that elicit turning responses. Morphologically, cells can be organized into 20 groups for analysis (Figure 1.7a, b). Two distinct groups, RoM1r in rhombomere 1 and the ventromedial cells of the rhombomeres 3-5 show preferential responses to stimuli that evoke turning behaviors (Figure 1.7c, d). These two laterally symmetrical populations were removed cell by cell with two photon laser ablations. After a short recovery period, the behavioral responses were measured, identifying the ventromedial cells as crucial for turning behaviors. These results demonstrate that the ventromedial cells in the hindbrain cells are a necessary part of the circuitry responsible for the optomotor response.

Figure 1.7

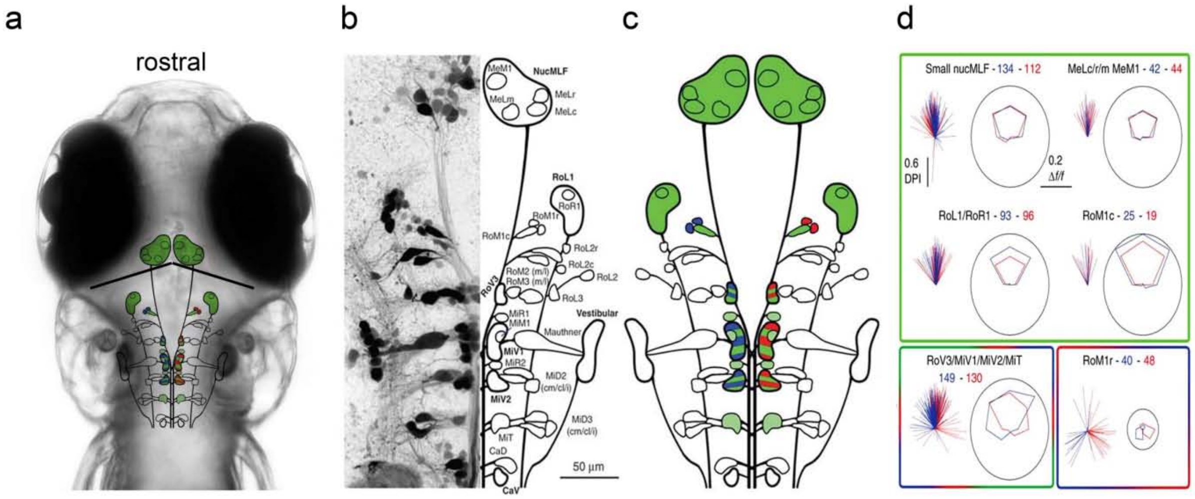
a
rostral
b
MeM1
NucMLF
MeLm
MeLr
MeLc
RoL1
RoR1
RoM1r
RoM1c
RoL2r
RoL2c
RoL2
RoM2 (m/l)
RoM3 (m/l)
RoV3
RoL3
MiR1
MiM1
Vestibular
Mauthner
MiV1
MiR2
MiD2 (cm/cl/i)
MiV2
MiD3 (cm/cl/i)
MiT
CaD
CaV
50 µm
c
d
Small nucMLF - 134 - 112
MeLc/r/m MeM1 - 42 - 44
0.6 DPI
0.2 Δf/f
RoL1/RoR1 - 93 - 96
RoM1c - 25 - 19
RoV3/MiV1/MiV2/MiT
149 - 130
RoM1r - 40 - 48

modified from Orger et al. Nat. Neurosci. 2008

Figure 1.7 - Reticular spinal projection cord neurons are responsive to whole field motion

Figure 1.7 - Reticular spinal projection cord neurons are responsive to whole field motion: a Dorsal view of a nacre-/- zebrafish head (6 dpf) overlaid with a schematic of the reticular projection neurons. Diagonal lines indicate the midbrain/hindbrain boundary. Other than the nucleus of the medial lateral fasciculus (midbrain), all other reticulospinal cord neurons reside within the hindbrain. b Schematic of the cell classification system according to Orger et al.: (right side) thin outlines represent single neurons and bold outlines represent groups of neurons. (left side) A projection of reticulopsinal neurons labeled with Texas Red dextran is shown for comparison with the classification scheme. c A summary diagram of the directional preference of spinal projection neurons. Neurons that preferred tail-to-head (forward) motion are colored green, neurons that had a left or right preference are colored blue or red, respectively, and mixed populations are displayed striped. d Two plots are shown for each cell group: the left plot of each pair shows the directionality vectors for every responsive cell recorded from that group and the right plots show the average tuning curves for the population. Data from cells/groups on the right side of the brain are shown in red, data from left cells/groups are in blue. Up represents the tail-to-head direction. The label for each plot gives the category name followed by the number of cells recorded on the left and the right side of the brain, respectively. The colored boxes group functionally similar classes of neurons according to their stimulus preference (forward, green; right and left turns, red and blue, respectively).

1.3.3.4 INFORMATION PROCESSING BETWEEN RETINA AND THE HINDBRAIN

How do these descending motor commands emerge from the information that the retina extracts from the visual world? The previously discussed research on both the sensory the motor ends of the neural circuit underlying the OMR has provided us with insights into how the retina detects changes in light levels and how networks of the spinal cord are controlled by projection neurons, yet the neural processing intermediate to the retina and the hindbrain remains largely unknown.

1.3.4 AIM1: INVESTIGATING THE NEURAL CIRCUITRY OF VISUAL WHOLE-FIELD MOTION DISCRIMINATION

How can a vertebrate neural circuit discriminate between different directions of whole field motion of a visual scene and translate this information into the appropriate behavioral choice? Simply because the OMR is controlled by the direction of the visual motion stimulus, the underlying neural circuitry must have the ability to discriminate and process different directions of motion information. For turning behaviors, patterns of light intensity arriving at the photoreceptors have to eventually be combined in lateralized neural structures to form the motor commands that enact the behavioral choice[53]. In order to understand how this is accomplished, it is necessary to 'trace' the sensory information through the nervous system and examine how the information is represented at each level of neuronal processing. With an unambiguous whole field motion stimulus, each eye receives information relevant to the control of the optomotor response. Therefore, sensory information arising from each eye should contribute to the behavioral output. For the investigation of aim 1, I used a psychophysics approach to investigate this crucial neural processing step which must take place in the neural circuitry between retina and the hindbrain. I reasoned that a detailed characterization of the behavioral responses to unambiguous binocular and monocular stimuli, as well as ambiguous (conflicting) stimuli, might provide useful clues about how the neural circuitry combines eye specific information. Importantly, such stimuli also allow isolating the associated activation of neurons by one eye. Moreover, conflicting stimuli presented to the same circuitry could reveal crucial processing stages in the sensory motor circuitry. The following specific questions guided the research for aim 1:

1. How are stimuli from both eyes integrated to guide the OMR behavioral responses? What are the behavioral responses to conflicting stimuli?
2. How are specific behaviors reflected at the level of the relevant hindbrain neurons?
3. Can genetically encoded calcium indicators be used to investigate large volume of the zebrafish brain to identify components of the neural circuitry that process whole-field visual motion? If yes, what is the neuronal substrate of the motion discrimination circuitry?
4. What are the specific response properties of the identified circuit components?
5. How does laser ablation of these components affect the behavior?
6. What model of the motion discrimination circuitry can be developed based on results from previous studies and new findings from this investigation?

1.4 BACKGROUND AND INTRODUCTION TO AIM 2:

MONITORING NEURAL ACTIVITY WITH BIOLUMINESCENCE DURING NATURAL BEHAVIOR

To correlate the activation of specific neurons with the execution of specific behaviors, it is necessary to monitor neural activity while an animal behaves. Neural recordings in freely moving animals are possible with electrophysiology, but the available techniques are invasive, often cannot target specific neurons, and are restricted to organisms that can physically transport the required electronics[131-135]. Optical techniques, using genetic strategies to target protein reporters to specific neurons and non-invasively monitor their activity, provide a promising alternative[86,136-138]. These tools have provided access to neurons in the larval zebrafish brain and allow monitoring and manipulating their activity *in vivo*[79,88,139,51,52]. In particular, synthetic and genetically-encoded fluorescent Ca^{2+}-indicators, targeted to distinct neural populations, have been used to relate the activity of defined cell-types to different stimuli or behaviors[53,79,140,85]. Therefore, I reasoned that the translucence of the larval zebrafish would be ideally suited for an optical approach for detecting neural signals during unrestrained behavior.

Optophysiology, the optical recording of brain activity, has employed optical Ca^{2+} indicators to relate a change in fluorescence intensity to a change in intracellular Ca^{2+}levels. Transient increases in intracellular Ca^{2+} resulting from action potentials and/or synaptic activation, detected by either synthetic or genetically-encoded fluorescent probes, have been used to infer neural activity in restrained larval zebrafish[52,53,141,142]. For measuring the neural activity in unrestrained zebrafish, a possible strategy would be to illuminate an entire behavior chamber with excitation light and monitor Ca^{2+}-dependent changes in fluorescence intensity. Although, spatial resolution would be lost, such a technique would provide temporal information about the activity of all neurons containing the Ca^{2+} -reporter. However, to regain specificity the Ca^{2+}-reporter could be targeted to the cell type of interest. Such fluorescence- based strategy for recording from genetically specified neurons in unrestrained zebrafish would provide a powerful tool for monitoring the activity of distinct neural populations during natural behavior [137].

Unfortunately, there are multiple limitations for the realization of such a fluorescence based strategy. First, all fluorescent reporters have at least moderate baseline emission intensity (fluorescence in absence of Ca^{2+} in addition to auto-fluorescence in neural tissue. This background emission poses a serious problem since any changes in excitation or detection efficiency caused by fish motion will produce substantial changes in detected fluorescence. This is especially since these baseline changes exceed the expected small intensity changes dependent on neural Ca^{2+}. This is particularly evident as motion artifacts resulting from a small tactile stimulus induce so much noise even in a restrained preparation. Thus, fluorescent signals are corrupted when motion causes fluorescently-labeled neurons to enter and exit the imaged region[79,85]. This sensitivity to movement has limited imaging techniques to restrained, paralyzed or anesthetized animals for which behavior is abolished or severely restricted[53,143-145].

1.4.1 NON IMAGING STRATEGIES

In principle, a "non-imaging" technique can allow monitoring neural activity in freely behaving zebrafish. Non-imaging systems do not attempt to form an image of the source at the light detector and thus do not require intermediate focusing optics. As a consequence, a large-area photo-detector can be positioned directly above the behavior arena. The detector receives light emitted from anywhere within the arena and the optical signals from the neurons labeled in a translucent organism are unaffected by the animal's movement throughout the collection volume. Although this approach sacrifices all spatial information, a conventional imaging approach will also suffer from a loss of spatial information when used with freely behaving animals: emitted light is scattered by intact tissue and movement of the labeled neurons out of the focal plane will severely limit the possible spatial resolution. In addition, natural behavior requires an arena size substantially larger than the animal and, unless behavior is slow enough to allow the imaging setup to accurately move along with the animal[146], the entire area must be imaged at high resolution to gain useful spatial information, all while maintaining the high frame rates necessary for monitoring activity on physiologically relevant timescales. Given the limited spatial information available to an imaging assay of behaving animals, I decided to pursue a non-imaging approach, which is technically straightforward, inexpensive, provides higher temporal resolution, and is able to detect a large portion of emitted light because the detector can be installed close to the behavior arena. Furthermore, spatial information can be gained indirectly by using a genetically-encoded reporter and targeting its expression only to the neurons of interest[137]. A non-imaging detection system with a genetically-encoded neural activity reporter would provide a powerful new tool for selectively recording from genetically-defined neurons during natural behavior.

Unfortunately, two features of the commonly-used fluorescent activity reporters preclude their use in a non-imaging setup. The baseline light emission when unbound to Ca^{2+} and, regardless of this basal fluorescence, auto-fluorescence will provide a significant background signal. With these sources of background emission, any changes in excitation or detection efficiency caused by motion within the collection volume will produce changes in the detected fluorescence unrelated to neural activity. Second, the use of fluorescent indicators in a non-imaging setup requires an intense visible excitation light to homogenously fill the behavior/collection arena. In addition to the technical challenge, the excitation light would also disrupt assays of vision and might confound other behavioral experiments (e.g. studies of sleep).

Given these above constraints, I can list the characteristics of an ideal optical Ca^{2+} reporter for use with freely swimming zebrafish: zero background emission at basal neural Ca^{2+} levels, excitation independence, genetically-encoded, non-toxic to neurons, stable at room temperature, fast Ca^{2+}-sensing kinetics, and sensitive to the large dynamic range in Ca^{2+}-concentrations in neurons. Conveniently, each of these criteria is met by the fascinating protein Aequorin, a Ca^{2+}-dependent bioluminescent enzyme produced in nature by the jellyfish *Aequorea Victoria* [71].

1.4.2 AEQUORIN AS CALCIUM INDICATOR IN NEURONS

In contrast to fluorescent reporters, Aequorin, has no background light emission at basal Ca^{2+} levels and does not require excitation light. Based on these properties alone, I reasoned that Aequorin might be well suited for non-imaging assays of neural activity in freely moving zebrafish. Furthermore, Aequorin has demonstrated excellent characteristics as a genetically-encoded Ca^{2+}sensor[72]. Upon binding calcium, Aequorin (luciferase) catalyzes the completion of the luciferase reaction, the oxidation of its substrate (luciferin) coelenterazine (CLZN), resulting in the production of a blue photon. Coelenterazine is a small molecule for which the biosynthetic pathway is unknown, must be delivered to the intracellular Aequorin. Fortunately, it readily permeates lipid membranes and under the correct conditions will be absorbed directly from the surrounding water by zebrafish larvae. In fact, many coelenterates are not thought to synthesize their own coelenterazine, but instead acquire it via their diet. Purified Aequorin has been employed as an optical indicator of intracellular Ca^{2+} in many cell-types, including neurons[147,148,70,149].

In jellyfish, Aequorin naturally occurs as a complex with green-fluorescent protein (GFP), and via a process termed chemiluminescence resonance energy transfer (CRET), the energy from CLZN oxidation is transferred to GFP and results in the emission of a green photon[149]. The efficiency of Ca^{2+}-dependent photoemission from Aequorin is enhanced when associated with GFP (from 10% to 90%), which inspired the development of a GFP-Aequorin fusion (GA)[150]. GA retains the fast kinetics of Aequorin (6-30 ms rise time[70]) and its sensitivity to Ca^{2+}-concentrations ranging from 100 nM-10 μM[151], which is on par with the best synthetic Ca^{2+} sensors. In addition, the associated GFP provides a fluorescent tag that can be imaged with conventional fluorescence methods to localize and quantify GA expression.

These improved features of GA have fostered new interest in bioluminescence assays for neural Ca^{2+} signals and it has been successfully employed to monitor pharmacologically evoked activity in neural populations of restrained flies[152], detect mitochondrial Ca^{2+} in the muscles of behaving mice[153], and image the bioluminescent signals from individual neurons in disassociated cell cultures and *in vitro* preparations[72,154,150,155].

1.4.3 AIM 2:

USING BIOLUMINESCENCE TO RECORD FROM GENETICALLY SPECIFIED NEURONS WHILE MONITORING BEHAVIOR SIMULTANEOUSLY

Understanding how the activity of a specific group of neurons in the brain drives specific behaviors requires monitoring neuronal activity in freely behaving animals. Linking the neural activity of such candidate neurons to specific behavioral responses is crucial in determining the role these neurons play in the underlying circuitry. Although, *in vivo* fluorescence imaging allows non-invasive monitoring of neuronal activity in awake fish, they are required to be restrained, paralyzed or even anesthetized. Fortunately, this approach is sufficient to monitor the activity of each individual neuron in their brain in response to behaviorally relevant stimuli, as described for aim 1. However for the investigation of neural activity in the brain of fish which are swimming freely in a natural environment, another technique is required.

The zebrafish's translucence invites the use of an optical technique. In order to develop a technique based on bioluminescence generated by the photoprotein GFP-Aequorin, many methodological details had to be resolved. The specific questions and requirements for aim 2 are as follows:

1. Can Aequorin be specifically expressed in neurons in stable transgenic fish?
2. How can Aequorin be constituted *in vivo* to allow for neural recordings?
3. Design, engineering and development of an assay to monitor single photons while monitoring behavioral responses in darkness and during natural illumination.
4. Design of control experiments to confirm the neural origin of light emitted from freely swimming fish.
5. Express Aequorin in the small population of HCRT positive neurons to investigate their role in behavioral regulation.

In result section 3.2, I describe the implementation of this novel technique that fundamentally extends previous bioluminescence studies: a non-imaging setup for long term monitoring of GA bioluminescence that can report the activity of a small number of genetically specified neurons in the larval zebrafish during natural, unrestrained behavior. Although initially limited to behaviors occurring in darkness, I also describe and implement a novel bioluminescence detection strategy that uses stroboscopic illumination to reproduce natural lighting, and thus further extend this technique to the investigation of visually-driven behaviors.

2 MATERIALS AND METHODS

Since different materials and methods were used for the experiments presented for the investigation of aim 1 and aim 2, I present them in separate sections in order to clarify the specifics of each experimental design, even for related experiments (i.e. two photon imaging) as some of the relevant details are different.

2.1 MATERIAL AND METHODS OF AIM 1

2.1.1 ZEBRAFISH

Five to seven day old wildtype *nacre* -/- zebrafish in AB, WIK or TL background strains were used to outcross transgenic lines; they lack pigment in the skin, but retain wildtype eye pigmentation. Their behavior was similar to wild-type siblings in the different assays. Zebrafish were maintained on a 14 hr light /10 hr dark cycle and fertilized eggs were collected and raised at 28°C. Embryos were kept in E3 solution (5 mM NaCl, 0.17 KCl, 0.33mM CaCl2, 0.33 mM MgSO4). All experiments were approved by Harvard University's standing committee on the use of animals in research and training.

2.1.2 BEHAVIORAL TESTING

Behavioral setup for freely swimming zebrafish:

Larval zebrafish (5 -7 dpf) swam freely in a clear 5 cm diameter petri dish. Illumination of the fish was achieved by an array of infrared light-emitting diodes directed from below. Their swimming behavior to various stimuli was recorded at 200 Hz using an infrared sensitive high speed, monochrome charge coupled device (CCD) camera (Pike F-032, 1/3", Allied Vision Technology, Germany) A zoom lens (Edmund Optics, USA) was used with an infrared filter pass filter (RG72, Hoya, Japan). The center of the dish was aligned with the center of an appropriately zoomed camera image such that the edge of the dish was not visible in the field of view, which simplifies the fish detection algorithm by not having to handle side-wall reflections. Stimuli were projected directly onto a 12 by 12 cm diffusing screen (Edmund optics, USA) 5 mm below the fish using a commercial DLP projector (Optoma, USA). Custom image processing software (Labview, National Instruments, USA andVisual C++, Microsoft, USA) extracted the position and orientation of the fish at the camera acquisition frame rate. This information was used to update a stimulus rendered in real-time using OpenGL. To begin each trial, fish were induced to swim to the center of the camera field of view by a concentric circular, converging sinusoidal grating. When the fish was detected near the center, a trial was triggered and would continue until either the fish left the camera field of view or the maximum trial duration was reached. To independently stimulate each eye, the stimulation was blanked directly underneath the fish, and the monocular stimulus regions started at a distance of 5 mm from either eye. Behavioral data were analyzed offline in Matlab (Mathworks, USA).

Behavioral setup for head restrained larval zebrafish:

Larval zebrafish (5 -7 dpf) were collected with a transfer pipette and fish medium was replaced with 100 µl of liquid, 37degree,drop of low melting agarose (1.5% w/v in fish medium) placed at the center of a 2cm petridish filled to 50% depth with clear sylgard, which improved agar adhesion to the bottom substrate. Fish were normally able to a upright themselves within the drop before the agar set. After the agar solidified (~4 minutes), the dish was filled with E3 fish medium. A surgical blade was then used to remove the agarose just caudal to each pectoral fin, thus liberating the fish tail. The "head-embedded" fish was then aligned under the camera with only the tail in the field of view. Illumination of the fish was achieved with an array of infrared light-emitting diodes directed from underneath the dish. The behavioral response of the tail motion was recorded at 500 Hz using an infrared sensitive, high speed, monochrome CCD camera (Pike F-032, 1/3", Allied Vision Technology, Germany). Stimuli were projected directly onto a 5 by 5 cm screen, 5 mm below the fish using a DLP projector (Optoma, USA). Custom image processing software (Labview, National Instruments, USA,Visual C++, Microsoft, USA) extracted the position of the fish tail at the acquisition frame rate. Stimuli were presented in random order and rendered in real-time using OpenGL. To ensure independent stimulation of each eye, 1 cm area directly, directly underneath the fish was left blank (black).

2.1.3 TWO PHOTON CALCIUM IMAGING

Synthetic indicators:

Spinal projection neurons were filled as previously described[75]. Briefly, a 50% w/v solution of dextran-conjugated calcium green (10,000 MW, Invitrogen, USA) was injected into the spinal cord of tricaine-anesthetized (0.02% 3-aminobenzoic acid ethyl ester in fish medium) fish. After injection, the fish were allowed to recover and were maintained for at least 24 hours in normal fish water before imaging. Fish were screened for sufficient labeling, and candidates were embedded in 1.5% low melting point agarose, and paralyzed with a bolus injection of a-bungarotoxin into the axial musculature of the caudal tail. Viability was monitored before and after imaging by observing the heartbeat and blood flow throughout the brain. The ventral descending spinal cord neurons were identified by anatomical details of the dendritic morphology and axonal projections of the reticular spinal cord neurons based on morphological criteria with a custom two-photon microscope, using a pulsed Ti-sapphire laser tuned to 920 nm (Spectra Physics, USA). The stimulus was projected from below with a DLP projector (Optoma, USA) after passing through a red long-pass filter (Thorlabs, USA), which allowed simultaneous visual stimulation and detection of green fluorescence. In each experiment, images were acquired at 3.6 Hz. After one or more repetitions of each stimulus set, the microscope focus was moved to a different z plane. The resulting image time and depth series were analyzed in Matlab (Mathworks, USA) to extract the positional origin of functional responses to different stimulation patterns.

Genetically encoded Calcium Indicators:

In-vivo two-photon imaging of GCaMP2 fluorescence were performed at age 5 dpf or as indicated in main text. Prior to imaging, larvae were anaesthetized using 0.02% Tricaine (Sigma, USA) in E3 and embedded in low melting point agarose (1.2% w/v). Tricaine was removed and α-Bungarotoxin (1 mg/ml, Sigma, USA) was injected into the ventral region of the spinal cord using a pulled glass pipette, inducing paralysis and preventing movement artifacts. Neurons and regions of interest were identified by anatomical details of the morphology and stereotypic blood vasculature. Imaging experiments were carried out as described above. All data acquisition and analysis was performed using custom Labview (National Instruments, USA), Matlab (Mathworks, USA) and C++ software.

2.1.4 TWO PHOTON LASER ABLATION

After embedding larval zebrafish in low melting agarose, targeted areas were identified by anatomical landmarks and stereotypical blood vasculature in the *HuC:GCaMP2* transgenic zebrafish (5-7dpf). A very small rectangular sub-region was selected. The power of a mode-locked laser (885 nm) was linearly increased while the beam was scanned in a spiral pattern throughout the targeted region. The laser scan was immediately terminated upon the detection of fluorescence saturation, which is presumed to result from the creation of highly localized plasma via multi-photon absorption by water molecules[156]. When using this procedure on single cells, it always results in the complete destruction of the cell despite immediately adjacent cells appearing unaffected[53]. Ablations in neuropil regions, which mostly consist of dendritic and axonal processes, the region of destruction is highly dependent on the surrounding neural tissue. The ablation of the posterior commissure is easily verified by taking a two photon stack immediately or hours after the ablation and the amount of recessed neural tissue can be easily assessed in transgenic lines (HuC:GCaMP2, HuC:YC2.1) .

2.1.5 GENERATION OF TRANSGENIC ZEBRAFISH LINES

The coding sequence of GCaMP2 (a kind gift from L. Looger), TnlXXL (a kind gift from O. Griesbeck) was subcloned via gateway vector cloning into a tol2 flanked HuC promoter expression vector (tol2:HuC:X:tol2), resulting in tol2:HuC:GCaMP2:tol2, tol2:HuC:TnlXXL:tol2. Plasmid DNA (20ng/µl in 100 mM KCl) was injected into nacre-/- zebrafish embryos at the single cell stage for transient expression. To generate stable transgenic zebrafish, tol2:HuC:GCaMP2:tol2 or tol2:HuC:TnlXXL:tol2 was co-injected with tol2 transposase mRNA. Injected embryos were grown in E3 solution and screened for expression at 2-5 dpf, and positive individuals (F0) were grown to adulthood and out-crossed to nacre zebrafish. F1 progeny of this cross were screened for expression at 2-5dpf, and transgenic founders with the best expression levels were identified. Most experiments with *HuC:GCaMP2* transgenic zebrafish were performed with progeny of crosses of stable transgenics (heterozygous) and wild-type nacre zebrafish. The stable transgenic lines *HuC:Chameleon* were a gift from the J. Fetcho, *athonal:GFP* from H. Baier.

2.2 MATERIAL AND METHODS OF AIM 2:

2.2.1 ZEBRAFISH

Zebrafish (Danio rerio) of the mitfa$^{-/-}$ (nacre) strain[73] were used in all studies; they lack body pigmentation and are therefore significantly more translucent than wild type strains. Zebrafish were maintained on a 14/10 hr light-dark cycle and fertilized eggs were collected and raised at 28°C. Embryos were kept in E3 solution (5 mM NaCl, 0.17 KCl, 0.33mM CaCl2, 0.33 mM MgSO4). All experiments were approved by Harvard University's Standing Committee on the Use of Animals in Research and Training

2.2.2 VECTOR CONSTRUCTION AND TRANSGENIC LINES

The coding sequence of GFP Aequorin, GA5v1 (a gift from L. Tricoire), referred to throughout the text as Ga, was subcloned via PCR into a neuro-β-tubulin expression vector (Nβt:GFP) (a gift from Paul Krieg) into an AgeI and NotI site, resulting in tol2:Nβt:Ga:tol2. UAS:Ga was constructed by subcloning the coding sequence after the UAS:E1B sequence in the UAS:Dsred Express-1 expression vector by replacing DsRed by blunt end insertion at the AgeI/Not I site. To express Ga in HCRT neurons, the zebrafish HCRT promoter, containing 1 kb of genomic DNA immediately upstream of the HCRT start codon, was subcloned upstream of Ga to yield tol2:HCRT:Ga:tol2. For specific expression of Ga in serotonergic neurons of the dorsal *raphe nuclei*, the zebrafish pet1 promoter (a kind gift from C. Lillesaar) was excised with BamHI and was subcloned upstream of Ga, yielding tol2:pet1:Ga:tol2. Plasmid DNA (20ng/µl in 100 mM KCl) was injected into nacre zebrafish embryos at the single cell stage for transient expression. To generate stable transgenic zebrafish, tol2:Nβt:Ga:tol2 or tol2:HCRT:Ga:tol2 was co-injected with tol2 transposase mRNA. Injected embryos were grown in E3 solution and screened for expression at 2-5 dpf, and positive individuals (F0) were grown to adulthood and out-crossed to nacre zebrafish. F1 progeny of this cross were screened for expression at 2-5dpf, and transgenic founders with the best expression levels were identified. Most experiments with Nβt:Ga transgenic zebrafish were performed with progeny (F3) of crosses of stable F2 transgenics (heterozygous) and wild-type nacre zebrafish. Hypocretin experiments were performed by crossing HCRT:Ga F0 founders to wild-type nacre zebrafish. For serotonin experiments, only transient pet1:Ga transient fish were used.

2.2.3 AEQUORIN RECONSTITUTION

Zebrafish larva were raised in E3 medium and screened for GFP fluorescence of Ga at 3 dpf. For reconstitution with coelenterazine (CLZN), 5-10 larvae were transferred into 2 ml of E3 solution containing a final concentration of 40 µM CLZN-h (Biotium, USA) or native CLZN (Invitrogen, USA or Biotium, USA) (all stock solutions at 10 mM dissolved in 45% 2-hydroxypropyl-b-cyclodextrin (Invitrogen, USA) were kept at -80°C to minimize auto-oxidation). After 24-48 hours, larvae were washed repeatedly in E3 medium and maintained in new E3 medium until they were transferred to the recording chamber (0-3 hours). In some experiments fish were transferred back into freshly prepared E3-CLZN solution after a neuroluminescence recording session and washing was repeated before the next set of experiments.

2.2.4 BIOLUMINESCENCE DETECTION AND BEHAVIOR MONITORING

Within a light-proof enclosure, the bioluminescence and behavior setup (Fig. 2b) was assembled and aligned using structural framing (80/20, USA) and optomechanic components (Thorlabs, USA). Zebrafish were placed in ~1 ml of E3 solution contained in a circular behavior chamber machined from clear-acrylic (12.5 mm in diameter and 6.25 mm in depth) enclosed on the top and bottom with cover glass. To avoid bubble formation in long term or overnight recordings, silicone sealant was used to keep the cover glass held in position. The chamber was mounted as close as physically possible (~5 mm) to a large-area photon-counting PMT (H7360-02: Hamamatsu, Japan) with USB interface counting unit (C8855: Hamamatsu, Japan), thus maximizing the angle of light collected by the detector (>60°). An 880 nm infrared LED ring light (Advanced Illumination, USA) was placed above the recording chamber, surrounding the PMT. The low-incident angle of the LEDs allowed the zebrafish to be illuminated while only minimally directing light into the PMT. To further limit bleed through of the IR illumination light into the sensitive detector, a 700nm short-pass filter (Chroma, USA) was placed at the entrance to the PMT. An infrared-sensitive CCD camera (C4900, Hamamatsu, Japan) was positioned beneath the behavior chamber and imaged the zebrafish behavior via a close-focus manual zoom lens (58-240: Edmund Optics, USA). The camera's sensitivity allowed for low-light IR illumination, but was limited to 30 Hz frame acquisition rates. However, software de-interlacing and cropping of the video signal resulted in 60 Hz frame rates (frame period of 16.67 ms) at 250x240 pixels.

Depending on the experiment, single fish or groups of up to 10 were included in the chamber. In some experiments, PTZ was added to induce epileptic events, while keeping the final volume constant. To evoke escape responses, zebrafish were stimulated with a mechanical tap delivered to the behavior chamber by a custom-designed computer controlled electromagnetic lever. For the prey capture experiments, paramecia cultures were filtered and 20µl (50- 100 paramecia) were added to the recording chamber. Photon count data from the PMT, behavior image data from the CCD, and experiment/stimulus control was accomplished with a custom multi-threaded C++ program. However, Labview drivers (National Instruments, USA) are available for the USB counter and the camera frame-grabber (PCI-1407, National Instruments, USA). To minimize the amount of behavioral data recorded, images were compressed with a custom compression algorithm that stored only pixels with intensity changes larger than the camera noise threshold and permitted continuous behavior monitoring for days. In some HCRT:GA experiments, IR illumination was strobed for 20 ms at 1 Hz and camera frames were synchronously acquired at 1 Hz, thus minimizing bleed-through into the PMT but allowing the classification of behavior into active and inactive seconds based upon whether the fish had moved since the last frame acquisition. All data analysis was performed with custom Matlab software (Mathworks, USA). Individual bioluminescent events were fitted with a double exponential function:

$$y(t) = A\ \frac{e^{\frac{O-t}{\tau_2}}}{1 + e^{\frac{O-t}{\tau_1}}}$$

where τ_1 is the time constant for the rising phase, τ_2 the time constant for the decay and A and O fit the Amplitude and the horizontal offset respectively.

2.2.5 IN VIVO TWO PHOTON IMAGING

In-vivo two-photon imaging of GA expression, coelenterazine loading and HUC: GCaMP2 fluorescence were performed at age 5 dpf or as indicated in main text. Prior to imaging, larvae were anaesthetized using 0.02% Tricaine (Sigma, USA) in E3 and embedded in low melting point agarose (1.2% w/v). Tricaine was removed and α-Bungarotoxin (1 mg/ml, Sigma, USA) was injected into the ventral region of the spinal cord using a pulled glass pipette, inducing paralysis and preventing movement artifacts. Expression profiles or coelenterazine loadings were imaged at high resolution with a custom built two-photon microscope[17] employing a Ti:Sapphire laser (Spectra Physics, USA) tuned to 920 nm for Ga and 850 nm for

CLZN. All data acquisition and analysis was performed using custom Labview (National Instruments, USA), Matlab (Mathworks, USA) and C++ software.

2.2.6 SINGLE PHOTON IMAGING

Using a modified commercial imaging system (Xenogen, USA), a custom designed microscope was built to allow magnification of the zebrafish brain onto an image intensifier, which amplifies light via an electron multiplication stage that is directed onto a phosphor screen that is imaged by a conventional CCD camera. The microscope incorporated an Blue-UV LED illuminated epifluorescence pathway for imaging GA expression prior to photon counting[74] and a 20X water immersion objective with a 0.95 numerical aperture (Olympus, Japan). A manual z-stage allowed adjustment of the focal plane within the zebrafish brain (Newport, USA). A USB frame-grabber (Sensoray, USA) was used to acquire raw images from the CCD, and custom C++ and Matlab (Mathworks, USA) software was used to detect single photon positions and exclude cosmic rays. After being treated with CLZN-h and washed with E3, zebrafish were prepared as described above for two-photon imaging. After acquiring a fluorescent image by exciting GA positive neurons with UV light and a bright field image to localize the GA positive neurons within the fish, baseline photon emission was recorded. To identify the neuronal source of any emitted photons, PTZ (10 mM) was used to maximally excite all neurons in the fish. Recordings were made continuously for approximately an hour. Analysis of the photon source position was performed by examining periods of transient increases in full field photon emission similar to those detected in the free-behavior assay. All analysis was performed with custom Matlab software.

2.2.7 BIOLUMINESCENCE DETECTION DURING NATURAL LIGHTING

.

Within a light-proof enclosure, the bioluminescence and behavior setups were assembled as described above. The following differences were implemented: A channel photon multiplier CPM (MP 1984 CPM, Perkin Elmer Optoelectronics, Germany) with a 520/60 nm band-pass filter (Chroma, USA) was mounted directly above the recording chamber. A yellow LED (peak emission: 587 nm, luminous intensity: 1900 mcd, RadioShack, USA) was directed towards the behavior chamber from the side. A high-speed, infrared-sensitive CCD camera (Pike, Allied Vision Technology, USA) was installed beneath the behavior chamber. An

Infrared filter (Hoya filter, R72, B and H Photo, USA) was mounted on the camera lens to prevent bleed through of the visible illumination light into the camera. The camera's sensitivity allowed for low-light IR illumination with frame rates exceeding 100 Hz.

During bioluminescence measurements, groups of up to 10 NβT GA fish were placed into the chamber. Computer generated timing signals (C++ and Labview, National Instruments, USA) controlled the IR illumination of the infrared LED ring light, the stimulus LED, and the camera exposure times. During one illumination cycle, the CPM was initially gated on for 9 ms and sensitive to individual bioluminescent photons after which it was rapidly gated OFF for 1 ms. While the CPM was off, the IR illumination and visible LED were briefly switched on for 0.8 ms and a camera exposure was acquired. This recording-illumination cycle was repeated at 100 Hz, producing the illusion of constant visible illumination while still allowing 90% of the emitted bioluminescence photons to be detected by the CPM.

3 RESULTS

3.1 RESULTS OF AIM 1: NEURAL CIRCUITRY UNDERLYING WHOLE-FIELD MOTION DISCRIMINATION IN LARVAL ZEBRAFISH

3.1.1 BEHAVIORAL RESPONSES TO MONOCULAR WHOLE-FIELD MOTION IN FREELY SWIMMING ZEBRAFISH

Figure 3.1

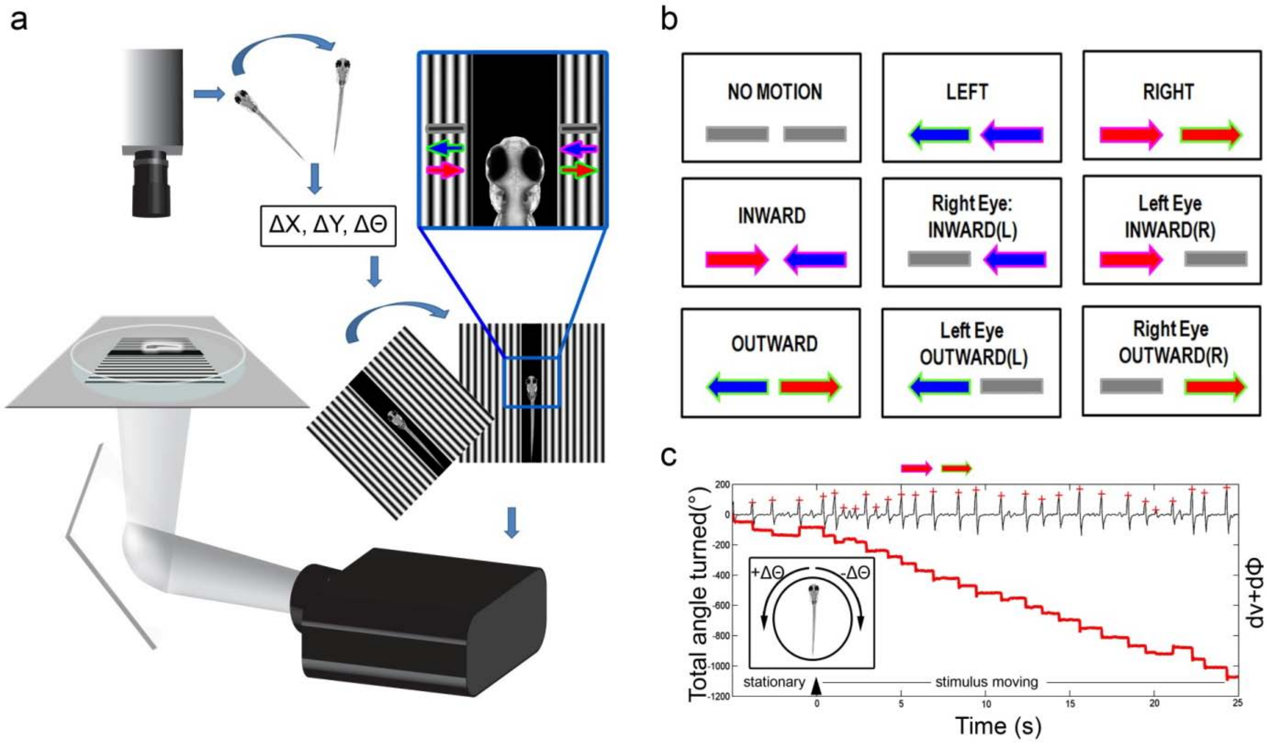
a
ΔX, ΔY, ΔΘ
b
NO MOTION
LEFT
RIGHT
INWARD
Right Eye: INWARD(L)
Left Eye INWARD(R)
OUTWARD
Left Eye OUTWARD(L)
Right Eye OUTWARD(R)
c
Total angle turned(°)
200
0
-200
-400
-600
-800
-1000
-1200
+ΔΘ
-ΔΘ
stationary
stimulus moving
0
5
10
15
20
25
Time (s)
dv+dΦ

Figure 3.1 - Behavioral set up for testing freely behaving zebrafish: **a** Schematic of the behavioral set up. A zebrafish is swimming freely in a clear behavioral arena while its behavior is monitored with a high speed camera. An image processing algorithm extracts the position and orientation of the fish and updates a visual stimulus that is presented from below. Enlarged region depicts the visual pattern that was used to permit stimulation of each eye independently. **b** Overview of the 9 different stimulation patterns that were used to probe the contribution of each eye's input to OMR turning behaviors: arrows on the right/left indicate the direction of stimulation for the right/left eye. Leftward motion is depicted in blue, rightward in red. The colored boundary around the arrows indicates inward (magenta) and outward (green) motion to either eye. Grey rectangles indicate no motion. **c** Example of a raw measurement of zebrafish orientation (cumulative angle) during presentation of a whole field RIGHT motion stimulus (red trace). The inset explains that negative and positive angle changes are associated with right and left turns, respectively. The summed velocity and angular change (dv+dΘ) of the fish was measured between each frame (upper gray trace) allowing individual swim events to be identified (+ symbols), extracted, aligned, and quantified.

To investigate how the information arriving from each eye contributes to the neural circuit controlling optomotor behavior, we designed a new setup that allows precise control of the monocular visual stimulus and simultaneous monitoring of the behavioral responses of freely swimming larval zebrafish (Figure 3.1a). This setup allows for real-time control of the visual environment (60 Hz) and online tracking of the behaving fish (200 Hz). Whole field motion moving orthogonal to the fish evokes directed turns. To investigate the contribution of each eye to these distinct behaviors, and assay how the system reacts to conflicting vs. coherent binocular motion stimuli, we used a set of stimuli (Figure 3.1b) that isolate the behavioral response to visual motion presented to each eye independently. To avoid accidental stimulation of one eye from stimuli directed to the other eye, a region 1 cm wide, directly underneath the fish and extending to the margins of the swim arena, was left blank (Figure 3.1a inset). Even if the field of view of each eye would extend to the full 180°, this exclusion ensured eye independent stimulation. Control experiments (data not shown) suggested that the non stimulated region could be completely removed without grossly affecting behavioral results; larger non-stimulated regions led to attenuation of the behavior, but not to differences in the overall structure of response patterns. To present a constant motion direction despite changes in the fish's orientation, the stimulus was locked to the fish body-axis in a closed loop configuration. The fish's position and orientation was tracked at high speed and this information was used to rotate and translate the visual stimulus with a minor delay introduced by the display refresh period (16 ms). For example, a whole field right moving stimulus (RIGHT) is presented and evokes a rightward turn (Figure 3.1a, c). This reorientation is detected by the video tracking program, which measures (and records) the amplitude of the turn and then rotates the stimulus in the same direction right by the same amplitude, thus the fish continues to experience rightward motion with respect to its body axis. The zebrafish body orientation was monitored continuously, and could easily detect left (+) and right (-) angle changes (Figure 3.1c inset) during each stimulus presentation (Figure 3.1 – rightward motion). Each trial began with the presentation of converging circles, which acted as an OMR stimulus to drive the fish to the center of the arena (Supplementary Movie 3.1). Upon entering the central area of the behavioral arena, the display then changed to a stationary stimulus, which persisted for 2 seconds, after which it began to move. Drifting at 1 cm per second, the motion stimulus lasted for 30 seconds. Even a reduced stimulus space, for which only right and left stimuli are presented in different combinations (Figure 3.1.5b), allowed investigating how unambiguous (coherent left/ right motion) and ambiguous (conflicting left/right motion) as well as exclusively monocular stimuli differentially affect the directed turning behaviors of the OMR. For a coherent rightward motion stimulus, which should be perceived as a whole field stimulus moving from left to right beneath the fish (RIGHT), the left eye receives an inward moving stimulus whereas the right eye receives an outward moving stimulus. As expected, the fish perceives this stimulus as congruent motion and responds robustly with turns to the right (Figure 3.1c). As a challenge to the OMR circuit, we used ambiguous stimuli simulating a visual motion situation that would not occur naturally as a result of zebrafish horizontal self-motion. These conflicting stimuli were the result of presenting both eyes, simultaneously, with either inward motion (INWARD) or outward motion (OUTWARD). Furthermore, by presenting inward or outward motion to only one eye while keeping the stimulus presented to the other eye stationary, the monocular contribution to the OMR behavior could be assessed. The monocular components of whole field LEFT motion are the stimulation of the right eye with inward motion (REI) and the left eye with outward motion (LEO). Analogously, the monocular components of whole field RIGHT are the stimulation of the left eye with inward motion (LEI), and the right eye with outward motion (REO). Furthermore, a no motion condition (NM) was used to assess spontaneous turning and swimming rates.

Figure 3.2

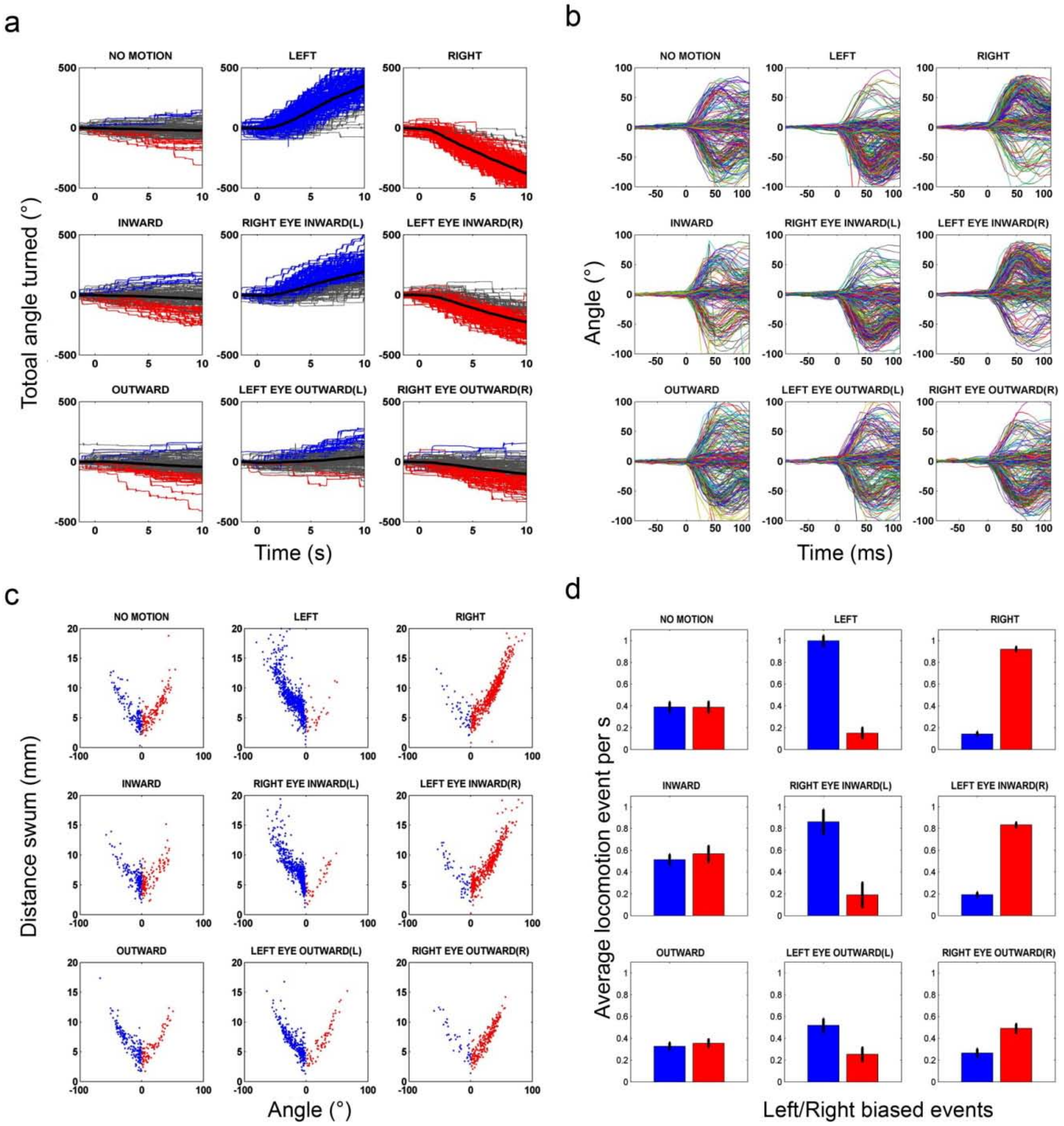

Figure 3.2 - Analysis of locomotion events to monocular and binocular motion stimuli. **a** Behavioral responses of a single zebrafish to the nine different stimulation patterns. Fish orientation during each stimulus presentations are plotted; trials are colored blue when the accumulated angle change exceeds more than 80 (resulting from many consecutive turns in the same direction) or red if below -80˚ by the time point 5 seconds following stimulus motion; otherwise traces are shown in gray. Average trajectories from all trials are overlaid in black. **b** The discrete behavioral events (swims, turns) of a single zebrafish are extracted and aligned to the detected onset of each event. The net angle change and distance swum following the event onset could be measured. **c** All of the discrete behavioral events produced by an individual zebrafish are plotted as the per event distance swum vs. per event angle change, for each stimulus type (blue, if angle change is associated with net negative angle change, red with net positive angle change). **d** Summary of average locomotion events per second (n = 12 fish) for the different stimulation patterns. The ratio of left or right biased locomotion events demonstrates which turn type predominates. Note that fish turn spontaneously as often to the left and right during the "no motion" condition.

For each experiment, these nine different simulation patterns (Figure 3.1b) were presented in a randomized order. Each individual fish received at least 25 presentations of the entire stimulus set. For one individual fish, we recorded more than 120 stimulus set repetitions over approximately 10 hrs of continuous monitoring (Figure 3.2a). The cumulative changes in fish body orientation that occurred during the individual stimulus presentations are plotted, with the average trajectory for each stimulus condition overlaid. This average cumulative angle change during stimulus presentation is indicative of how the fish responded to each stimulus, but the details of the turning behavior are not apparent. However, given that larval zebrafish swim and turn with discrete bouts, each individual motion bout could be extracted and analyzed separately. These discrete behavior events were identified (Figure 3.1c), extracted (Figure 3.2b) and characterized by two parameters, distance swum forward and total angle turned (Figure 3.2c). Each event was classified as a net right or left angle change (right/left turns as well as directionally biased forward swims) and the average number of behavior events in each category, per second of motion stimulation, is compared for each stimulus type (Figure 3.2d). The ratio of directed left vs. right events per second to each stimulus was consistent across individuals. As expected, the fish move and turn spontaneously when stationary gratings are shown, but with an equal number of events towards either direction.

As in Orger et al.[53], we found that the behavior was strongly tuned for the stimulus direction when both eyes were presented congruent whole field motion (LEFT and RIGHT, Figure 3.2d). To compare the net angle change across multiple fish, we adjusted for an individual fish's bias towards one or the other direction measured during the no-motion stimulus and calculated the bias-corrected angle change per second of stimulus presentation (Figure 3.3a). Each motion stimulus that contained a net motion, in either direction, evoked a larger angle change per second than the stationary stimulus, and, as expected for the OMR, this change was always in the direction of the stimulus motion. Surprisingly, monocular inward stimulation (REI and LEI) evoked much larger angle changes per second than monocular outward stimulation (REO and LEO), suggesting that the inward component of whole field motion contributes significantly more than the outward component to normal OMR turning behavior. The conflicting conditions (INWARD and OUTWARD) did not bias the net angle change in either direction. Interestingly, the average number of locomotion events per second (Figure 3.3b), with respect to the spontaneous rate occurring for the no motion condition, increased for any stimulus with an inward component (RIGHT, LEFT, REI, LEI and INWARD), even for binocular INWARD, which otherwise showed no influence on the directional bias of locomotion events. When the fish was stimulated with a monocular outward motion (REO, LEO), the rate of behavior was unchanged with respect to the rate of no motion events, however, when presented with binocular outward (OUTWARD) the rate of behavior events was significantly attenuated (for locomotion events per second: 12 fish, < 25 stimulus repetitions, Student's t-test, INWARD versus OUTWARD: $p < 0.00001$, INWARD versus LEO: $p < 0.001$, INWARD versus REO: $p < 0.001$, OUTWARD versus NM: $p < 0.001$). To determine what types of behavior events underlie the stimulus driven changes in the rate of motor activity, we compared the distribution of turn amplitudes that occurred during the different motion stimuli (Figure 3.3c).

Figure 3.3

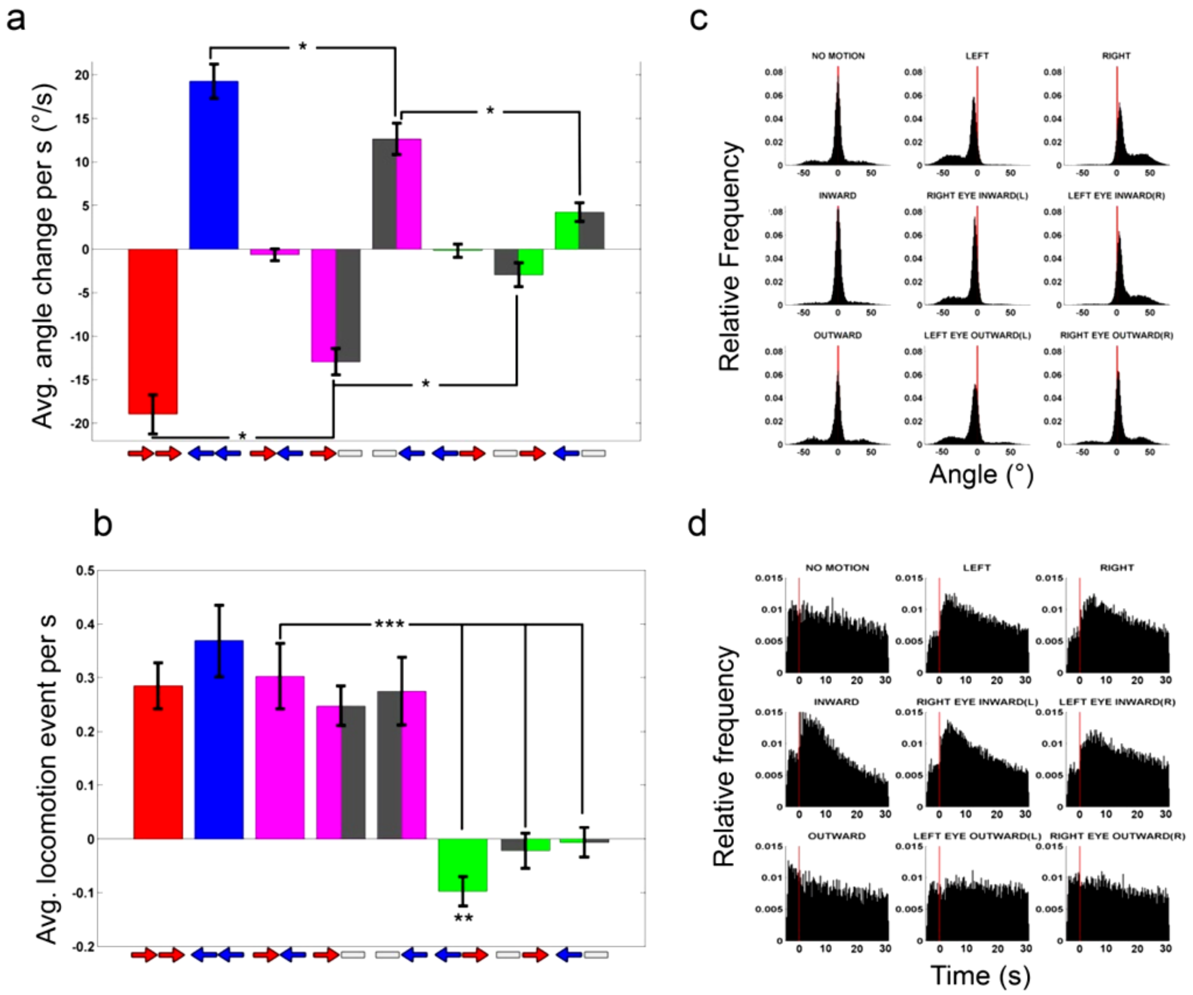

Figure 3.3 - Behavioral responses to variations of monocular and binocular motion stimuli. a Average angle change per second for all stimulation conditions, adjusted to the baseline “no motion” condition. Different colors of the bars indicate different stimulus conditions: red: binocular RIGHT, blue: binocular LEFT, magenta: binocular INWARD, magenta/gray: monocular inward stimulation/no motion stimulation for other eye, green: binocular OUTWARD, green/gray: monocular outward stimulation/no motion stimulation for the other eye. Arrows below each bar graph indicate the direction of motion that was presented to each eye. Gray bar indicates that a stationary stimulus was presented to that eye; error bars indicate s.e.m. (n =12 fish). Unambiguos stimuli evokes significantly increased angle changes per second than monocular inward and outward; monocular inward motion induces more turning than monocular outward stimulation. **b** Average number of locomotion events per second for all stimulation conditions, adjusted to the baseline no motion condition. Labels are the same as in **a**; error bars indicate s.e.m. (n =12 fish). Binocular inward stimulation evokes significantly more locomotor activity than outward stimulation. Binocular outward stimulation shows significantly supressed locomotor activity compared to the no motion condition. **c** Histograms of the relative frequency of per event angle changes for behavior events occurring during the different stimulation patterns. Note how the population of large angle turns is influenced by the coherent/conflicting motion stimuli. **d** The relative frequency of behavior events over the time course of each stimulus presentation. Most locomotion events occur 2 seconds after stimulus onset. Note, since fish can leave the experimental phase at different time points, the frequency of events for each time bin decays over the trial.

The distribution of angle changes reveals two distinct classes of events, large and small amplitude turns. During the no motion stimulus, as expected, the distribution is symmetric around the center, for both small and even large angle events. The whole field motion stimuli

(LEFT and RIGHT) appear to bias small angle turns towards the stimulus direction and increase the frequency of large angle turns in the same direction. Interestingly, large angle turns towards opposite the stimulus direction are absent, suggesting that the stimulus is able to suppress spontaneously occurring large angle turns in the “incorrect” direction. For the monocular inward stimulation (REI and LEI) the frequency of “incorrect” large angle turns is also greatly reduced, but not for the monocular outward stimulation (REO and LEO), for which large angle turns in the opposite direction still occur. If, as it appears, monocular inward stimulus components can somehow suppress large angle turns in the opposite direction, it is not surprising to find that INWARD stimuli do not drive large angle turns in either direction (for angle change per second: 12 fish, > 25 stimulus repetitions, Student’s t-test, RIGHT versus INWARD: $p < 0.00001$, RIGHT versus OUTWARD: $p < 0.00001$, RIGHT versus LEI: $p < 0.01$, RIGHT versus REO: $p < 0.00001$, LEI versus REO: $p > 0.002$, LEFT versus INWARD: $p > 0.000001$, LEFT versus OUTWARD: $p > 0.000001$, LEFT versus REI: $p > 0.01$, LEFT versus LEO: $p > 0.0001$, REI versus LEO: $p > 0.01$, LEO versus NM: $p > 0.002$, REO versus NM: $p > 0.0001$). Conflicting, binocular INWARD stimulation leads to an elevated locomotion level, albeit no directed turning, which suggests that a fish is still in an excited behavioral state while turning is inhibited; this suggests that inward motion (REI, LEI) stimuli may suppress neural activity on the contralateral side and thereby prevent accidental turning in the wrong direction. In addition, this finding also demonstrates that binocular INWARD stimuli do not cause the network to oscillate between the two turn directions, whereas binocular OUTWARD information might be allow for bistable behavioral states. Furthermore, the time course of the locomotion activity with respect to the stimulus onset (Figure 3.3d) reveals a fast onset of behavioral activity following the all directed turn inducing stimuli (LEFT, RIGHT, REI, LEI) as well as binocular INWARD (Figure 3.3d). These behavioral responses are stereotyped across individuals.

Together, these behavioral results demonstrate that different combinations of monocular motion stimuli can evoke different responses. Interestingly, the inward or outward components of whole field stimuli differentially influence OMR behavior, suggesting the possible independent neuronal processing of these stimulus types. However, whole field motion evokes stronger turning behaviors than monocular inward stimulation alone, and therefore inward and outward stimuli must be combined somewhere in the brain to produce these stronger responses. The conflicting combination of these elementary monocular motion stimuli gives clues about the underlying neuronal computation: binocular INWARD modulates locomotion event frequency, but does not drive large angle turns or net change in direction. Therefore, the neural circuitry must be stable enough to deal with such stimuli, which could be effectively accomplished by reciprocal inhibition. Taken together, these specific behavioral results suggest the following predictions about the neural control circuit: 1. Inward and outward stimuli are processed separately. 2. Inward and outward stimuli have to be integrated across eyes, i.e. combined within the brain, to drive the full whole-field, binocular OMR behavior. 3. All stimuli with a net direction of motion in one direction should show activation of the neural circuitry in the motor stages of neural processing. 4. INWARD conflicting stimuli must activate the same neural circuitry that allows for turning behavior but somehow compensate for activation from both sides. 5. Given the exclusive contralateral retinofugal projection, outward information must cross back over the midline to achieve lateralized activation neurons controlling directed turns.

However, before we can investigate the neural circuitry underlying these behaviors, we tested whether our stimuli can evoke equivalent behavior in a head-restrained zebrafish, a condition that most closely resembles the preparation used in the forthcoming neural recordings.

3.1.2 BEHAVIORAL RESPONSES TO MONOCULAR MOTION IN HEAD RESTRAINED ZEBRAFISH

To ensure that the behavioral responses found in freely swimming fish can be compared to neural correlates from restrained fish, the same stimulus set was presented to partially restrained (head-embedded, tail-free) zebrafish (Figure 3.4a). Zebrafish larvae (5-7dpf) were fully immersed in low melting temperature agarose dorsal side up on a clear, sylgard coated petri dish. Part of the solidified agarose was carefully removed to leave the fish tail free to move, while the head position was stable, even during vigorous swimming. Again, stimuli were presented from below and the zebrafish was centered and aligned on an eye-segregating blank region. To further assure the independence of eye stimulation, the blank region was made larger (1.5 cm), because the fish was slightly further away from the projection screen than in the freely-swimming assay. This preparation allowed measuring tail motion from above with a high speed camera (500Hz) in response to visual stimuli from below. A simple algorithm that tracks the left-right tail position was used to detect behavioral responses (Figure 3.4a, b) during stimulus presentation. Deviation of the fish tail center of mass from the resting position, in either direction, was used to measure the net movement of the fish tail in response to each visual stimulus (Figure 3.4c). The average net tail movement for 12 fish reveals that coherent whole field stimuli evoked the most movement, monocular inward stimulation evoked less movement, and the other stimuli evoked no movement. Interestingly, the time course of the response was much slower than for freely behaving fish; the onset of tail movement did not begin until 2 seconds following motion stimulus onset and did not peak until six seconds. The raw tail position data from individual trials was used for the classification of each distinct tail behaviors into four distinct classes: right turns, left turns, swims and struggles (Figure 3.4d). Whereas turns are indentified by high amplitude tail motion with sluggish rebound to the resting tail position, swims show small amplitude changes with an oscillation (multiple zero-crossings) component. Struggles show both high amplitude and multiple oscillations. Summary data for 12 fish analyzed for behavioral choices in response to the 9 stimulus combinations are shown for swims and struggles (Figure 3.4e) and for directed turns (Figure 3.4f). Compared to the measurements from freely behaving fish, the data from head restrained fish suggest that the monocular outward and binocular conflicting stimuli do not drive any behavior. However, since spontaneous motion in head embedded zebrafish is suppressed (see also Figure 3.24) it was not surprising to find that the no motion condition shows little or no activity. In freely swimming fish, binocular OUTWARD visual motion or monocular outward stimuli appear to inhibit spontaneous motion, thus it was not surprising that the directional bias in the behavioral responses in these conditions is not detectable either. However, tail movement evoked by whole field motion and monocular inward stimuli follow the general pattern of responses found in freely swimming fish, which suggests that the essential neural processing of these behaviors is present in head restrained animals, and thus imaging techniques can be used to monitor the associated neural activity.

Figure 3.4

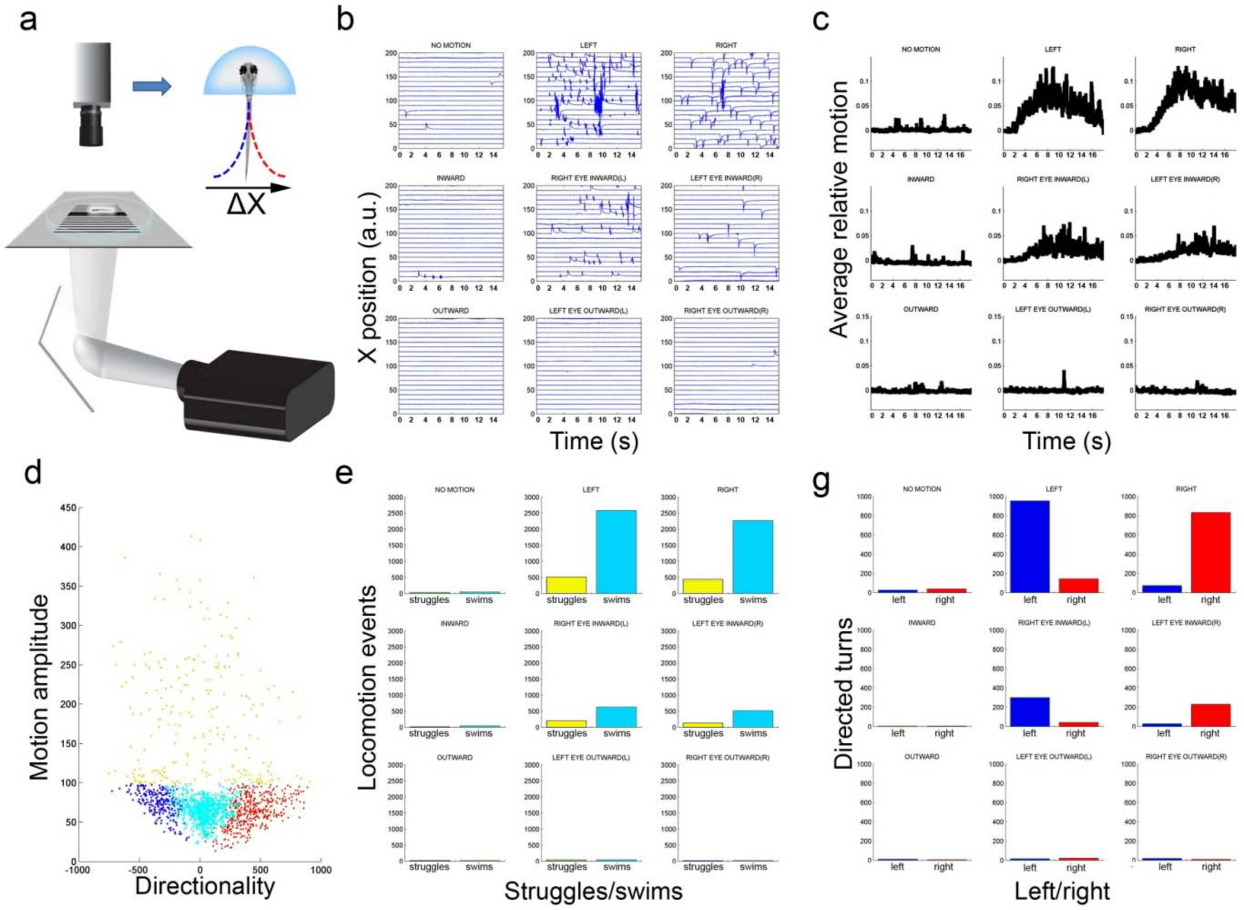

Figure 3.4: **Behavioral responses to variations of monocular and binocular motion stimuli in head restrained zebrafish:** **a** Schematic of behavioral set up. Head restrained zebrafish were presented with motion stimuli from below while their tail motion was monitored with a high-speed camera (500 Hz). **b** Raw example traces of 10 stimulus repetitions for each stimulus condition. Positive and negative changes from baseline correspond to tail motion to the left and right, respectively. **c** Time course of average relative tail motion of 11 zebrafish. Note, that behavioral events only begin 2 seconds after stimulus onset. **d** Single tail motion events can be sorted into 4 different catagories: events with high motion amplitude (to either left or right) are classified as struggles (yellow), events with low motion amplitude, but with a high frequency zero crossings are classified as swims (cyan). Directed turns with low motion amplitude, high directionality and a low frequency zero crossings can be classified as either left turns (left) or right turns (red). **e** Locomotion events classified as struggles or swims in response to the 9 stimulation patterns for all 11 fish. **f** Directed turns for all 11 fish in response to the 9 stimulation patterns.

3.1.3 NEURAL RESPONSES TO MONOCULAR MOTION STIMULATION

To identify components of the neural circuitry that mediate OMR behaviors, we recorded from neurons within the zebrafish during the presentation of whole field motion stimuli. In order to analyze the neural activity patterns for each eye contribution independently, we again used the elementary motion stimuli (Figure 3.1b). Neural activity was measured with functional imaging experiments, using both synthetic and genetically encoded calcium indicators, employing two-photon microscopy[157]. Two-photon excitation was essential because infrared excitation light is invisible to the fish and, furthermore, facilitates access to the deepest cells of the fish' brain. Typically, OMR responses were stable for longer than 15 hours, which allowed imaging at many focal planes and analysis of the response properties spanning large brain volumes. We began our investigation from the 'bottom up', since we knew from previous studies which neurons are involved in controlling OMR turning behaviors at the level of the reticulospinal projection neurons.

3.1.4 NEURAL RESPONSES OF HINDBRAIN SPINAL PROJECTION NEURONS REFLECT THE BEHAVIOR

Previously, a small, identifiable subpopulation of functionally lateralized ventromedial reticulospinal cord neurons (ventromedial cells) was found to be a necessary component in the circuit underlying visually evoked turning responses of the OMR. To determine which role these cells play in the behaviors evoked by the monocular stimulation described above, we monitored the activity of these neurons with synthetic calcium indicators during presentation of visual stimuli (Figure 3.5). The same set of nine stimuli, as used in the head restrained behavioral experiments, were presented to fish positioned beneath a two photon-microscope, except that only the red spectrum of the stimulus was used to avoid the stimulus detection by the photon multiplier tubes. For these experiments, zebrafish were injected with dextran-conjugated Oregon Green BAPTA into the spinal cord and screened for labeling in the reticulospinal cord neurons 24 hours later (Figure 3.5a). A projection of spinal projection neurons labeled with Texas Red dextran in a zebrafish expressing a green fluorescent protein (HuC:GCaMP2) shows the location of the ventromedial cells with respect to the rest of the zebrafish brain (Figure 3.5b,c). Fish with sufficient labeling in the low residing ventromedial cells were embedded in agarose and paralyzed to avoid motion artifacts during imaging. The average responses from 10 stimulus repetitions for 8 fish were analyzed by grouping the ventromedial cells according to their location either left or right of the midline (Figure 3.5e-g). As shown previously, cells on the right or left side of the midline show strong preference for stimuli moving to the right or left, respectively. Some neurons in this cluster did not respond at all to the presented stimuli, which was not surprising given that some ventromedial cells are mostly responsive to stimuli moving forward. Notably, the amplitude of the average responses resembles the behavioral data in that neurons responded stronger to whole field motion, less so to monocular inward stimulation, and much less so to monocular outward stimulation. Activity of the majority of these reticulospinal cord neurons reflects the behavioral responses, which suggests that inward and outward motion information from each eye has been combined prior to reaching this stage of neural processing (Figure 3.5d-f). To identify the upstream neural circuitry, which provides the input to the ventromedial cells, we required a technique other than the retrograde labeling from the spinal cord. Ideally, a sensitive calcium indicator in all neurons, which serves as both functional and anatomical marker, would allow the investigation neural responses throughout the rest of the brain. Although bolus loaded synthetic calcium indicators provide a means to image populations of neurons, they need to be delivered with invasive techniques and cannot be delivered to all regions of the brain simultaneously. In contrast, neural activity could be measured in transgenic zebrafish that express a genetically encoded calcium indicator (GECI) in all neurons.

Figure 3.5

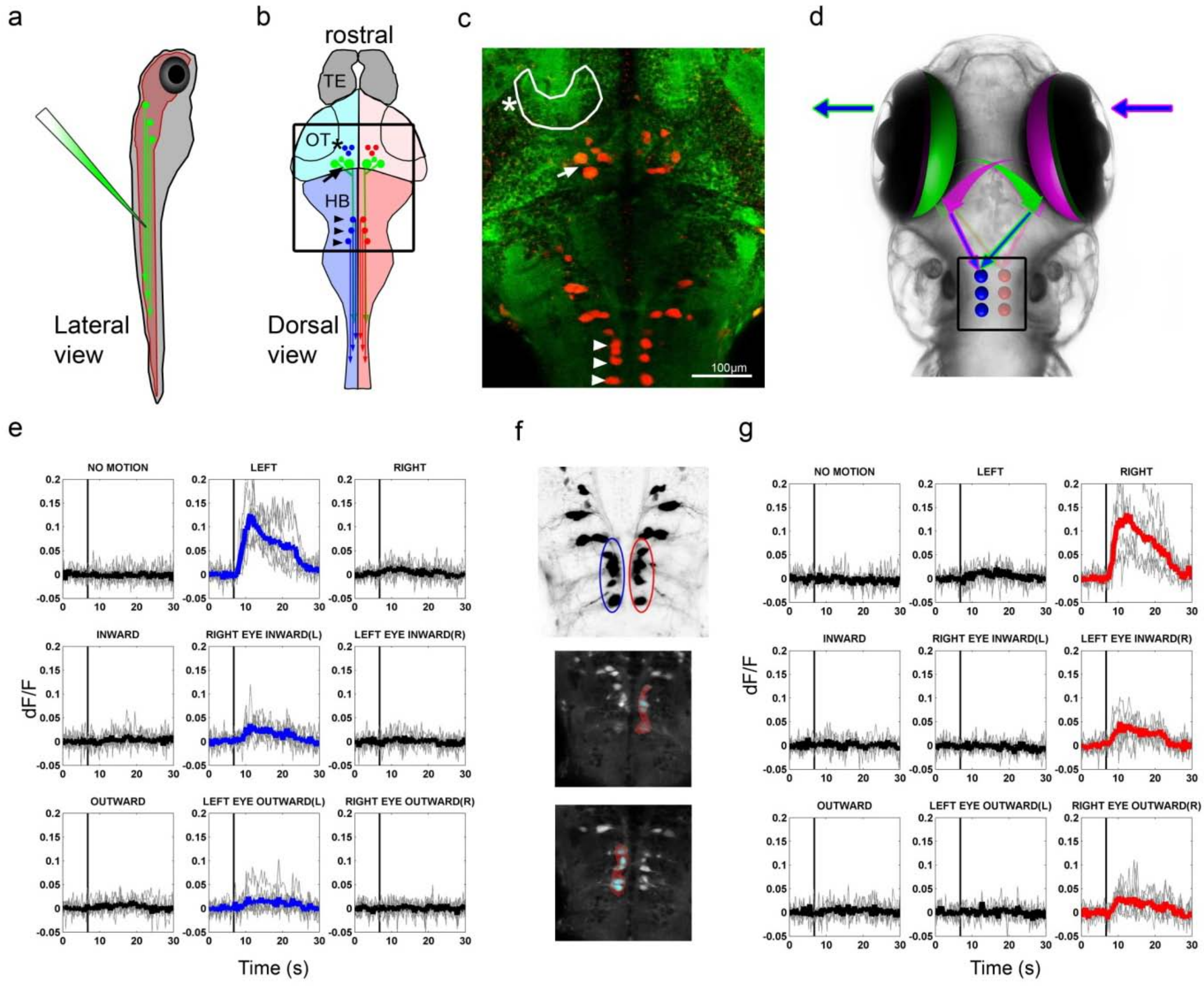

Figure 3.5 - Ventromedial reticulospinal neuron responses to monocular and binocular whole-field motion stimuli

Figure 3.5 - Ventromedial reticulospinal neuron responses to monocular and binocular whole-field motion stimuli: **a** Schematic of the technique of labeling the descending reticulospinal neurons with dextran conjugated dyes. A beveled glass electrode is used to sever the axons of the spinal cord while injecting fluorescent dye. The dye is taken up by the axon and retrogradely labels the cell bodies within the brain. **b** Schematic of zebrafish brain showing pretectal neurons (asterix) in blue and red and the NucMLF (arrow) in green in the midbrain. Caudal to midbrain boundary, the ventromedial cells (arrow heads) are shown in blue and red. TE: telencephalon, OT: optic tectum, HB: hindbrain. Rectangle demarcates area shown in c. **c** Z-projection of two-photon optical sections (200 µm below the surface) of a transgenic *HuC:GCaMP2* fish with Texas red labeled reticulospinal cord neurons, most neurons of the zebrafish brain in green and reticulospinal cord neurons in red. Asterix (*) and outline demarcate the pretectal area. Large red neurons of the NucMLF are indicated (arrow) on the left of the midline and, on the right, some of the smaller NucMLF cells are also labeled. Further caudal, the 3 clusters of the ventral medial cells are indicated by arrow heads. **d** Schematic illustrating the location of the ventromedial cells with respect to zebrafish head (rectangle) and the minimum necessary circuit that would allow these cells to acquire lateralized motion responses. Illustrated here for a fish that sees whole field motion to the left, inward and outward information (magenta and green) could be combined directly by the ventromedial cells by direct connection to retinal ganglion cells (arrows) arriving from the each brain hemisphere. **e** Calcium responses from left ventro medial cells for the 9 different stimulation patterns. Averages from 10 repetitions of individual fish are shown in light gray and average of all fish are shown in black or blue for unambigous motion stimuli to the left (n = 8 fish). Vertical line demarkates stimulus motion onset. **f** Texas red labelled cells show the cells that were chosen for analysis in **e** and **g**. Z-projection of example recording with region of interest are shown below. **g** Calcium responses from right ventromedial cells.

3.1.5 GENERATION AND EVALUATION OF PAN NEURONAL TRANSGENIC LINES

Figure 3.6

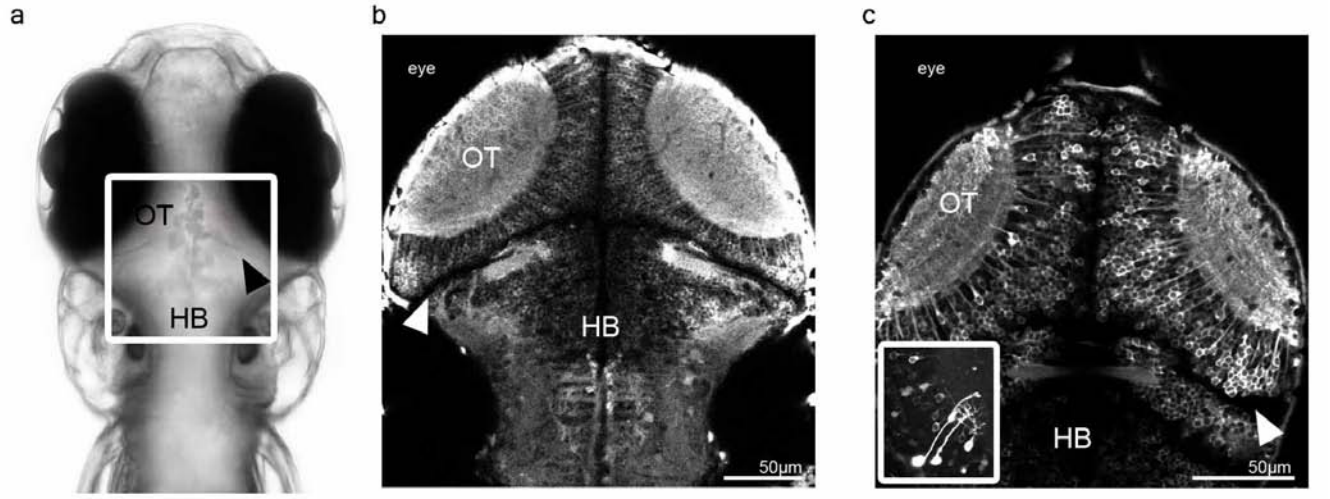

Figure 3.6 – Stable expression of GECIs throughout the zebrafish brain: **a** Bright-field image of the zebrafish with an overlaid rectangle indicating the location of the two-photon micrographs displayed in **b** and **c**. OT = optic tectum, HB = hindbrain, arrowhead points to the midbrain hindbrain boundary. **b** A two-photon optical section through a *HuC:GCaMP2* transgenic fish, approximately 100 µm below the dorsal surface. **c** A two-photon optical section through a Nbt:TnlXXL transgenic fish at a similar location and depth to the one shown in **b**. Inset shows neurons that transiently express TnlXXL in the optic tectum. Many neurons in the stable transgenic lines show labeling in this nucleus as well.

For the purpose of generating transgenic zebrafish that express a genetically encoded indicator in all neurons, different DNA constructs were produced with the cDNAs TnlXXL[82], GCamP1.6[80], and GCamP2[158]. These genetically encoded calcium indicators show great promise for such applications[159-161,82,162,163].These were subcloned into expression vectors that contained a neural specific promoter. The complete form of the HuC promoter[48] was used to achieve quasi panneuronal expression. Since the endogenous protein encoded by the HuC gene is expressed in all (or almost all) differentiated neurons, this promoter is likely to reproduce a panneuronal expression pattern (Figure 3.6). To facilitate transgenesis, the expression vectors containing a promoter followed by the encoding DNA of a GECI, were flanked with Tol2 transposable elements. These DNA constructs were co-injected with mRNA for the Tol2 transposase into one cell stage zebrafish embryos[47]. Transiently expressing fish were used for preliminary experiments to test the constructs in zebrafish and all constructs were confirmed to be functional (data not shown). To generate stably transgenic fish, embryos with fluorescence were selected, raised and out-crossed to wild type to screen the fry for founder candidates which were offspring form germ cells that had successfully integrated the foreign DNA. Due to positional effects, these founders can differ tremendously in expression pattern and level. Fish with the best expression patterns were again raised to adulthood and out-crossed again to produce the stable F2 fish that were used in most experiments. Although all constructs were functional in transiently expressing larvae, the ratiometric indicators showed either small or no signals to stimuli that evoked large responses in two of the *HuC:GCaMP2* lines. In our hands, multiple transgenic lines with stable expression showed side effects due to over expression or no fluorescence signal changes (Figure 3.6c). For our application, two particular *HuC:GCaMP2* stable lines emerged as the best choice for our application. Most likely, these stable transgenic lines had expression levels that strike a good balance between bright fluorescence, for high signal to noise ratio, and low toxicity. All data presented and discussed here was acquired from a offspring of one particular line of stable *HuC:GCaMP2* transgenic zebrafish. Although it is unlikely that few or single action potentials can be detected within this fish, it provides a powerful tool to map the neural circuitry with stimuli that are expected to drive strong neural activity, such as stimulation with whole field motion.

To test whether we can detect neuronal activation of neurons with known response properties, we performed some functional imaging experiments with *HuC:GCaMP2* fish focusing on the easily detectable NucMLF neurons. These neurons can be identified by position and size near the midbrain hindbrain boundary. We presented whole field motion gratings drifting in eight different directions to paralyzed fish while recording the neural activity. As reported previously, these neurons show a strong forward direction preference (tail to head motion). In Figure 3.6.1, exemplary data for these NucMLF cell responses are shown.

Figure 3.6.1

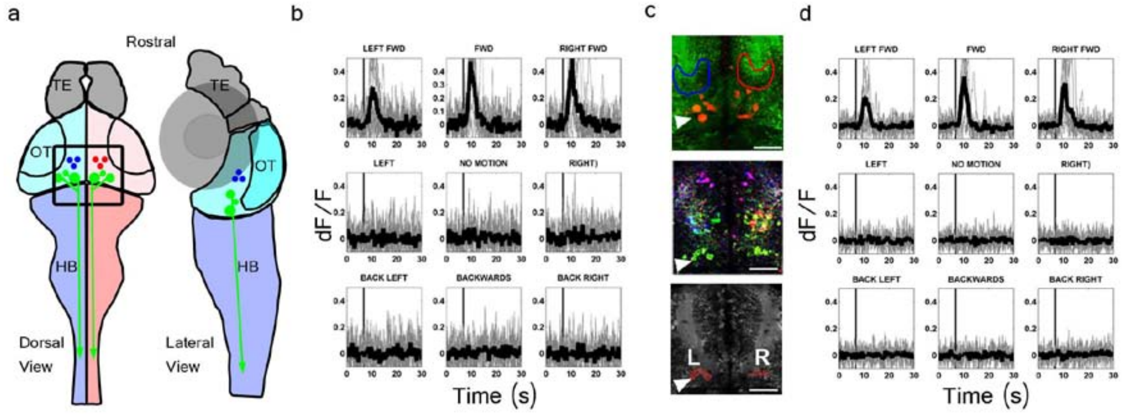

Figure 3.6.1- Calcium responses within then NucMLF of *HuC:GCaMP2* transgenic fish: a Dorsal and lateral view of a schematized zebrafish brain, highlighting the pretectal neurons (blue and red) and the NucMLF (green neurons within the midbrain). The rectangle demarcates the region of interest shown in **c**. TE: telencephalon, OT: optic tectum, HB: hindbrain. **b** and **d** Average calcium responses of NucMLF neurons recorded in a *HuC:GCaMP2* transgenic fish that were presented whole field sinusoidal gratings moving in eight different directions. The vertical line indicates the time of stimulus motion onset. Single repetitions (gray) are overlaid with the average responses (black); **b** shows responses from the left and **d** from right NucMLF neurons. **c** Top: Two-photon section revealing green neurons in a *HuC:GCaMP2* transgenic fish and red NucMLF neurons that were backfilled with Texas Red dextran. Blue outline demarcates pretectal areas to the left of the midline, red outline for the right. Middle: Two photon image acquired during calcium recording with pixels colored according to dF/F changes from baseline for each of the stimulus directions: green – (forward), blue – (forward left, left, back left) and red – (forward right, right, back right). Each pixel is coded by the intensity of the response and with a color depending on the activation by the stimulus in a particular direction. Bottom: the same two photon section, showing the region of interest taken for the left and right NucMLF neurons for which the time series data is shown in **b** and **d**. Scale bar = 20µm.

3.1.6 NEURAL RESPONSES OF RETINAL GANGLION ARBOURIZATION FIELDS REFLECT SENSORY INFORMATION

In order to identify the arbourisation field(s) of the retinal ganglion cells that carry the visual information driving the OMR, we performed calcium imaging experiments using the *HuC:GCaMP2* transgenic line within brain regions that are known to receive retinal ganglion cell afferents. The retinorecipient tectum (AF10) and AF9 were reported to not be involved in mediating the OMR response of zebrafish (Figure 1.6)[60]. Therefore, we concentrated our efforts to regions that contain the remaining AFs. Due to the complete crossing of retinal ganglion cells and the response properties found in reticulospinal cord neurons involved in the OMR, we expected to find persistent activity that would be eye specific at the early sensory level and show no modulation of activity during stimulation of the other eye. *HuC:GCaMP2* transgenic zebrafish were embedded in agarose, paralyzed, and neural activity was recorded in response to the set of nine stimuli. We found a region with strong activation by these stimuli deep below the tectum, which we identified as AF6 by comparing anatomical landmarks within the *athonal:GFP* transgenic fish and previous tracing studies (Figure 3.7a,b). Other retinorecipient regions, the optic tectum and regions with other suspected arbourisation fields, showed no, or very transient, activation to the stimuli presented. In Figure 3.7c and d average data of the functional imaging experiments in either the left or right AF6 is shown. To visualize the neuronal structures activated during stimulus presentation, the dF/F time series measurements from all pixels were analyzed and stimulus associated fluorescence changes were translated into intensity values and color coded for a particular type of stimulus. These color-coded images of the functional imaging experiments provide information on the location of neural activation evoked by a particular stimulus. For example, in Figure 3.7c and d the region that is activated by stimuli to the contralateral eye can be clearly delineated, whereas other stimuli do not activate this region at all. As neither AF6 shows activation of stimuli presented to the ipsilateral eye, activation patterns of this region can serve as an additional demonstration of that the monocular stimulation pattern is able to deliver motion information to each eye independently (Figure 3.7). In contrast to the responses from reticulo spinal cord neurons, at this level of visual processing all stimuli are equally represented. For example, average data for multiple fish clearly shows that each stimulus component (inward or outward) evokes the expected sensory activation for both directions, indiscriminate of the context in which the motion stimuli were shown (Figure 3.7f,g). Furthermore, when single regions of interest are analyzed; distinct regions can be separated into inward and outward responsive regions (Figure 3.7e). This spatial separation of direction selectivity indicates that inward motion and outward motion enter the brain via two separate pathways and that the activity evoked by inward and outward stimuli are potentially mediated by a different set of retinal ganglion cells, as has been proposed previously[121,105,108,164,110]. As the changes in calcium most likely reflect the activation of presynaptic terminals, these may form specific synapses with their postsynaptic partners, which, we speculate, might be involved in the processing of information coming from the retina. Notably, the activation for monocular inward stimulation is of the same magnitude as the inward stimulation that occurs as part of a whole field coherent or binocular conflicting stimuli. The same is true for outward stimuli components (Figure 3.7). These results are consistent across fish and none of the animals that were analyzed deviated from this activation pattern.

Figure 3.7

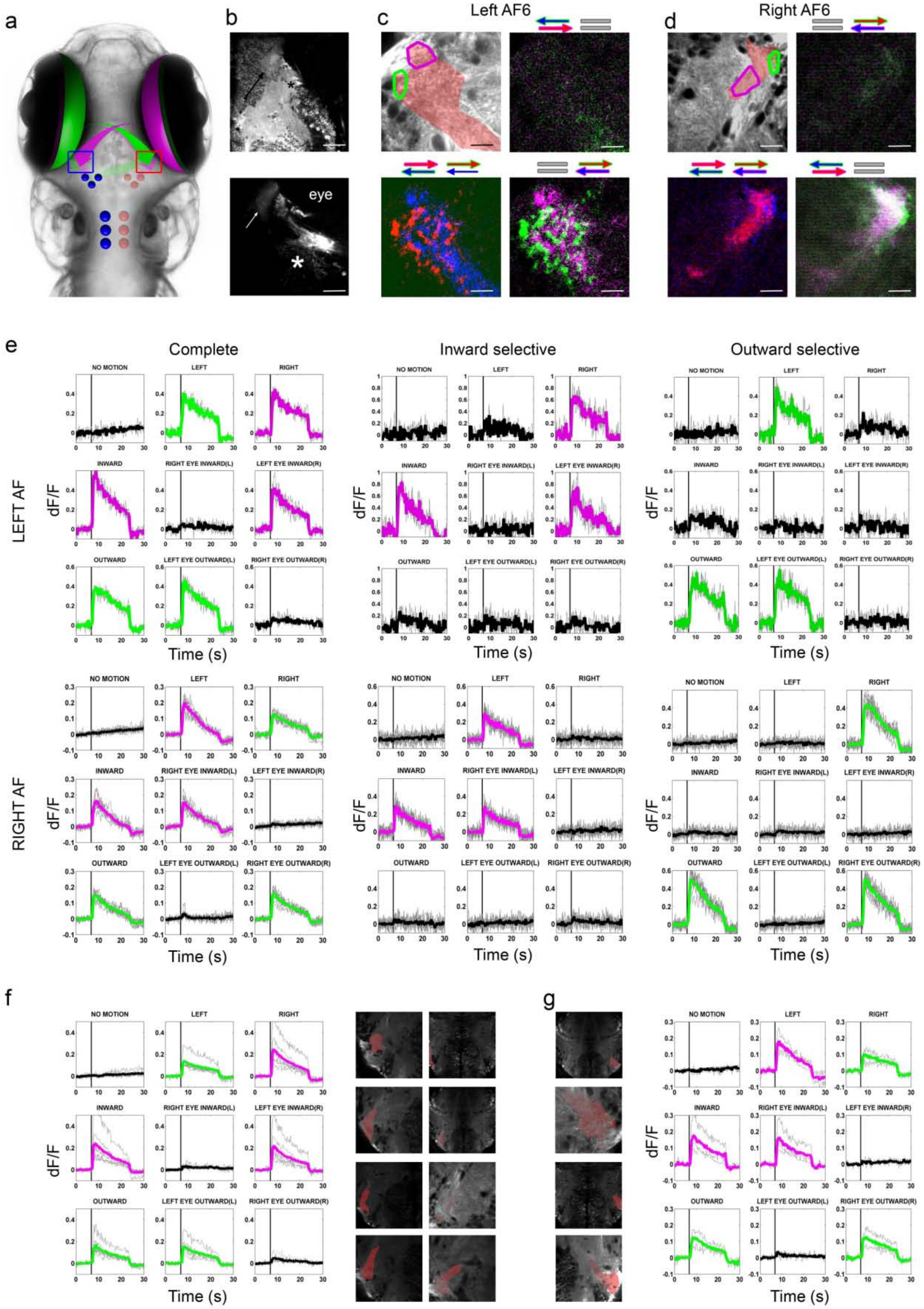

Figure 3.7 - Retinal ganglion arbourisation field calcium responses to monocular and binocular whole-field motion stimuli

Figure 3.7 - Retinal ganglion arbourisation field calcium responses to monocular and binocular whole-field motion stimuli: **a** Schematic depiction of the targeted imaging site (blue and red rectangle). **b** Top: Z-projection of two-photon optical sections through a HuC:Chameleon pan-neuronal fish showing the lower part of the right AF 9 (arrow) and the region we term AF6. Bottom: Z-projection of two-photon optical sections through the ath5:GFP transgenic fish, at approximately the same depth, both lower portions of AF9 and AF6 is visible. Scalebar = 10 μm **c** Top Left: The left AF6 in *HuC:GCaMP2* transgenic fish is shown with the ROIs for the time series shown in **e** (left AF6). Top Right: The color-coded average calcium data shown for stimulation of the left (ipsilateral) eye. No activation was detected, as expected, because retinal ganglion cells cross exclusively to the contralateral side. Bottom Left: Stimulation of the contralateral eye evokes strong activation. Average calcium data is color-coded for whole field LEFT and RIGHT motion. A clear delineation of regions with selectivity for one or the other direction is visible as they appear in either blue (LEFT) or red (RIGHT) with little overlap, which would appear purple. Bottom Right: When color-coded for inward (magenta) and outward (green) motion, it is apparent that AF6 is segregated into inward and outward regions responsive to the contralateral eye. Scalebar = 5 μm **d** Top Left: Further zoomed out (Scalebar = 25 μm) projection of the right AF6 in *HuC:GCaMP2* transgenic fish is shown with ROIs for the time series shown in **e** (right AF6). Top Right: The color-coded average calcium data shown for stimulation of the right (ipsilateral) eye results in no activation. Bottom Right: Average calcium data colorcoded for whole field LEFT and RIGHT motion. Selectivity for one or the other direction is visible as they appear in either blue (LEFT) or red (RIGHT). In this plane more overlap appearing purple can be detected. Right: Colorcoded for inward (magenta) and outward (green) motion calcium average data collapsed from 30 μm calcium imaging data shows overlap of both regions within the center (white regions), whereas regions specifically selective to inward or outward motion stimulation can still be detected. Above and below these 30 μm, no activation could be measured, suggesting that this volume of neural tissue (~30x15x15 μm) represents a specific region that is involved in whole field motion processing. **e** Average calcium time course for both left and right AF6 is shown from the ROIs indicated in **c** and **d**. ROIs integrated data over the whole region that was activated during motion stimulation. Inward vs. outward selective regions of interest were selected manually. Average calcium data is color coded magenta for inward and green for outward stimulus components presented to the contralateral eye. **f** Average calcium data from the right AF6 is shown (n = 8). ROIs are shown to the right. **g** Average calcium data from left AF6 is shown (n = 4). ROIs are shown to the left.

To further investigate whether the same region is involved in mediating the OMR to motion directions other than left and right, we performed similar calcium imaging experiments with different stimuli. Instead of the set of nine stimuli, the fish were presented with just one large moving grating, drifting in eight directions (Figure 3.8). As the same region (AF6) is activated by all motion stimuli, it suggests that this could be the neural substrate that is the generic entry site for other whole field motion stimuli. All directions are represented at this level of processing, even though activation is biased towards forward motion and motion in the direction of the side of the brain in which the AF itself is located: leftward motion in the left AF and rightward motion in the right AF. Together, these results identify this region as a potential entry site for OMR relevant visual motion information, but also demonstrate that, at this stage, all sensory information is represented and available for the further processing necessary for the reported specificity of the neuronal responses in the ventromedial cells and behavioral choices.

Figure 3.8

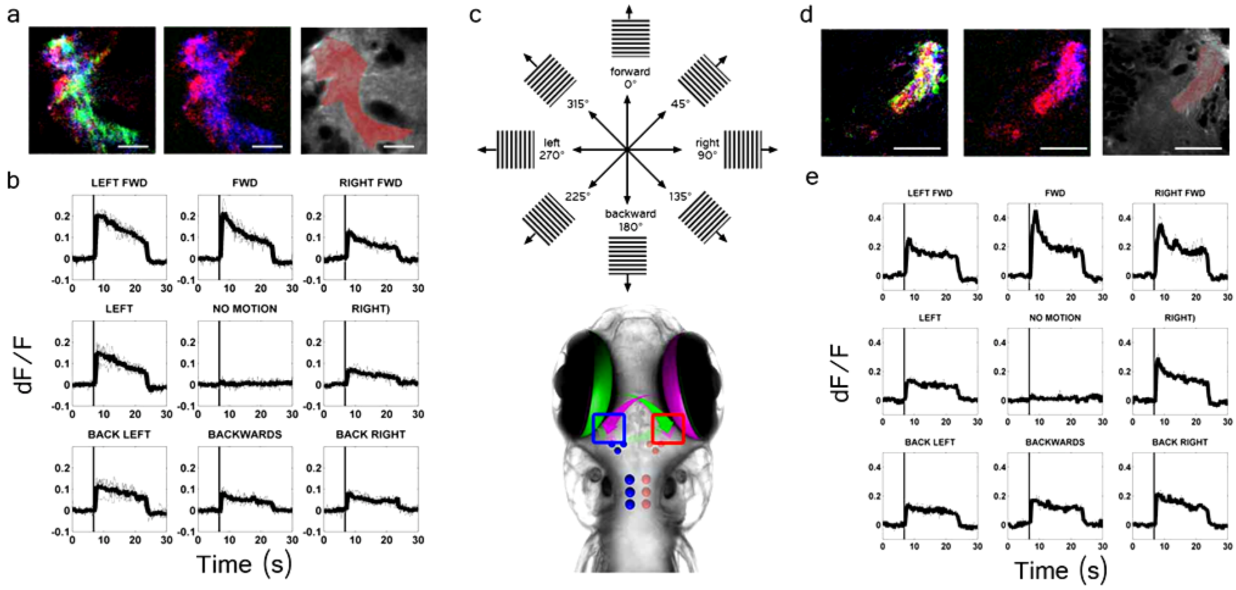

Figure 3.8 - Direction selectivity of retinal ganglion arbourisation field 6: **a** Left AF6 calcium recordings in *HuC:GCaMP2* fish. Left: Color-coded activity image (left stimulus in blue, right stimulus in red and forward stimulus in green). Middle: Removing forward motion from the dataset results in regions segregated into right and left selective regions. Right: Z-projection of two photon sections shows the ROI used for the time series analysis shown in **b**. The left AF6 is responsive to all directions with stronger activation to motion with a leftward or forward component. **c Top:** Schematic of stimulation patterns. Bottom: Blue and red rectangles indicate the region of imaging within the fish. **d** Right AF6 calcium recordings in *HuC:GCaMP2* fish. Right: Color-coded (as in **a**) activity image. Middle: Removing *forward* motion from the dataset results in regions segregated into right and left selective regions. Right: Z-projection of two photon sections shows the ROI used for time series analysis in **e**. The right AF6 is responsive to all directions with stronger activation to motion with a rightward or forward component. (Scalebars = 10µm)

3.1.7 NEURAL RESPONSES OF PRETECTAL NEURONS RESEMBLE THE BEHAVIOR

In order to identify neuronal substrates that are involved in the further processing of the visual information present at the level of AF6, we performed preliminary calcium imaging experiments in the vicinity of the AF6 with the same nine stimulation patterns. We expected neurons that provide input to Ventromedial cells to show activation by stimuli that evoke turns, and therefore show lateralized responses with a functional counterpart on the other side of the midline that would be activated by motion stimuli moving in the opposite direction. By performing imaging experiments throughout the whole midbrain region of the zebrafish brain, we were able to detect a number of direction selective, but only transiently activated neurons in the upper region of the tectal subventricular zone (data not shown). By far the strongest and most consistent activation could be detected in a region ventral to the posterior medial tectum, but dorsal to the NucMLF. We believe this region to be the pretectum and will term cells in this region pretectal neurons (Figure 3.9).

Figure 3.9

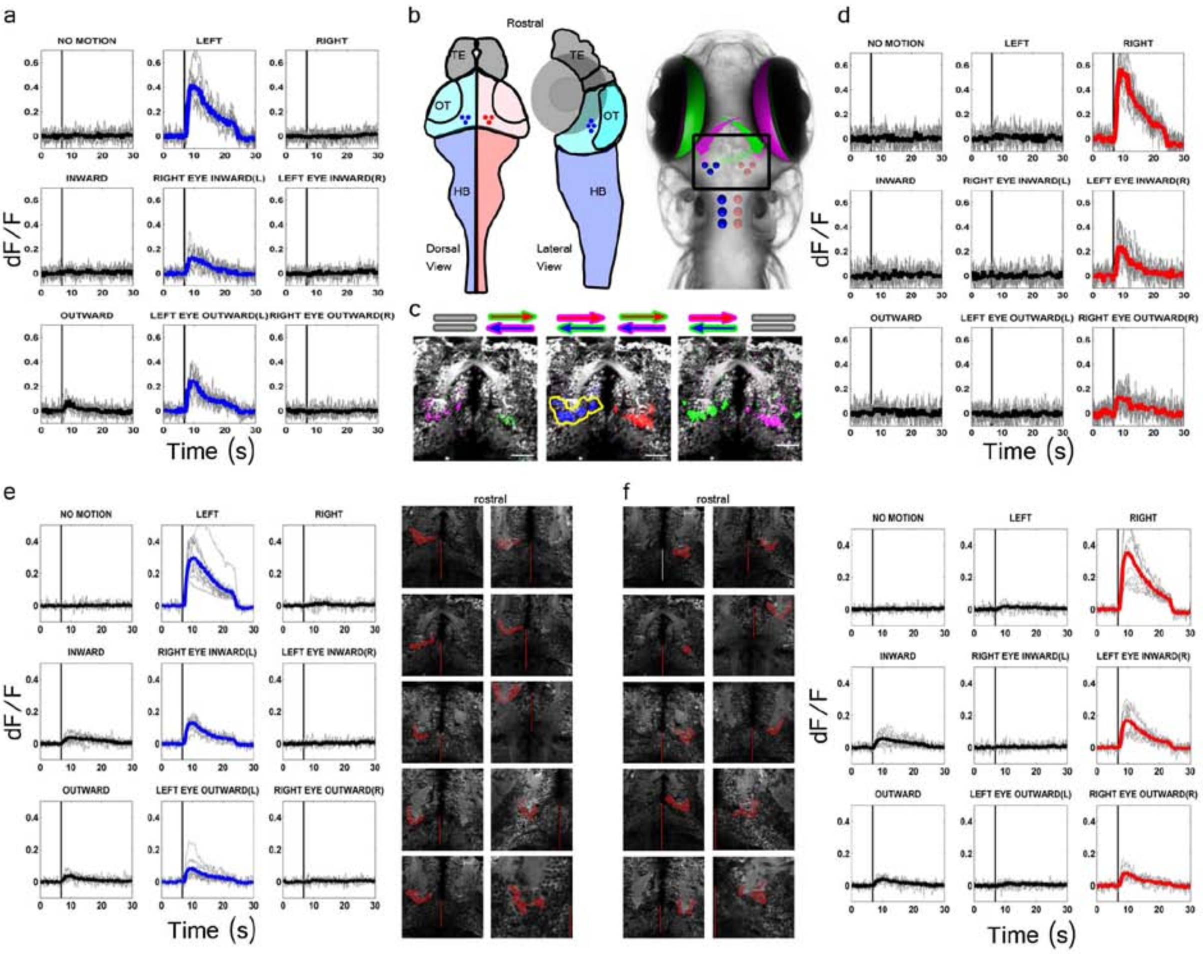

Figure 3.9- Pretectal neuron responses to monocular and binocular whole-field motion stimuli: **a** Calcium responses measured in a single plane of a *HuC:GCaMP2* transgenic fish in the left pretectal area to the 9 stimulation patterns. Ten stimulus repetitions are shown in light gray and averages are shown on top as thick lines. For stimuli with net motion to the left, averages are shown in blue. **b** Dorsal and lateral view of schematic zebrafish brain, showing the location of pretectal neurons in the midbrain, below the optic tectum. Schematic that illustrates the location of pretectal neurons within the zebrafish head (rectangle) and suggests the flow of information that the circuit might use to produce lateralized motion responses. **c** An average two photon section acquired during the calcium measurements shown in **a** and **d**. Responses greater than 0.1 dF/F for the different stimuli are overlaid to show the location of the active of regions during a particualr stimulus combination. From left to right: The first panel shows responses for stimulation of the right eye, magenta or green for either inward (blue/magenta arrow) or outward motion (red/green arrow) to the right eye, respectively. Second panel: responses to either left or right stimuli in blue and red. Yellow outline shows an examplary ROI for data shown in **a**. Third panel: responses to left eye stimulation only, inward motion responses are shown in magenta or green for outward motion. Scalebar = 20µm. Note: stimulation to one eye evokes responses in both halfs of the brain, suggesting the combination of congruent moton stimuli in this population of neurons. **d** Calcium responses in right pretectal neurons, from the same recording shown in **a**. **e** Average calcium responses in left pretectal ROIs (regions shown at the right). Single fish averages are shown in gray (n = 10 fish). **f** Average calcium responses of left pretectal ROIs (regions shown at the left). Single fish averages are shown in gray (n = 10 fish).

Similar to ventromedial cells, the pretectal neurons are activated strongly and persistently by whole field motion in their preferred direction, which is right for neurons right of the midline and left for neurons left of the midline (Figure 3.9e,f). Analysis of their response properties reveals that the majority of neurons within this region receive input from both eyes. Evident from their response patterns, neurons respond to inward motion from the contralateral eye and to outward motion to the ipsilateral eye. This activation pattern is particularly evident when data is color-coded for eye specific stimuli (Figure 3.9c). This finding suggests that the inward information that might enter the brain via specific direction selective retinal ganglion cells via the optic chiasm could simply provide input to the pretectal neurons without crossing the midline. Outward information from the ipsilateral eye, however, must somehow cross back over. In many cases, monocular inward motion leads to stronger activation than monocular outward information, possibly providing the grounds for stronger turning responses for monocular inward stimulation. Furthermore, we find that some of these neurons that combine the input from both eyes also respond weakly or strongly to conflicting stimuli (binocular INWARD and OUTWARD) as evident in the average responses (Figure 3.9e,f). However, we also find pretectal neurons that only respond to conflicting stimuli and congruent whole field motion. Further evidence of the independent processing of inward and outward motion stimuli are provided by neurons that are only responsive to stimulation of either inward or outward motion to one eye. A few cells with such different response types are depicted in Figure 3.10, but further experiments are necessary to quantify the proportion of different cell types based on response properties.

Figure 3.10

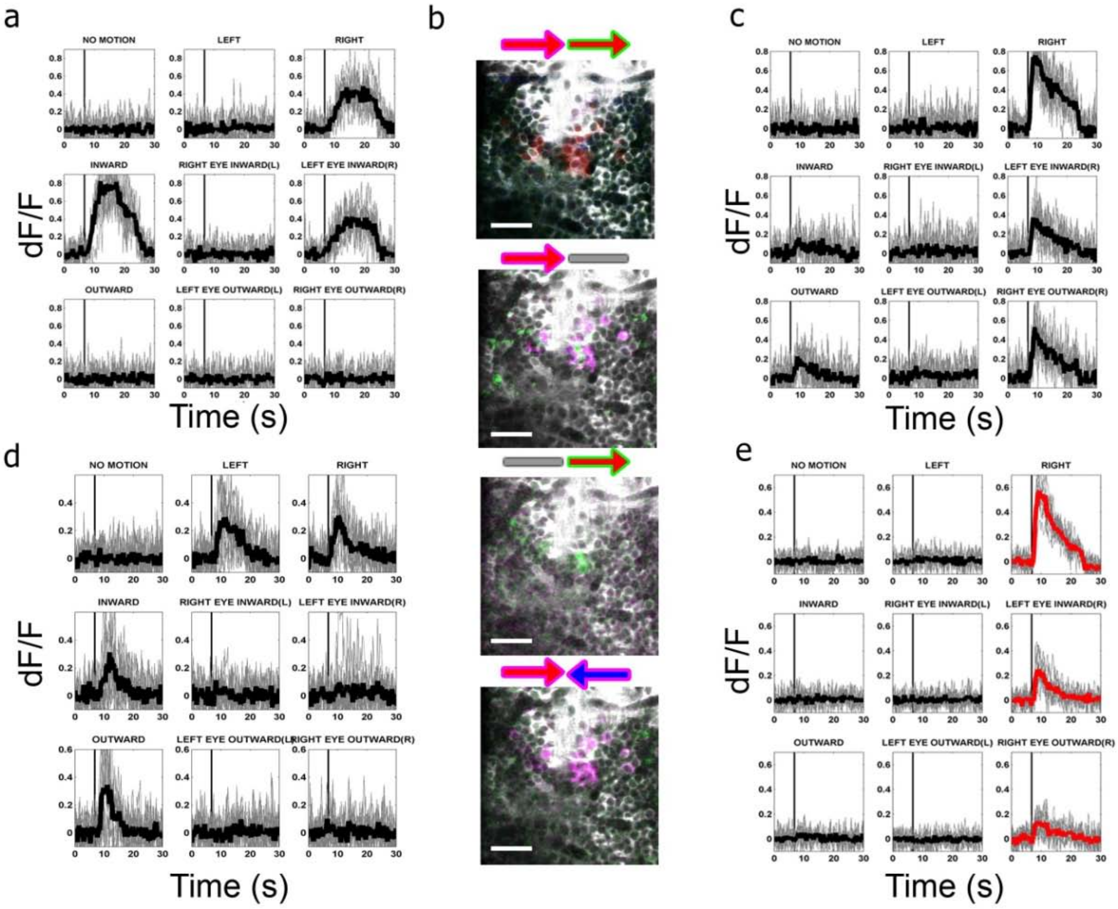

Figure 3.10 - Different combinations of visual motion information in different pretectal neurons: **a**, **c-e** Average calcium responses found in single neurons of the right pretectal area. Responses to single stimulus repetitions are shown in gray, average response in black/red. **a** Exemplary neuron showing responses to all inward components of a rightward stimulus. **b** Z-projections of two photon optical sections showing neurons responding to different types of motion stimulation. Scalebar = 20µm. **c** Pretectal neuron responding primarily to rightward motion, but also weakly to INWARD and OUTWARD stimuli. **d** Pretectal neuron responds exclusively to binocular stimulation. **e** Typical right pretectal neuron response.

Furthermore, we monitored the activity of these pretectal neurons while stimulating the fish with whole field motion drifting in eight different directions (Figure 3.11). Most neurons were tuned to forward motion and had lateralized responses, but many also had strong forward selective properties, whereas others showed strongly lateralized responses. In deeper regions adjacent to the pretectum, neurons of similar response properties can be found.

Figure 3.11

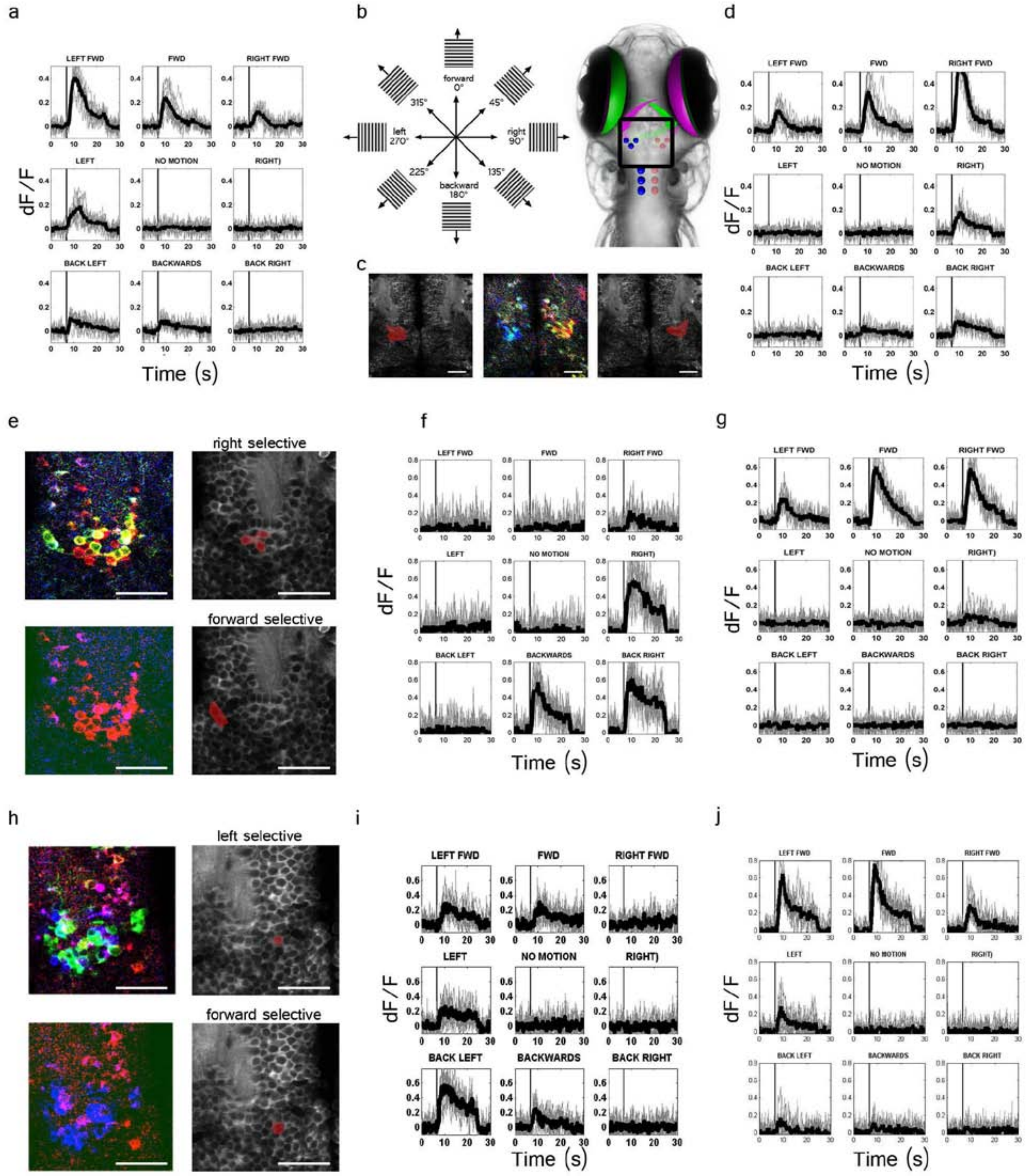

Figure 3.11 - Direction selectivity of pretectal neurons: **a** Calcium responses from left pretectal neurons of the ROI shown in **c**. **b** Stimulation paradigm: sinusoidal gratings were presented moving in 8 different directions. The schematic shows the brain area investigated with respect to the fish. **c** Z-projections of calcium recordings indicating the ROI recorded in **a** (left) and **d** (far right). The middle panel shows color-coded calcium responses of different regions (left - blue, right - red, green - forward). Neurons that are both forward and left direction selective appear in cyan and yellow for forward and right selectivity. **d** Calcium responses of left pretectal neurons in the ROI shown in **c**. **e** Top row: Color-coded (as in c) average data of right pretectal neurons. Some neurons are predominantly rightward selective (cells marked in red in the right image), time series date is shown in **f**. Some neurons are forward selective, their time series is shown in **g**. Bottom row: Color-coded average data without forward or backwards stimuli. Most neurons in the right pretectum are strongly rightward selective. An ROI for the forward selective cells in **g**. **f** Calcium responses of back right selective pretectal neurons. **g** Calcium responses of forward selective pretectal neurons. **h** Top row: Color-coded (as in c) average data of left pretectal neurons. Some neurons are predominantly leftward selective (cells marked in red), time series data shown in **i**. Some neurons are more forward selective, time series data shown in **j**. Bottom row: Color-coded average data, without forward or backwards stimuli. Most neurons in the left pretectum are strongly left selective. An ROI for mostly forward selective cells in **g**. **i** Calcium responses of back right selective pretectal neurons. **j** Calcium responses of forward selective pretectal neurons. (For all images, scalebars = 20µm).

Furthermore, since the pretectal neurons are responsive to outward stimuli from the ipsilateral eye, it is necessary that this information must cross back over the midline as the sensory information enters the brain through a purely contralateral projection from the retina. In functional imaging experiments in dorsal regions of the pretectum, the posterior commissure, which passes from the right pretectal region to the left, shows activation to outward motion (Figure 3.10). This lead to the speculation that it is via this commissure that outward information is relayed to the opposite pretectal region.

Figure 3.12

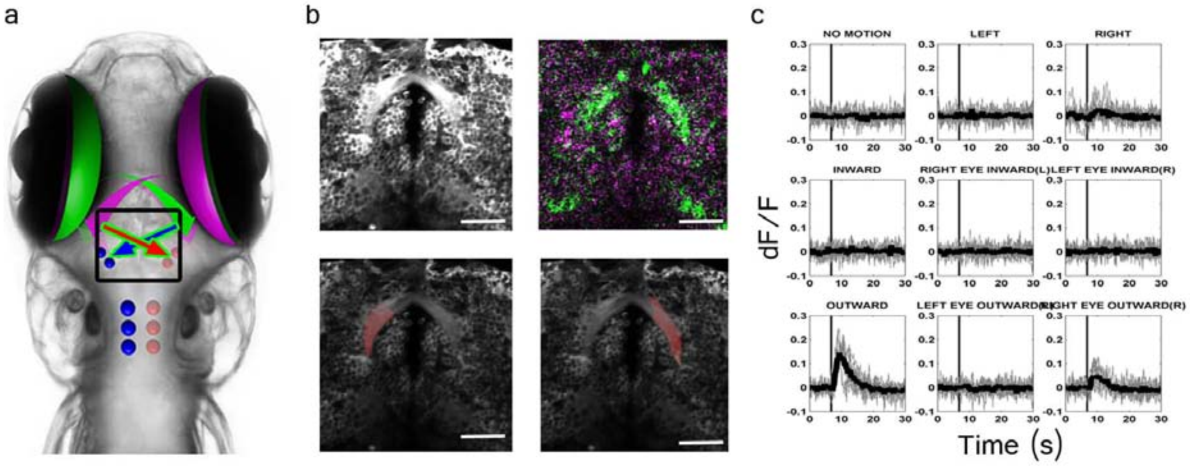

Figure 3.12 - **Outward responsive commissural connections:** **a** The black rectangle on the schematic fish head shows the brain area investigated. Outward information for whole-field right and left motion (arrows in blue and red with green outline) must cross the midline in order to activate the ipsilateral side pretectal or ventromedial neurons. **b** Top Left: Two-photon micrograph showing the posterior commissure, anatomically positioned to suggest it as candidate conduit for outward information. Top Right: A color-coded calcium recording showing all outward stimuli in green and all inward stimuli in magenta. Intensely green coloring of the commissural structure indicates a strong response to outward stimuli. Bottom, Left and Right: projections showing the location of ROIs for time series analysis shown in **c**. (Scalebar = 10µm) **c** Examplary calcium responses of right commissural section of the ROI shown in **b**, data for the left ROI is not shown.

Together, the majority of the neurons in this region show response properties that are very similar when compared to those found in the ventromedial cells (compare Figure 3.5 and Figure 3.9e, f), suggesting that they may provide direct input to this small subpopulation of spinal cord neurons that are necessary for the resultant turning behavior. As their activation patterns indicate, they combine inward and outward sensory information from both eyes, providing evidence that this is a site necessary for the sensory neural processing required for directing OMR turning, and consistent with separate processing of inward and outward stimuli. Single neurons that respond exclusively to inward or outward stimuli support this hypothesis

(Figure 3.8). Furthermore, the response properties of neurons that are activated during binocular INWARD stimulation suggest that they could mediate the reciprocal inhibition predicted by the behavioral responses. Finally, these results demonstrate that this strategy of monitoring the neural activity throughout the zebrafish brain during presentation of stimuli that have specific behavioral correlates is able to identify and characterize neurons that might be involved in the circuitry dedicated for the processing of whole field motion stimuli.

3.1.8 LASER ABLATIONS OF FUNCTIONALLY IDENTIFIED NEURAL STRUCTURES

Although correlational data from functional imaging has provided evidence that certain neurons are active during the processing of certain stimuli, causality cannot be established with this method. To establish a causal relationship between neurons and a particular function, perturbation of the neural activity or transient/permanent removal should result in a change or loss of its associated behavioral response. For this reason, we used laser ablations to confirm the role of the functionally identified neural structures. Our data suggest that AF6 is the neuroanatomical basis of the visual information entry point for the visual information controlling the OMR. To test whether this region is necessary for the associated behavior, we specifically ablated this region and then tested the treated fish for behavioral deficits. For the ablation, fish were briefly anesthetized and embedded in low melting agarose to restrain their movement. We used an ablation technique based on the non-linear absorption of femtosecond pulsed infrared light, which allowed for highly localized ablation restricted to a small focal volume. Scanning a 4 μm spiral pattern over fluorescent neuropil regions led to the formation of highly localized plasma, destroying the small targeted region, but leaving adjacent tissue intact. We used *HuC:GCaMP2* transgenic fish to localize the target area (Figure 3.13). In the case of the AF6, the target is composed of just neural processes and multiple (4-5) ablation sites were selected. A pre and post image of the entire region shows clearly intact tissue prior to ablation and cellular debris within the targeted region following ablation. However, even with the non linear absorption of the pulsed infrared laser, unspecific out of focal plane heating can occur. This is most evident when blood vessels above the ablated regions appear to be damaged or cauterized. To avoid these unspecific effects, after a successful ablation, only fish with normal blood flow in all blood vasculature above the ablated region were used for behavioral recordings. This procedure is only minimally invasive and fish recovered within 5-10 min, with normal spontaneous swim activity and an upright posture. Importantly, fish were able to turn in both directions spontaneously. For visually guided behaviors, the unilateral ablation of the left

AF6 led to results that mimic the negation of visual input to the right eye (Figure 3.13c- e). Most strikingly, the INWARD stimulus that normally does not evoke a net angle change in either direction produced a response identical to the monocular inward motion stimulation of the left eye following ablation of the left AF6. For all other stimulus conditions that contain stimulation to the right eye, similar changes were observed. For example, for OUTWARD stimulation, the behavioral response is similar to a monocular outward stimulation of the left eye only. For monocular right eye stimulation, the behavioral phenotype resembles the behavioral response to the no motion condition. In addition, after ablation, the average number of locomotion events per second is changed in a manner that resembles locomotion that would normally result from monocular input to the left eye. Together, these results further support that AF6 is the site of entry for the visual motion information, for, at least, stimuli that evoke directed turning behaviors. Although, these results confirm our model, these results must be considered preliminary, control ablations in adjacent tissue must be performed and behavioral responses statistically analyzed.

Figure 3.13

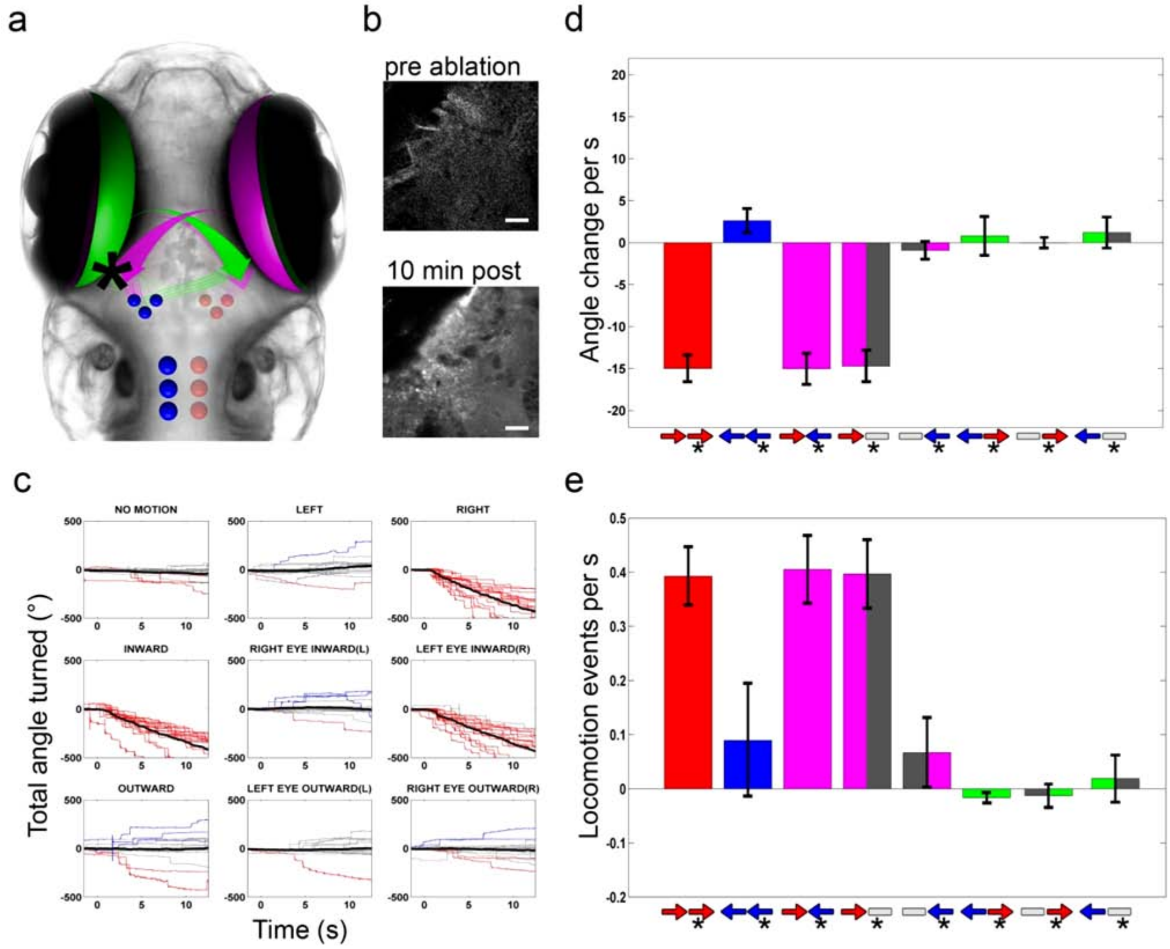

Figure 3.13 - Laser ablation of retinal ganglion arbourisation field 6

Figure 3.13 - Laser ablation of retinal ganglion arbourisation field 6: **a** Schematic showing site of ablation (asterix). **b** Top: Ablation site within a *HuC:GCaMP2* fish showing the intact left AF6 region. Bottom: After multiple small focal ablations within AF6, cell debris is visible 10 min post ablation. (Scalebar = 5 µm) **c** Behavioral recording after a successful ablation of the left AF6. Note, fish turns consistently to the right when presented with the normally coflicting INWARD stimuli. **d** Behavioral average data for angle change per second adjusted to the no motion condition with ablations to the left AF6 (n = 4 fish). As expected for an ablation of the input from the right eye's whole field motion processing circuit, behavioral responses show changes that turn previously conflicting stimuli into monocular stimuli. Labels as described above, asterix underneath arrow symbolizing the eye specific stimulation suggests that this input should no longer perceived with this type of ablation. **e** Locomotion events per second following successful ablations of left AF6 reveal a similar result. The large variation between fish presented with leftward motion might be due to incomplete ablation of the sensory input.

Based on anatomical data and calcium imaging, we hypothesized that the posterior commissure (Figure 3.14) could serve as either the conduit of the outward information that activates the pretectal neurons and/or the contralateral inhibition. We used the transgenic *HuC:GCaMP2* fish to localize the region identified by functional imaging and ablated the central region of the commissure. Multiple small sites were targeted and, after successful ablation, only fish with intact blood vasculature were used for behavioral experiments (Figure 3.14c). Ablation of the posterior commissure altered the behavior such that the fish appears to be only driven by inward information. For example, there is no longer a significant difference between the whole field stimuli and the monocular inward stimuli. Furthermore, the monocular outward stimuli show no statistically significant bias in direction compared to not treated animals (Figure 3.14e) (for angle change ablated fish = 9 fish, > 25 stimulus repetitions, Student's t-test, RIGHT versus LEI: p = 0.9, LEFT versus REI: p > 0.6, LEO versus NM: p = 0.54, REO versus NM: p= 0.6). Based on this data we hypothesized that the ablation is affecting the outward information added to the whole field stimulus. When we quantified the amount of turning that is added from monocular outward to the monocular inward stimulus yield the response to whole field motion (difference between monocular inward and whole field motion). Measured in percent increase, we find that fish with ablated commissures had a significantly smaller outward "boost effect" than untreated animals (CONTROL versus ablated: p = 0.03) (Figure 3.14b). Although the results from fish to fish were variable, likely due to insufficient ablation of the large commissure, these data are suggestive of the role the posterior commissure might play in the conveying of outward information to the contralateral side. Another interesting finding is that the monocular outward stimuli in the ablated fish also suppress the locomotion activity. This allows us to speculate that the outward information remaining on the contralateral side (entering via AF6) is likely inhibiting locomotion, whereas outward information that back-crossed to the ipsilateral side activates the 'turning circuitry'.

Interestingly, this ablation invariably resulted in processes connected to the ablated central area of the commissure increasing their fluorescence intensity (Figure 3.14d). Presumably, when the axons were severed, the influx of Ca^{2+} ions induced the fluorescence change by binding to the exposed *GCaMP2* molecules. Since this increase in fluorescence was stable, we could image the area and localize the projection patterns of the commissural projections. The axons either ended or passed by the pretectal neurons in all fish that we ablated in this specific way. In addition, when ablating pretectal neurons (data not shown), the fluorescence in the commissure projecting to the contralateral side was increased as well. Although we are encouraged by these results, the time of this report, they must be considered preliminary and more experiments will be necessary to confirm the role of the posterior commissure in the neural circuit underlying OMR turning responses.

Figure 3.14

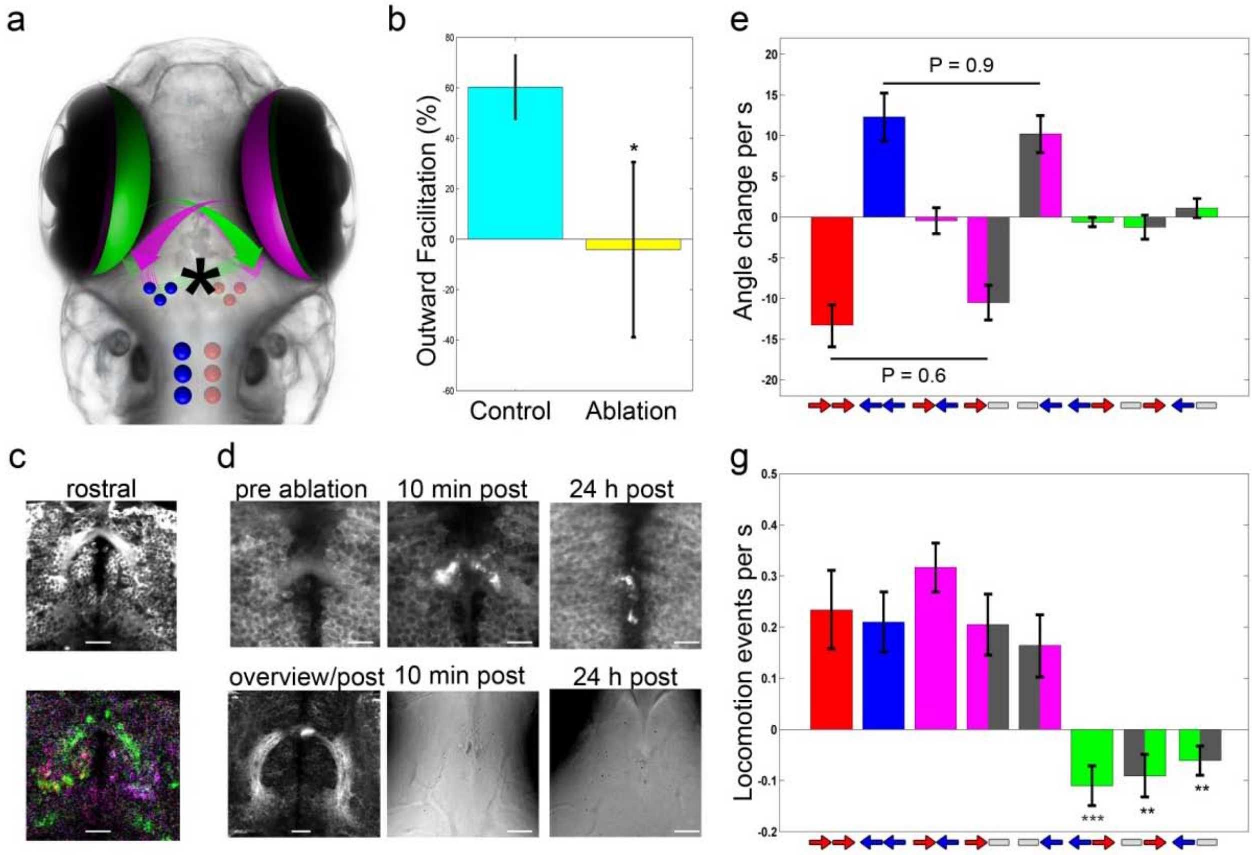

Figure 3.14: Laser ablation of posterior commissure

Figure 3.14: Laser ablation of posterior commissure. **a** Schematic showing site of ablation (asterix). **b** Summary of the ablation effect: By ablating the posterior commissure, the difference between responses to whole field, coherent motion and those to monocular inward stimulation alone were quantified in percent of response added by the outward component; this "outward facilitation" was significantly smaller in ablated fish. Comparison of control (n = 12) and ablated fish (n = 6). Large variation between ablated fish might be due to incomplete ablations. **c** Ablation site within a *HuC:GCaMP2* fish showing the intact commissure at the same depth as the pretectal neurons. Below: Color coded calcium imaging data showing green areas in which cells respond exclusively to outward motion and magenta for inward motion. **d** Top: Posterior commissure within a *HuC:GCaMP2* fish, before, 10 min and 24 hr after ablation of the commissure. Bottom: A zoomed out projection of a two photon section, 10 minutes after a successful ablation, showing the increase in fluorescence in neurons passing through the ablation site. Interestingly, projections pass or terminate in the pretectal region. Right: transmission images 10 minutes and 24 hr after an ablation. Scalebar = 50 µm. **e** Behavioral average data for angle change per second baseline adjusted to the no motion condition for 6 fish with ablations of the posterior commissure. Results are consistent with the attentuation of behavioral responses due to removal of additional outward stimulation. **e** Average locomotion events per second, adjusted to the no motion condition for ablations of the commissure show that whole field motion stimuli are now only able to evoke locomotion levels comparable to monocular inward stimulation.

3.1.9 Comparison of behavioral responses and neural correlates

Figure 3.15

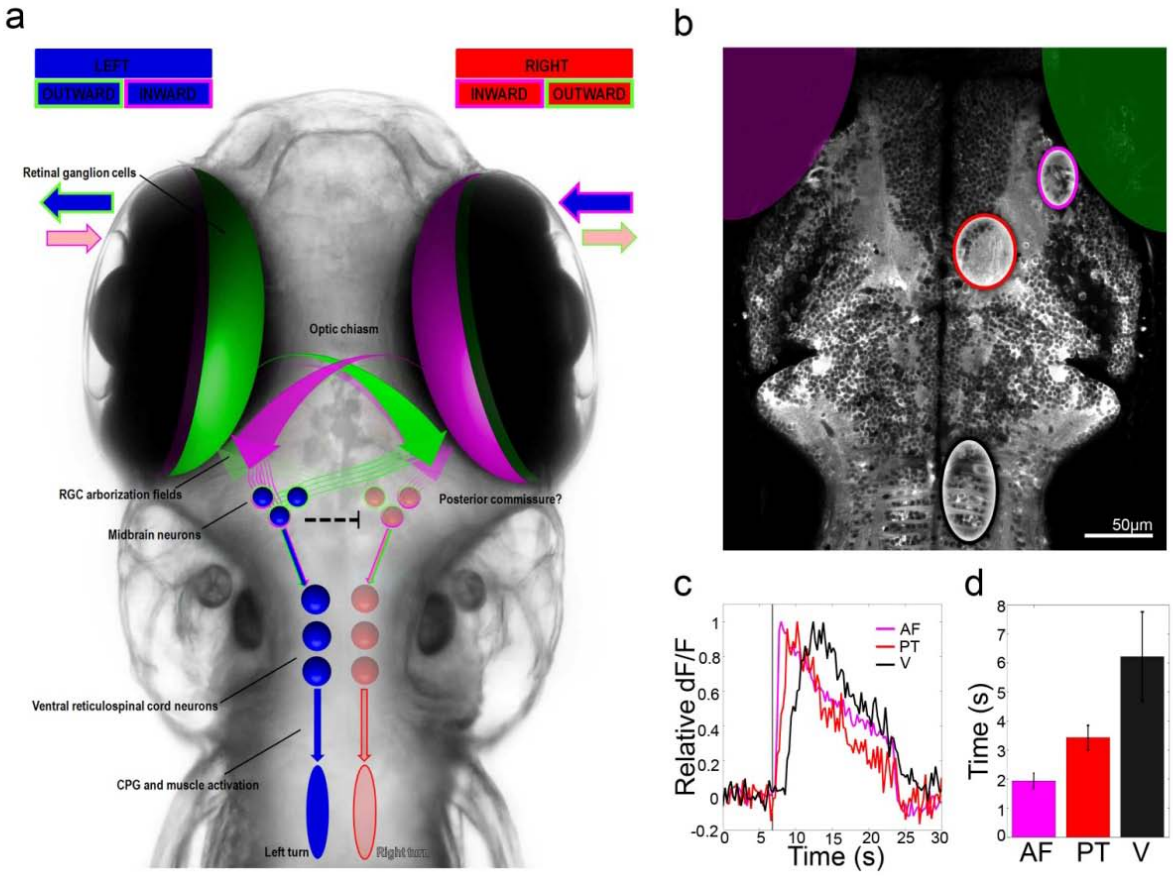
a
LEFT
OUTWARD
INWARD
RIGHT
INWARD
OUTWARD
Retinal ganglion cells
Optic chiasm
RGC arborization fields
Posterior commissure?
Midbrain neurons
Ventral reticulospinal cord neurons
CPG and muscle activation
Left turn
Right turn
b
50µm
c
Relative dF/F
1
0.8
0.6
0.4
0.2
0
-0.2
0
5
10
15
20
25
30
Time (s)
AF
PT
V
d
Time (s)
8
7
6
5
4
3
2
1
0
AF
PT
V

Figure 3.15 – 'Working Model' of zebrafish whole field motion discrimination circuitry: **a** Schematic of fish overlaid with a depiction of the identified components and necessary neural computations predicted from available data. **b** Two photon optical section of a HuC:Chameleon fish showing ROIs for the time series analysis shown in **c** (magenta - AF6, red - midbrain region, pretectal area, black -ventromedial descending reticulospinal neurons). **c** Normalized average calcium responses from 10 stimulus presentations of whole whole-field RIGHT motion from area AF6, pretectal neurons, and ventromedial cells. Response to rightward is fastest in AF6, followed by the pretectum, and then the ventromedial cells. **d** Average data from 7 fish for each region reveals the time of peak calcium responses driven by motion stimulus onset for the different brain regions (+/- SEM). This timecourse of calcium responses corresponds with the slow onset of tail motion in head restraint fish. (AF = arbourisation field 6, PT = pretectum, V = ventromedial cells).

Information from prior research and the presented behavioral and functional data, allow the development of a 'working model' for whole field motion discrimination in zebrafish. In Figure 3.15, we schematize our current understanding of the flow of whole field motion information within the zebrafish brain. Orthogonal motion stimuli can be described as visual motion moving either lateral to medial (inward) or medial to lateral (outward) with the respect to the fish’s midline. Combinations of inward and outward are unambiguous stimuli (LEFT and RIGHT) and drive the strongest and clearest behavioral choices, whereas only monocular inward stimulation results in extra directed turns, instead of just biasing spontaneous turns in stimulus direction as was found for monocular outward. This can be explained by our model, in which direction selective ganglion cells project to AF6 where they make specific connections to neurons in the pretectum for inward stimulation and to relay neurons for outward stimulation. These relay neurons connect, possibly via the posterior commissure, to the other side of the pretectum, creating the observed response properties in the pretectum. The combined (inward and outward) information can then be passed along to the ventromedial cells of the hindbrain that mediate turning behavior. These reticulo spinal neurons then activate their downstream targets, i.e. central pattern generators (CPG) in the spinal cord. Furthermore, as binocular INWARD stimuli result in more locomotion, but not in increased number of large angle turns, and the group of neurons that are activated by unambiguous stimuli are not necessarily overlapping with the group of neurons that are activated by binocular INWARD only, in addition to the fact that ventromedial cells are not activated by binocular INWARD, it is possible that the specific group of neurons that are responsive to binocular INWARD drive the strong locomotion behavior while inhibiting the contralateral side, preventing large angle turns. Binocular OUTWARD suppresses spontaneous locomotion; neurons activated by binocular OUTWARD could be inhibiting the locomotion circuitry, but not the turning circuitry. Importantly, all behavioral and imaging results are all consistent with the fact that inward and outward information is processed via different channels within the brain, at least in the early stages.

Moreover, as the head-restrained behavioral data indicates, the onset of the optomotor response is relatively slow (~2 s latency) and the maximum turning rate of freely behaving fish only peaks after ~1s. This seemingly long delay could indicate that the neuronal circuitry integrates the sensory information until it reaches a certain threshold, at which point behavior is initiated. To explore this hypothesis, we compared the signals of calcium recordings in the 3 different regions: AF6, pretectal neurons and ventromedial neurons. The peak activation times of the calcium responses in these regions are staggered in time, as predicted by our model (Figure 3.15b-d). As AF6 is predicted to provide the input to the pretectal neurons, the fast onset in AF6 (within one frame time of 0.275ms) and a peak time around 2 seconds after stimulus onset, which is ~2 seconds before the pretectal neurons and ~4 seconds before the ventromedial cell calcium peaks, is not surprising. Future experiments should address whether pretectal or ventromedial cells could function as a temporal integrator of visual motion information.

3.2 RESULTS OF AIM 2: MONITORING NEURAL ACTIVITY WITH BIOLUMINESCENCE DURING NATURAL BEHAVIOR

3.2.1 NEUROLUMINESCENCE REPORTS NEURAL ACTIVITY IN FREELY BEHAVING ZEBRAFISH

The mechanism of Ca^{2+}-dependent bioluminescence from GFP-Aequorin (GA) and the steps to use GA as a neural activity reporter are schematized in Figure 3.16. Neuron-specific expression of GFP-apoAequorin (Ga), (Figure 3.17) was achieved by injecting single-cell embryos with plasmid encoding Ga downstream of the neuro-β-tubulin promoter (Nβt). High resolution 2-photon imaging also revealed the absence of any nonspecific expression in muscle), (Figure 3.18) and variegated expression levels in different brain regions (Figure 3.19).

Figure 3.16

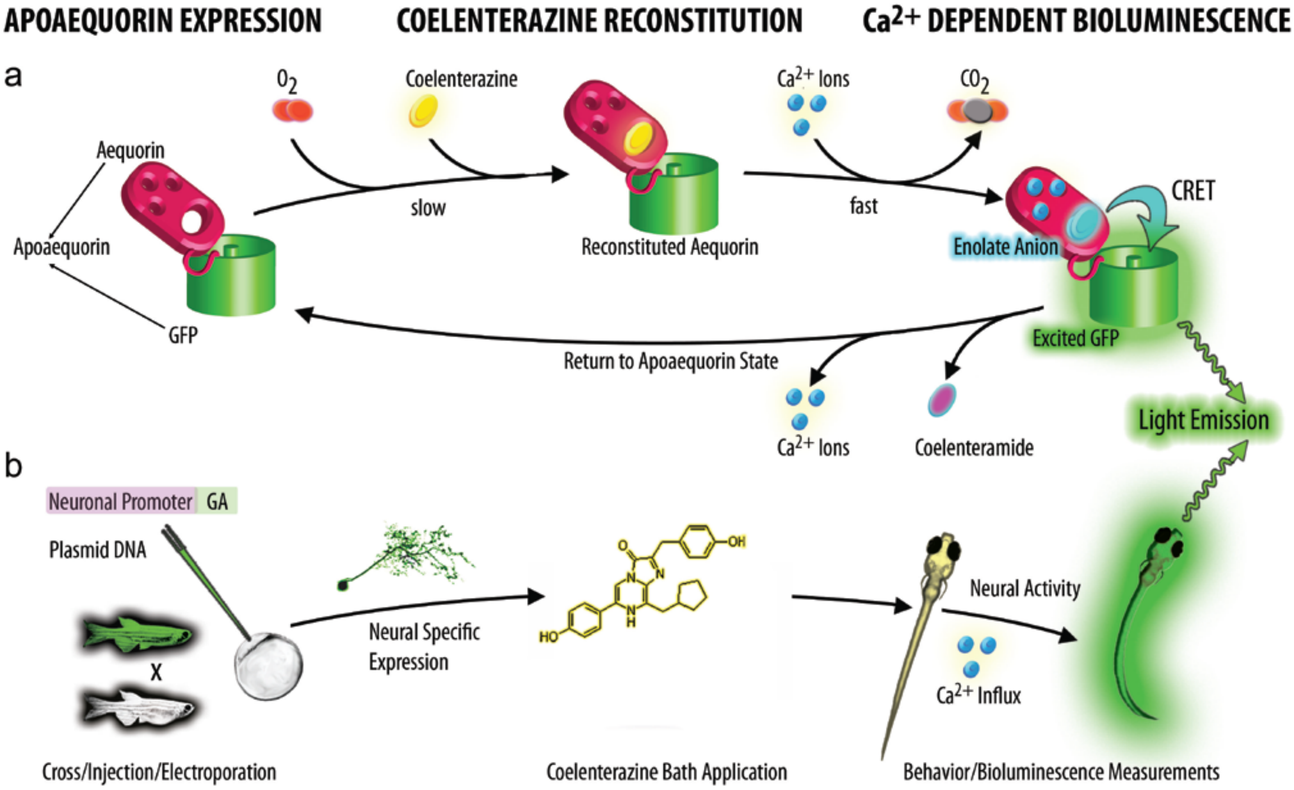
APOAEQUORIN EXPRESSION
COELENTERAZINE RECONSTITUTION
Ca2+ DEPENDENT BIOLUMINESCENCE
a
O2
Coelenterazine
Ca2+ Ions
CO2
Aequorin
Apoaequorin
GFP
slow
Reconstituted Aequorin
fast
CRET
Enolate Anion
Excited GFP
Return to Apoaequorin State
Ca2+ Ions
Coelenteramide
Light Emission
b
Neuronal Promoter GA
Plasmid DNA
X
Neural Specific Expression
HO
OH
O
N
H
Neural Activity
Ca2+ Influx
Cross/Injection/Electroporation
Coelenterazine Bath Application
Behavior/Bioluminescence Measurements

Figure 3.16 – Neuroluminescence in zebrafish: mechanism and method

Figure 3.16 – Neuroluminescence in zebrafish: mechanism and method: The upper diagram (**a**) schematizes the molecular reaction underlying the Ca^{2+}-dependent light emission of GFP-Aequorin (GA) and the lower diagram (**b**) shows how GA was employed as a bioluminescence reporter of neural activity in freely swimming zebrafish. **a** Light emission first requires the reaction of GFP-apoAequorin (Ga) with coelenterazine. After reacting with oxygen to form a stable peroxide intermediate, a coelenterazine molecule will stably bind to Ga to form GA. In this reconstituted form, the binding of Ca^{2+} ions induces a conformational change in GA that initiates the oxidative decarboxylation of coelenterazine, releasing CO_2 and producing an excited enolate anion. By a process known as non radiative chemiluminescent resonance energy transfer (CRET), the energy from the excited anion is transferred to GFP and results in the emission of a green photon. After photon emission, both the coelenteramide and Ca^{2+} are released and Ga is again available for reconstitution. **b** Neural expression of Ga is achieved by microinjecting embryos at the single-cell stage with plasmid DNA encoding Ga under control of a neuron specific promoter. Generation of stable transgenic fish or other expression targeting methods (e.g. electroporation) can also be used to introduce Ga into neurons of interest. Neuronal Ga is exposed to coelenterazine *in* vivo, in order to form the luminescent GA, by immersing the entire zebrafish larva in embryo medium containing coelenterazine dissolved in cyclodextrin. After an incubation time, neural Ca^{2+}-dependent light emission, neuroluminescence, can be detected during unrestrained behavior.

Figure 3.17

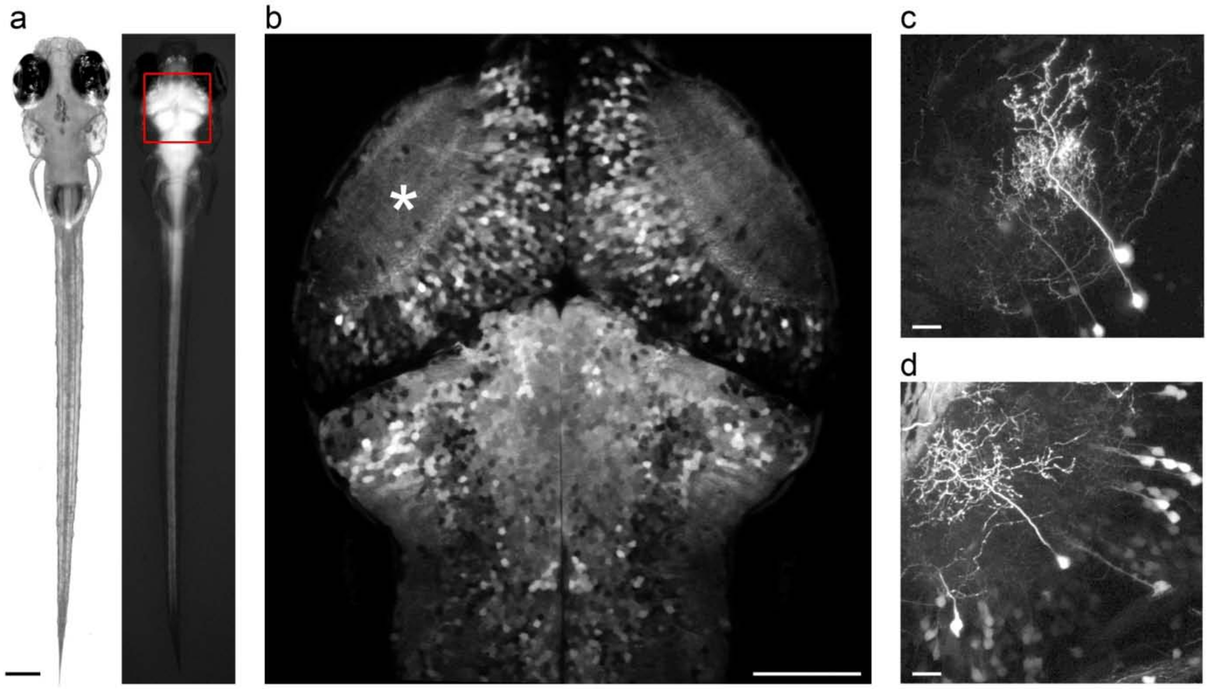

Figure 3.17 - Neural specific expression of GFP-Aequorin (Ga): a Bright field and fluorescence micrographs of a 7 dpf transgenic NβT:Ga larval zebrafish (scale bar: 0.2 mm). **b** A two-photon optical section through the dorsal midbrain and hindbrain (scale bar: 100 µm). **c-d** Two-photon maximum intensity z-projections of the left optic tectum in two zebrafish larvae that transiently expressed Ga following plasmid injection at the single-cell stage. The *neural-β-tubulin* promoter specifically targets Ga expression to neurons, which appear healthy during all observed developmental stages (3-10 dpf) (scale bar: 20 µm).**c** Mosaic expression of Ga with *neural*-β-*tubulin:Ga* (6 dpf).**d** Expression of Ga by co-injection of plasmids encoding *neural*-β-*tubulin:Gal4* and *UAS:Ga,* demonstrating that a binary expression system can be used to target Ga expression to specific neurons (6 dpf).

Figure 3.18

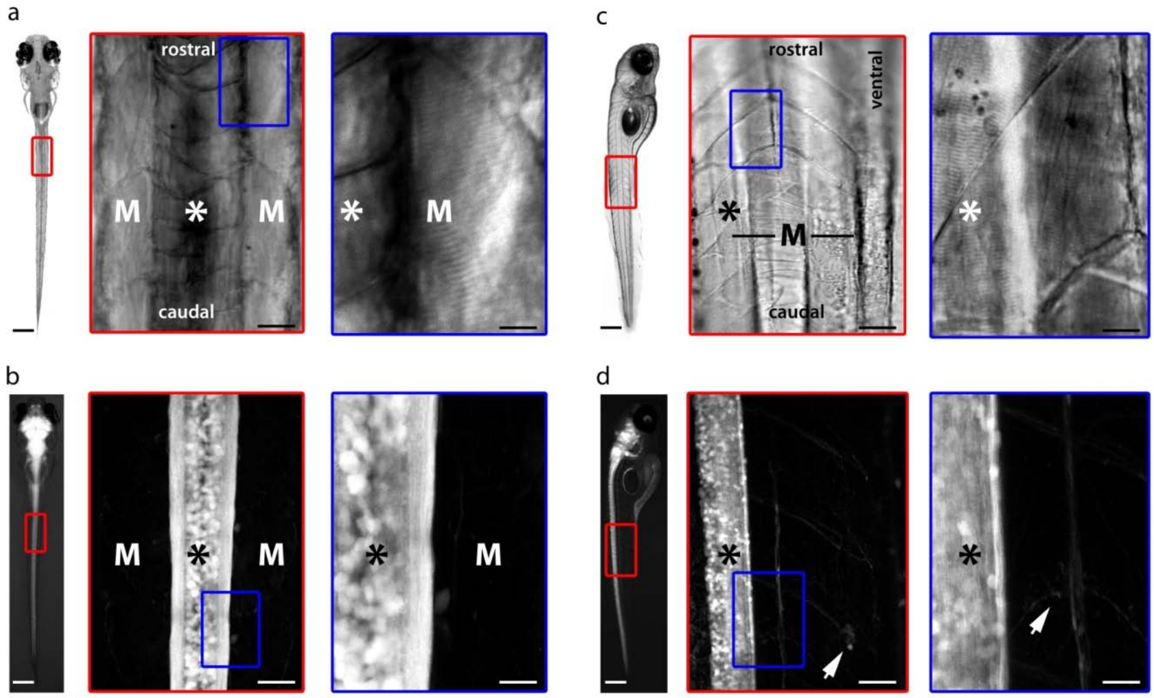

Figure 3.18 - Neural specific expression of GFP-Aequorin (Ga) in the zebrafish tail: **a** (left) Dorsal bright field micrograph of a 7 dpf zebrafish (scale bar: 0.3 mm). (middle) An expanded view of the region indicated (red rectangle) focusing on the tail of the fish. Neurons of the spinal cord (*) are located along the midline above the notochord. Axial musculature surrounds the fish tail. Epaxial muscles are not easily visible on the dorsal side, but the lateral hypaxial muscles (M), and the segregated myotomes, are clearly visible (scale bar: 50 µm). (right) A higher magnification image of the indicated region (blue rectangle) reveals the dark stripes characteristic of the sarcomeres of skeletal muscles (M) (scale bar: 20 µm). **b** (left) Dorsal bright field and fluorescence micrograph of a 7 dpf transgenic Nβt:Ga zebrafish (scale bar: 0.3 mm). The indicated region (red rectangle) shows the position of subsequent two-photon investigation of Ga expression. (middle) A maximum intensity projection of a series of images acquired with a two-photon microscope through the complete depth, 370 µm, of the tail (scale bar: 50 µm). Specific neural expression in spinal cord neurons and lateral axon tracks (*) can be seen in the center; a few neural processes and auto-fluorescence from skin is detected in the region overlapping with the lateral hypaxial muscles (M). (right) A zoom-in on the indicated region (blue rectangle) further demonstrates that Ga expression is only detected in neuronal structures (scale bar: 20 µm). **c** (left) Lateral bright field micrograph of a 7 dpf zebrafish (scale bar: 0.3 mm). (middle) An expanded view of the region indicated (red rectangle) focusing on the tail of the fish. Neurons (*) of the spinal cord are positioned dorsal to the notochord. The segregated myotomes of the axial musculature that surrounds the fish (M) can be seen (scale bar: 50 µm). (right) A higher magnification of the indicated region (blue rectangle) also reveals dark stripes characteristic of the sarcomeres of skeletal muscles (M) and the location of the spinal cord track(*) (scale bar: 20 µm). **d** (left) Lateral bright field and fluorescence micrograph of a 7 dpf transgenic Nβt:Ga zebrafish (scale bar: 0.3 mm). The indicated region (red rectangle) shows the position of subsequent two-photon investigation of Ga expression. (middle) A maximum intensity projection of a series of images acquired with a two-photon microscope through the complete depth, 250 µm, of the tail (scale bar: 50 µm). Specific neural expression in spinal cord is apparent; only neural processes and auto-fluorescence from skin is observed in the region overlapping with the axial muscles (M). (right) A zoom-in on the indicated region (blue rectangle) further demonstrates that Ga expression is only detected in neuronal structures (scale bar: 20 µm). Arrows indicate neural processes innervating the musculature.

Figure 3.19

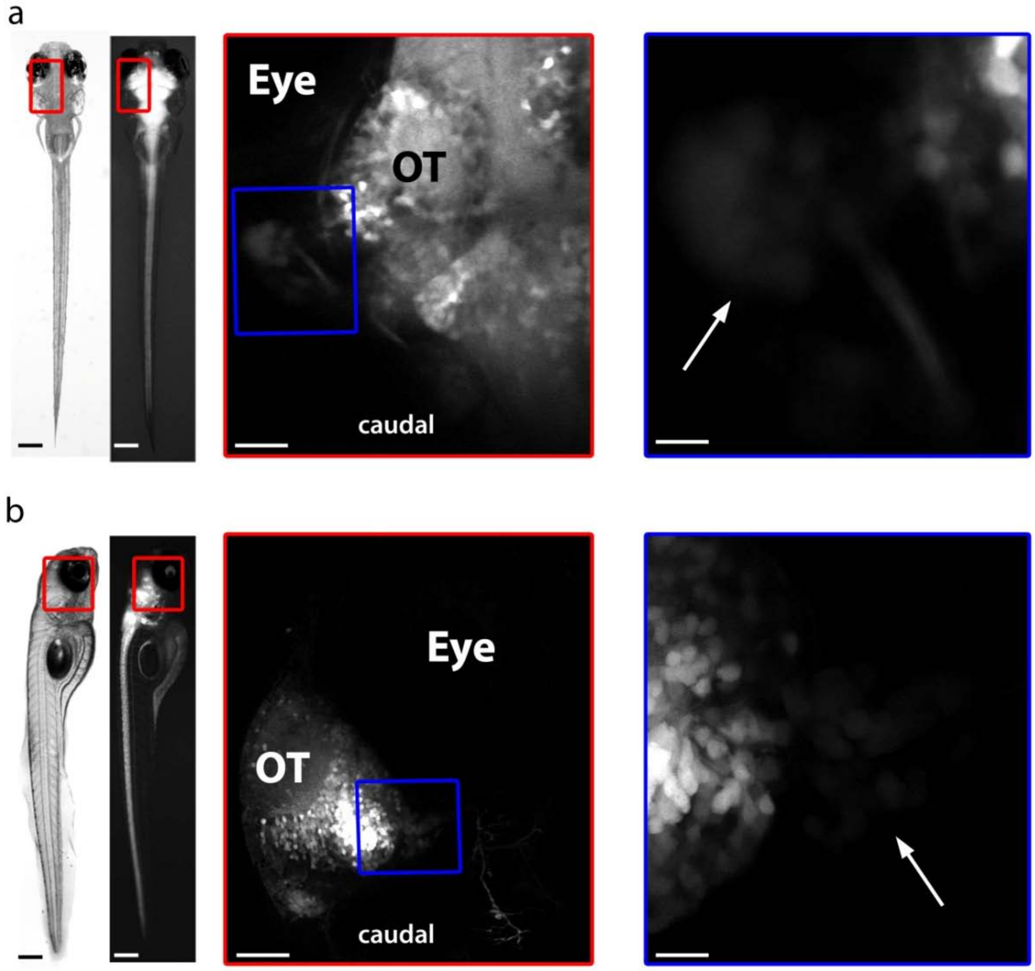

Figure 3.19 - Neural specific expression of GFP-Aequorin (Ga) in Trigeminal Neurons: **a** (left) Dorsal bright field and fluorescence micrographs of a 7 dpf transgenic Nβt:Ga zebrafish (scale bar: 0.3 mm). Rectangle indicates the region imaged with two-photon microscopy. (middle) A maximum intensity projection through the ventral portion of the left optic tectum (OT) and trigeminal nucleus (scale bar: 50 µm). (right) A higher magnification image of the indicated region (blue rectangle) reveals the low expression level of Ga in trigeminal neurons (arrow) compared to other neurons of the zebrafish brain (scale bar: 20 µm). **b** (left) Lateral bright field and fluorescence micrographs of a 7 dpf transgenic Nβt:Ga zebrafish (scale bar: 0.3 mm). Rectangle indicates the region imaged with two-photon microscopy. (middle) A maximum intensity projection of sagittal sections through the right optic tectum (OT) and trigeminal nucleus (scale bar: 50 µm). (right) A higher magnification image of the indicated region (blue rectangle) again reveals the low expression level of Ga in trigeminal neurons (arrow) compared to the more dorsal neurons of the zebrafish brain (scale bar: 20 µm). Note that only neural structures are visible, even though expression level varies, and that there is no detectable expression in regions where facial and axial muscles are located.

Following a 24 hour exposure to coelenterazine (CLZN), transgenic Nβt:GA zebrafish (Figure 3.20a) were placed into the recording device (Figure 3.20b), where they swam freely within a behavior chamber positioned directly beneath a large-area photomultiplier tube (PMT). While the PMT detected single photons emitted within the arena, an infrared CCD camera simultaneously tracked fish movement. Most bouts of spontaneous swimming coincided with the emission of large flashes of green light (Figure 3.20 c-g, Movie 1), which occasionally were also observed without concurrent locomotion (Figure 3.20d, arrowhead).

Figure 3.20

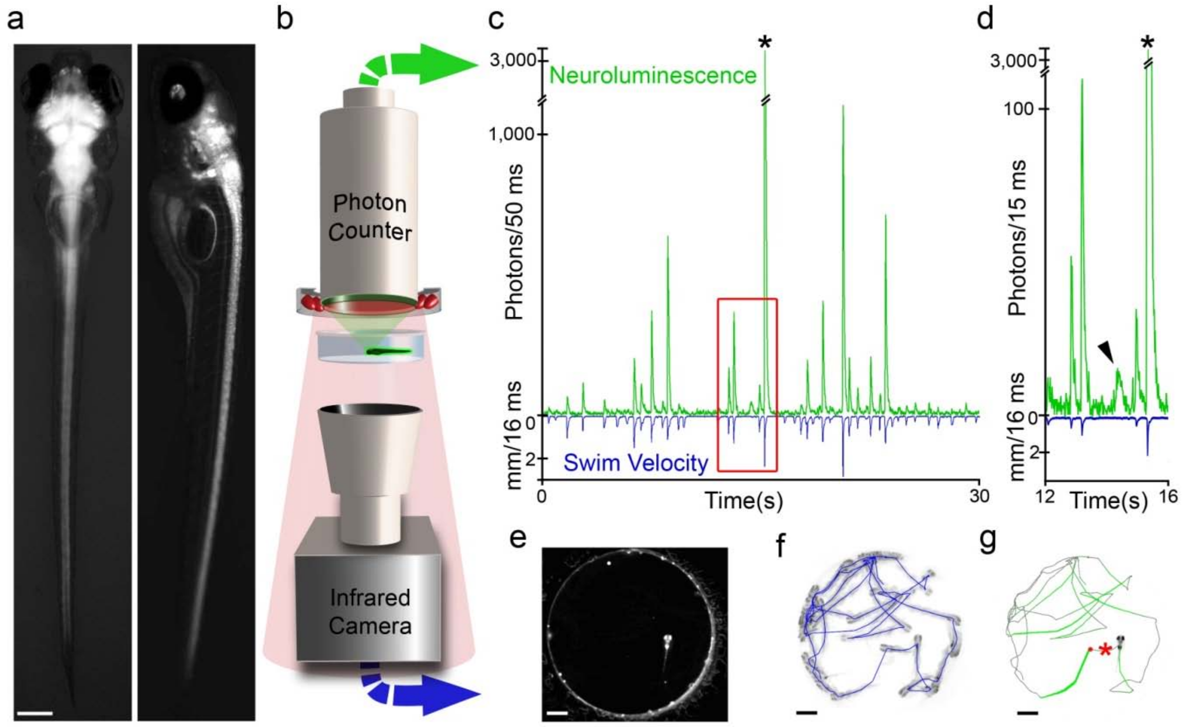

Figure 3.20 – Monitoring the neural activity of freely behaving zebrafish: **a** Dorsal (left) and lateral (right) fluorescence/bright-field micrographs of a 7 dpf *Nβt:Ga* transgenic zebrafish larva (scale bar: 0.20 mm). **b** Neuroluminescence setup: A large-area (25 mm diameter) photon-counting PMT is situated above a transparent behavior chamber (12.5 mm diameter). The highly-sensitive light detector is protected by an infrared (IR)-blocking filter such that a ring of 880 nm light-emitting diodes can be used to illuminate the behavioral chamber. Fish are imaged with an IR-sensitive CCD camera positioned below the chamber. The large spectral separation between GA bioluminescence and the IR illumination allows the simultaneous recording of neuroluminescence signals and the behavior of freely swimming zebrafish larvae. **c** Exemplary neuroluminescence recording of a 7 dpf *Nβt:Ga* transgenic zebrafish larva previously exposed to coelenterazine. Photon emission and behavior (swim speed in millimeter moved per frame period (mm/16.67 ms)) are shown for a 30 second recording. A mechanical stimulus was delivered at 15 s (*), inducing a fast startle response and a large increase in neuroluminescence. **d** An expanded view of the boxed region indicated in **c** highlights a neuroluminescence event not associated with locomotion (arrowhead). **e** Raw image acquired by the IR CCD camera during neuroluminescence recording (scale bar: 1.5 mm). **f** Superposition (inverted grayscale) of all frames acquired during the 30 second recording period shown in **c**, the entire fish trajectory is shown. **g** The fish trajectory shown in **f** is overlaid with a colored line for which the neuroluminescence amplitude at each segment is coded as the line-width, (*) indicates the time of the mechanical stimulus.

The absence of any signal in Ga animals, untreated with CLZN, as well as in wild-type fish (with or without CLZN treatment) demonstrated that neuroluminescence required both the expression of Ga as well as exposure to CLZN (Figure 3.21a). Previous studies used alcohol as a solvent for CLZN reconstitution solutions 38, but we found that dissolving CLZN in 2-hydroxypropyl-β-cyclodextrin (CLZN-CDX)[165] also allowed, and possibly facilitated, in vivo formation of GA (Figure 3.21b) and avoided the negative effects of exposure to ethanol or methanol[166]. Fish tested in cyclodextrin solution at a tenfold higher concentration then normally required showed no detectable changes in health or behavior (Figure 3.21d). With periodic replacement of the CLZN-CDX bath starting at 3 days-post-fertilization (dpf), large neuroluminescence signals were detected until at least 11 dpf, the last day tested (Figure 3.21c). Differences in neuroluminescence signal amplitude between individual larvae (Figure 3.22a-c) were apparent, possibly due to differential CLZN loading (Figure 3.22d-e) and animals that showed little or no responses were not tested further. Also, signal amplitude was found to depend on the type of CLZN used for GA constitution. Analogs of native CLZN have been developed that confer different binding affinities for calcium resulting in a range of sensitivities for the indicator. We found that coelenterazine-h (CLZN-h) consistently produced better results than the native version and was therefore used in our experiments.

Figure 3.21

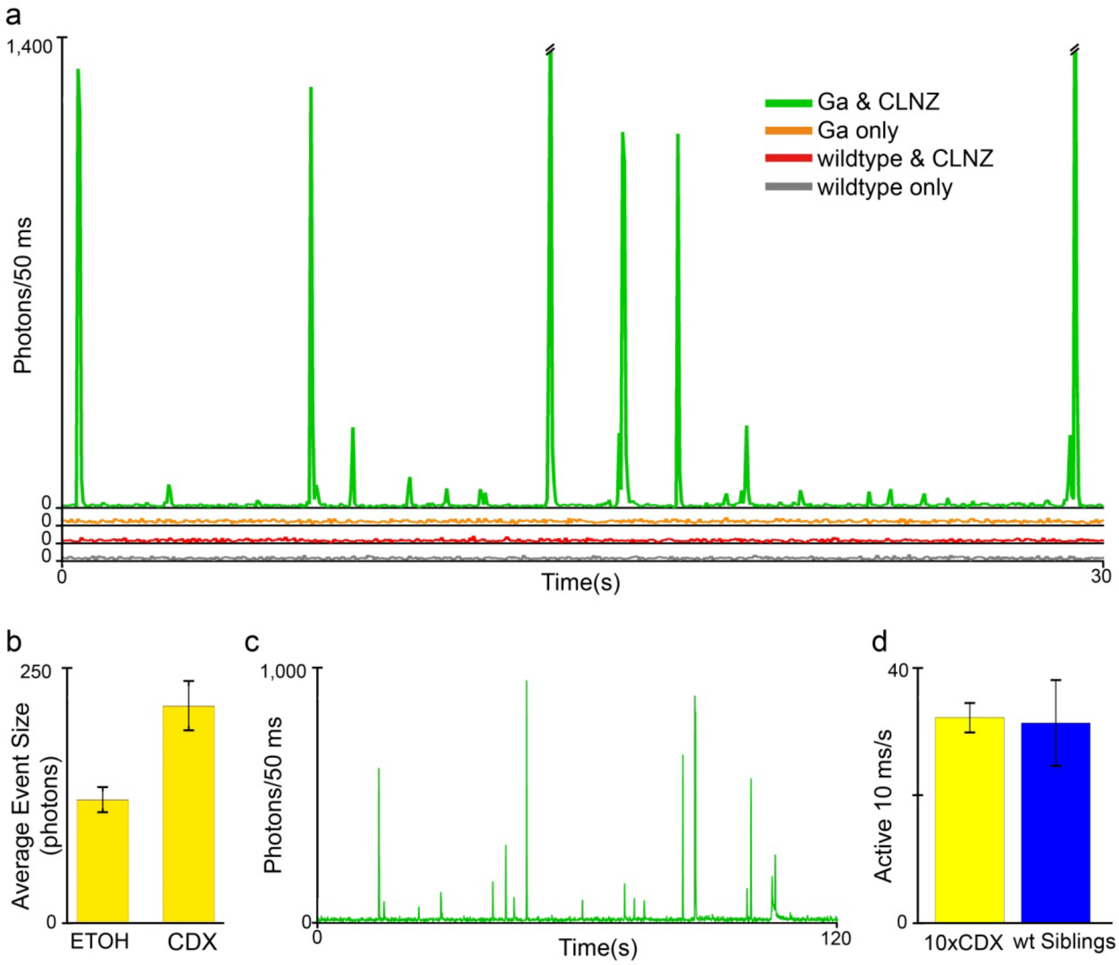

Figure 3.21 - Variation in signal amplitude and coelenterazine loading: **a-c** Neuroluminescence signals produced by three 6 dpf zebrafish siblings and their corresponding swim velocity (mm/frame period (16.67 ms)). Each sibling was exposed to CLZN-*h* for 24 hours under identical conditions (in the same rearing dish). Neuroluminescence corresponding to behavioral events can be detected in all 3 individuals; however, the peak signal amplitudes vary from fish to fish. For the fish shown in **a**, small neuroluminescence events are visible, but almost no baseline neuroluminescence is detectable, whereas the fish in **b** and **c** show not only larger transient neuroluminescence signals, but also an increase in the baseline neuroluminescence which possibly reflects a corresponding increase in background neural activity. **d-e** Two-photon horizontal sections through the optic tectum and the otic vesicle comparing the amount of CLZN-fluorescence in 4 dpf non-transgenic *nacre* zebrafish (scale bar: 40 µm). A control zebrafish not exposed to CLZN exhibits strong auto-fluorescence from the skin, but weak auto-fluorescence within the brain. **e** Individual larvae exposed to CLZN 24 hours prior to imaging exhibit strong fluorescence in neural tissue resulting from the excitation of CLZN that was absorbed into the brain. Each image is color coded according to reflect the calibrated CLZN concentration (see gradient scale). Weak signal in cell body regions could be caused by exclusion of CLZN from the nucleus of neurons, however, CLZN is clearly detected within the brain of each larva and the observed differences in concentration may explain some of the observed variability in peak neuroluminescence signals.

Figure 3.22

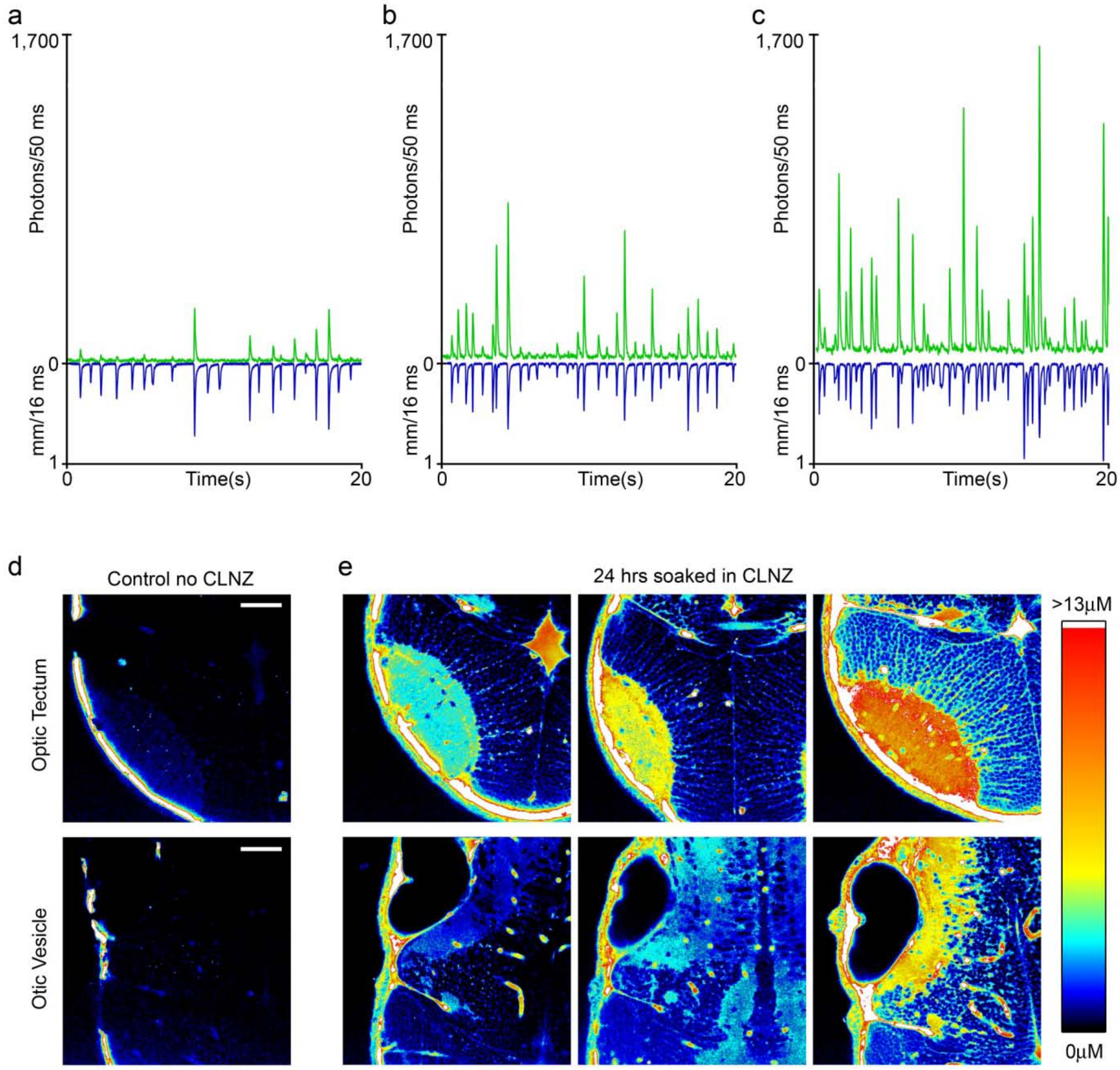

Figure 3.22 - Variation in signal amplitude and coelenterazine loading: a-c Neuroluminescence signals produced by three 6 dpf zebrafish siblings and their corresponding swim velocity (mm/frame period (16.67 ms)). Each sibling was exposed to CLZN-*h* for 24 hours under identical conditions (in the same rearing dish). Neuroluminescence corresponding to behavioral events can be detected in all 3 individuals; however, the peak signal amplitudes vary from fish to fish. For the fish shown in **a**, small neuroluminescence events are visible, but almost no baseline neuroluminescence is detectable, whereas the fish in **b** and **c** show not only larger transient neuroluminescence signals, but also an increase in the baseline neuroluminescence which possibly reflects a corresponding increase in background neural activity. **d-e** Two-photon horizontal sections through the optic tectum and the otic vesicle comparing the amount of CLZN-fluorescence in 4 dpf non-transgenic *nacre* zebrafish (scale bar: 40 μm). A control zebrafish not exposed to CLZN exhibits strong auto-fluorescence from the skin, but weak auto-fluorescence within the brain. **e** Individual larvae exposed to CLZN 24 hours prior to imaging exhibit strong fluorescence in neural tissue resulting from the excitation of CLZN that was absorbed into the brain. Each image is color coded according to reflect the calibrated CLZN concentration (see gradient scale). Weak signal in cell body regions could be caused by exclusion of CLZN from the nucleus of neurons, however, CLZN is clearly detected within the brain of each larva and the observed differences in concentration may explain some of the observed variability in peak neuroluminescence signals.

Neuroluminescence signals were large (signal to noise ratio >> 100), stable for long periods of time (>24 hours) (Figure 3.23a), and coincident with spontaneous and evoked swim events (Figure 3.20c, Figure 3.23). Spontaneous signals detected from individual zebrafish spanned a range of sizes (Figure 3.23b-c), exhibiting a smooth amplitude distribution with a high frequency of small events phasing into a long tail of increasingly large and rare events (Figure 3.23d). After aligning individual signals to the initial onset inflection we estimate a time-to-peak of 5-10 ms and a slower decay time of ~ 25 ms (Figure 3.23c), consistent with expectations for Aequorin and comparable to popular synthetic Ca^{2+}-indicators.

To measure neuroluminescence signals produced during stimulus-evoked behaviors, we delivered a mechanical tap below the swim chamber to elicit a startle response. Repeatedly evoked neuroluminescence signals were fast and consistently similar in amplitude (Figure 3.23e). In order to isolate the sensory component of this response we then paralyzed the fish via a bolus injection of α-Bungarotoxin and repeated the experiment in the same animals (Figure 3.23f). Figure 3.23g shows the aligned evoked signals from freely swimming fish in blue and from the same but paralyzed fish in red. The reduction in signal size following paralysis is not surprising; restrained fish show a substantial reduction spontaneous activity, possibly reflecting s state of behavioral suppression that affects both spontaneous and evoked behaviors (Figure 3.24). Furthermore, we find very weak Ga expression levels in the trigeminal ganglion, one of the primary somatosensory ganglia known to mediate the tap-evoked escape response (Figure 3.19), which can serve as an additional explanation for the reduction of the isolated sensory response in paralyzed fish.

To further investigate the origins of neuroluminescence, we exposed zebrafish to pentylenetetrazole (PTZ, 10 mM), an inhibitor of GABA-A receptors that induces epileptic-like neuronal discharges in humans, rodents and zebrafish[167,168]. Approximately thirty seconds after bath application of PTZ, zebrafish exhibited sustained periods of uncoordinated swimming accompanied by very large waves of neuroluminescence (Figure 3.23h, Movie 3.2). These early episodes (~3-5 min) were followed by periodic bouts of clonus-like convulsions and prolonged waves of neuroluminescence that extended beyond the swimming bouts. (Figure 3.23i, Movie 3.3). PTZ evoked neuroluminescence signals of similar size and shape can also be detected in fully paralyzed fish (Figure 3.23j, Movie 3.4) and serve as a clear example of bioluminescence evoked in the absence of any motor activity.

Figure 3.23

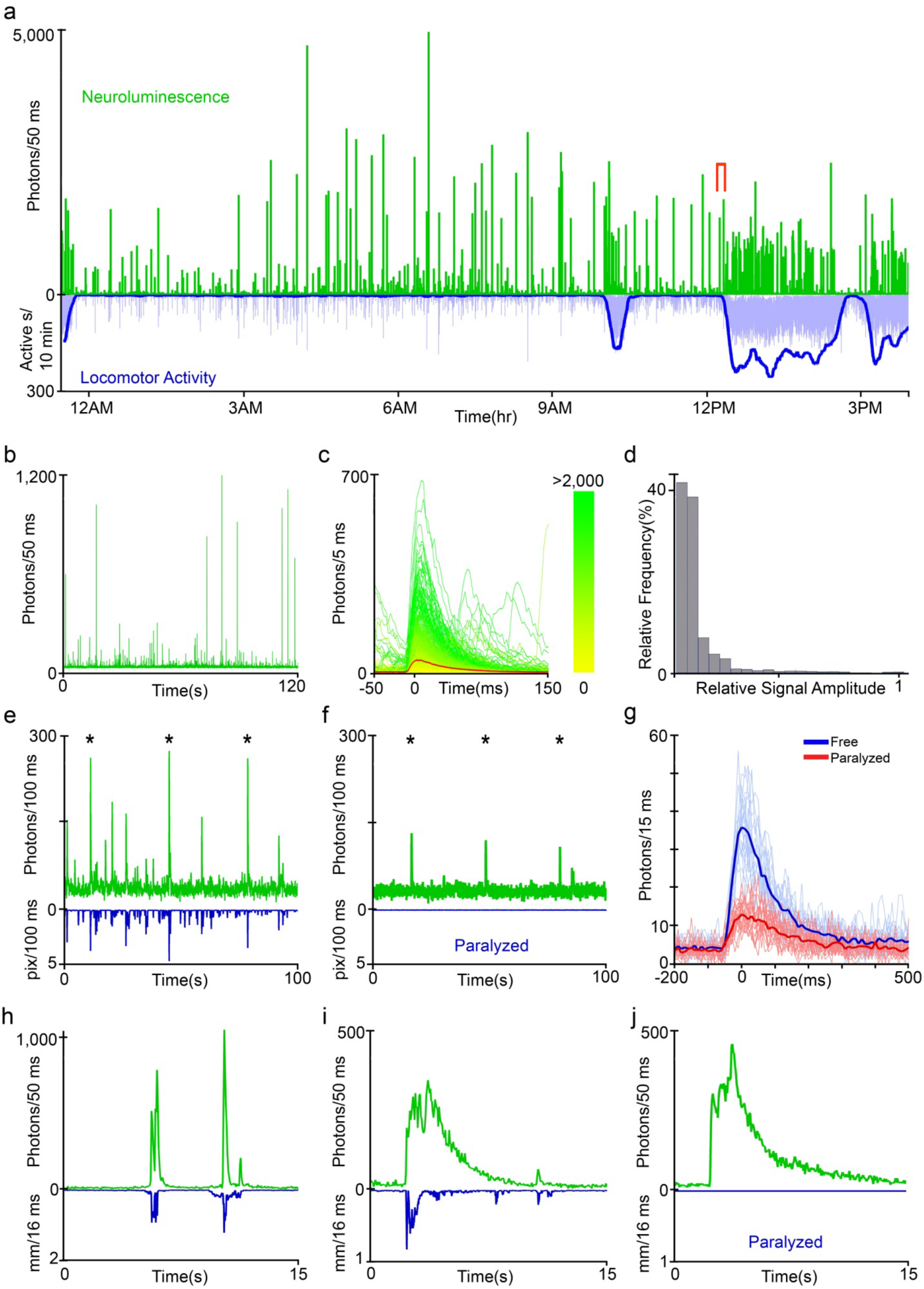

Figure 3.23 – Neuroluminescence and behavior of NβT GA zebrafish

Figure 3.23 – **Neuroluminescence and behavior of NβT GA zebrafish:** a Neuroluminescence signals and behavior can be monitored continuously for several days; a 16 hour excerpt of the recording from a 6 dpf *Nβt:Ga* transgenic zebrafish, following 24 hours of exposure to coelenterazine, is shown. Despite the constant dark conditions of the assay, an increase in locomotor activity, measured as the number of active seconds in a ten minute sliding window (bold line), and a corresponding increase in neuroluminescent events occurs soon after the previously experienced light-on time (9 AM) of the zebrafish light-dark rearing cycle. This is expected from a circadian modulation of spontaneous swimming [75]. b Expanding the bracketed region indicated in a reveals the range of neuroluminescence signal amplitudes that occur during spontaneous behavior. c Upon aligning all the signals detected during the 16 hour recording to each signals onset time and color coding each event by the number of photons arriving in a 50 ms window (0 to >2,000, see color bar), we find that neuroluminescence events consist of a fast rise and slower decay in light emission with a large range of peak amplitudes. d The histogram of signal amplitudes observed from NβT GA zebrafish (n = 6 fish, 3,125 events), normalized to the maximum signal detected from each individual, demonstrates the frequent occurrence of small amplitude events and a long tail of the distribution populated by increasingly large and rare events. e A mechanical stimulus was delivered to a group of freely swimming zebrafish (n = 6) by tapping the recording chamber (stimulus times indicated by the star symbol (*)). The stimulus resulted in neuroluminescence signals coincident with the evoked startle responses, surrounded by intermittent and variable spontaneous signals. f The same fish shown in e were paralyzed with α-Bungarotoxin and received the same mechanical stimulus (*). Paralysis permitted isolating the sensory component of the neuroluminescence event from the full escape response behavior elicited in freely-swimming animals. g The aligned stimulus-driven events in each condition are compared, revealing an attenuated but clearly detectable sensory signal in paralyzed zebrafish. h PTZ induced epileptic behavior, characterized by uncoordinated rapid swimming, is associated with large, fast bursts of neuroluminescence consistent with the strong neural activation expected during seizure episodes (t_0 = 1 min after initial PTZ exposure). i Following extended exposure to PTZ (t_0 > 17 min), long, slow neuroluminescence events are observed independent of swimming. j Paralyzed zebrafish exposed to PTZ also exhibit long, slow neuroluminescence events, suggesting that motor activity may modulate the amplitude and timescale of PTZ induced epileptic episodes.

Figure 3.24

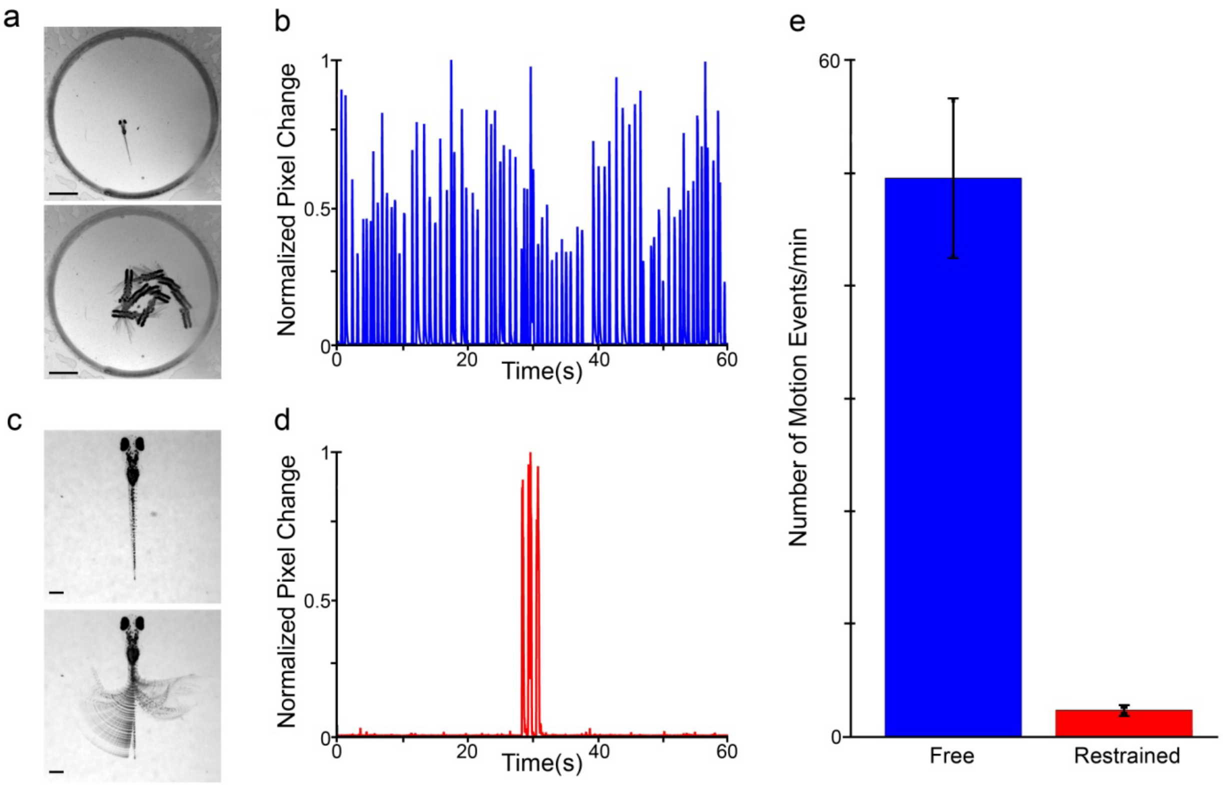

Figure 3.24 - Restraining zebrafish substantially reduces spontaneous activity: a A single image of a freely swimming zebrafish (top) and the minimum intensity projection of a 3 second image sequence (bottom) (scale bar: 2.5 mm). **b** The activity of a 6 dpf fish, measured as the frame to frame pixel change (acquired at 50 Hz) normalized to the maximum value, is plotted for a 60 second time period. Each peak in the activity recording, which corresponds to a discrete swim bout, is counted as a single motion event. **c** A single image of a partially restrained zebrafish (top), and a maximum intensity projection of a 3 second image sequence (bottom) during a bout of spontaneous behavior (scale bar: 0.35 mm). The fish's head is embedded in low melting agarose, but the tail is free to move. **d** The activity of a head-restrained 6 dpf fish, measured as the frame to frame pixel change (acquired at 50 Hz) normalized to the maximum value, is plotted for a 60 second time period. Each peak in the activity recording, which corresponds to a discrete bout of tail motion, is counted as a single motion event. Note that a complete lack of activity in the restrained fish is interrupted by a brief burst of struggle-like bouts of tail motion. **e** A comparison of the mean number of spontaneous motion events per minute in free versus head-restrained zebrafish reveals a dramatic reduction in spontaneous activity during restraint (n = 10 zebrafish in each group, 5-6 dpf).

Imaging the PTZ induced fluorescence changes of a large brain region in a transgenic fish expressing *GCaMP2* under the HUC promoter[48] with two-photon microscopy uncovers long slow waves of correlated neural activity (Figure 3.25) that are comparable with the neuroluminescence shown in Figure 3.23h. These imaging experiments highlight the similarity of the bioluminescence signals to those obtained with conventional techniques. Together, these results obtained with Nβt:GA indicate that neuroluminescence allows the non-invasive and long-term recording of population activity from freely behaving zebrafish larvae.

Figure 3.25

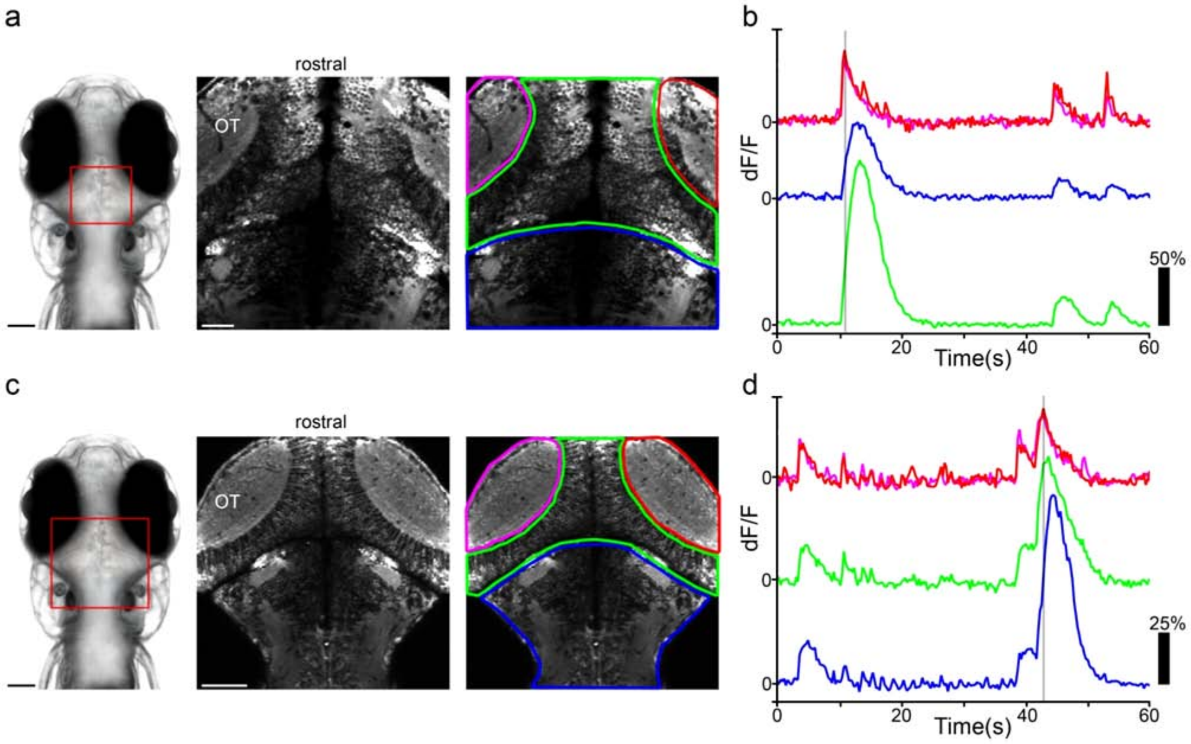

Figure 3.25 - PTZ evoked calcium responses in *HuC:GCaMP2* transgenic zebrafish: **a** (left) Dorsal bright field micrograph of a 7 dpf zebrafish (scale bar: 0.15 mm). The rectangle indicates the region selected for calcium imaging. (middle) A *HuC:GCaMP2* zebrafish was embedded in low melting agarose, paralyzed, and imaged with a two-photon microscope. The average intensity image of the acquired time-series reveals expression of GCaMP2 in the optic tectum (OT), midbrain, and hindbrain of this transgenic zebrafish (scale bar: 50 μm). (right) Regions of interest within the right and left tectal neuropils, midbrain somatic region, and hindbrain are shown; these regions were used in analysis of the calcium-dependent fluorescence signal. **b** During PTZ exposure, sporadic waves of correlated activity were detected throughout the zebrafish brain. The integrated δF/F (%) signals from each region are shown in the corresponding color; a vertical line aligned to the earliest signal peak (in the tectal neuropil) is shown to facilitate comparison of the peak signal times in the different brain regions. These transient responses have time courses comparable to the sustained neuroluminescence events observed in paralyzed Nβt:GA zebrafish (**Figure 3j**). **c-d** An additional example of the experiment described in **a-b** in which a larger, more dorsal plane of the zebrafish brain was investigated. **c** (middle image, scale bar: 100 μm) **d** Unlike in **b**, the hindbrain is the final region to reach peak signal intensity.

3.2.2 MONITORING NEUROLUMINESCENCE IN GENETICALLY TARGETED NEURONS

The hypocretin/orexin (HCRT) system in the hypothalamus consists of a group of neurons that is distinct, small in number (~ 20) and sits at the ventral limit of the diencephalon. It has been implicated in the control of arousal in mammals and fish[35,169,170,171,172,173] and its disruption in dogs and mice[174,175] produces symptoms similar to those of human narcolepsy, a disorder characterized by the sudden, spontaneous onset of sleep. Electrical recordings from HCRT neurons in rodents have found that these cells are active during periods of wakefulness and exhibit transient bouts of activity during phasic REM sleep[176,177,178]. In addition, specific optical stimulation of channelrhodopsin-2 expressing HCRT neurons in mice increased the probability of awakening from slow-wave sleep[179]. Over-expression of HCRT in zebrafish larvae promotes and consolidates wakefulness, induces hyperarousal and inhibits rest[180]. However, it has not been determined whether the activity of HCRT neurons in zebrafish is associated with periods of heightened activity, as has been observed in mammals. To directly measure the activity of HCRT neurons during rest and wakefulness, we expressed Ga under the control of a HCRT promoter (Figure 3.26) and monitored neuroluminescence throughout a circadian period. To record from this group of neurons is a significant test of the sensitivity of the neuroluminescence approach, because there are less than 20 HCRT neurons within ~100,000 neurons of the larval zebrafish nervous system. In addition, their location deep below the dorsal surface (>300 μm) results in considerable light scattering. Zebrafish larvae expressing Ga in HCRT neurons were treated with CLZN-h at 3 dpf and neuroluminescence was measured on subsequent days. With exposure to a natural light-dark cycle, zebrafish maintain a circadian periodicity in their rate of spontaneous swimming under constant lighting conditions [181]. In the constant darkness of the neuroluminescence assay, larvae were found to increase their rate of swim bouts each morning, shortly after the time of normal lights-ON in the fish rearing facility (Figure 3.23a, 3.27a). During these morning-active periods, as well as other periods of increased swimming activity[180], we observed an increase in the frequency of neuroluminescent signals from HCRT neurons (Figure 3.27a). This is consistent with recordings from HCRT neurons in mammals[176]. Furthermore, when compared to Nβt:GA larvae (Figure 3.23a), less neuroluminescence was detected in HCRT:GA fish when they were at rest or during brief arousals during the night (Figure 3.27a). This suggests that HCRT neurons are specifically active during periods of consolidated locomotor activity and is in agreement with the hypothesis that HCRT promotes wakefulness and inhibits rest in zebrafish larvae [180], as in mammals [179].

Figure 3.26

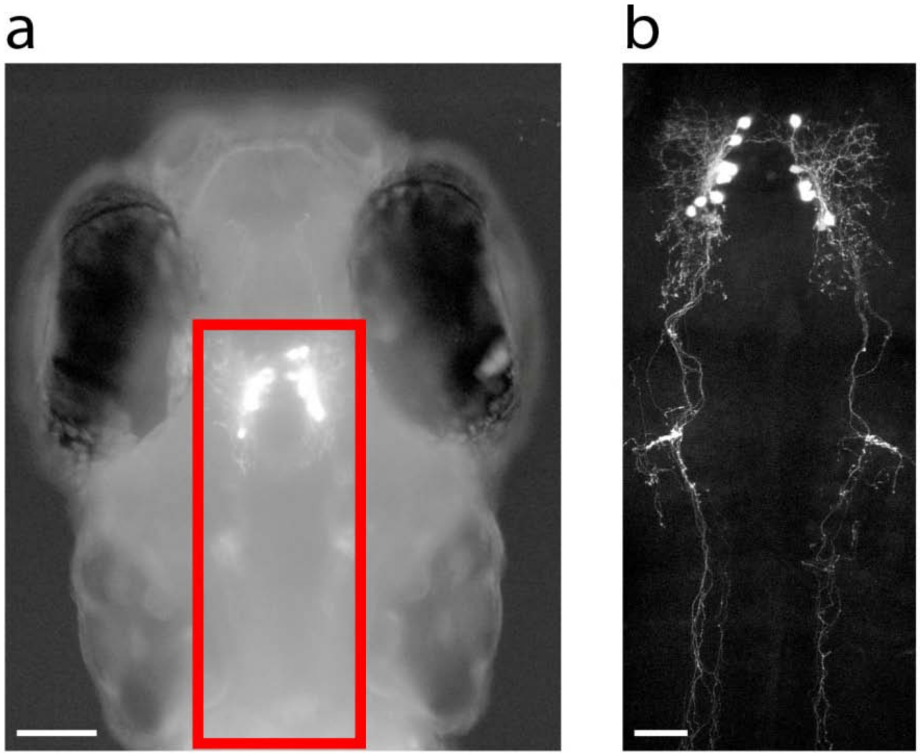

Figure 3.26 – Targeted Ga expression in Hypocretin neurons: **a** Expression of Ga in the ~20 Hypocretin (HCRT) neurons of a transgenic 4 dpf zebrafish larva are imaged with a wide-field fluorescence microscope, demonstrating their position within the posterior diencephalon (scale bar: 100 µm). **b** Ga-expressing HCRT neurons shown in a maximum intensity projection of image sections acquired with a two-photon microscope (imaged region indicated by red rectangle in a); note the long, dorsal-caudal projecting axons with an expansive arborization near the zebrafish otic vesicle (scale bar: 50 µm).

Figure 3.27

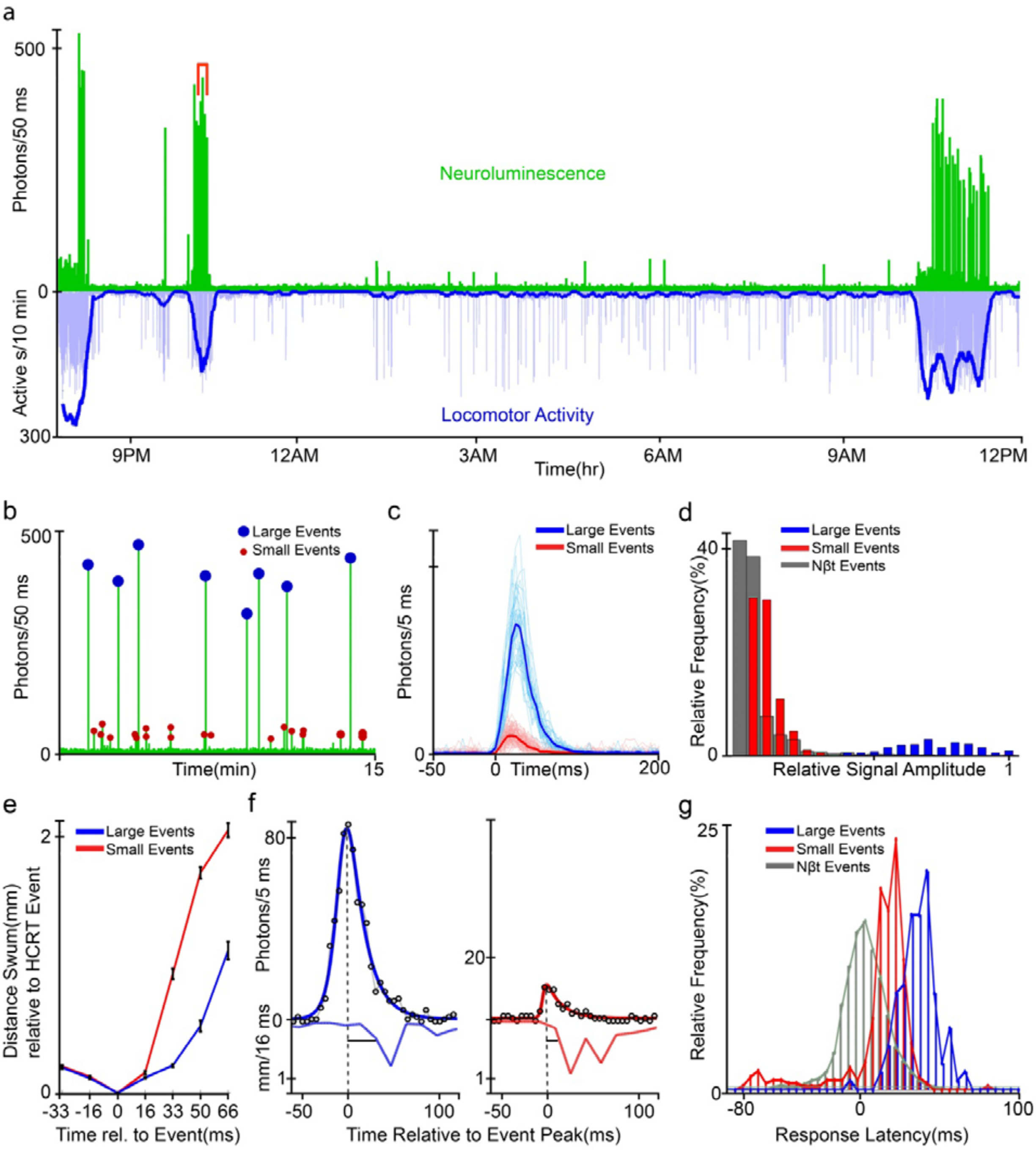

Figure 3.27 –Activity in Hypocretin neurons during natural behavior

Figure 3.27 –Activity in Hypocretin neurons during natural behavior: **a** A freely behaving 4 dpf zebrafish larva exhibits periods of increased spontaneous locomotor activity. The longest active period occurs soon after the light-on time (9 AM) of the normal rearing light cycle. Neuroluminescence events primarily occur during these periods of heightened activity. **b** Expanding the bracketed region indicated in **a** reveals that these neural signals fall into two distinct amplitude classes. Manually determined thresholds (200 photons/50 ms in **b**) were used to classify individual events into a large and small amplitude group. **c** The amplitude classified signals from the entire recording of the larva shown in **a** are aligned and the thick lines indicate the average signal time course within each class. **d** Histogram of the amplitudes for all HCRT neuroluminescence events (n = 1,064, 8 fish), normalized to the maximum response within each fish, are compared to the response amplitude of NβT:GA fish (NβT) shown in **Figure 3d**. Signals classified as large and small are colored accordingly and are clearly distinct. **e** The mean distance swum, aligned to the position of the fish at the time of a HCRT signal (0 ms), is plotted for the frames immediately before and after HCRT signals of each amplitude class (error-bars represent 1 SEM). Notably, fish swim sooner and further following small HCRT events than following large HCRT events. **f** A double exponential fit of neuroluminescence signals was used to identify the peak of the event. Example fits (solid curves) are shown for events (open circles) from the two amplitude classes along with the corresponding swim-velocities. Latency was measured as the time from the peak of the response to time at which the zebrafish achieved a threshold swim velocity (0.25 mm/16 ms). **g** Histograms of event-to-behavior latencies for the large and small HCRT events as well as events analyzed for NβT:GA zebrafish (NβT); the distributions are distinct.

To determine whether any proportion of the signals in HCRT:GA larvae were due to non-specific background effects, we used an imaging approach to localize the origin of the luminescence. Using an intensified-CCD camera in a custom-built bioluminescence/ fluorescence microscope (Figure 3.28a), we imaged restrained zebrafish and compared the spatial location of neuroluminescence to the location of GA expression as reported by the fluorescence of the tethered GFP (Figure 3.28b). Again, bath application of PTZ was used to induce epileptic events. As demonstrated in the whole brain two-photon imaging experiments (Figure 3.25), PTZ exposure induces strong and unspecific activity in most, if not all neurons across the brain, thus highlighting the usefulness of this treatment for control-experiments that test for the contribution of non-specific background expression to the neuroluminescent signals.

Although the zebrafish were paralyzed, this pharmacological stimulation produced transient increases in the total luminescence, similar to those detected in the non-imaging assay (Figure 3.27c). During these transient neuroluminescence signals, ~90% of the emitted photons came from a region containing the HCRT somata (Figure 3.28d-e). Photons originating from elsewhere within the fish head or tail were largely explained by the background dark-count rate generated by the detector. In addition, the small increase observed with respect to background might result from neuroluminescence generated in the processes of the HCRT neurons, which extend caudally into the spinal cord (Figure 3.26). Similar experiments in restrained, but non-paralyzed, Nβt:GA and HCRT:GA fish confirm the absence of any detectable bioluminescence from muscle or other non-neuronal tissues (Figure 3.29, 3.30 and 3.31).

Figure 3.28

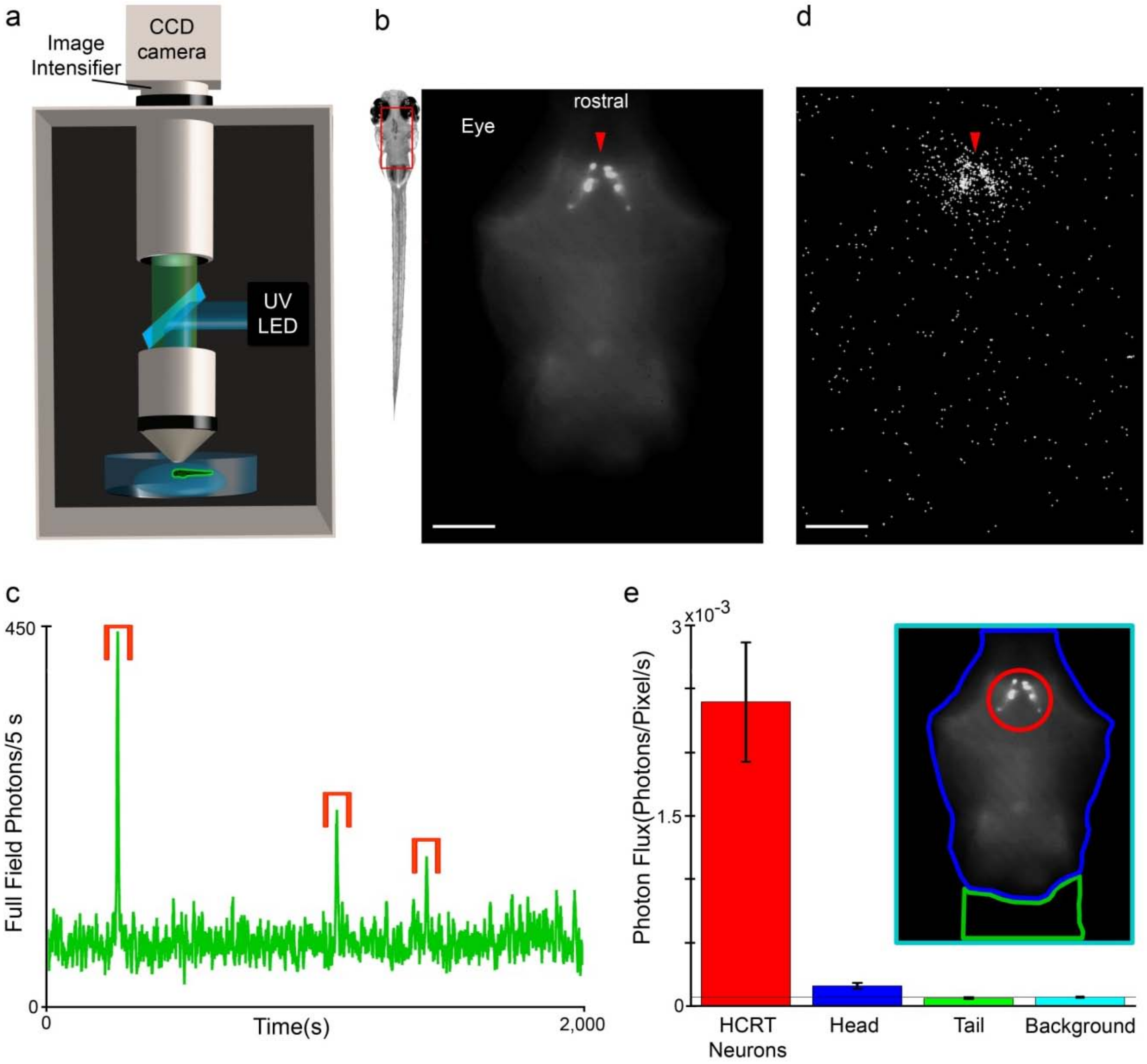

Figure 3.28 – Bioluminescent photons are generated by the GA-targeted HCRT neurons: **a** Schematic diagram of photon-counting imaging apparatus: an intensified CCD camera, custom epi-fluorescence microscope, and excitation light (UV LED) are assembled within a light tight enclosure. **b** The rectangle overlay indicates the region imaged to localize Aequorin expression via GFP fluorescence in a HCRT-GA larva immobilized in low melting point agarose and paralyzed with α-Bungarotoxin. The arrow indicates the HCRT somata (scale bar: 100 μm). **c** When epileptic-like neural activity is induced by the addition of PTZ (10 mM), transient increases in the total number of photons arriving throughout the entire image field were observed (brackets). **d** The positional origin of the detected photons during these transient events is plotted. The majority of photons arrive from the region containing the HCRT neurons; the spread is likely caused by scattering in the biological tissue while the homogenous background signal results from dark counts at the detector (scale bar: 100 μm, arrow shown at same position as **b**). **e** The photon flux arriving from within four regions of interest (see inset): the HCRT somata, the imaged portion of the zebrafish head excluding the HCRT somata, the rostral tail, and the background. The number of photons arriving from non-HCRT region of the zebrafish head is only slightly above the background dark counts and may represent photons originating from the axonal processes of the HCRT neurons (see Figure 4). However, after adjusting for the dark count signal, we still observe that >90% of photons arrive from the region containing the HCRT somata.

Figure 3.29

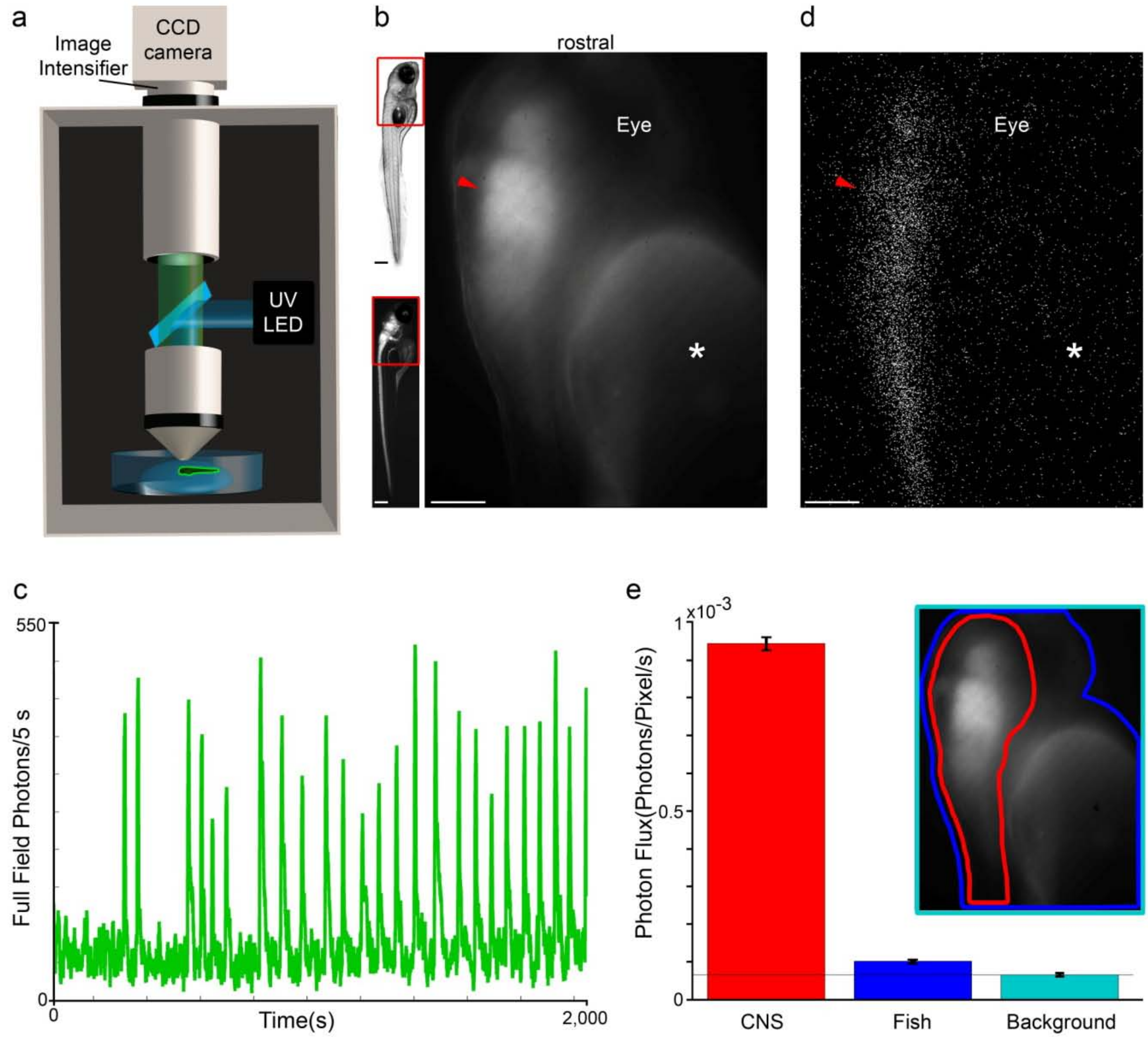

Figure 3.29 – **Photons are generated by neural structures in Nβt:GA transgenic fish: a** Schematic diagram of photon-counting imaging apparatus: an intensified CCD camera, custom epi-fluorescence microscope, and excitation light (UV LED) are assembled within a light tight enclosure. b A 5 dpf Nβt:GA larva was immobilized on its side in low melting point agarose and the rectangle overlay indicates the region imaged to localize Aequorin expression via GFP fluorescence. The arrow indicates the dorsal portion of the zebrafish brain and the auto-fluorescent swim bladder is indicated with a star symbol (*) (scale bar: 100 μm). c When epileptic-like neural activity is induced by the addition of PTZ (10 mM), transient increases in the total number of photons were observed . d The positional origin of the detected photons during these transient events is plotted. Also in a non-paralyzed zebrafish, the majority of photons arrive from the region containing neurons of the brain and spinal cord (CNS); arrow and start symbol (*) are located at the same position as in b (scale bar: 100 μm). e The photon flux (photons/pixel/second) from within three regions of interests (see inset): CNS, the imaged portion of the zebrafish excluding the CNS, and the background. Photon flux from the non-neuronal region of the zebrafish is slightly above the background dark counts, which could result from photons that originate from neurons being scattered by the fish body tissue or from neural processes located throughout the fish.

Figure 3.30

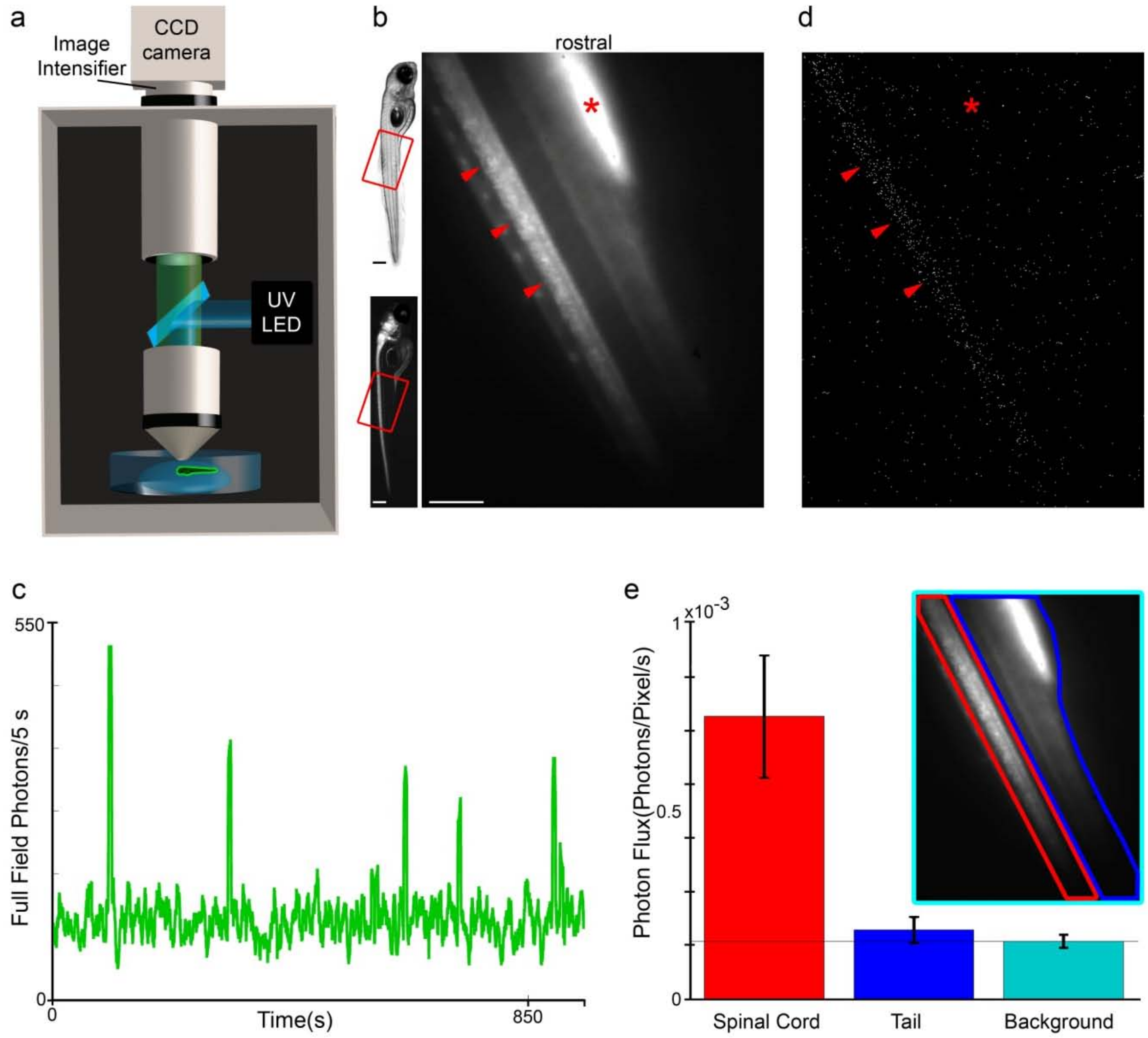

Figure 3.30 – Photons are exclusively generated by neural structures in the spinal cord: **a** Schematic diagram of photon-counting imaging apparatus: an intensified CCD camera, custom epi-fluorescence microscope, and excitation light (UV LED) are assembled within a light tight enclosure. **b** A 5 dpf Nβt:GA larva was immobilized on its side in low melting point agarose and the rectangle overlay indicates the region imaged to localize Aequorin expression via GFP fluorescence. The arrows indicate regions of the spinal cord and the auto-fluorescent swim bladder is indicated with a star symbol (*) (scale bar: 100 µm). **c** When epileptic-like neural activity is induced by the addition of PTZ (10 mM), transient increases in the total number of photons were observed . **d** The positional origin of the detected photons during these transient events is plotted. The majority of photons arrive from the region containing neurons of the spinal cord; arrows and star symbol (*) are located at the same position as in **b**. **e** The photon flux (photons/pixel/second) from within three regions of interests (see inset): spinal cord, the imaged portion of the zebrafish excluding the spinal cord, and the background. Photon flux from the non-neuronal region of the zebrafish is slightly above the background dark counts, which could result from photons that originate from neurons being scattered by the fish body tissue or from neural processes located throughout the fish.

Figure 3.31

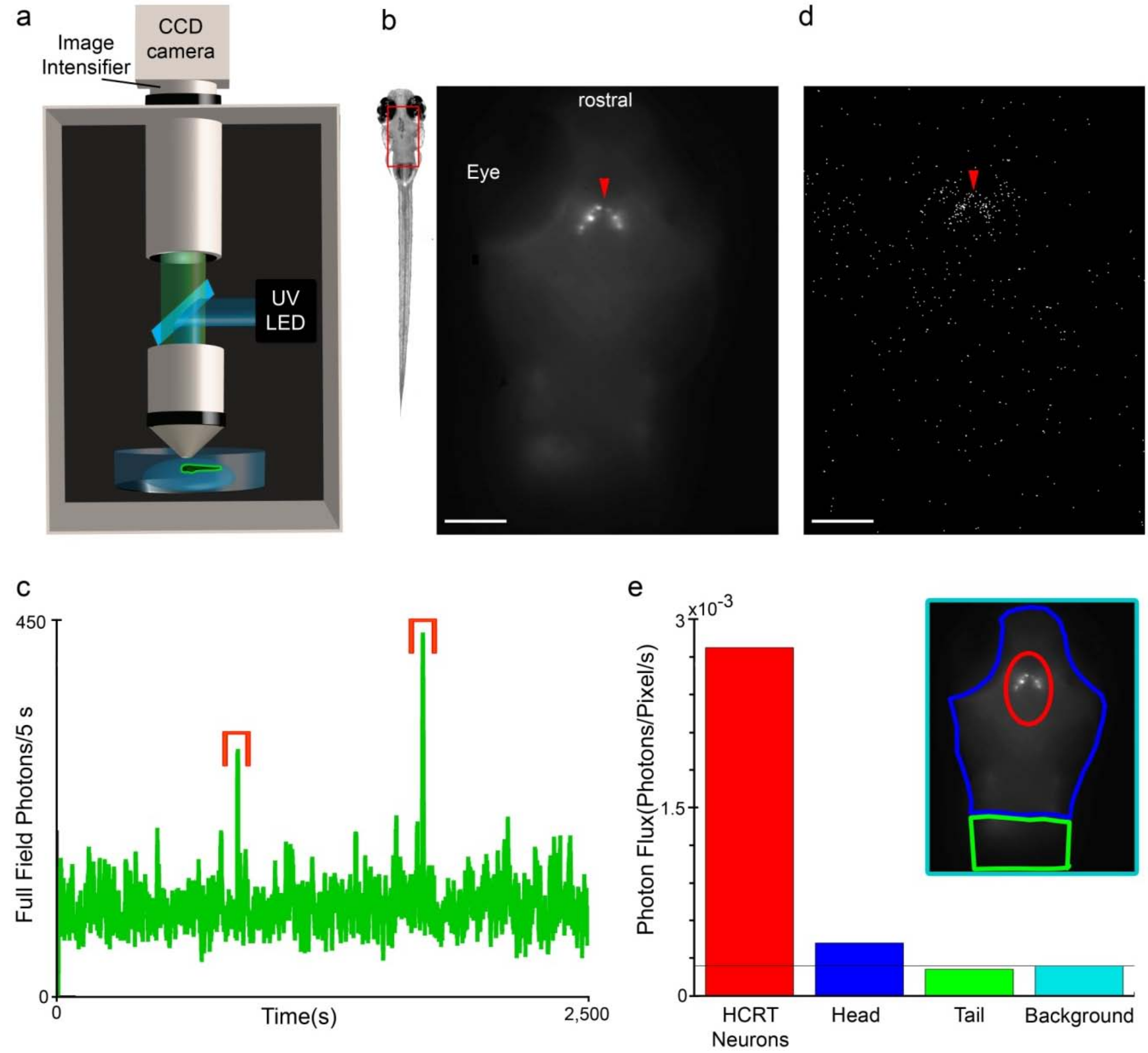

Figure 3.31 – Photons are generated by GA-targeted HCRT neurons in restrained fish: **a** Schematic diagram of photon-counting imaging apparatus: an intensified CCD camera, custom epi-fluorescence microscope, and excitation light (UV LED) are assembled within a light tight enclosure. **b** A 5 dpf HCRT-GA larva was immobilized in low melting point agarose and the rectangle overlay indicates the region imaged to localize Aequorin expression via GFP fluorescence. The arrow indicates the HCRT somata (scale bar: 100 µm). **c** When epileptic-like neural activity is induced by the addition of PTZ (10 mM), transient increases in the total number of photons were observed . **d** The positional origin of the detected photons during these transient events is plotted. Also in a non-paralyzed zebrafish, the majority of photons arrive from the region containing the HCRT neurons; the arrow is located at the same position as in **b** (scale bar: 100 µm). **e** The photon flux (photons/pixel/second) from within four regions of interests (see inset): HCRT neurons, the imaged portion of the zebrafish head excluding the HCRT region, the rostral tail, and the background. Photon flux from the non-HCRT head region of the zebrafish is slightly above the background dark counts, which may represent photons originating from the axonal processes of the HCRT neurons or photons from HCRT neurons that are scattered within the fish body tissue.

Having confirmed the spatial origin of the neuroluminescence produced by HCRT:GA zebrafish, we next examined the properties of individual signals and their association with zebrafish behavior. Individual neuroluminescence signals produced by HCRT neurons fell into two distinct amplitude categories (Figure 3.32b). The aligned signals from individual zebrafish were easily classified into large or small signals with a manually determined threshold of peak amplitude (Figure 3.32c). This bi-modal amplitude distribution differed from the continuous distribution measured for Nβt:GA neuroluminescence events (Figure 3.32d). Both large and small signals were associated with swim bouts, but the latency of a behavioral response and the distance swum following either signal amplitude consistently differed (Figure 3.27e). Signals classified as small HCRT events were followed by a short latency behavior. In contrast, behaviors following large HCRT events occurred 15-30 ms later. Accurate estimation of the neuroluminescence-to-behavior latency was accomplished by fitting the raw photon signal with a dual-exponential function, determining the peak-time, and measuring the time from the peak until the subsequent behaviors exceeded a velocity threshold (Figure 3.27f). The histograms of response latencies for large and small HCRT signals are distinct and the average latencies are significantly different ($p < 0.001$; Student’s T-test: n = 359 small events, n = 135 large events from 5 fish). Furthermore, small HCRT signals were more likely to be preceded by a behavioral response than large HCRT signals. These preceding behavior events result in latency estimates less than zero. Excluding events of clearly inverted causality, (latencies of less than -50ms, 47 of 359 small events versus only 1 of 135 large events) the average response latencies for both amplitude classes of HCRT signals were significantly longer than the latencies observed for Nβt:GA neuroluminescence signals (Figure 3.27g), suggesting that swim bouts associated with HCRT events represent a distinct subset of the spontaneous behaviors produced by larval zebrafish (5 HCRT fish, small events (S): 17.6 +/- 1.0 ms, n = 312, large events (L): 40.8 +/- 1.6 ms, n = 134; 6 NβT fish: 11.3 +/- 0.4 ms, n = 1667 – S versus PN: $p < 0.001$, L versus PN: $p < 0.001$). Further analysis of the behaviors associated with the different amplitude HCRT signals (Figure 3.32) revealed that the peak velocity following the small events significantly exceeds that of large events. This analysis also revealed that large events are preceded by increased swim activity compared to small events in a one second time window preceding the HCRT event.

These results highlight that neuroluminescence signals have sufficient temporal resolution to compare neurophysiologic and behavioral responses on a time scale of ~10 ms in addition to the capability of distinguishing between responses that differ in amplitude. Whether the small and large HCRT signals result from activating different subsets of the labeled neurons or whether the different amplitudes originate from distinct activation states of the entire population is unknown.

To explore the limits of neuroluminescence sensitivity, we investigated whether our technique can detect signals from a single HCRT neuron (Figure 3.33). For this we expressed transiently Ga in HCRT neurons and screened for fish that showed expression in only a single cell (Figure 3.33a). After treatment with CLZN-h and exposure to PTZ we observed neuroluminescent signals that were small but still well above the detection limit (Figure 3.33b), a clear demonstration that neuroluminescence can be detected from single neurons.

Figure 3.32

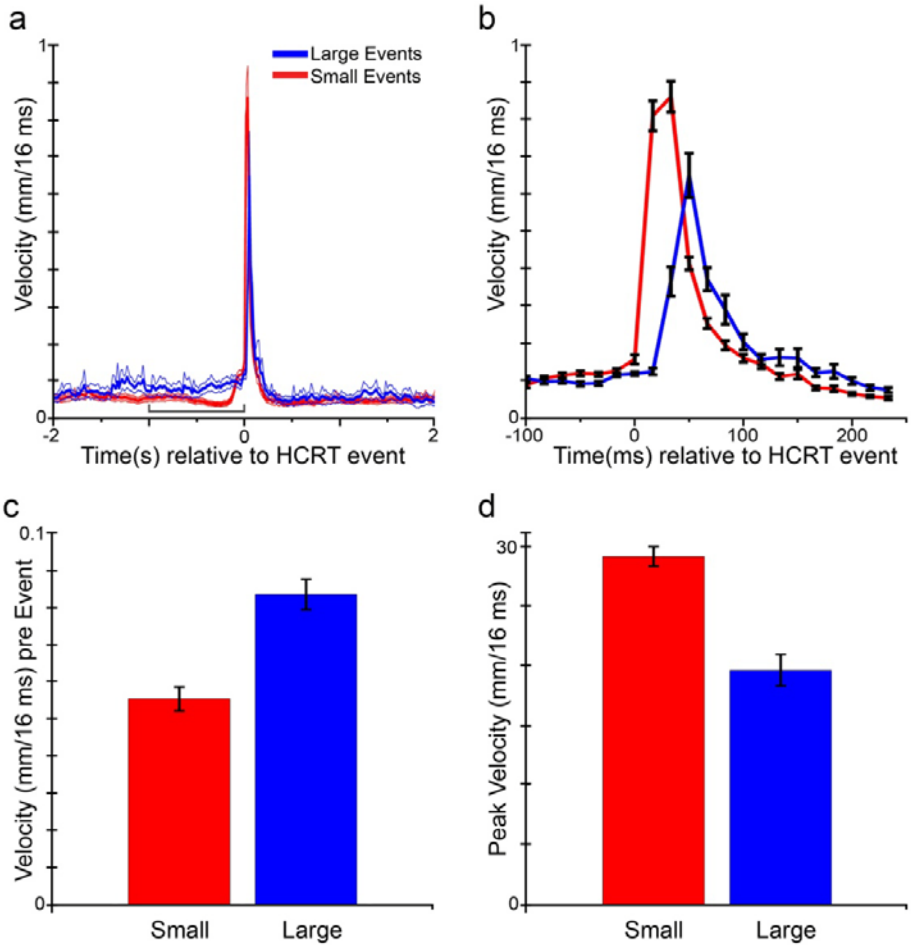

Figure 3.32 - Different amplitude signals from HCRT neurons are correlated with different behaviors: a The mean velocity of freely swimming HCRT:GA zebrafish in the two second time period surrounding large and small HCRT events (event time = 0 ms).The thin lines surrounding each mean plot demarcate a boundary of +/- 2 SEM. **b** An expansion of the time immediately surrounding the HCRT event. The difference in response latency for large and small HCRT events is apparent, as well as different velocity profiles. **c** Comparing the mean velocity within 1 second preceding the HCRT events (bracketed time region shown in **a**), demonstrates that zebrafish are more active prior to a large HCRT event than a small HCRT event. **d** Comparing the mean peak velocity reached following different HCRT events reveals that fish swim faster after a small HCRT event than after a large HCRT event.

Figure 3.33

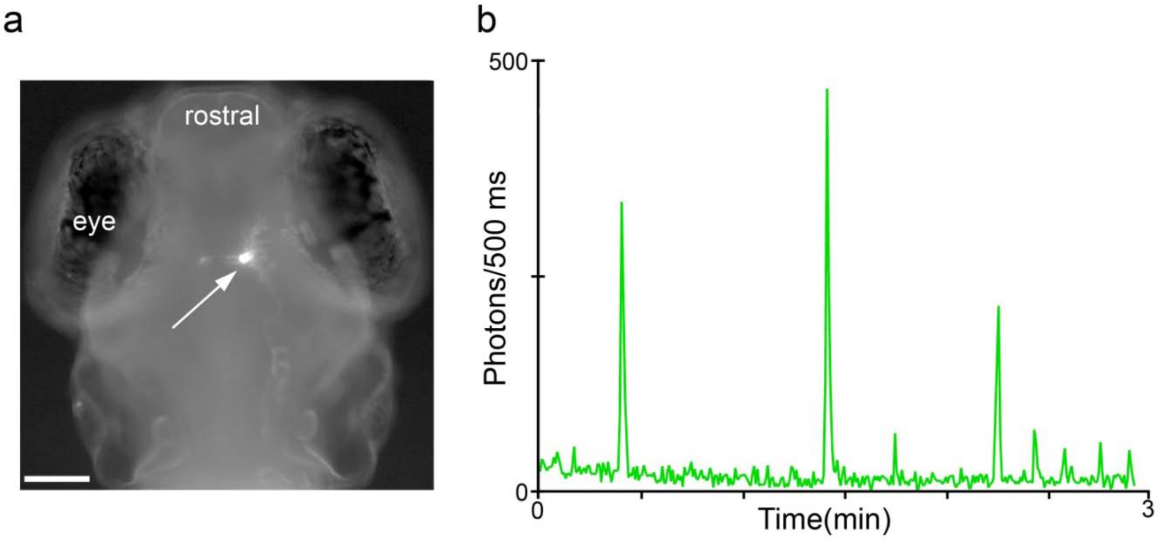

Figure 3.33 – Neuroluminescence detection from single HCRT **neurons:** a Fluorescence micrograph of a zebrafish larva transiently expressing HCRT: Ga in a single neuron (soma indicated by arrow, scale bar: 100 µm). **b** Following constitution with CLZN for 24 hours, epileptic-like neural activity was induced by the addition of PTZ (10 mM), and large neuroluminescence signals were easily detected from an individual neuron in a freely moving animal.

3.2.3 AEQUORIN RESPONSES IN SEROTONERGIC NEURONS

The serotonergic system (5-hydroxytryptamine (5-HT), serotonin) of the *dorsal raphe nuclei* (DRN) is involved in feeding, depression, anxiety, and sleep regulation. For many associated psychiatric disorders, treatments target serotonin function in one way or another. Despite many investigations on its function, there seems to be little agreement about which behaviors the serotonergic neurons in the DRN are regulating. However, evidence from different studies points towards a role in reward processing. For example, single-unit recordings in neurons within the DRN in primates show modulation of serotonergic neuronal activity during reward processing[182,183]. In rodents, intracranial self-stimulation of the DRN region seems to be strongly reinforcing, indicating that serotonin could be modulating motivational states. A recent study, that measured neuronal activity in the DRN in freely moving rats performing a decision-making task, report that a large majority of DRN neurons are rapidly and transiently modulated by sensory and motor as well as reward variables[184]. If serotonergic neurons in zebrafish also process a similarly wide range of information, this would not be surprising. In order to study the role of this specific neural population in spontaneous and feeding behaviors, we investigated the neural activity of serotonergic neurons of the DRN of larval zebrafish during spontaneous behavior and in presence of food (paramecia) (Figure

3.34). Using an available promoter for the serotonergic DRN[49,185], we transiently expressed the Aequorin-GFP in just this neural population (Figure 3.34a). With DNA microinjection we were able to transiently express GFP-Aequorin in more than 50-100 neurons of these serotonergic neurons. Without the presence of food most of the signals that we recorded were short and burst like during locomotion (Figure 3.34b). When paramecia were added to the recording chamber, long low amplitude signals could be recorded (Figure 3.34d), possibly resulting from a successful prey capture event that might serve as a reward signal. These signals are longer than any signal recorded before the paramecia were added. This finding is consistent with the classical view of tonically acting neuromodulatory systems. Notably, these long signals are further evidence that Aequorin signals can be detected independent of locomotion. Although, we repeated these experiments four times, these results are considered to be preliminary. However, the fact that we could simply express Aequorin in a neural population of interest and record the neural activity within this group of neurons during natural behavior highlights the power of this technique for the investigation of specific neuronal populations. Furthermore, the highly visual zebrafish hunts paramecia guided by its vision and in order to properly investigate the role of serotonergic neurons in prey tracking, we need to implement first a strategy that allows studying behaviors with bioluminescence in natural lighting conditions.

Figure 3.34

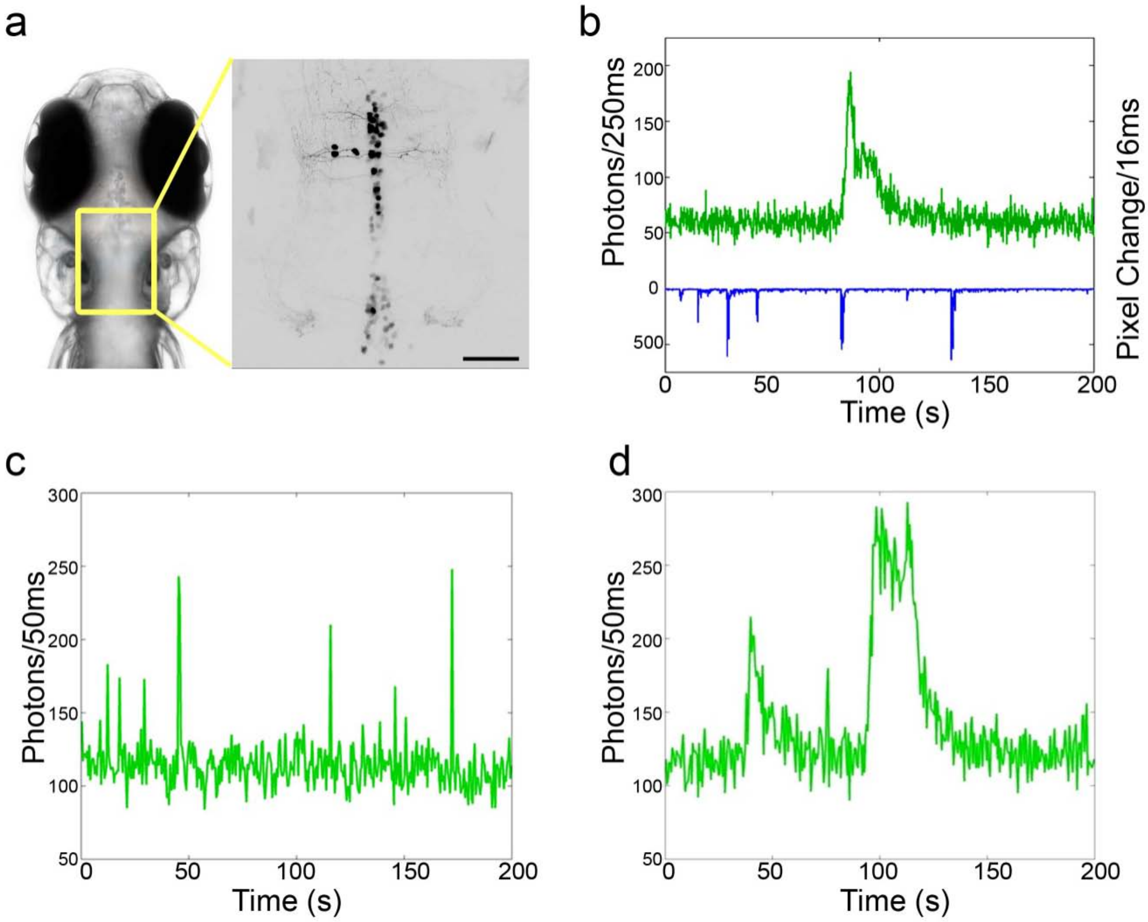

Figure 3.34 – Neuroluminescence detection from serotonergic neurons: **a** Schematic illustrating the location (yellow rectangle) of a projection of two photon sections transiently expressing pet1: Ga in the *dorsal raphe nucleus* along the midline of the zebrafish (scale bar: 20 µm). **b** Exemplary neuroluminescence signals from serotonergic neurons recorded in the presence of paramecia. Note that the neuroluminescence signals are decorrelated with the simultaneously recorded locomotion. **c** Typical short lived neuroluminescence signals without paramecia. **d** Typical signals after 10 minutes after addition of paramecia to the recording chamber. (4 experiments, 5 fish per experiments)

3.2.4 MONITORING NEUROLUMINESCENCE DURING VISUAL BEHAVIOR

Using existing detection methods, bioluminescence experiments have been limited to behaviors that occur naturally in darkness. Imperfections in spectral filters, particularly their inability to adequately reject the high-angle (>30°) light incident on the detector, have necessitated that the photon-counting sensor be protected from all but infrared illumination, to which most sensors are largely insensitive. To overcome this problem, we have designed a novel detection system that uses a cathode-gated channel photon multiplier (CPM) with a temporal gating strategy that allows fast flickering visible illumination during the detection of the bioluminescence signal.

In our design, computer generated gating signals control the cathode-voltage of the CPM, a visible LED, and the IR illumination light source for a behavior monitoring camera. During each 10 ms cycle, the CPM is gated “ON” for 9 ms, and is able to detect individual bioluminescence photons. In the final 1 ms, the CPM is rapidly gated “OFF” and both the visible LED and IR illumination are briefly activated, sending ~1012 visible photons towards the now insensitive detector for 1 ms. In the next cycle, the CPM is again gated “ON” and able to count single bioluminescent photons. With this 100 Hz repetition rate and a 90% detection duty cycle, natural illumination conditions can be simulated while only 1 of 10 emitted bioluminescent photons is discarded (Figure 3.35a).

We have tested our time-gated detection/illumination strategy by exposing groups of Nβt:GA zebrafish to short visible light cycles (5 min ON, 5 min OFF). Zebrafish respond to transient decreases in illumination with an increase in swim activity, while an elevation in light levels is followed by a period of suppressed activity (Figure 3.35b-c). These transient behavioral responses to changes in light intensity are in line with previously reported observations. We were able to record this visually-driven behavior while simultaneously recording neuroluminescence signals, demonstrating that the neuroluminescence assay can be extended to experiments requiring natural lighting conditions.

Figure 3.35

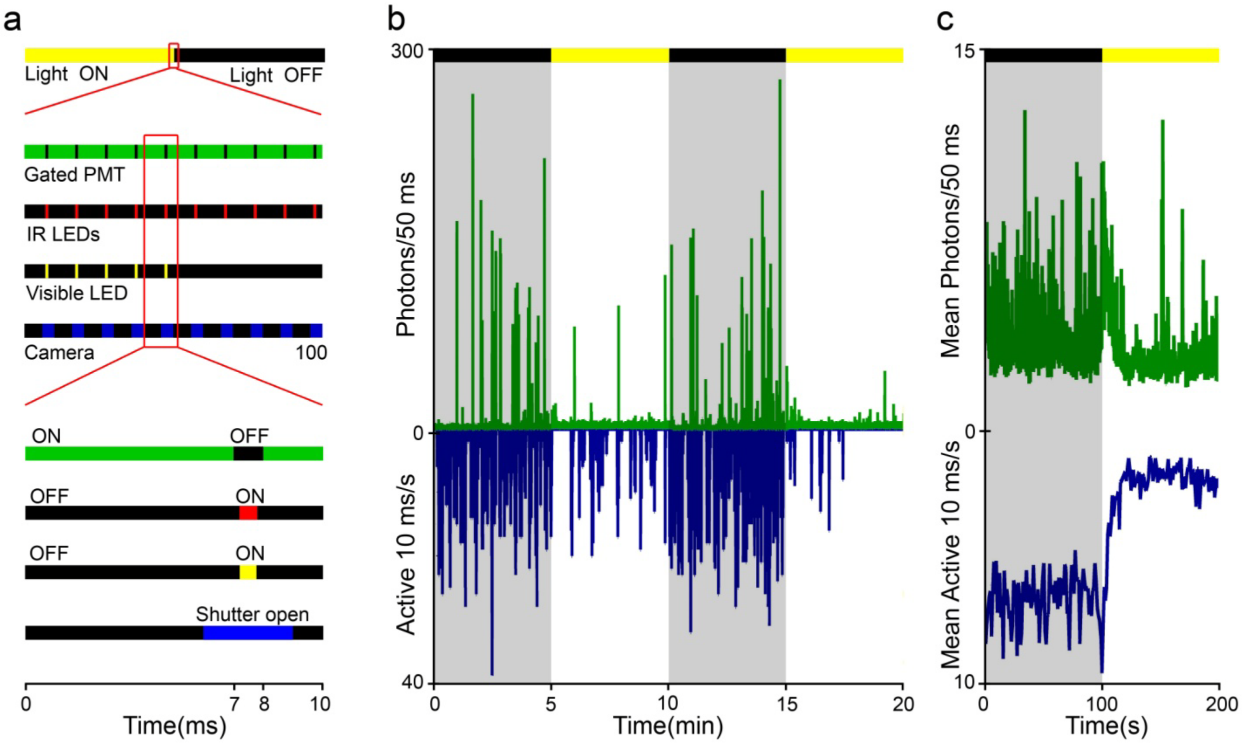

Figure 3.35 – Temporally gated detection for monitoring neuroluminescence during visual stimulation: **a** Schematic of timing protocol for stroboscopic visual stimulation and gating of a Channel Photon Multiplier (CPM) during a "light ON" to "light OFF" transition. Close-ups of the 100 ms surrounding the transition and 10 ms of a "light ON" gate cycle demonstrate the synchronous control of the bioluminescence detection and behavior monitoring. When visual stimulation is required, the visible LED is switched on for 0.8 ms while the CPM is off gated. **b** Example of neuroluminescence and visually-evoked behavior recorded during periodic changes in whole-field illumination. 6 dpf Nβt:GA transgenic zebrafish larvae, previously exposed to CLZN, show reduced locomotor activity and Nβt:GA neuroluminescence signal during "light ON" periods. **c** The mean neuroluminescence and behavioral response surrounding an step increase in whole-field illumination (63 light transitions, 7 experiments, 49 fish).

4 DISCUSSION

4.1 GENERAL DISCUSSION

4.1.1 GENERAL SIGNIFICANCE

The work presented in this thesis addressed two separate aims, both related to the dissection of the neural circuitry that generates behavior in a vertebrate model system, the larval zebrafish. Understanding the anatomy and function of neural circuits that generate behavior is the fundamental goal of system neuroscience. The two different aims shared the goal of connecting specific neural activity to specific behavioral responses.

The first aim was to identify and investigate the neural circuitry that processes and combines visual whole-field motion information to produce an appropriate behavior. For this I developed a strategy, which could be implemented with available technologies. Given that the larval zebrafish brain is small, translucent, and genetically accessible, it provides a near ideal experimental system for optically investigating the role of any neuron in the entire intact vertebrate brain. I made use of this excellent opportunity to identify the components of the neural circuit underlying a sensory discrimination and the associated behavioral choices. Informed by previous studies, I focused on the central processing portion of this neural circuit that is tasked with directing and combining the visual motion information arriving from the each retina to a population of neurons that likely provide the input to motor control regions of the brainstem, the reticulospinal cord neurons, which have been shown to be necessary for the turning behavior of the OMR. The behavioral assay allowed stimulating the eyes of a freely swimming zebrafish independently and recording of the behavioral responses during this discrimination task. The generation of stable transgenic lines that express GECIs throughout their nervous system was used, along with two-photon microscopy, for the systematic analysis of the activity of single neurons throughout the brain. These technological advances resulted in the identification of the entry site of visual whole-field motion information (AF6) and neurons in the mid-brain whose response properties suggest a role as the integration site of whole-field motion. These findings are important as they outline a previously unknown neural circuit[53,186] that controls the robust OMR behavior in zebrafish. In addition, with the laser ablation of both the AF6 and the commissure, I have begun to demonstrate the necessity of these structures for normal behavioral execution. Together, these results not only demonstrate a viable strategy to identify and probe dedicated neural circuits in zebrafish, but these biological findings add to our understanding of how whole-field visual motion is transformed by the brain of a living vertebrate into the appropriate behavioral response. Identification of this motion discrimination circuitry opens up many new avenues to probe and investigate this neural circuit within a genetically accessible model organism. In addition, the same experimental strategy can be adapted to other behaviors that zebrafish are able to perform in a head restrained configuration.

The study of more complex behaviors, such as prey capture or predator avoidance, was not possible with existing techniques since the behavior is abolished or strongly attenuated in the restrained animal (Figure 3.24). Therefore, as the second aim of this thesis, I sought to circumvent these limitations of available techniques, again making use of the optical advantages the larval zebrafish has to offer, I implemented a novel technique that uses bioluminescence to non-invasively monitor the activity of genetically specified neurons in freely behaving zebrafish. For this technique, I generated expression vectors to introduce the photoprotein GFP-apoAequorin (Ga) in neurons of larval zebrafish and explored different methods to constitute Ga *in vivo* with its substrate coelenterazine (CLZN) to form the Ca^{2+}-sensitive bioluminescent sensor GFP-Aequorin (GA). In order to record the neural activity dependent light emission, ‘neuroluminescence’, in collaboration with Dr. A. Kampff, I designed and engineered an assay equipped with a large-area photon-counting detector and an infrared-sensitive camera allowing the simultaneous recording of neural activity and associated behaviors. This use of Aequorin to determine the role of genetically identified neurons in behavioral execution is a novel technique with the potential to dissect the complete neural circuitry of the zebrafish’s behavioral repertoire- one cell type at a time. A particular advantage of this technique is that neural activity of different neuronal populations can be recorded continuously for many days. Through improvements and refining of this strategy, and by performing many control experiments, the technique is now easily implemented by other laboratories.

Furthermore, I tested the limits of this technique by specifically targeting Ga to hypocretin-positive neurons of the hypothalamus. As expected from previous findings, the resulting neuroluminescence generated by this group of ~20 neurons was associated with periods of increased locomotor activity. Furthermore, it was possible to correlate two classes of neural activity corresponding to distinct swim latencies. However, in order to use the technique for the application that it was intended for initially, to study prey capture, it was necessary to overcome a major limitation of bioluminescence measurements, which previously required a completely dark environment. Therefore, I developed, tested and optimized a method for fast temporal gating of the photon detector that allowed lighting conditions in which the fish could use vision to hunt. Therefore, it is now possible to use this technology to study a small population of serotonergic neurons while zebrafish are hunting and feeding, for the first time in their life. Other investigations, focusing on different cell types (dopaminergic and HCRT receptor positive neurons) are currently in progress. In conclusion, this neuroluminescence assay can report, with high temporal resolution and stability, the activity of small subsets of neurons during unrestrained, visual behavior and can serve as an alternative strategy to study behavior and the associated neural circuits.

4.1.2 METHODOLOGICAL CONSIDERATIONS FOR USING LARVAL ZEBRAFISH IN THE INVESTIGATION OF NEURAL CIRCUITS

To examine how the use of the experiment strategy outlined in the introduction (section 1.2.6) has allowed the investigation of the neural circuitry underlying zebrafish behaviors, the achieved results will be discussed in the following.

Arguments for the use of zebrafish in the study of neural circuitry are based on the model organism's practical advantages: rapid development, large clutches of genetically similar animals, translucence, genetic accessibility and easily quantifiable behaviors. In the results of both aim 1 and aim 2, these useful properties were essential for the success of both investigations. In each study, the total optical accessibility of the zebrafish nervous system, which is otherwise only available for invertebrate preparations, was used to make neural recordings throughout the entire brain. The fast and relatively inexpensive generation of multiple stable transgenic lines allowed choosing the most suitable founder animal. This was not only convenient, but even necessary to achieve the quality of results (i.e. for the testing of different genetically encoded calcium indicators). In addition to the fast generation time, the ease of screening for the correct expression pattern was crucial to select the best transgenic from many founder animals with differential positional insertions into the genome, which produced varied expression patterns. Although promoter sequences are selected for their expression specificity (i.e. neuronal specific), once integrated into the genome surrounding enhancer elements can have a strong influence on the actual expression pattern of the reporter gene. These positional insertion effects can also result in leaky expression (i.e. not only in the neurons in question, but in muscle tissue, other neurons, etc.), which can be extremely detrimental for the interpretation of any results from the neuroluminescence assay. Therefore, for the generation of the transgenic lines used in the neuroluminescence assay, up to 20 different founder animals were screened for their specific expression profile before a suitable founder, with both the correct phenotype and a single genome insertion of the transgene could be identified and selected for further breeding. Fortunately, due to the rapid screening process, this is a routine procedure. Furthermore, for many experiments it was not only advantageous, but sometimes necessary to be able to use sibling animals for controls and comparisons in which conditions are kept as identical as possible (Figure 3.21 and Figure 3.22); thus the large clutch size was not just a mere convenience for the experimenter, but offered a valuable experimental condition.

In addition, the ease with which it is possible to track the larval zebrafish's behavior was essential for the detailed behavioral observations presented both in the results of experiments of aim 1 (long, stable recordings of turning behaviors in freely swimming fish and head restrained animals) and of aim 2 (long stable monitoring of fish locomotion, even under difficult, low light conditions). In particular, the nacre pigmentation mutant facilitated robust tracking of the fish position and orientation. This robustness was necessary to allow the detailed quantification of the turning behavior under aim 1 (Figures 3.1, 3.2, 3.3, 3.4). For aim 2, the robust circadian locomotor activity patterns were crucial to the study of arousal and sleep (Figures 3.20, 3.27, 3.32). The easy quantification of locomotor activity in response to lighting changes was a simple and effective method to prove that visual behaviors can be studied with bioluminescence (Figure 3.35). Together, I demonstrate that these useful properties of the zebrafish are readily applicable to the study of neural circuits in this impressive vertebrate.

Regarding the implementation of the strategy for the study of neural circuits, I claim that the strategy developed in the introduction has been very successful for both aim 1 and aim 2. As the study of the optomotor response is possible in head restrained fish, the use of detailed behavioral characterization, whole-brain functional imaging and laser ablations allowed the identification of neural circuit elements and the description of a working model for the neural circuitry underlying the specific behavioral phenotypes. Although, many details of the motion discrimination circuitry presented in the results of aim 1 await further confirmation and experimental tests, detailed analysis of response properties and evidence for necessity and sufficiency, the main cellular components of this neural circuit appear to be sufficiently, albeit coarsely, explained by the presented data. With aim 2, I showed that a group of genetically specified candidate neurons show activity patterns that are associated with particular locomotion events. Although this technique did not allow us to characterize the details of the response properties of the HCRT positive neurons and further experiments are needed to determine what exact role these neurons play in the regulation of arousal states, this technique fulfills the criterion of non-invasively recording the neural activity of defined groups of neurons while providing the possibility of simultaneously monitoring the behavior at high temporal and spatial resolution. Therefore, the combination of the different techniques used, developed, and reviewed in the presented work promises to be a powerful toolset for unraveling the neural circuitry used to perform behaviors of the larval zebrafish. These two examples, along with other recent studies of neural circuitry[31,89,44,142,53], demonstrate that insights and conclusions can be gained from this level of circuit analysis using larval zebrafish. For, at least, the behaviors that zebrafish display at this young age, it is likely that we will have good understanding of the underlying neural circuitry in the near future.

4.1.3 PROGRESS IN UNDERSTANDING THE NEURAL CIRCUITRY OF LARVAL ZEBRAFISH

At this point, the major limitation of the zebrafish as a model organism in systems neuroscience and the investigation of neural circuits are the necessity of studying zebrafish at a very early stage in development, thus exploiting their translucence and ease of manipulation, which is lost later developmental stages. Furthermore, findings from studies of the nervous system of larval zebrafish can only be interpreted for developing brains, i.e. the brains of the larval zebrafish (4-10 dpf) used in these and similar studies, which change rapidly both anatomically and functionally. This is particularly apparent when considering the fact that the animal under study was not even able to move, or see, just hours earlier. Similarly, as larval zebrafish will not have to eat before 10 dpf, in most experiments the animals are extremely naïve, suggesting that their nervous system is at the very least, in a different state than that of an individual that is required to possess survival skills beyond escape and OMR responses. Indeed, many more complex behaviors, which would represent interesting behavioral paradigms, appear only later in development or as adults. However, newly available pigmentation mutants do retain their translucence throughout life, such as the double pigmentation mutant for *nacre* and *roy,* called ‘c*aspar’*[187]. Furthermore, few studies have investigated behaviors of juvenile fish (before they require breathing through their gills and acquire an optically opaque skull) and which may present a greater variety of complex behaviors while retaining some, if not all, of the advantages of the larvae; juvenile zebrafish may very well present a convenient compromise.

As for now, there are many open questions about the neural circuitry of behaviors that the larval zebrafish readily display. Even for behaviors like the OMR, that can be studied in head restrained fish, and therefore allowing the functional imaging presented in the result section 3.1, many open questions await elucidation. The detailed description of the circuit elements both developmentally and genetically will allow further investigation of both connectivity and function. The genetic tools available to the zebrafish suggest that the identification of the type of retinal ganglion cells projecting to the pretectal area is a reasonable possibility. In particular, the increasing sophistication with which promoter elements can be isolated and combined to achieve specific expression encourages a 'genetic dissection' of this and other neural circuits[23]. Such genetic access would allow many investigations combining developmental and functional questions about retinofugal projections. Furthermore, genetic targeting of other specific elements of this neural circuitry could enable the comparison of neural recordings from freely swimming fish in the neuroluminescence assay and those made in the restrained condition. Such recordings would not only serve to confirm findings, but will be helpful to determine their role in the behavior in different environmental contexts. For such investigations, it was thus particularly important to develop the neuroluminescence technique reported as aim 2, which allowed for neural recordings during visual behaviors.

Furthermore, the strategy I developed in the introduction, if used together with the neuroluminescence technique presented in section 3.2, could be used to investigate neural circuits underlying the neural implementation of prey capture[58,63]. This relatively complex behavior could serve as a model for investigating the neural processing of appetitive and aversive stimuli. Since the optic tectum is necessary for prey capture and predator avoidance, the identification of specific neural cell types that can be genetically targeted[188] offers the promise that the role of these different cell types might ultimately be understood. Many other behavioral paradigms (i.e. phototaxis[189]) will benefit from a similar approach. Using the appropriate combination of techniques, including behavioral analysis, functional imaging, neuroluminescence and optogenetic tools, promises to yield great insights into the function of this remarkable, miniature vertebrate in the near future.

4.2 SPECIFIC DISCUSSION OF AIM 1:

NEURAL CIRCUITRY OF VISUAL WHOLE-FIELD MOTION DISCRIMINATION

In order to identify the neural circuitry underlying visually evoked turning behavior, we first characterized the contribution of each eye to behaviors evoked by the presentation of whole field motion and its monocular components. We then used functional imaging to identify the retinal arbourization fields that carry whole field motion information, and to find that neurons of the pretectum combine and translate this sensory input into motor relevant neural responses. We hypothesize that these pretectal neurons provide direct input to hindbrain neurons that control turning behavior, thus completing the sensory to motor neural circuit. This represents a significant step towards understanding the optomotor response (OMR) in fish, but also the neuronal basis of sensory motor transformations in general. Importantly, the experiment strategies and techniques developed for this study offer further promise for studies of this and other neural circuits found in other genetically-accessible model organisms. In the following, I will discuss how our behavior-based, neuroethological, approach was used to identify putative elements of a motion discrimination neural circuit and compare these findings with information from other vertebrate, and mammalian, neural circuits. I will then highlight interesting directions for future experiments and describe which technical developments will make these exciting experiments possible.

4.2.1 PSYCHOPHYSICS AND NEURAL CIRCUIT IDENTIFICATION

To characterize the information processing performed by the neural circuit underlying whole-field motion discrimination, we used a psychophysics approach to assay how visual information arising from each eye contributes to the resultant behavior. It was known that retinal ganglion cells project exclusively to the contralateral brain [123] hemisphere and that lateralized activity in a group of hindbrain neurons is necessary for turning behavior[53]. Therefore, we hypothesized that a crucial processing stage in the circuit will involve the combination of sensory information from both eyes. Surprisingly, the whole-field motion information that evokes turning behaviors was not balanced between the eyes (Figure 3.3). Instead, our behavioral results demonstrate that OMR turning behavior is primarily evoked by the inward motion information arriving at either eye; the right eye for leftward motion and the left eye for rightward motion. This result presented a dilemma: what happens when both eyes experience inward (or outward) conflicting motion? For these conflicting stimuli, different behavioral responses might have been expected: Given that the monocular inward motion components can alone evoke strong turning behavior, we speculated that the fish might show a bistable behavior. When humans and other non-human primates are presented with different images to each eye, these conflicting monocular images compete dynamically for access to conscious perception and control of behavior[190,7,191]. Such "rivalry" phenomena have been particularly useful to neuroscientists, as they facilitate attempts to identify the stage of neural processing where perceptual decisions are made. Although, in primates, binocular rivalry does occur for conflicting monocular motion stimuli[192,193], presentation of binocular inward conflicting motion stimuli to zebrafish did not result in a bistable behavioral output. The behavioral data, as well as subsequent neural recordings in the zebrafish pretectum, suggests that inward motion stimuli are able to suppress neural activity on the contralateral side and that the network remains stable when binocular inward motion is un-naturally presented. Given the likely importance of the OMR for larval zebrafish, this stability may be an adaptive property of the network, one that suppresses ‘wrong’ or ‘wasteful’ behavioral choices.

Notably, all stimuli that contained an inward stimulus component also caused strongly increased locomotor activity when compared to the no motion baseline condition. Normal whole field motion, inward motion to one eye and the outward motion to the other, leads to an additional increase of large angle turns, but not to more motor activity with respect to monocular inward stimulation alone. The preliminary data about the direction selectivity of the pretectal neurons suggests that the inward stimuli also activate neurons responsive to forward stimuli and therefore activate a different part of the neural circuitry, one that induces heightened motor activity.

Interestingly, the behavioral results for binocular or monocular outward motion suggest that these stimuli are not only unable to drive this heightened motor activity circuit, but might even suppress it: Monocular outward stimuli bias spontaneous turns in the stimulus direction, whereas binocular conflicting motion lowers the spontaneous locomotor activity significantly. After ablation of the posterior commissure, we found that even monocular outward motion suppresses motor activity, while no longer biasing the turn direction (Figure 3.14). As monocular outward stimuli activate neurons in the ipsilateral pretectum that also respond to inward stimuli, they should drive the turning and locomotor circuitry. However, as we cannot detect increased locomotor activity for these stimuli, it is possible that outward stimuli, suppress locomotor activity on the contralateral side, while activating the ‘turning circuitry’ of the pretectum. For monocular outward stimulation, this activation could balance such inhibitory outward information that does not cross via the posterior commissure. So far, this hypothesis is consistent with the behavioral data for binocular conflicting stimuli and the locomotor suppression after commissure ablation; however the details of these phenomena should be addressed in future experiments.

The use of psychophysics to probe and challenge the nervous system has helped us speculate about how each stimulus might be represented within the underlying neural processing circuitry. Fortunately, the larval zebrafish preparation allows direct, optical investigation of neural activity during the presentation of visual stimuli to an intact animal. We used this advantage, along with available techniques, to study the neural implementation of the motion discrimination behavior tested with our zebrafish psychophysics assay.

4.2.2 COMPONENTS OF THE ZEBRAFISH MOTION DISCRIMINATION CIRCUIT

4.2.2.1 MOTOR CONTROL OF THE OPTOMOTOR RESPONSE

We began our investigation of the OMR circuit from the output stage, starting with the spinal projection neurons that are known to be involved in visually guided turning behavior. Previous studies reported that the ventromedial cells of the hindbrain were functionally heterogeneous, showing different tuning properties; neurons with forward motion responses were found bilaterally while those responding to leftward and rightward motion were lateralized. As expected, given that the ventromedial neurons are necessary for turning behaviors, their responses to our set of monocular stimuli reflected the associated behavioral response (strongest for unambiguous motion stimuli, and attenuated responses to monocular inward and even less for monocular outward stimulation). Therefore, at this stage in the circuit, these neurons have integrated congruent visual motion information across eyes and also report the graded responses to monocular stimuli (stronger response to inward motion versus outward motion) and no activation to binocular inward stimulation. Could these neurons receive and integrate sensory information coming directly from the eyes or are they activated by intermediate neurons? There are no major projections of retinal ganglion cells directly to the hindbrain and we therefore set out to investigate the known terminal fields for visual information. Calcium imaging experiments using transgenic *HuC:GCaMP2* zebrafish found neurons in the pretectal region of the midbrain that exhibited activity patterns resembling the ultimate turning behavior, and although we currently do not have any information about the connectivity of these neurons, we hypothesize that these neurons provide direct input to the ventromedial cells. We next sought to characterize this region of pretectal neurons in more detail.

4.2.2.2 INFORMATION PROCESSING IN THE MIDBRAIN

Similar to the ventromedial neurons, whole field motion responsive pretectal neurons are functionally heterogeneous. Some neurons display a strong forward motion preference, but the majority most had a lateralized preference for turn-evoking motion stimuli. It is appears that the processing of the binocular visual information is accomplished by these pretectal neurons and that they then provide a graded output to the reticulospinal cord neurons of the mid- and hindbrain, including the ventromedial cells, which fine tune and direct the behavioral response.

Many of the responses observed in pretectal neurons require the combination of inward information from the contralateral eye with outward information from the ipsilateral eye. In zebrafish, since all retinal ganglion cells cross the midline via the optic chiasm, the outward information must re-cross the midline in order to activate the pretectal neurons which are contralateral inward responsive. Furthermore, as suggested by behavioral data, we predict that at least some of the pretectal neurons which are activated by binocular (as well as monocular) inward stimulation are inhibitory neurons that suppress the contralateral, whole-field motion responsive pretectal neurons. Consistent with the behavioral results, these neurons are also strongly forward selective, and may also facilitate the observed increase in forward swimming while suppressing 'incorrect' large angle turns.

Detailed analysis of these different response properties of the neurons within the pretectum will reveal more about how the processing is distributed across this population. However, as the neurons of the pretectum have been identified based on their visual responses, the first questions arise are how these pretectal neurons acquire their functional properties: How is the information of the visual whole-field motion relayed from the retina?

4.2.2.3 WHOLE-FIELD MOTION INFORMATION PROCESSED BY DIRECTION SELECTIVE GANGLION CELLS

In order to identify and understand the neural circuitry underlying motion discrimination, it is necessary to know where and how the sensory information is represented when it enters the brain. Therefore, I performed targeted functional imaging experiments in the ten retinorecipient areas (AF1-10) of the larval zebrafish. AF6 showed the strongest activation to the visual motion stimuli. Therefore, I postulate that AF6 conveys at least part of the visual information to the neural circuit that drives the OMR. The eye specific persistent activation during visual stimulation corresponded well with expectations for responses at the early sensory level and showed no modulation of activity during stimulation of the other eye. Anatomical landmarks (the optic nerve can be traced from the eye to the area in question) and preliminary ablation results confirm the role of this region as the entry site of the visual motion by retinal afferents. It has been long known, that distinct types of retinal ganglion cells respond to different visual features, such as changes in light intensities (ON and OFF cells, and ON-OFF cells), or even moving objects[194,119,105]. About a dozen different retinal ganglion cell types with distinct morphology and function are supposed to relay visual information to the brain in parallel pathways[22]. Included are the direction selective retinal ganglion cells that were discovered over 40 years ago in the rabbit retina[109]. Many studies have investigated the cellular mechanisms for their direction selectivity[194], explaining some of their functional properties with their specific connectivity within the retina itself (with e.g. amacrine or bipolar cells). The two main types of direction-selective ganglion cells, ON and ON-OFF direction selective ganglion cells are common to many vertebrates including the zebrafish[194,195,119]. Interestingly, a particular visual zebrafish mutant (*nrc*) that had been previously characterized as lacking an OKR[195], whereas nearly responding normally to light decreases, provides us with some further clues about which retinal ganglion cells could be involved in the motion discrimination. Physiological experiments on the *nrc* fish demonstrated that they have normal OFF responses, but abnormal ON-OFF responses and no ON response at all. These findings, together with a pharmacological blocking of the ON pathway, strongly suggest that the ON pathway is necessary to drive the OKR in the larval zebrafish[195]. It is possible that the same ON direction selective retinal ganglion cells also mediate the OMR. Future experiments should both address which types of retinal ganglion cells terminate in AF6 and also how exactly they are connected to their downstream target. Despite many open questions, the identification of AF6 which could be specifically connected to pretectal neurons presents a first description of the neural circuitry underlying the visually guided turning responses in the larval zebrafish.

4.2.3 COMPARISON TO OTHER MOTION DISCRIMINATION NEURAL CIRCUITRY

In mammals, the midbrain region MTN of the AOS[112], has already been implicated in the processing of whole-field motion stimuli and is important for an OMR related behavior, the OKR[103]. For fish however, little is known about the core sensory processing of whole-field motion stimuli for either OKR or OMR. One study showed with electrophysiological recordings that a putative homolog retinorecipient pretectal area (*corpus geniculatum laterale*) in the small-spotted dog fish (*Scyliorhinus canicula*) is direction selective[196]. Another investigation from the same group in the gold fish reports on similarly visually direction selective neurons in a pretectal area[127]. However, since they can only with great difficulty stimulate both eyes simultaneously, the authors report that binocular responses are rare or even nonexistent. They argue that the pretectal areas are not interconnected and therefore only visual input from the contralateral retina can drive the neural activity in the pretectal neurons. This leads them to postulate that neurons that can combine the visual information and therefore allow for the correct analysis of self-motion in the three-dimensional space would only appear at a later processing stage (i. e. in the *vestibulocerebellum* or the *inferior olive*)[127].

However, with the data presented here, I show that the pretectum of zebrafish contains not only neurons with activity strongly related to the behavioral output evoked during binocular and monocular visual motion stimulation, but also a likely connection between the bilateral pretectal nuclei. In addition, I also find that the pretectum itself is the processing stage in which information from both eyes is combined.

The specific response properties to inward and outward motion in the pretectum in the zebrafish could be explained by specific retinal connections to their downstream target, the pretectal neurons[119]. Such retinofugal connections have already been found in the homologous midbrain (pretectal) regions identified in mammals[186,118,197,112]. However, to connect the anatomy with functional properties of these retinal ganglion cells is difficult and only few examples exist. By examining electrophysiologically a genetically specified types of retinal ganglion cells (SPIG1+ and SPIG1-), which project to the putative mammalian pretectal homologue (MTN), it could be shown that these neurons respond preferentially to upward and downward motion, respectively. Additional labeling experiments demonstrated that these neurons also form specific connections in the MTN. These results suggested that information about a certain image motion is not only transmitted by distinct ON direction selective ganglion cells, but also processed separately in the MTN. Similarly, the findings about the segregation in AF6 and the response properties in the pretectum in the zebrafish presented in the result section point toward a neural mechanism in which whole-field motion information is preprocessed by the retina, segregated into different direction selective pathways, and then passed on to the midbrain where this information is combined and deciphered.

Another example of this preprocessing and formation of specific connections of the retinal output to the downstream targets can be found in a particularly elegant set of studies by Kim et al.[110,120]. The authors demonstrate that a genetically identified (by the junctional adhesion molecule B (JAM-B)) upward motion direction selective OFF retinal ganglion cell type in mice forms connections in discrete laminar zones within the *lateral geniculate nucleus* or *superior colliculus.* The specificity of their morphology (highly asymmetric dendritic arbors aligned dorso-laterally across the retina), their functional motion selectivity for stimuli moving from soma to dendrite, and their specific connectivity to their downstream targets suggests that such retinal ganglion cells can provide specific preprocessed visual information to the brain. In another study, a similarly restricted connectivity between retina and its downstream targets was demonstrated for another specific type of ON-OFF direction-selective ganglion cells, which exclusively project to the *dorsal lateral geniculate nucleus* and *superior colliculus*[121]. These examples at least suggest that different functional subtypes of retinal ganglion cells could be connected to their dedicated neural target via distinct parallel information pathways.

In conclusion for the neural mechanism in zebrafish, a similar direct connection from specific retinal ganglion cell types to their pretectal partners is suggested by the finding that AF6 is segregated into distinct regions, selective for different motion directions (Figure 3.7). I speculate that the pretectum receives directional motion information via a class of whole-field direction selective retinal ganglion cells and that sensory information from each eye is combined within pretectal neurons. The integrated output of these pretectal neurons can then activate descending reticulospinal cord neurons to trigger behaviors, coordinated by spinal locomotor pattern generators.

4.2.4 CONCLUSION AND FUTURE DIRECTIONS FOR AIM 1

The characterization of the cellular information pathways that define the OMR circuit is the first step towards understanding the function of this neural processing unit. Future work should investigate how the neurons of this circuit are interconnected with other neural circuits that process different sensory information, e.g. touch or is regulated by other brain systems, such as neuromodulators. For these questions further technical developments and assay design will be necessary. However, even with our current techniques, a number of general questions about the function and structure of neural circuits can be explored. For example, a particular interesting phenomenon is revealed by the finding that fish do not immediately start turning when presented with whole-field motion stimuli, for both the freely behaving assay and, with even longer latencies, when head restrained. It appears that motion is integrated over time, and it is thus possible to investigate how information accumulates within the identified neural elements of the OMR circuit. Do the pretectal neurons and/or the ventromedial cells function as neural integrators of motion information? Forthcoming experiments will address this question with a slightly modified behavioral assay, in which motion stimulus saliency is varied (i.e. speed, contrast), and whole-brain calcium imaging experiments address the functional correlates throughout the motion discrimination circuitry.

Addressing the connectivity of the identified circuit components, however, will require further technical developments. The translucency of larval zebrafish, again, suggests the use of (genetically encoded) optical tools. Anatomical mapping of the dendrites and axon targets of circuit-relevant neurons (e.g. the pretectal neurons) can be visualized with a variety of labeling techniques and fluorescence microscopy. In particular, photo-activated fluorescent proteins, which change their emission properties after an optical conversion, show great promise to map the coarse connectivity of the OMR and other neural circuits. A promising strategy makes use of a modified green fluorescent protein that dramatically increases its emission yield following photo-activation. Photo-activatible GFP (paGFP) variants[198] allow the targeted photo-conversion of individual neurons in densely packed brain tissue of pan-neuronally expressing transgenic zebrafish (M. Orger, unpublished). In combination with a panneuronal red fluorescent transgenic fish line, paGFP will likely be useful for tracing the morphology of neurons of interest, like the neurons in the pretectal area. Or perhaps could be useful for the small regions of neuropil of AF6 in which the neuropil could be photoactivated and by diffusion of the photoconverted pGFP can reveal neurons that project to that neuropil. On a smaller scale, if regions surrounding dendrites of neurons (i.e. ventromedial cells) of interest are activated, the axons of connecting upstream, presynaptic neurons could be labeled and their somata identified. Although, helpful in establishing possible links between distinct neural populations, this technique is not sufficient to demonstrate synaptic connections.

Other strategies for proving synaptic connectivity of circuit components, such as viral gene delivery of a recombinant Rabies virus that retrogradely infects connected neurons[199], or combinatorial expression of fluorescent protein fragments that can identify synaptic partners(GRASP)[200] will ultimately be required. However, the standard for demonstrating synaptic connections between the neurons of a neural circuit is electron microscopy (EM). A serial EM reconstruction of the zebrafish brain will render the model organism an even more powerful for investigating neural circuits, and a comprehensive database is currently being pursued, but will likely not be available in the near future. However, many of the other technical developments are already available today and promise to make the further investigation of this and different neural circuits within the larval zebrafish an exciting endeavor.

Together, the behavioral and functional imaging data and preliminary results from ablations collected to address aim 1 present a consistent model of the neural circuitry which allows the fish to discriminate whole-field visual motion to guide its behavior. The characterization of this neural sensory motor circuit in zebrafish opens many new opportunities to address the computation, function and development underlying vertebrate behavior.

4.3 SPECIFIC DISCUSSION OF AIM 2: MONITORING NEURAL ACTIVITY WITH BIOLUMINESCENCE DURING NATURAL BEHAVIOR

Our results demonstrate a novel technique for monitoring neural activity in freely behaving animals. We show that Ca^{2+}-dependent bioluminescence can be detected from a small number of genetically specified neurons, even just a single cell, and that this signal can be monitored continuously for days while an animal freely behaves within an illuminated environment. This technique offers great potential for future investigations of the neural control of behavior in zebrafish and other neuroscience model systems. However, before exploring the future potential of our neuroluminescence assay, I will first discuss some of the technique's main caveats.

4.3.1 THE RELATION BETWEEN NEUROLUMINESCENCE AND NEURAL ACTIVITY

It is likely that the current version of GA, as is the case for existing fluorescent genetically-encoded Ca^{2+} indicators, lacks the sensitivity to detect individual action potentials[84]. We thus expect that the neuroluminescence responses detected with our system primarily result from bursts of firing rather than from individual action potentials. With existing versions of Aequorin, bioluminescence signals evoked by as little as five action potentials have been detected from individual pyramidal neurons in brain slices[201] and these signals showed relatively linear characteristics at higher stimulus intensities. This indicates that our technique is comparable in its sensitivity to existing genetically encoded calcium indicators[84,162,163,160]. However, in order to relate neuroluminescence signals quantitatively to the underlying number of action potentials, it is necessary to conduct careful electrophysiological studies separately in each model system and, ideally, in each neuronal sub-population. Nonetheless, these preliminary results suggest that while individual action potentials are likely to remain undetected, bursts of a few spikes should result in identifiable bioluminescent signals. An indicator that reliably reports bursts of activity is unquestionably useful, especially if it can be targeted to specified subclasses of neurons that are hypothesized to be involved in a natural behavior.

Evidently, a thorough calibration of the bioluminescent signals with conventional methods such as electrophysiology or fluorescent calcium imaging would be invaluable to allow correct interpretation of the signals. The question of how many action potentials underlie a bioluminescence signal is indeed pressing, but very difficult to assess in a context comparable to our assay for freely-swimming zebrafish. Even if restrained, paralyzed fish are used, targeted on-cell recordings from neurons that are deep within the intact brain, as opposed to superficial structures like the trigeminal nucleus, is a technique with which is much more difficult. Although, ideally, a calibration should be done for every type of neuron under study, this particular endeavor would be a goal for a complete set of other studies. Also, we would like to note that this calibration dilemma is not exclusive to our bioluminescent technique, but shared with other genetically encoded calcium indicators and that our present work might be viewed in comparison with most of the other work employing genetically encoded indicators for which precise *in vivo* calibration remains very difficult. However, results from the investigations of the *in vitro* properties of GFP-Aequorin[150,153,202] provide a comparison to similar *in vitro* calibrations of genetically-encoded Calcium indicators[162]. Until additional *in vivo* calibration experiments can be performed, this can serve as preliminary reference for the calcium sensitivity of the GFP-Aequorin in zebrafish neurons.

Calcium imaging offers another possibility to compare our bioluminescence signals to those acquired with established techniques, but this also requires additional calibration steps for a conclusive relation to underlying electrical activity. In order to get a first qualitative impression of the relationship between bioluminescence and the popular GCaMP2 fluorescent calcium indicator, we compared whole brain imaging in transgenic zebrafish expressing GCaMP2 under the HuC promoter to the Nβt GFP-Aequorin fish. We find that the long waves of correlated neural activity that we observe throughout the brains of paralyzed GCaMP2 fish exposed to PTZ, nicely resemble the rise and decay timescales of bioluminescence signals observed in paralyzed and non-swimming Nβt GFP-Aequorin fish exposed to PTZ (Figure 3.28, 30). These imaging experiments also provide a useful demonstration that PTZ treatment indeed drives waves of correlated activity throughout the brain. Therefore, PTZ treatment offers an ideal tool to test for low-level non-specific expression of GFP-Aequorin in our photon imaging setup (Figure 3.28-31). The correlated activity during the induced epileptic events represents a “worst-case scenario” for non-specific expression collectively contributing to the transient signals we detect with our assay. The fact that even under these epileptic conditions, >90% of observed photons during a transient event arise from the targeted neurons (Figure 3.28) lends additional evidence to our conclusion that bioluminescence events detected in freely swimming fish are specific to the targeted neuronal population.

A further difficulty in comparing *in vitro* calibration studies to our data from freely behaving animals arises from the behavioral change - and likely change in neural activity- due to restraint. Even when partially restrained – head embedded in agar with the tail free to move - zebrafish behavior is dramatically altered in comparison to freely swimming animals. This effect is illustrated in Figure 3.24, which demonstrates that the frequency of spontaneous swim events is reduced by more than tenfold in restrained fish. The severe influence of restraint on fish behavior illustrates the necessity of having a technique for recording neural activity in freely behaving animals, but it also highlights a major difficulty in comparing the observations from electrophysiology and calcium imaging experiments performed in restrained animals to the data collected in our freely swimming assay. It is perhaps worth noting that it is exactly these changes in behavior under head-fixed conditions that originally motivated us to develop a technique for monitoring neural activity in freely behaving zebrafish.

4.3.2 CORRELATION OF BIOLUMINESCENCE SIGNALS WITH LOCOMOTION

The finding that most of the bioluminescence signals we observe were tightly linked to locomotion of the zebrafish could raise the concern that the bulk of the bioluminescence signal could originate from non-specifically expressed GFP-Aequorin in muscle or from some other motion-related process. However, as larval zebrafish swim in discrete bouts (Orger et al. 2008), we expected to find a strong correlation between neural activity, and thus bioluminescence signals, and zebrafish locomotion. Thus, it is perhaps not surprising, that the neural activity underlying these swim bouts is reported as motion correlated bursts of neuroluminescence. Furthermore, in the larval zebrafish, even weak sensory stimulation often results in some type of swim event. In fact, it has been shown that a single AP in a single trigeminal neuron is sufficient to evoke an escape-response. At the timescales we can record, it would be difficult to disambiguate the initial sensory response from the resulting motor behavior. Nonetheless, although most signals are associated with activity, we do occasionally detect signals in the absence of locomotion. We have highlighted one such event in Figure 3.5 as the zoom-in panel that indicates a slow bioluminescence event not associated with swimming and gives a clearer picture of the complex relationship between amplitude of bioluminescence signals and the associated behavior events. Furthermore, we investigated in detail the potential contribution of non-neuronal structures (e.g. muscles) to the bioluminescence signal. First, the expression patterns in Nβt GFP-Aequorin zebrafish with two-photon microscopy. Figure 3.3 shows clearly that there is no detectable expression in tail muscles. Next, we conducted additional experiments to demonstrate that bioluminescence from non-motor processes can also be detected in our assay as well. The iCCD imaging of the head and swim-bladder of fully-embedded but non-paralyzed zebrafish exposed to PTZ Nβt GFP-Aequorin zebrafish, areas that could show non-specific expression and thus contribute to the bioluminescence signal (Figure 3.30,31), demonstrate clearly that the vast majority of photons detected above general dark noise arise from areas of the nervous system (brain and spinal cord).

Next, in order to isolate the sensory component of a bioluminescence signal, we compared the tap response of freely swimming fish to the same group of fish when paralyzed with alpha-bungarotoxin. As is expected, the isolated sensory response is smaller than the signal observed during the full escape response produced by freely swimming fish, but nonetheless, clearly shows that sensory processes giving rise to bioluminescence signals can also be detected with our method. Additionally, the expression levels in one of the sensory structures thought to be involved in mediating the tap evoked escape response – the trigeminal nucleus shows very weak expression (Figure 3.19) of GFP-Aequorin in this neuronal population for the Nβt transgenic line. This finding suggests an additional explanation for the reduced tap evoked sensory signal in paralyzed fish.

Although preliminary, a new series of experiments, in which GFP-Aequorin was expressed under control of the pet1 promoter[49] in the serotonergic neurons of the dorsal *raphe* nucleus, also demonstrate that bioluminescence signals can occur in the absence of locomotion. In Figure 3.34b depicts an example of the slow bioluminescent events that only occur when paramecia, a natural prey of the larval zebrafish, are added to the assay chamber. A brief motion burst by the fish is followed by a long and slow bioluminescent signal in the absence of any swimming. We hypothesize that these signals may be the result from successful prey-capture events, but our current behavior monitoring camera lacks sufficient resolution to detect paramecia (in fact, the high background nose in the data resulted from increasing the IR illumination in an, unsuccessful, attempt to detect the single-celled paramecia) and we are in the process of designing a new assay around a high-sensitivity, high-resolution IR CMOS camera that should be able to monitor both predator (zebrafish) and prey (paramecia/artemia) during simultaneous bioluminescence monitoring. Although, more experiments are necessary to investigate the function of the serotonergic neurons, these preliminary results can serve as a further demonstration of bioluminescence signals not associated directly with locomotion and also highlight the future potential of the technique.

4.3.3 INVESTIGATION OF NEURAL CIRCUITS WITH NEUROLUMINESCENCE

Investigations of neural circuits would be greatly advanced by a systematic, functional analysis of neuronal cell types[137]. One way to classify a cell type is by expression profile and neurotransmitter type, and with the investigation of the serotonergic and HCRT systems with our bioluminescence assay, we have demonstrated that it is now possible to monitor the neural activity of genetically specified groups of neurons, i.e. defined cell types, during free, unrestrained, natural behaviors. This functional characterization is a first step towards understanding how these neurons participate in behaviors and thus in specific neural circuits. Although our data on the serotonergic system is still too preliminary, the data from the HCRT system suggests a strong correspondence between Hcrt neural activity and movement, which is consistent with mammalian studies of Hcrt *in vivo* activity. Mileykovskiy et al. recorded from 9 putative Hcrt neurons using microwires inserted into the rat hypothalamus[176]. They found that the “activity of Hcrt neurons was correlated with the presence of motor activity” and that “Hcrt neurons strongly decreased their firing rates or ceased discharge during quiet wakefulness and virtually ceased activity in slow wave sleep”. These results are in complete agreement with ours. Lee et al. recorded from 6 Hcrt neurons in head-fixed rats[178]. They found that Hcrt “neurons discharge during active waking”, “decrease discharge during quiet waking in absence of movement, and virtually cease firing during sleep”. They also show a strong correlation between Hcrt neuron discharge and EMG activity, and observed that “when the neurons did discharge with one or two spikes during sleep, they usually did so at a time when a small movement or twitch occurred”. In contrast to Mileykovskiy et al., Lee et al. also observed that Hcrt neurons “increase firing before the end of paradoxical sleep, and thereby herald by several seconds the return of waking and muscle tone”. This difference between the studies could result from recording from different classes of Hcrt neurons since each study only recorded 9 or 6 Hcrt neurons. Alternatively, the use of head-fixed rats by Lee et al. may have caused abnormal Hcrt firing that does not occur in the freely behaving rats analyzed by Mileykovskiy et al. or the freely behaving zebrafish larvae analyzed in our study. We also note that both rodent papers presented their data over timescales (seconds) that were much longer than those analyzed by us (milliseconds), so the rodent studies do not resolve the relationship between Hcrt neuron discharge and locomotor activity as precisely as our study. However, they do show that maximal Hcrt neuron discharge is coincident with behavior, similar to our observations in zebrafish, suggesting a direct link between Hcrt neuron discharge and behavior. Nonetheless, independent confirmation of the Hcrt signals we observe in freely swimming fish with conventional techniques is clearly desirable. Obviously the best way would be targeted electrical recordings from this deep group of neurons during different wake and sleep states. However, this probably will be a challenging, but worthwhile undertaking. An alternative comparison would be to perform calcium imaging with genetically encoded or synthetic indicators. Ultimately, the experiments to determine the exact function of the Hcrt neurons will require new techniques for reversibly activating and inactivating these neurons over long timescales and during natural behavior.

4.3.4 OPTOGENETICS AND NEUROLUMINESCENCE

Optogenetic activation and inactivation techniques (such as ChR2 and Halorhodopsin, respectively)[86], often employ a non-imaging strategy to excite the entire population of expression positive neuron. These popular techniques thus face similar technical problems (simultaneously recording behavior during intense photo-stimulation (photon detection), achieving specific expression of the protein in the population of neurons of interest) similar to our non-imaging technique for monitoring bioluminescence. We expect that our technique can thus benefit from many of the technical advances in the rapidly developing field of optogenetics, while also providing a means of *monitoring* the activity during natural behavior in the groups of neurons that these other techniques are able to *manipulate*. For example, experiments in stable transgenic HCRT:ChR2 fish lines would be very informative to specifically activate Hcrt neurons.

4.3.5 CONCLUSION AND FUTURE DIRECTIONS OF AIM 2

The future development of modified forms of Aequorin, akin to the significant enhancement of other genetically encoded calcium indicators [84], as well as the use of existing or novel CLZN analogs [70] that confer increased Ca^{2+} sensitivity to Aequorin will further extend the sensitivity of the neuroluminescence technique. Indeed, recent advances in optimizing emission properties of different bioluminescent probes have facilitated their use at the single cell level [72] and manipulated their calcium sensitivity[203]. Furthermore, the development of new light detectors with improved quantum efficiency for both non-imaging assays (e.g. with large-area avalanche photodiodes and gallium-arsenide-phosphate PMTs) and photon-counting imaging setups (e.g. with electron multiplying CCDs)[204] offer exciting future possibilities for improving GA signal detection.

We are also highly encouraged by the quantitative properties of neuroluminescence demonstrated by the results with HCRT:GA zebrafish (Figure 3.27 b-g). Not only are we able to isolate two distinct event amplitudes in a freely swimming zebrafish, but the two amplitude classes were reliable predictors of distinct behaviors. As this technique is applied to different populations of neurons, we expect not only to gain insights about the timing of activity in such a population in the context of natural behaviors, but also to get a reliable report of the magnitude of these activations - another valuable source of information to assist in decoding how the neurons of the brain control an animal's behavior.

We look forward to the use of expression targeting strategies, including cell-type specific promoters and binary expression systems such as UAS/Gal4[205-207] to target GA to a wide variety of brain regions and specific neural populations. For example, available promoters for the serotonergic dorsal *raphe nuclei*[185] or the dopaminergic system[208] can be used to investigate the role of these neurotransmitters and the associated cell populations in various behavioral contexts. With the continued development of behavioral assays and techniques for stimulating and ablating neurons[86,53,209] neuroluminescence has the potential to provide an essential tool for determining how the brain choreographs the complex behavioral patterns of a simple vertebrate.

In addition to the larval zebrafish, neuroluminescence detection during free behavior could be applied to other popular neuroscience model systems. For example, the fruit fly *Drosophila melanogaster* has been used successfully in bioluminescent imaging assays to study circadian clock genes[210] and to image neural activity in restrained fruit flies[152]. Similarly, using a neuroluminescence strategy in the small and genetically accessible *Drosophila* larvae or the nematode *C. elegans* should facilitate the long-term and cell-specific recording of neural activity in any behavioral assay. In mammals, the bulk neuroluminescence from genetically distinct neuron types could be recorded during natural behavior with chronically implanted optical fibers[211]. We believe that the fast, stable properties of GA's report of neural activity along with non-imaging detection strategies provide a useful, easily implemented tool for monitoring the activity of genetically specified cell types during natural behavior; an attractive alternative to more technically challenging imaging approaches currently being pursued.

4.4 CONCLUSION

In order to understand the brain, it is necessary to analyze its function at the level of single neurons. For this functional analysis, an adequate definition of what the neural circuit is accomplishing is a prerequisite. This definition is often achieved by a detailed description of behavior. Using the behavioral response to particular stimuli to elucidate the underlying neural function can be accurately termed a ‘neuroethological’ approach to the investigation of neural circuitry. To comprehend how such neural circuitry allows an organism to detect, integrate and process information to produce appropriate behaviors is a general goal of systems neuroscience. Most of the examples for which we understand a dedicated neural circuit come from the combined study of behavior and neural function. Therefore, perhaps the first question should be: for which behaviors should the neural circuitry be understood? Examples such as the neural circuitry of the stomatogastric ganglion of the lobster seem, at first glance, an odd neural circuit not worthy of any detailed investigation. However, the amount of insight about how simple neuronal groups function together, are regulated by neuromodulators, and can adapt in order to match a target network activity, provide us with one of the most informative examples of neural circuitry[12,11,13].

I conclude that a similarly reductionist model of more complex behaviors, like the larval zebrafish, could be similarly successful, and will ultimately expand our understanding of the neural processing underlying the fascinating array of animal behaviors.

5 CONTRIBUTIONS AND ACKNOWLEDGEMENTS

5.1 AIM 1

The results investigating questions of aim one report on behavioral and imaging experiments, in which I designed the assay, performed the experiments and analyzed both behavioral and imaging data. For many experiments I used stable transgenic zebrafish expressing genetically encoded calcium indicators. The generation of different transgenic lines was a collaborative effort shared with Dr. Michael Orger, Drew Robson and Jen Li, who generated the particular transgenic zebrafish line used in this study (HuC:GCamP2). The experiments performed for the investigation of aim 1 has not been published yet and some the results must be considered incomplete awaiting further elucidation by additional experiments and analysis.

We thank A. Kampff for generous advice, discussion, and the construction of the two photon microscope used in this study. We also thank O. Griesbeck for the kind gift of the TN-XXL construct; members of the Engert and Schier labs for comments and advice; and D. Robson, J. Li and M. Orger for the *HuC:GCaMP2* transgenic fish.

5.2 AIM 2

The results addressing aim two, reports on a technique I developed in collaboration with Dr. Adam Kampff. We worked together in developing the bioluminescence assay, experimental protocols, and data analysis. I cloned various DNA constructs for the preliminary experiments and generated the Nβt:GA transgenic fish. Dr. David Prober generated the transgenic Aequorin-Hypocretin zebrafish used in this study. The work presented in the results section has been published in Nature Neuroscience[1], excluding the data regarding the expression of Aequorin in serotonergic neurons and bioluminescence recordings from *pet:Ga* fish.

We thank W. Hastings and T. Wilson for bountiful advice, discussion, and generously providing an intensified CCD camera. We also thank L. Tricoire for the kind gift of the GA construct; M. Orger, A. Douglass, P. Ramdya, and members of the Engert and Schier labs for comments and advice; A. Douglass for Nβt:gal4 vectors; P. Ramdya for providing the nacre strains; and D. Robson, J. Li and M. Orger for the HuC:GCaMP2 transgenic fish. For both aims, we thank Steven Zimmerman, Karen Hurley, and Jessica Miller for excellent zebrafish care.

6 REFERENCES

1. Naumann, E.A., Kampff, A.R., Prober, D.A., Schier, A.F. & Engert, F. Monitoring neural activity with bioluminescence during natural behavior. *Nat. Neurosci* 13, 513-520 (2010).
2. Zimmer, C. *Soul made flesh: the discovery of the brain-- and how it changed the world*. (Simon and Schuster: 2004).
3. Gross, C.G. *A Hole in the Head: More Tales in the History of Neuroscience*. (MIT Press: 2009).
4. Damasio, H., Grabowski, T., Frank, R., Galaburda, A.M. & Damasio, A.R. The return of Phineas Gage: clues about the brain from the skull of a famous patient. *Science* 264, 1102-1105 (1994).
5. Fadiga, L., Craighero, L. & D'Ausilio, A. Broca's area in language, action, and music. *Ann. N. Y. Acad. Sci* 1169, 448-458 (2009).
6. Deweer, B., Pillon, B., Pochon, J.B. & Dubois, B. Is the HM story only a "remote memory"? Some facts about hippocampus and memory in humans. *Behav. Brain Res* 127, 209-224 (2001).
7. Sheinberg, D.L. & Logothetis, N.K. The role of temporal cortical areas in perceptual organization. *Proc.Natl.Acad.Sci.U.S.A* 94, 3408-3413 (1997).
8. Quiroga, R.Q., Reddy, L., Kreiman, G., Koch, C. & Fried, I. Invariant visual representation by single neurons in the human brain. *Nature* 435, 1102-1107 (2005).
9. Padoa-Schioppa, C. & Assad, J.A. Neurons in the orbitofrontal cortex encode economic value. *Nature* 441, 223-226 (2006).
10. Desmurget, M. et al. Movement intention after parietal cortex stimulation in humans. *Science* 324, 811-813 (2009).
11. Marder, E. & Bucher, D. Understanding circuit dynamics using the stomatogastric nervous system of lobsters and crabs. *Annu. Rev. Physiol* 69, 291-316 (2007).
12. Marder, E. & Goaillard, J. Variability, compensation and homeostasis in neuron and network function. *Nat. Rev. Neurosci* 7, 563-574 (2006).
13. Destexhe, A. & Marder, E. Plasticity in single neuron and circuit computations. *Nature* 431, 789-795 (2004).
14. Chen, H., Hippenmeyer, S., Arber, S. & Frank, E. Development of the monosynaptic stretch reflex circuit. *Current Opinion in Neurobiology* 13, 96-102 (2003).
15. Lisberger, S.G. Visual guidance of smooth-pursuit eye movements: sensation, action, and what happens in between. *Neuron* 66, 477-491 (2010).
16. Straka, H. & Dieringer, N. Basic organization principles of the VOR: lessons from frogs. *Prog. Neurobiol* 73, 259-309 (2004).
17. Ito, M. Control of mental activities by internal models in the cerebellum. *Nat Rev Neurosci* 9, 304-313 (2008).
18. Rose, G.J. Insights into neural mechanisms and evolution of behaviour from electric fish. *Nat. Rev. Neurosci* 5, 943-951 (2004).
19. Lorenz, K. *On Aggression*. (Routledge: 2002).
20. Tinbergen, N. *The study of instinct*. (Clarendon Press: 1951).
21. Tinbergen, N. *The Animal in Its World (Explorations of an Ethologist, 1932-1972): Field Studies*. (Harvard University Press: 1972).
22. Kandel, E.R., Schwartz, J.H. & Jessell, T.M. *Principles of neural science*. (McGraw-Hill, Health Professions Division: 2000).
23. Luo, L., Callaway, E.M. & Svoboda, K. Genetic dissection of neural circuits. *Neuron* 57, 634-660 (2008).
24. O'Connor, D.H., Huber, D. & Svoboda, K. Reverse engineering the mouse brain. *Nature* 461, 923-929 (2009).
25. Hyde, P.S. & Knudsen, E.I. The optic tectum controls visually guided adaptive plasticity in the owl's auditory space map. *Nature* 415, 73-76 (2002).
26. Konishi, M. Behavioral guides for sensory neurophysiology. *J. Comp. Physiol. A Neuroethol. Sens. Neural. Behav. Physiol* 192, 671-676 (2006).
27. McAlpine, D. & Grothe, B. Sound localization and delay lines--do mammals fit the model? *Trends Neurosci* 26, 347-350 (2003).
28. Brainard, M.S. & Doupe, A.J. What songbirds teach us about learning. *Nature* 417, 351-358 (2002).
29. Gerlai, R. High-throughput behavioral screens: the first step towards finding genes involved in vertebrate brain function using zebrafish. *Molecules* 15, 2609-2622 (2010).
30. Genetic and optical targeting of neural circuits a... [Curr Opin Neurobiol. 2009] - PubMed result. at <http://www.ncbi.nlm.nih.gov/pubmed/19781935>
31. Wyart, C. et al. Optogenetic dissection of a behavioural module in the vertebrate spinal cord. *Nature* 461, 407-410 (2009).
32. Gahtan, E. & Baier, H. Of lasers, mutants, and see-through brains: functional neuroanatomy in zebrafish. *Journal of Neurobiology* 59, 147-161 (2004).
33. Streisinger, G., Walker, C., Dower, N., Knauber, D. & Singer, F. Production of clones of homozygous diploid zebra fish (Brachydanio rerio). *Nature* 291, 293-296 (1981).

34. Fadool, J.M. & Dowling, J.E. Zebrafish: a model system for the study of eye genetics. *Prog Retin Eye Res* 27, 89-110 (2008).
35. Rihel, J. et al. Zebrafish behavioral profiling links drugs to biological targets and rest/wake regulation. *Science* 327, 348-351 (2010).
36. Karlstrom, R.O., Trowe, T. & Bonhoeffer, F. Genetic analysis of axon guidance and mapping in the zebrafish. *Trends Neurosci* 20, 3-8 (1997).
37. Granato, M. & Nüsslein-Volhard, C. Fishing for genes controlling development. *Curr. Opin. Genet. Dev* 6, 461-468 (1996).
38. Fetcho, J.R. & Bhatt, D.H. Genes and photons: new avenues into the neuronal basis of behavior. *Current Opinion in Neurobiology* 14, 707-714 (2004).
39. Denk, W. et al. Anatomical and functional imaging of neurons using 2-photon laser scanning microscopy. [Review] [35 refs]. *Journal of Neuroscience Methods* 54, 151-162 (1994).
40. Svoboda, K. & Yasuda, R. Principles of two-photon excitation microscopy and its applications to neuroscience. *Neuron* 50, 823-839 (2006).
41. Neuhauss, S.C.F. Behavioral genetic approaches to visual system development and function in zebrafish. *J. Neurobiol* 54, 148-160 (2003).
42. Portugues, R. & Engert, F. The neural basis of visual behaviors in the larval zebrafish. *Curr. Opin. Neurobiol* 19, 644-647 (2009).
43. Meng, A. et al. Transgenesis. *The zebrafish, genetics and genomics* 133-147 (2003).
44. McLean, D.L., Fan, J., Higashijima, S., Hale, M.E. & Fetcho, J.R. A topographic map of recruitment in spinal cord. *Nature* 446, 71-75 (2007).
45. Sumbre, G., Muto, A., Baier, H. & Poo, M. Entrained rhythmic activities of neuronal ensembles as perceptual memory of time interval. *Nature* 456, 102-106 (2008).
46. McLean, D.L. & Fetcho, J.R. Using imaging and genetics in zebrafish to study developing spinal circuits in vivo. *Dev Neurobiol* 68, 817-834 (2008).
47. Kawakami, K. Transposon tools and methods in zebrafish. *Dev. Dyn* 234, 244-254 (2005).
48. Park, H.C. et al. Analysis of Upstream Elements in the HuC Promoter Leads to the Establishment of Transgenic Zebrafish with Fluorescent Neurons. *Dev.Biol.* 227, 279-293 (2000).
49. Lillesaar, C., Stigloher, C., Tannhäuser, B., Wullimann, M.F. & Bally-Cuif, L. Axonal projections originating from raphe serotonergic neurons in the developing and adult zebrafish, Danio rerio, using transgenics to visualize raphe-specific pet1 expression. *J. Comp. Neurol* 512, 158-182 (2009).
50. Higashijima, S., Hotta, Y. & Okamoto, H. Visualization of cranial motor neurons in live transgenic zebrafish expressing green fluorescent protein under the control of the islet-1 promoter/enhancer. *J. Neurosci* 20, 206-218 (2000).
51. Niell, C.M. & Smith, S.J. Functional imaging reveals rapid development of visual response properties in the zebrafish tectum. *Neuron* 45, 941-951 (2005).
52. Ramdya, P. & Engert, F. Binocular Circuit Properties Emerge Following Retinotectal Rewiring. *Nature Neuroscience* in press, (2008).
53. Orger, M.B., Kampff, A.R., Severi, K.E., Bollmann, J.H. & Engert, F. Control of visually guided behavior by distinct populations of spinal projection neurons. *Nat.Neurosci.* 11, 327-333 (2008).
54. Lister, J.A., Robertson, C.P., Lepage, T., Johnson, S.L. & Raible, D.W. nacre encodes a zebrafish microphthalmia-related protein that regulates neural-crest-derived pigment cell fate. *Development* 126, 3757-3767 (1999).
55. O'Malley, D.M. et al. Optical physiology and locomotor behaviors of wild-type and nacre zebrafish. *Methods Cell Biol* 76, 261-284 (2004).
56. Nakayama, K. Biological image motion processing: a review. *Vision Res* 25, 625-660 (1985).
57. Huang, Y. & Neuhauss, S.C.F. The optokinetic response in zebrafish and its applications. *Front. Biosci* 13, 1899-1916 (2008).
58. Portugues, R. & Engert, F. The neural basis of visual behaviors in the larval zebrafish. *Curr. Opin. Neurobiol* 19, 644-647 (2009).
59. Brockerhoff, S.E. Measuring the optokinetic response of zebrafish larvae. *Nat Protoc* 1, 2448-2451 (2006).
60. Roeser, T. & Baier, H. Visuomotor Behaviors in Larval Zebrafish after GFP-Guided Laser Ablation of the Optic Tectum. *Journal of Neuroscience* 23, 3726-3734 (2003).
61. Rick, J.M., Horschke, I. & Neuhauss, S.C. Optokinetic behavior is reversed in achiasmatic mutant zebrafish larvae. *Curr.Biol.2000.May.18.;10(10):595.-8.* 10, 595-598 (2000).
62. Neuhauss, S.C. Behavioral genetic approaches to visual system development and function in zebrafish. *Journal of Neurobiology* 54, 148-160 (2003).
63. Gahtan, E., Tanger, P. & Baier, H. Visual prey capture in larval zebrafish is controlled by identified reticulospinal neurons downstream of the tectum. *Journal of Neuroscience* 25, 9294-9303 (2005).
64. Kampff, A.R., PhD Thesis. (2008).

65. Borla, M.A., Palecek, B., Budick, S. & O'Malley, D.M. Prey capture by larval zebrafish: evidence for fine axial motor control. *Brain Behav.Evol.* 60, 207-229 (2002).
66. Budick, S.A. & O'Malley, D.M. Locomotor repertoire of the larval zebrafish: swimming, turning and prey capture. *Journal of Experimental Biology* 203 Pt 17, 2565-2579 (2000).
67. Smear, M.C. et al. Vesicular glutamate transport at a central synapse limits the acuity of visual perception in zebrafish. *Neuron* 53, 65-77 (2007).
68. Fetcho, J.R. & Liu, K.S. Zebrafish as a model system for studying neuronal circuits and behavior. *Ann.N.Y.Acad.Sci.* 860, 333-345 (1998).
69. Spence, R., Gerlach, G., Lawrence, C. & Smith, C. The behaviour and ecology of the zebrafish, Danio rerio. *Biol.Rev.Camb.Philos.Soc.* 83, 13-34 (2008).
70. Shimomura, O., Musicki, B., Kishi, Y. & Inouye, S. Light-emitting properties of recombinant semi-synthetic aequorins and recombinant fluorescein-conjugated aequorin for measuring cellular calcium. *Cell Calcium* 14, 373-378 (1993).
71. Shimomura, O. A short story of aequorin. *Biol Bull* 189, 1-5 (1995).
72. Baubet, V. et al. Chimeric green fluorescent protein-aequorin as bioluminescent Ca2+ reporters at the single-cell level. *Proc.Natl.Acad.Sci.U.S.A* 97, 7260-7265 (2000).
73. Grewe, B.F. & Helmchen, F. Optical probing of neuronal ensemble activity. *Curr. Opin. Neurobiol* 19, 520-529 (2009).
74. Hille, B. *Ionic channels of excitable membranes*. (Sinauer Associates: 1992).
75. Svoboda, K., Denk, W., Kleinfeld, D. & Tank, D.W. In vivo dendritic calcium dynamics in neocortical pyramidal neurons. *Nature* 385, 161-165 (1997).
76. Tsien, R.Y. New calcium indicators and buffers with high selectivity against magnesium and protons: design, synthesis, and properties of prototype structures. *Biochemistry* 19, 2396-2404 (1980).
77. Ramdya, P., Reiter, B. & Engert, F. Reverse correlation of rapid calcium signals in the zebrafish optic tectum in vivo. *J.Neurosci.Methods.* (2006).
78. Fetcho, J.R. & O'Malley, D.M. Visualization of active neural circuitry in the spinal cord of intact zebrafish. *J.Neurophysiol.* 73, 399-406 (1995).
79. O'Malley, D.M., Kao, Y.H. & Fetcho, J.R. Imaging the functional organization of zebrafish hindbrain segments during escape behaviors. *Neuron* 17, 1145-1155 (1996).
80. Nakai, J., Ohkura, M. & Imoto, K. A high signal-to-noise Ca(2+) probe composed of a single green fluorescent protein. *Nat.Biotechnol.* 19, 137-141 (2001).
81. Heim, N. & Griesbeck, O. Genetically encoded indicators of cellular calcium dynamics based on troponin C and green fluorescent protein. *Journal of Biological Chemistry* 279, 14280-14286 (2004).
82. Mank, M. et al. A genetically encoded calcium indicator for chronic in vivo two-photon imaging. *Nat. Methods* 5, 805-811 (2008).
83. Reiff, D.F., Plett, J., Mank, M., Griesbeck, O. & Borst, A. Visualizing retinotopic half-wave rectified input to the motion detection circuitry of Drosophila. *Nat. Neurosci* 13, 973-978 (2010).
84. Mank, M. & Griesbeck, O. Genetically Encoded Calcium Indicators. *Chem.Rev.* 108, 1550-1564 (2008).
85. Higashijima, S.I., Masino, M.A., Mandel, G. & Fetcho, J.R. Imaging neuronal activity during zebrafish behavior with a genetically encoded calcium indicator. *J.Neurophysiol.* 90, 3986-3997 (2003).
86. Deisseroth, K. et al. Next-generation optical technologies for illuminating genetically targeted brain circuits. *Journal of Neuroscience* 26, 10380-10386 (2006).
87. Volgraf, M. et al. Allosteric control of an ionotropic glutamate receptor with an optical switch. *Nat. Chem. Biol* 2, 47-52 (2006).
88. Douglass, A.D., Kraves, S., Deisseroth, K., Schier, A.F. & Engert, F. Escape behavior elicited by single, Channelrhodopsin-2-evoked spikes in zebrafish somatosensory neurons. *Current Biology* 18, 1133-1137 (2008).
89. Arrenberg, A.B., Del Bene, F. & Baier, H. Optical control of zebrafish behavior with halorhodopsin. *Proc. Natl. Acad. Sci. U.S.A* 106, 17968-17973 (2009).
90. Curado, S., Stainier, D.Y.R. & Anderson, R.M. Nitroreductase-mediated cell/tissue ablation in zebrafish: a spatially and temporally controlled ablation method with applications in developmental and regeneration studies. *Nat Protoc* 3, 948-954 (2008).
91. Bulina, M.E. et al. Chromophore-assisted light inactivation (CALI) using the phototoxic fluorescent protein KillerRed. *Nat Protoc* 1, 947-953 (2006).
92. Asakawa, K. et al. Genetic dissection of neural circuits by Tol2 transposon-mediated Gal4 gene and enhancer trapping in zebrafish. *Proc. Natl. Acad. Sci. U.S.A* 105, 1255-1260 (2008).
93. Sugrue, L.P., Corrado, G.S. & Newsome, W.T. Choosing the greater of two goods: neural currencies for valuation and decision making. *Nat. Rev. Neurosci* 6, 363-375 (2005).
94. Newsome, W.T., Britten, K.H. & Movshon, J.A. Neuronal correlates of a perceptual decision. *Nature* 341, 52-54 (1989).

95. Feierstein, C.E., Quirk, M.C., Uchida, N., Sosulski, D.L. & Mainen, Z.F. Representation of spatial goals in rat orbitofrontal cortex. *Neuron* 51, 495-507 (2006).
96. Kepecs, A., Uchida, N., Zariwala, H.A. & Mainen, Z.F. Neural correlates, computation and behavioural impact of decision confidence. *Nature* 455, 227-231 (2008).
97. Yang, T. & Shadlen, M.N. Probabilistic reasoning by neurons. *Nature* 447, 1075-1080 (2007).
98. Orger, M.B., Smear, M.C., Anstis, S.M. & Baier, H. Perception of fourier and non-fourier motion by larval zebrafish. *Nat.Neurosci.* 3, 1128-1133 (2000).
99. Panerai, F. & Sandini, G. Oculo-motor stabilization reflexes: integration of inertial and visual information. *Neural Netw* 11, 1191-1204 (1998).
100. Borst, A. & Egelhaaf, M. Principles of visual motion detection. *Trends Neurosci* 12, 297-306 (1989).
101. Krapp, H.G. & Hengstenberg, R. Estimation of self-motion by optic flow processing in single visual interneurons. *Nature* 384, 463-466 (1996).
102. Borst, A., Haag, J. & Reiff, D.F. Fly Motion Vision. *Annu Rev Neurosci* (2010).doi:10.1146/annurev-neuro-060909-153155
103. Cahill, H. & Nathans, J. The optokinetic reflex as a tool for quantitative analyses of nervous system function in mice: application to genetic and drug-induced variation. *PLoS ONE* 3, e2055 (2008).
104. Cochran, S.L., Dieringer, N. & Precht, W. Basic optokinetic-ocular reflex pathways in the frog. *J. Neurosci* 4, 43-57 (1984).
105. Sanes, J.R. & Zipursky, S.L. Design principles of insect and vertebrate visual systems. *Neuron* 66, 15-36 (2010).
106. Egelhaaf, M. Fly Vision: Neural Mechanisms of Motion Computation. *Current Biology* 18, R339-R341 (2008).
107. Olsen, S.R. & Wilson, R.I. Cracking neural circuits in a tiny brain: new approaches for understanding the neural circuitry of Drosophila. *Trends Neurosci* 31, 512-520 (2008).
108. BARLOW, H.B., HILL, R.M. & LEVICK, W.R. RETINAL GANGLION CELLS RESPONDING SELECTIVELY TO DIRECTION AND SPEED OF IMAGE MOTION IN THE RABBIT. *J. Physiol. (Lond.)* 173, 377-407 (1964).
109. Oyster, C.W. & Barlow, H.B. Direction-selective units in rabbit retina: distribution of preferred directions. *Science* 155, 841-842 (1967).
110. Kim, I., Zhang, Y., Yamagata, M., Meister, M. & Sanes, J.R. Molecular identification of a retinal cell type that responds to upward motion. *Nature* 452, 478-482 (2008).
111. Baier, H. Zebrafish on the move: towards a behavior-genetic analysis of vertebrate vision [In Process Citation]. *Current Opinion in Neurobiology* 10, 451-455 (2000).
112. Masseck, O.A. & Hoffmann, K. Comparative neurobiology of the optokinetic reflex. *Ann. N. Y. Acad. Sci* 1164, 430-439 (2009).
113. Beck, J.C., Gilland, E., Tank, D.W. & Baker, R. Quantifying the ontogeny of optokinetic and vestibuloocular behaviors in zebrafish, medaka, and goldfish. *J. Neurophysiol* 92, 3546-3561 (2004).
114. Brockerhoff, S.E. et al. A behavioral screen for isolating zebrafish mutants with visual system defects. *Proc. Natl. Acad. Sci. U.S.A* 92, 10545-10549 (1995).
115. Maximova, E., Govardovski, V., Maximov, P. & Maximov, V. Spectral sensitivity of direction-selective ganglion cells in the fish retina. *Ann. N. Y. Acad. Sci* 1048, 433-434 (2005).
116. Orger, M.B. & Baier, H. Channeling of red and green cone inputs to the zebrafish optomotor response. *Vis. Neurosci* 22, 275-281 (2005).
117. Euler, T., Detwiler, P.B. & Denk, W. Directionally selective calcium signals in dendrites of starburst amacrine cells. *Nature* 418, 845-852 (2002).
118. Yonehara, K. et al. Expression of SPIG1 reveals development of a retinal ganglion cell subtype projecting to the medial terminal nucleus in the mouse. *PLoS ONE* 3, e1533 (2008).
119. Gollisch, T. & Meister, M. Eye smarter than scientists believed: neural computations in circuits of the retina. *Neuron* 65, 150-164 (2010).
120. Kim, I., Zhang, Y., Meister, M. & Sanes, J.R. Laminar restriction of retinal ganglion cell dendrites and axons: subtype-specific developmental patterns revealed with transgenic markers. *J. Neurosci* 30, 1452-1462 (2010).
121. Huberman, A.D. et al. Genetic identification of an On-Off direction-selective retinal ganglion cell subtype reveals a layer-specific subcortical map of posterior motion. *Neuron* 62, 327-334 (2009).
122. Yonehara, K. et al. Identification of retinal ganglion cells and their projections involved in central transmission of information about upward and downward image motion. *PLoS ONE* 4, e4320 (2009).
123. Stuermer, C.A. Retinotopic organization of the developing retinotectal projection in the zebrafish embryo. *J. Neurosci* 8, 4513-4530 (1988).
124. Fricke, C., Lee, J.S., Geiger-Rudolph, S., Bonhoeffer, F. & Chien, C.B. astray, a zebrafish roundabout homolog required for retinal axon guidance. *Science* 292, 507-510 (2001).
125. Burrill, J.D. & Easter, S.S. Development of the retinofugal projections in the embryonic and larval zebrafish (Brachydanio rerio). *J.Comp Neurol.* 346, 583-600 (1994).

126. Springer, A.D., Easter, S.S. & Agranoff, B.W. The role of the optic tectum in various visually mediated behaviors of goldfish. *Brain Res* 128, 393-404 (1977).
127. Klar, M. & Hoffmann, K. Visual direction-selective neurons in the pretectum of the rainbow trout. *Brain Res. Bull* 57, 431-433 (2002).
128. Zhang, H.Y. & Hoffmann, K.P. Retinal projections to the pretectum, accessory optic system and superior colliculus in pigmented and albino ferrets. *Eur. J. Neurosci* 5, 486-500 (1993).
129. Korn, H. & Faber, D.S. The Mauthner cell half a century later: a neurobiological model for decision-making? *Neuron* 47, 13-28 (2005).
130. Gahtan, E., Sankrithi, N., Campos, J.B. & O'Malley, D.M. Evidence for a widespread brain stem escape network in larval zebrafish. *J.Neurophysiol.* 87, 608-614 (2002).
131. Fee, M.S. Active stabilization of electrodes for intracellular recording in awake behaving animals [In Process Citation]. *Neuron* 27, 461-468 (2000).
132. Kralik, J.D. et al. Techniques for long-term multisite neuronal ensemble recordings in behaving animals. *Methods* 25, 121-150 (2001).
133. Miller, E.K. & Wilson, M.A. All my circuits: using multiple electrodes to understand functioning neural networks. *Neuron* 60, 483-488 (2008).
134. Wilson, M.A. & McNaughton, B.L. Reactivation of hippocampal ensemble memories during sleep. *Science* 265, 676-679 (1994).
135. Hahnloser, R.H., Kozhevnikov, A.A. & Fee, M.S. An ultra-sparse code underlies the generation of neural sequences in a songbird. *Nature* 419, 65-70 (2002).
136. Denk, W. & Svoboda, K. Photon upmanship: why multiphoton imaging is more than a gimmick. *Neuron* 18, 351-357 (1997).
137. Luo, L., Callaway, E.M. & Svoboda, K. Genetic dissection of neural circuits. *Neuron* 57, 634-660 (2008).
138. Adelsberger, H., Garaschuk, O. & Konnerth, A. Cortical calcium waves in resting newborn mice. *Nat.Neurosci.2005.Aug.;8.(8.):988.-90.Epub.2005.Jul.10.* 8, 988-990 (2005).
139. Brustein, E., Marandi, N., Kovalchuk, Y., Drapeau, P. & Konnerth, A. "In vivo" monitoring of neuronal network activity in zebrafish by two-photon Ca(2+) imaging. *Pflugers Arch.* (2003).at
140. Takahashi, M., Narushima, M. & Oda, Y. In vivo imaging of functional inhibitory networks on the mauthner cell of larval zebrafish. *Journal of Neuroscience* 22, 3929-3938 (2002).
141. Niell, C.M., Meyer, M.P. & Smith, S.J. In vivo imaging of synapse formation on a growing dendritic arbor. *Nat.Neurosci.* 7, 254-260 (2004).
142. Fetcho, J.R. & O'Malley, D.M. Imaging neuronal networks in behaving animals. *Current Opinion in Neurobiology* 7, 832-838 (1997).
143. Dombeck, D.A., Khabbaz, A.N., Collman, F., Adelman, T.L. & Tank, D.W. Imaging large-scale neural activity with cellular resolution in awake, mobile mice. *Neuron* 56, 43-57 (2007).
144. Galizia, C.G., Sachse, S., Rappert, A. & Menzel, R. The glomerular code for odor representation is species specific in the honeybee Apis mellifera. *Nat.Neurosci.* 2, 473-478 (1999).
145. Briggman, K.L., Abarbanel, H.D. & Kristan, W.B. Optical imaging of neuronal populations during decision-making. *Science* 307, 896-901 (2005).
146. Clark, D.A., Gabel, C.V., Gabel, H. & Samuel, A.D. Temporal activity patterns in thermosensory neurons of freely moving Caenorhabditis elegans encode spatial thermal gradients. *Journal of Neuroscience* 27, 6083-6090 (2007).
147. Smith, S.J. & Zucker, R.S. Aequorin response facilitation and intracellular calcium accumulation in molluscan neurones. *J Physiol* 300, 167-196 (1980).
148. Ashley, C.C. & Ridgway, E.B. Simultaneous recording of membrane potential, calcium transient and tension in single muscle fibers. *Nature* 219, 1168-9 (1968).
149. Hastings, J.W. & Johnson, C.H. Bioluminescence and chemiluminescence. *Methods Enzymol* 360, (2003).
150. Rogers, K.L. et al. Visualization of local Ca2+ dynamics with genetically encoded bioluminescent reporters. *European Journal of Neuroscience* 21, 597-610 (2005).
151. Curie, T., Rogers, K.L., Colasante, C. & Brulet, P. Red-shifted aequorin-based bioluminescent reporters for in vivo imaging of Ca2 signaling. *Mol Imaging* 6, 30-42 (2007).
152. Martin, J.R., Rogers, K.L., Chagneau, C. & Brulet, P. In vivo bioluminescence imaging of Ca signalling in the brain of Drosophila. *PLoS ONE* 2, e275 (2007).
153. Rogers, K.L. et al. Non-invasive in vivo imaging of calcium signaling in mice. *PLoS ONE* 2, e974 (2007).
154. Rogers, K.L. et al. Electron-multiplying charge-coupled detector-based bioluminescence recording of single-cell Ca2+. *J Biomed Opt* 13, 031211 (2008).
155. Agulhon, C. et al. Bioluminescent imaging of Ca2+ activity reveals spatiotemporal dynamics in glial networks of dark-adapted mouse retina. *J Physiol* 583, 945-58 (2007).
156. Vogel, A. & Venugopalan, V. Mechanisms of pulsed laser ablation of biological tissues. *Chem.Rev.* 103, 577-644 (2003).

157. Denk, W., Strickler, J.H. & Webb, W.W. Two-photon laser scanning fluorescence microscopy. *Science* 248, 73-76 (1990).
158. Tallini, Y.N. et al. Imaging cellular signals in the heart in vivo: Cardiac expression of the high-signal Ca2+ indicator GCaMP2. *Proc Natl Acad Sci U S A* 103, 4753-8 (2006).
159. Mao, T., O'Connor, D.H., Scheuss, V., Nakai, J. & Svoboda, K. Characterization and subcellular targeting of GCaMP-type genetically-encoded calcium indicators. *PLoS ONE* 3, e1796 (2008).
160. Tian, L. et al. Imaging neural activity in worms, flies and mice with improved GCaMP calcium indicators. *Nat. Methods* 6, 875-881 (2009).
161. Hendel, T. et al. Fluorescence changes of genetic calcium indicators and OGB-1 correlated with neural activity and calcium in vivo and in vitro. *J. Neurosci* 28, 7399-7411 (2008).
162. Pologruto, T.A., Yasuda, R. & Svoboda, K. Monitoring neural activity and [Ca2+] with genetically encoded Ca2+ indicators. *J Neurosci* 24, 9572-9 (2004).
163. Reiff, D.F. et al. In vivo performance of genetically encoded indicators of neural activity in flies. *Journal of Neuroscience* 25, 4766-4778 (2005).
164. Barlow, H.B. & Levick, W.R. The mechanism of directionally selective units in rabbit's retina. *J. Physiol. (Lond.)* 178, 477-504 (1965).
165. Teranishi, K. & Shimomura, O. Solubilizing Coelenterazine in Water with Hydroxypropyl-Iý-cyclodextrin. *Biosci Biotechnol Biochem* 61, 1219-1220 (1997).
166. Matsui, J.I., Egana, A.L., Sponholtz, T.R., Adolph, A.R. & Dowling, J.E. Effects of ethanol on photoreceptors and visual function in developing zebrafish. *Invest Ophthalmol Vis Sci* 47, 4589-4597 (2006).
167. Leweke, F.M., Louvel, J., Rausche, G. & Heinemann, U. Effects of pentetrazol on neuronal activity and on extracellular calcium concentration in rat hippocampal slices. *Epilepsy Res.* 6, 187-198 (1990).
168. Baraban, S.C., Taylor, M.R., Castro, P.A. & Baier, H. Pentylenetetrazole induced changes in zebrafish behavior, neural activity and c-fos expression. *Neuroscience* 131, 759-768 (2005).
169. Sakurai, T. The neural circuit of orexin (hypocretin): maintaining sleep and wakefulness. *Nat Rev Neurosci* 8, 171-181 (2007).
170. Appelbaum, L., Skariah, G., Mourrain, P. & Mignot, E. Comparative expression of p2x receptors and ecto-nucleoside triphosphate diphosphohydrolase 3 in hypocretin and sensory neurons in zebrafish. *Brain Res* 1174, 66-75 (2007).
171. Faraco, J.H. et al. Regulation of hypocretin (orexin) expression in embryonic zebrafish. *J Biol Chem* 281, 29753-61 (2006).
172. Yokogawa, T. et al. Characterization of sleep in zebrafish and insomnia in hypocretin receptor mutants. *PLoS Biol* 5, e277 (2007).
173. Kaslin, J., Nystedt, J.M., Ostergard, M., Peitsaro, N. & Panula, P. The orexin/hypocretin system in zebrafish is connected to the aminergic and cholinergic systems. *J Neurosci* 24, 2678-89 (2004).
174. Chemelli, R.M. et al. Narcolepsy in orexin knockout mice: molecular genetics of sleep regulation. *Cell* 98, 437-451 (1999).
175. Lin, L. et al. The sleep disorder canine narcolepsy is caused by a mutation in the hypocretin (orexin) receptor 2 gene. *Cell* 98, 365-376 (1999).
176. Mileykovskiy, B.Y., Kiyashchenko, L.I. & Siegel, J.M. Behavioral correlates of activity in identified hypocretin/orexin neurons. *Neuron* 46, 787-798 (2005).
177. Takahashi, K., Lin, J.S. & Sakai, K. Neuronal activity of orexin and non-orexin waking-active neurons during wake-sleep states in the mouse. *Neuroscience* 153, 860-870 (2008).
178. Lee, M.G., Hassani, O.K. & Jones, B.E. Discharge of identified orexin/hypocretin neurons across the sleep-waking cycle. *J Neurosci* 25, 6716-6720 (2005).
179. Adamantidis, A.R., Zhang, F., Aravanis, A.M., Deisseroth, K. & de Lecea, L. Neural substrates of awakening probed with optogenetic control of hypocretin neurons. *Nature* 450, 420-424 (2007).
180. Prober, D.A., Rihel, J., Onah, A.A., Sung, R.J. & Schier, A.F. Hypocretin/orexin overexpression induces an insomnia-like phenotype in zebrafish. *J Neurosci* 26, 13400-13410 (2006).
181. Cahill, G.M., Hurd, M.W. & Batchelor, M.M. Circadian rhythmicity in the locomotor activity of larval zebrafish. *NeuroReport* 9, 3445-3449 (1998).
182. Bromberg-Martin, E.S., Hikosaka, O. & Nakamura, K. Coding of task reward value in the dorsal raphe nucleus. *J. Neurosci* 30, 6262-6272 (2010).
183. Schweighofer, N., Tanaka, S.C. & Doya, K. Serotonin and the evaluation of future rewards: theory, experiments, and possible neural mechanisms. *Ann. N. Y. Acad. Sci* 1104, 289-300 (2007).
184. Ranade, S.P. & Mainen, Z.F. Transient firing of dorsal raphe neurons encodes diverse and specific sensory, motor, and reward events. *J. Neurophysiol* 102, 3026-3037 (2009).
185. Lillesaar, C., Tannhauser, B., Stigloher, C., Kremmer, E. & Bally-Cuif, L. The serotonergic phenotype is acquired by converging genetic mechanisms within the zebrafish central nervous system. *Dev Dyn* 236, 1072-1084 (2007).

186. Masseck, O.A. & Hoffmann, K. Question of reference frames: visual direction-selective neurons in the accessory optic system of goldfish. *J. Neurophysiol* 102, 2781-2789 (2009).
187. White, R.M. et al. Transparent adult zebrafish as a tool for in vivo transplantation analysis. *Cell Stem Cell* 2, 183-189 (2008).
188. Scott, E.K. & Baier, H. The cellular architecture of the larval zebrafish tectum, as revealed by gal4 enhancer trap lines. *Front Neural Circuits* 3, 13 (2009).
189. Burgess, H.A., Schoch, H. & Granato, M. Distinct retinal pathways drive spatial orientation behaviors in zebrafish navigation. *Curr. Biol* 20, 381-386 (2010).
190. Logothetis, N.K., Leopold, D.A. & Sheinberg, D.L. What is rivalling during binocular rivalry? *Nature* 380, 621-624 (1996).
191. Leopold, D.A. & Logothetis, N.K. Activity changes in early visual cortex reflect monkeys' percepts during binocular rivalry. *Nature* 379, 549-553 (1996).
192. Tailby, C., Majaj, N.J. & Movshon, J.A. Binocular integration of pattern motion signals by MT neurons and by human observers. *J. Neurosci* 30, 7344-7349 (2010).
193. Tong, F., Meng, M. & Blake, R. Neural bases of binocular rivalry. *Trends Cogn. Sci. (Regul. Ed.)* 10, 502-511 (2006).
194. Demb, J.B. Cellular mechanisms for direction selectivity in the retina. *Neuron* 55, 179-186 (2007).
195. Emran, F. et al. OFF ganglion cells cannot drive the optokinetic reflex in zebrafish. *Proc. Natl. Acad. Sci. U.S.A* 104, 19126-19131 (2007).
196. Masseck, O.A. & Hoffmann, K. Responses to moving visual stimuli in pretectal neurons of the small-spotted dogfish (Scyliorhinus canicula). *J. Neurophysiol* 99, 200-207 (2008).
197. Wylie, D.R., Bischof, W.F. & Frost, B.J. Common reference frame for neural coding of translational and rotational optic flow. *Nature* 392, 278-282 (1998).
198. Patterson, G.H. & Lippincott-Schwartz, J. A photoactivatable GFP for selective photolabeling of proteins and cells. *Science* 297, 1873-1877 (2002).
199. Zhu, P. et al. Optogenetic Dissection of Neuronal Circuits in Zebrafish using Viral Gene Transfer and the Tet System. *Front Neural Circuits* 3, 21 (2009).
200. Feinberg, E.H. et al. GFP Reconstitution Across Synaptic Partners (GRASP) defines cell contacts and synapses in living nervous systems. *Neuron* 57, 353-363 (2008).
201. Drobac, E., Tricoire, L., Chaffotte, A., Guiot, E. & Lambolez, B. Calcium imaging in single neurons from brain slices using bioluminescent reporters. *J. Neurosci. Res* 88, 695-711 (2010).
202. Drobac, E., Tricoire, L., Chaffotte, A.F., Guiot, E. & Lambolez, B. Calcium imaging in single neurons from brain slices using bioluminescent reporters. *J Neurosci Res* (2009).
203. Tricoire, L. et al. Calcium dependence of aequorin bioluminescence dissected by random mutagenesis. *Proc Natl Acad Sci U S A* 103, 9500-5 (2006).
204. Roncali, E. et al. New device for real-time bioluminescence imaging in moving rodents. *J Biomed Opt* 13, 054035 (2008).
205. Higashijima, S., Mandel, G. & Fetcho, J.R. Distribution of prospective glutamatergic, glycinergic, and GABAergic neurons in embryonic and larval zebrafish. *Journal of Comparative Neurology* 480, 1-18 (2004).
206. Okamoto, H., Sato, T. & Aizawa, H. Transgenic technology for visualization and manipulation of the neural circuits controlling behavior in zebrafish. *Dev Growth Differ.* 50 Suppl 1, S167-S175 (2008).
207. Scott, E.K. et al. Targeting neural circuitry in zebrafish using GAL4 enhancer trapping. *Nat Methods* 4, 323-326 (2007).
208. Wen, L. et al. Visualization of monoaminergic neurons and neurotoxicity of MPTP in live transgenic zebrafish. *Dev Biol* 314, 84-92 (2008).
209. Zhang, F. et al. Multimodal fast optical interrogation of neural circuitry. *Nature* 446, 633-639 (2007).
210. Plautz, J.D., Kaneko, M., Hall, J.C. & Kay, S.A. Independent Photoreceptive Circadian Clocks Throughout Drosophila. *Science* 278, 1632-1635 (1997).
211. Flusberg, B.A. et al. High-speed, miniaturized fluorescence microscopy in freely moving mice. *Nat.Methods* 5, 935-938 (2008).

CURRICULUM VITAE

Eva Aimable Naumann

Contact Information:

16, Divinity Avenue, room 2073
Cambridge, MA 02143

Mobile: 001-857-233-8701
Lab: 001-617-384-9773

email: eva@mcb.harvard.edu

Date of Birth: 16th September 1978, Germany
Nationality: German, Permanent Resident of USA

Education:

August 2005 – present:
PhD candidate at Ludwig Maximillian University/MPI for Neurobiology, Munich, Germany
- Research at Harvard University, Department of Molecular and Cellular Biology, Prof. Florian Engert

January 2005:
MSc. (Diploma) in Biology, Universität Konstanz, Germany
- Exchange semester 2003/04 Portland State University, OR, USA

November 2001:
BSc. (Prediploma) in Biology Universität Konstanz, Germany

January – June 1999:
Studium Generale Universite Stendahl, Grenoble, France

Fall semester 1998:
German Literature, University of Kassel, Germany

1989 – 1998:
Friedrichsgymnasium Kassel, Germany (humanistic, classical language highschool)
- Abitur (High school degree), Majors: Art, Biology, and German Literature

Relevant Research and Teaching Experience:

Summer 2010:
Grass Fellow: Independent Research Position at the Marine Biological Laboratories, Woods Hole, USA
“Neural correlates of behavioral variability. How the brain changes behavior”
Development of behavioral paradigms to study the necessary behavioral variability in reinforcement learning.
(Rodent behavior, Highspeed videography, color analysis, C++)

Spring 2010:
Teaching fellow: Harvard OEB57: Animal Behavior (Prof. N. Pierce & B.P.Olvezcky)

Fall 2009:
Teaching fellow: Harvard MCB145: Neurobiology of Perception and Decision Making (Prof. N. Uchida)
- ("Derek C. Bok Award for Excellence in Graduate Student Teaching of Undergraduates")

April 2009:
Coordinator of the Mind Brain Behavior Senior Honor Thesis workshops (MBB Harvard)

Fall 2008:
Teaching fellow: Harvard MCB145: Neurobiology of Perception and Decision Making (Prof. N.Uchida)

Spring 2008 – Spring 2009:
Supervision of Honor Thesis Research: Student, Annie Xiao Wang

"Using GFP-aequorin to study the role of serotonergic neurons in the dorsal *raphe nuclei* of larval zebrafish"

Spring 2008:
Teaching fellow: Harvard MCB105: Systems Neuroscience (Prof. F.Engert)

April 2008:
Coordinator of the Mind Brain Behavior Senior Honor Thesis workshops (MBB Harvard)

Fall 2007:
Group leader/teaching fellow in undergraduate research course: Harvard LS100 (Prof. A. Viel)
"Experimental Neuroscience: Expression and two photon imaging of fluorescent probes in larval zebrafish"

Spring 2007:
Teaching fellow: Harvard Science B-29: Evolution of Human Nature (Prof. M. Hauser and Prof. J. Dowling)
Interdisciplinary Introduction in Psychology/Neuroscience/Evolution.

Fall 2006:
Teaching fellow, Harvard MCB 117: Experimental Neuroscience (Prof. F. Engert)
Practical and theoretical introduction to microscopy in modern neuroscience

August 2005 - August 2006:
PhD Candidate at Max Planck Institute for Neurobiology, Munich, Germany
Computational and Systems Neurobiology Group (Prof. A. Borst/ Prof. O. Griesbeck)

> *Comparison of different FRET based genetically encoded Calcium indicators in rat hippocampal neurons*
> *(Primary neuronal cell culture, Patch Clamp, Calcium imaging, Programming in Labview)*

2004 - 2005:
Diplomarbeit (Master Thesis) in Prof. Engert Laboratory, MCB Harvard:

> "Using G-CaMP 1.6 to Monitor Visually-Evoked Synaptic Activity in Tectal Neurons *in vivo*"
> (molecular biology, genetically encoded Calcium indicators, anatomy, 2-photon microscopy)

Summer 2003:
Laboratory assistant, University Lausanne, Switzerland (Prof. L. Keller)

> *Competition over local resources between queens and males: Testing the queen-replenishment hypothesis to understand the colony sex ratio investment in the highly polygynous ant Formica exsecta.*
> *(Field work, quantitative and statistical analysis of sex ratio, molecular biology, kin selection)*

Spring 2003:
Laboratory assistant in Developmental Neurobiology Lab, University Konstanz (Prof. C. Stuermer)

> *Differential expression of reggie genes1a, 1b, 2a, 2b in the central nervous system during early zebrafish (Dario rerio) development.*
> *(Anatomy, immunohistochemistry, morpholino analysis)*

Spring 2002:
Laboratory assistant in Evolutionary Biology Lab, University Konstanz, Germany: (Prof. A. Meyer)

> *Polymorphic DNA microsatellites in the poisonous frog species Heterixalus and Mantella madagascariensis*
> *(Genomic DNA isolation, molecular clock genes, comparative phylogenomic analysis)*

Fall 2001:
Teaching Fellow: Introduction to Cell Biology, University Konstanz, Germany: (Prof. H. Plattner)
Section and Discussion for Cell biology 1 and 2

Publications & Posters:

"In vivo Ca^{2+} imaging of neural activity throughout the zebrafish brain during visual discrimination"
Eva A. Naumann, Adam R. Kampff, and Florian Engert
Conference Abstract: Computational and systems neuroscience 2010. doi: 10.3389/conf.fnins.2010.03.00328

"Monitoring Neural Activity with Bioluminescence during Natural Behavior"
Eva A. Naumann, Adam R. Kampff, David A. Prober, Alexander F. Schier and Florian Engert
Nature Neuroscience 13 513-20 (2010)

"*In vivo* calcium imaging of perceptual decision related neural activity within zebrafish brain by *in vivo*"
Eva A. Naumann, Adam R. Kampff, and Florian Engert
Society for Neuroscience Annual Meeting (Poster Presentation) 2009:

"Neuroluminescent Zebrafish: Using Aequorin to monitor the activity of genetically identified neurons in behaving animals"
Eva A. Naumann, Adam R. Kampff, David A. Prober, Alexander F. Schier and Florian Engert
Society for Neuroscience Annual Meeting (Poster Presentation) 2007:

"Using G-CaMP 1.6 to Monitor Visually-Evoked Synaptic Activity in Tectal Neurons *in vivo*"
Eva A. Naumann Diplomarbeit (Master Thesis)
(accessible at: http://kops.ub.uni-konstanz.de/volltexte/2005/1510/pdf/Naumann.pdf)

Fellowships and Awards:

March 2010:
"Grass Fellowship 2010"
Early career independent research fellowship supported by the Grass Foundation

Fall 2009:
"Derek C. Bok Award for Excellence in Graduate Student Teaching of Undergraduates"
Harvard University Certificate of Distinction in Teaching

Fall 2003:
"The Baden-Württemberg Scholarship"
Exchange program scholarship of highly qualified German students to study abroad

Extracurricular:

2007-8 Ultimate Frisbee Harvard's women's team (Quasar)
2002 –2005 ski instructor for the German Alps Club, Ultimate Frisbee team University of Konstanz
2002 June-September: Bicycle Tour Eastern Europe (Konstanz, Germany –Istanbul, Turkey)
2002 Academic year: Member of Student Senate University Konstanz, Germany (Environmental group)
2001 June-September: Bicycle Tour West Europe (Konstanz, Germany –Cordoba, Spain)
1999 Aug.- Oct. PADI Dive Master for VISA DIVERS, Kho Phi Phi, Thailand
1999 Spring: Volunteer Amata Bird Sanctuary, Chonburi, Thailand
1998 Summer: Camp Counselor in Camp Robin Hood, ME, USA (arts, lifeguard, crew)
1997 Fall: Exhibition in former communist KGB prison, Potsdam, Germany
1998 DLRG life guard
1995-1997 Occasional Icelandic horse trainer, Stud Karstens, Schneeverdingen, Germany
1992-1997 Crew instructor for Friedrichsgymnasium, Kassel

Other Interests:

Everything about human nature and culture, Art, Psychology, Surfing, Yoga, Skiing, Ski touring, Snowboarding, Sailing, Cooking, Ultimate Frisbee, German literature, Modern Dance, Music, Traveling, Life.

Computer Skills:

Labview, Matlab, and C++ (incl. OpenGL), excellent Adobe Photoshop and Illustrator skills

Languages:

German: Native language
English: Fluent
French: conversational
Italian and Spanish: basic
Latin: Extensive

EHRENWÖRTLICHE VERSICHERUNG UND ERKLÄRUNG

Ich, Eva Aimable Naumann, versichere hiermit ehrenwörtlich, dass die vorgelegte Dissertation von mir selbstständig und ohne unerlaubte Beihilfe angefertigt wurde.

Hiermit erkläre ich, dass ich mich nicht anderweitig einer Doktorarbeit ohne Erfolg unterzogen habe und die vorliegende Arbeit nicht bei einer anderen Hochschule eingereicht habe.

Eva Aimable Naumann